UNIVERSITÄT
BERN

Ischemia reperfusion injury: The role of immune response and the endothelium during myocardial infarction

Graduate School for Cellular and Biomedical Sciences

University of Bern

PhD Thesis

Submitted by

Pranitha Jayadev Kamat

from India

Thesis advisor

Prof. Dr. Robert Rieben
Department of Clinical Research
Medical Faculty of the University of Bern

Accepted by the Faculty of Medicine, the Faculty of Science and the Vetsuisse Faculty of the University of Bern at the request of the Graduate School for Cellular and Biomedical Sciences

Bern,	Dean of the Faculty of Medicine
Bern,	Dean of the Faculty of Science
Bern,	Dean of the Vetsuisse Faculty Bern

Preface

Playing with a rubber band is a common involuntary action we all do while listening or talking to someone. We wrap the band around one or several fingers obstructing the flow of blood to the tips. In medical terms the phase when any tissue (in this case the finger tip) is devoid of blood, is called Ischemia. When we then remove the wrap from our finger, we allow the blood to reflow, which in medical terms is called reperfusion. This phenomenon of ischemia reperfusion could be just an involuntary action in our routine. But for a few clinicians and researchers who are working in the field of transplantation and surgery, this phenomenon of ischemia reperfusion is a battle to fight in their routine.

Organs before transplantation are blood less and served with blood flow once transplanted into the accepting patient. During surgery, it is necessary to work in a blood free condition to allow clear field for surgery and avoid blood loss. In both these clinical situations the tissue is put on a long phase of ischemia and reperfusion. The tissue response to this is deleterious and results in death of parts or the entire organ contributing to the failure of organ transplantation or surgery.

My work in the past years as a PhD student was to learn and contribute to our understanding of the mechanisms involved during ischemia reperfusion. I have worked on individual projects each focusing on different aspects of ischemia reperfusion injury. In this thesis, each project is presented as a manuscript and is preceeded by a common background, which is ischemia reperfusion injury. As you read along the background you will find the projects mentioned at areas most relevant to their aims.

I would like to take the opportunity in this preface to thank the people behind the success of this thesis. Firstly, I would like to thank my supervisor Prof. Robert Rieben for his expert guidance all through the thesis. A big part of my acknowledgement goes to my big family for tolerating my hormonal changes due to the PhD and in return providing with moral support. Special thanks to my grandfather Mr. M.N. Shenoy, for his never-ending doses of motivation. Finally I would like to thank one and all, who have directly and indirectly contributed to the finish of this thesis.

TABLE OF CONTENTS

ABSTRACT 7

INTRODUCTION 9

1. ISCHEMIA/REPERFUSION INJURY 7

1.1 CHANGES IN AN ISCHEMIC CELL 7
1.1.1 REDUCTION OF INTRACELLULAR ATP PRODUCTION 9
1.1.2 IMBALANCED IONIC HOMEOSTASIS 9
1.1.3 CELLULAR CONTENT OF BIOMOLECULES 10
1.1.4 MITOCHONDRIAL CHANGES 11
1.2 CONSEQUENCES OF REPERFUSION 11
1.3 PROJECT UNDERTAKEN TO STUDY PROCESSES AT THE ONSET OF REPERFUSION 12

2. REACTIVE OXYGEN SPECIES (ROS) 13

2.1 INTRODUCTION 13
2.2 REACTIVE OXYGEN SPECIES DURING ISCHEMIA/REPERFUSION 13
2.2.1 MAJOR SOURCES OF REACTIVE OXYGEN SPECIES DURING ISCHEMIA/REPERFUSION 14
2.2.1.1 Xanthine oxidase 14
2.2.1.2 Mitochondria 15
2.2.1.3 NADPH oxidase 17
2.2.1.4 Arachidonic acid metabolites 17
2.2.2 CONSEQUENCES OF REACTIVE OXYGEN SPECIES DURING ISCHEMIA REPERFUSION 17
2.2.2.1 Reactive oxygen species the bad guy 17
- Oxidation of biomolecules 17
- Contribution to inflammation and coagulation 18
- Membrane permeability 18

2.2.2.2 Reactive oxygen species the good guy (mechanism of pre- and post-conditioning) 18
2.3 THE ROLE OF ANTIOXIDANTS 19
2.4 CONCLUSION 20
2.5 PROJECT IN THE CONTEXT OF REACTIVE OXYGEN SPECIES 21

3. INFLAMMATION 23

3.1 INTRODUCTION 23
3.1.1 HUMORAL IMMUNE RESPONSE 23
3.1.1.1 The complement system 23
3.1.1.1.1 Pathways of complement activation 24
3.1.1.1.2 Complement activation during ischemia/reperfusion 26
3.1.1.1.3 Consequences of complement activation 29
3.1.1.2 Cytokine generation during ischemia/reperfusion and its consequences 30
3.1.1.3 Chemokine generation and consequences during ischemia/reperfusion 30
3.1.2 CELLULAR IMMUNE RESPONSE 32
3.2 CONSEQUENCES OF INFLAMMATION 33
3.3 PROJECTS IN THE CONTEXT OF INFLAMMATION 35

4. COAGULATION **37**

4.1 INTRODUCTION **37**
4.2 INHIBITORS OF COAGULATION CASCADE **38**
4.3 COAGULATION IN ISCHEMIA REPERFUSION INJURY **39**
4.4 CONSEQUENCE OF ACTIVATION OF COAGULATION DURING ISCHEMIA/REPERFUSION **41**

5. VASCULAR SYSTEM **43**

5.1 VASOACTIVE FACTORS DURING ISCHEMIA/REPERFUSION **43**
5.1.1 NITRIC OXIDE 43
5.1.2 ENDOTHELIN 44
5.2 NO-REFLOW: A CAUSE AND CONSEQUENCE OF REPERFUSION INJURY **45**
5.3 PROJECT TO ATTENUATE MYOCARDIAL INFARCTION BY MAINTAINING VASCULAR TONE **46**

6. ENDOTHELIAL GLYCOCALYX **47**

6.1 INTRODUCTION – GLYCOCALYX AS AN ENDOTHELIAL FRINGE **47**
6.1.1 PROTEOGLYCANS- AND THE VERSATILITY IN THEIR NATURE 48
6.1.1.1 Proteoglycans during ischemia/reperfusion injury 49
6.1.1.1.1 Syndecans 49
6.1.1.1.2 Glypican, mimecan and biglycan 50
6.1.2 GLYCOSAMINOGLYCAN (ESSENTIALS OF GLYCOCALYX) 51
6.1.2.1 Glycosaminoglycans in ischemia/reperfusion injury 52

7. GLYCOCALYX ARE CENTRAL TO PATHWAYS INVOLVED IN ISCHEMIA/REPERFUSION **53**

7.1 INTERACTION OF GLYCOCALYX WITH OTHER PATHWAYS IN ISCHEMIA/REPERFUSION **53**
7.1.1 INTERACTION WITH SHEAR STRESS 53
7.1.2 INTERACTION WITH ROS 55
7.1.3 INTERACTION WITH COMPLEMENT SYSTEM 56
7.1.4 INTERACTION WITH CYTOKINES 57
7.1.5 INTERACTION WITH GROWTH FACTORS 59
7.1.6 INTERACTION WITH COAGULATION CASCADE 60
7.2 CONCLUSION **61**
7.3 PROJECT TO STUDY SHED GLYCOSAMINOGLYCANS DURING MYOCARDIAL INFARCTION **63**

8. SUMMARY AND DISCUSSION **65**

9. REFERENCES **67**

PAPER I 87

ENDOTHELIAL CELL ACTIVATION, COMPLEMENT AND CYTOKINES AT THE ONSET OF REPERFUSION AFTER TOURNIQUET APPLICATION IN HAND SURGERY

PAPER II 111

TESTING DEXRAZOXANE AS AN ATTENUATOR OF ISCHEMIA/REPERFUSION INJURY IN A CLOSED-CHEST PORCINE MODEL

PAPER III 129

DETECTION OF ACUTE MYOCARDIAL INFARCTION BY POSTMORTEM MAGNETIC RESONANCE IMAGING

PAPER IV 143

ANTIBODIES AND COMPLEMENT ARE DEPOSITED IN VIABLE MYOCARDIUM IN A PORCINE MODEL OF ACUTE CORONARY SYNDROME

PAPER V 161

EFFECT OF PRESSURE-CONTROLLED INTERMITTENT CORONARY SINUS OCCLUSION (PICSO) ON MYOCARDIAL ISCHEMIA AND REPERFUSION IN A CLOSED-CHEST PORCINE MODEL

PAPER VI 189

CHARACTERIZATION OF SHED HEPARAN SULFATES IN PIG MODEL OF MYOCARDIAL ISCHEMIA / REPERFUSION INJURY.

PAPER VII 209

DEVELOPMENT OF AN IN VITRO SYSTEM TO GROW AND INVESTIGATE VASCULAR ENDOTHELIAL CELLS UNDER PHYSIOLOGICAL FLOW CONDITIONS

GENERAL CONCLUSION 233

ACKNOWLEDGEMENTS 235

CURRICULUM VITAE 237

Abstract

A tissue devoid of blood (ischemia) undergoes changes that are augmented when it is resupplied with blood (reperfusion). Together these changes result in considerable amount of necrosis of the tissue known as ischemia reperfusion (IR) injury. IR is a common phenomenon in many clinical and pathological conditions and is therefore an interesting topic of research.

This thesis introduces the different pathways involved in IR injury, especially during myocardial infarction (MI), as most of the studies were conducted in an experimental model of MI. Every pathway although contributes significantly to the injury during IR, also functions in regaining homeostasis. Furthermore, the pathways highly interact with each other making the complete removal of any one of the pathways undesirable.

The aim of this thesis was to investigate the role of immune response and the endothelium during IR. This was studied in human skeletal muscles subjected to tourniquet induced IR and in pig hearts subjected to MI. The studies conclude an early participation of cytokines and the endothelial glycocalyx during IR. Deposition of complement components in the viable area of the infarcted myocardium indicated the role on complement in process other than mediating injury. Further, the pig model was used to test two different strategies to attenuate MI. One of the strategies hypothesized the use of a potential inhibitor of reactive oxygen species thereby reducing the injury caused by them. The other was a technique of mechanically regulating blood flow before and after reperfusion to ensure perfusion of the microvasculature. Although the treatments did not attenuate gross injury, the study identified specific parameters where the treatment was effective. Detection of infarcted myocardium with the help of a magnetic resonance imaging technique was also conducted in the hearts from our study. This added valuable data in forensics for detection of an infarct post mortem. Lastly an in vitro model for culturing endothelial cells and investigating them under pathological conditions was developed.

In summary this thesis highlights the major pathways of IR injury and demonstrates the significant role of immune responses and the endothelium in the same.

Introduction

1 Ischemia/reperfusion injury

An important component of any life form is its source of energy. For vertebrates this is mainly oxygen and glucose that is served by the transporting blood. Blood vessels make the pipelines through which this blood can reach different parts of the body. The heart acts as a central organ which pumps blood through the blood vessels and together they form the cardiovascular system. There are many episodes in our daily life when the cardiovascular system is not able to do its job of serving blood to all body parts. For instance if a rubber band was fastened on a finger, it cuts off the blood supply to the fingertip. On releasing the band the blood reflows into the tip. This phenomenon of a no blood flow (ischemia) region resupplied with blood (reperfusion) and the injury that follows is called ischemia reperfusion (IR) injury. In healthy individuals a short-term IR event is harmless, but ischemia due to a clinical condition followed by reperfusion/revascularization as a treatment to the condition could be potentially harmful. Table1 summarizes a few of such conditions.

It was is 1960 when Lennings first postulated the mechanism for IR injury. Since then a tremendous amount of in vitro, ex vivo and in vivo studies also in human patients has helped us better understand IR pathophysiology. During my PhD I focused mainly on ischemia/reperfusion injury occurring in the heart due to myocardial infarction (MI). The thesis therefore discusses IR injury in the myocardium elucidated by animal models of myocardial infarction and human clinical studies. Under topics where such knowledge is unavailable studies from other experimental models have been discussed.

1.1 Changes in an ischemic cell

In vitro models have largely helped elucidate cellular events during IR. A recent article reviews these events [1], which are briefed below.

Table 1: Clinical conditions where pathology is due to ischemia reperfusion injury

Cause	Description	Affected regions
Thrombosis	Blood clot within vessel	Heart (myocardial infarction), Brain (Stroke), Limbs (limb ischemia)
Emboli (venous and arterial)	Intravascular mass carried by circulation and capable of clogging vessels	Heart (myocardial infarction), Brain (Stroke) Limbs (limb ischemia)
Transplantation	Moving of organs and limbs from a donor or patient	The transplanted organ or limb
Sepsis	Systemic inflammatory response	Liver
Shock	Not enough availability of blood	Liver
Surgery (including replantation and flap surgery)	Clinical intervention that needs to be carried out in a blood less environment	Organs, limbs, skin
Volvulus	Twisting of all or part of organ obstructing flow of material	Stomach, Intestine
Intussusception	Sliding of one portion of bowel into another	Intestine
Hypoxic hepatitis	Arterial hypoxemia usually following heart failure	Liver
Vasculitis	Vascular obstruction due to inflammation	Kidney, skin

1.1.1 Reduction of intracellular ATP production

Adenosine triphosphate (ATP) is the major energy transfer molecule essential for every living cell and in the heart it is essential for sarcomere contraction and regulation of mitochondrial membrane potential. An interruption in oxygen supply during ischemia drives the ischemic cell to utilize other sources of oxygen than the physiological oxygen carriers namely oxyhemoglobin, myoglobin and neuroglobin [2, 3]. As the demand for ATP rises, the cell takes on to anaerobic metabolism resulting in an increase in inorganic phosphate, creatine, lactate and reduction in nicotinamide adenine dinucleotide phosphate ($NADPH_2$) oxidation. This results in accumulation of H^+ within the cell also known as cell acidosis. ATP production in ischemic cell is ultimately terminated due to acidosis and NADPH, which reduce glyceraldehyde-3-phosphate dehydrogenase (GAPDH) [4, 5]. Depletion of ATP was for example shown in isolated rabbit hearts subjected to ischemia [6].

1.1.2 Imbalanced ionic homeostasis

Anaerobic respiration results in cell acidosis with an excess of H^+ ions inside the cell. The Na^+/H^+ ion channel pumps out this excess H^+ and replaces it with Na^+ ions. In conjunction, the loss of ATP results in malfunctioning of the ATP dependent ion channel Na^+/K^+/ATPase, adding to the accumulation of intracellular sodium. Exceeding levels of Na^+ activates the Na^+/Ca^{2+} pump thereby increasing intracellular calcium. In parallel Ca^{2+} efflux is hindered by loss of Ca^{2+}/ATPase activity [7-10] (Figure 1).

An ischemic cell is therefore hypercalcemic and the high calcium content executes several protein modifications within the cell. One such modification is that of myocyte contracture proteins resulting in hypercontracture. Studies have shown that hypercontracture in an ischemic cell occurs before ATP depletion in the mitochondria. Suppression of contraction during an initial period of reperfusion, when cardiomyocytes recover from ionic derangements, was shown to limit infarct size [11, 12]

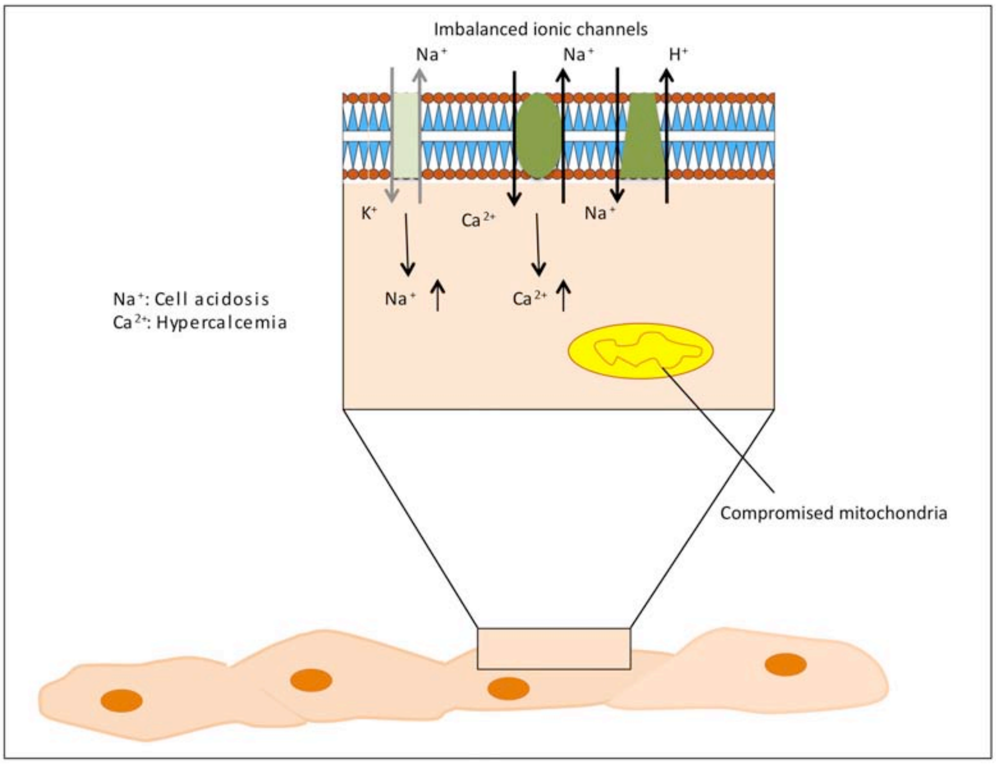

Figure 1: Ionic imbalance in an ischemic cell. Anaerobic respiration increases cellular content of H^+ ions, which is replaced by Na^+. The concentration of Na^+ also increases due to failure of ATP dependent K^+/Na^+ pump. Ca^{2+}/Na^+ pump finally replaces Na^+ ions with Ca^{2+} ions resulting in hypercalcemia (own illustration).

1.1.3 Cellular content of biomolecules

An ischemic period of 45-60 min increases cytoplasmic osmolarity by more than 100 mOsm resulting in cell edema [13]. The edema could be a consequence of formation of several osmotically active biomolecules like lactate, sodium, creatine and inorganic phosphate during anaerobic respiration. An ischemic cell in the absence of ATP seeks to cover its need for energy from ADP and eventually AMP resulting in formation of free adenosine that can freely diffuse out of the cell. There is therefore no adenosine available for ATP catabolism during reperfusion. Other molecules secreted by cardiomyocytes into the extracellular environment are bradykinin, adrenaline, acetylcholine or opioids. Detoxification of cellular metabolites is also largely affected due to reduction in glutathione, ascorbic acid and tocopherol.

1.1.4 Mitochondrial changes

During ischemia ATP depletion first occurs in the cytosol of the cell. Majority of the ATP generated by anaerobic metabolism is consumed by the cells mitochondria. Longer ischemic periods eventually deplete the mitochondrial ATP resulting in hypercalcemia within the mitochondria thereby damaging it. As a result, mitochondrial complex I followed by complex III and cytochrome oxidase is compromised [14].

1.2 Consequences of reperfusion

In vitro, in chicken cardiomyocytes, hypoxic conditions sustained for 4 hours resulted in 17% of cell death. This was significantly increased by following normoxia (simulated reperfusion) that caused 73% of cell death [15]. Reperfusion injury was clearly demonstrated in vivo in rats with 15, 30, 45 or 90 min of myocardial ischemia. One half of the rats in each group were further subjected to 14 min reperfusion. Although tissue damage increased with ischemia time, the injury in ischemia-reperfusion groups was significantly higher than in ischemia only groups [16].

It is clear that after certain duration of ischemia, the cell undergoes changes that may eventually lead to necrosis. Although the restoration of blood is a requisite to salvage the ischemic cell, from the experiments mentioned above it is clear that the injury may be aggravated by reperfusion. This phenomenon is known as reperfusion injury and is postulated to occur as a consequence of several factors.

The reflow of blood washes out accumulated H^+ in the extracellular space adding to the massive Ca^{2+} overload within the cell [7]. The Ca^{2+} overload activates calpain, a protease that reduces Na^+/K^+ functioning. This delays the normalization of Na^+ and as a consequence Ca^{2+} homeostasis during reperfusion. Reperfusion also contributes to generation of reactive oxygen species via the formation of xanthine oxidase. Protein modifications occurring within an ischemic cell and/or cell necrosis during ischemia may form epitopes for complement activation. Activated complement further aggravates injury during reperfusion. Various biomolecules formed during ischemia, like bradykinin, may also aggravate tissue injury during reperfusion and regulate the vascular tone.

From an eagle's view, the mechanisms mediating IR injury fall under five major systems namely, reactive oxygen species, inflammation, coagulation, vascular system and the endothelial glycocalyx. The role of these systems during IR is individually explained in the following sections.

1.3 Project undertaken to study processes at the onset of reperfusion

A clinical study with tourniquet induced ischemia reperfusion injury in the upper arm of patients was undertaken to study processes involved at the onset of reperfusion. Blood samples and biopsies were analyzed for measuring endothelial glycocalyx and inflammation. Results from this study are summarized in Paper I.

2 Reactive oxygen species (ROS)

2.1 Introduction

Reactive oxygen species are formed by incomplete reduction of oxygen leaving an unpaired electron in its outermost shell thereby making it highly reactive. A few examples of oxygen radicals are super oxide anion (O_2.-), hydrogen peroxide (H_2O_2), hydroxyl radical (•OH), etc. The incomplete outer shell renders the oxygen group instable and therefore highly reactive with surrounding molecules. The most reactive oxygen species is the hydroxyl radical which also makes it the most deleterious.

At physiologic concentrations ROS participates largely in signaling, redox homeostasis, inflammatory system, etc [17]. What is also present at normal physiologic condition is a substantial amount of antioxidants that neutralize excess ROS thereby maintaining homeostasis. However, in vascular diseases like IR injury, the ROS generation overwhelms the available antioxidants. This results in oxidation of surrounding biomolecules thereby compromising on their structure and function. Generation of ROS therefore contributes significantly to the pathology of IR injury. The first evidence of involvement of ROS in low oxygen conditions was the work from Rubanyi and Vanhoutte in 1986 [18]. They showed ex vivo in canine arterial rings that endothelium dependent vasodilation was improved by superoxide dismutase (a natural antioxidant). Since then studies have increasingly contributed to the source and consequence of ROS in IR injury.

2.2 Reactive oxygen species during ischemia/reperfusion

Reactive oxygen species are produced already during ischemia and as early as 5 min upon reperfusion of hypoxic cardiomyocytes with normoxic perfusate [19]. The formation of ROS during reperfusion is known to be due to a burst of oxygen in previously hypoxic cells also known as the ‘oxidative burst‘. Other studies have confirmed the formation of oxidative burst already at 10 and 15-20 seconds after reperfusion of isolated rabbit hearts with Krebs-Henseleit buffer [6, 20]. Sources of ROS generation during ischemia and reperfusion are listed below. Becker in 2004 postulated that the source of ROS during ischemia might be different from the source during reperfusion [21].

2.2.1 Major sources of reactive oxygen species during ischemia/reperfusion

2.2.1.1 Xanthine oxidase

Hypoxanthine is an intermediate product during degradation of the purine adenosine. The hypoxanthine is converted to xanthine and finally to uric acid, which is excreted from the body. In normal conditions xanthine dehydrogenase participates in the degradation of hypoxanthine to uric acid. However during ischemia, adenosine is generated and xanthine dehydrogenase is converted to xanthine oxidase (XO). XO still has the capacity to degrade hypoxanthine to xanthine and finally to uric acid in the presence of molecular oxygen, which is provided during reperfusion. This process of adenosine degradation by XO generates ROS early during reperfusion (Figure 2).

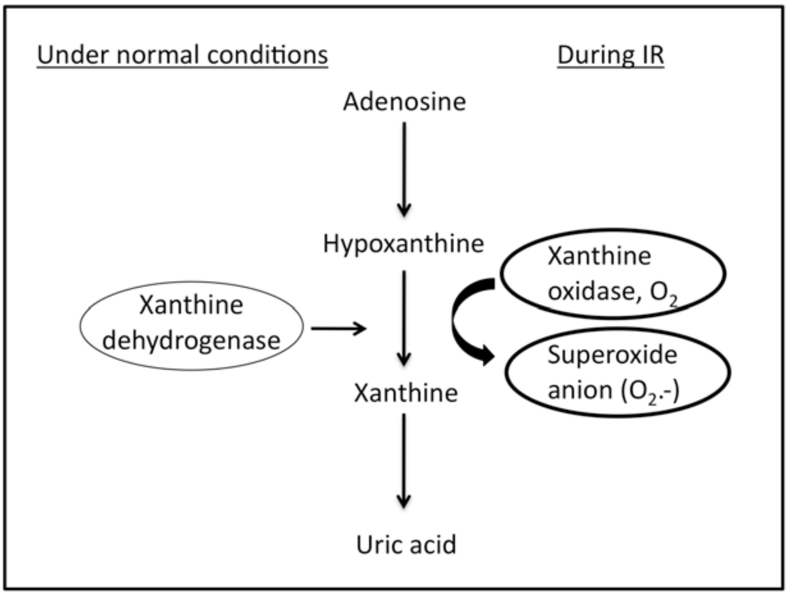
Under normal conditions
During IR
Adenosine
Hypoxanthine
Xanthine dehydrogenase
Xanthine oxidase, O2
Superoxide anion (O2.-)
Xanthine
Uric acid

Figure 2: Xanthine oxidase formed during ischemia reperfusion generates ROS. Under normal conditions, adenosine degradation occurs in the presence of xanthine dehydrogenase. During IR, xanthine dehydrogenase is replaced by xanthine oxidase that is also capable of degrading adenosine but results in the production of ROS (own illustration).

An important point to note here is that the occurrence of XO is tissue specific, and the human heart lacks this enzyme. However the role of XO in ROS generation cannot by overlooked in human myocardial IR. This is suggested by a study that showed significant rise of xanthine oxidase in circulating plasma in humans during aortic cross clamp procedure [22]. The possible source for XO in humans could be platelets the localization of which in the myocardium are elevated during MI [23]. Furthermore, the internalization of exogenous XO has been demonstrated in vitro in bovine endothelial cells [24].

2.2.1.2 Mitochondria

Mitochondria are responsible for the oxidative burst as a major contributor to the generation of ROS [25]. Mitochondrial ROS generation occurs via two pathways.

Electron transport chain: Traditionally referred to as the powerhouse of the cell, the mitochondria generate ATP via the electron transport chain (ETC). ETC is a series of redox enzymes that help in transporting electrons from a donor (NADH) to the acceptor (O_2) (Figure 3). On accepting the electrons O_2 is reduced to water. Normally, 95% of O_2 is reduced to H_2O by the mitochondrial ETC with 1% loss of electrons, which react directly with O_2 to form O_2. - [26].

Ischemia causes damage to ETC components complex I followed by complex III and cytochrome oxidase [27, 28]. The compromised cytochrome system allows leakage of electron to the oxygen present around an ischemic cell, therefore contributing largely to ROS production [29, 30] (Figure2). As a matter of fact the ischemic damage to ETC is enough to increase the overall production of ROS by mitochondria [31] (Figure 3).

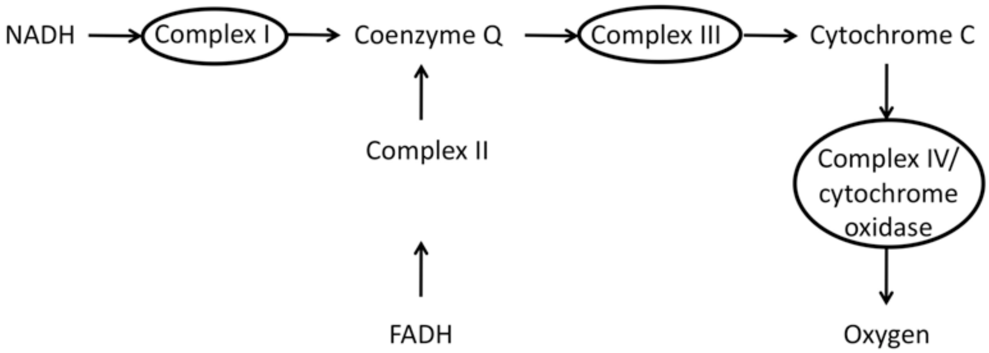

Figure 3: Mitochondrial electron transport chain. Electrons are transported via the ETC to generate ATP within the mitochondria. IR causes damage to ETC components, Complex I, Complex III and Complex IV resulting in leakage of electrons and thereby generation of ROS (own illustration).

Univalent pathway: The univalent pathway is a secondary to the ETC and reduces the remaining 5% O_2 left out by the ETC. It is a step-by-step process where oxygen accepts a single electron to form superoxide anion radical (O_2-). Superoxide is normally present in equilibrium with its protonated form $^\bullet HO_2$. In ischemic conditions the protonated form is more favored due to acidosis. The preferred $^\bullet HO_2$ is highly reactive and oxidizes the surrounding microenvironment including lipids that constitute the cell membrane. The cell dismutates this via superoxide dismutase (SOD) to form H_2O_2. H_2O_2 in small amounts is non-toxic and is converted to water in a normal cell via catalase and glutathione oxidase. In an ischemic cell, H_2O_2 is converted to a much more reactive hydroxyl radical (OH•) in the presence of metal ions, hence the rationale for metal chelation during oxidative stress [21] (Figure 4).

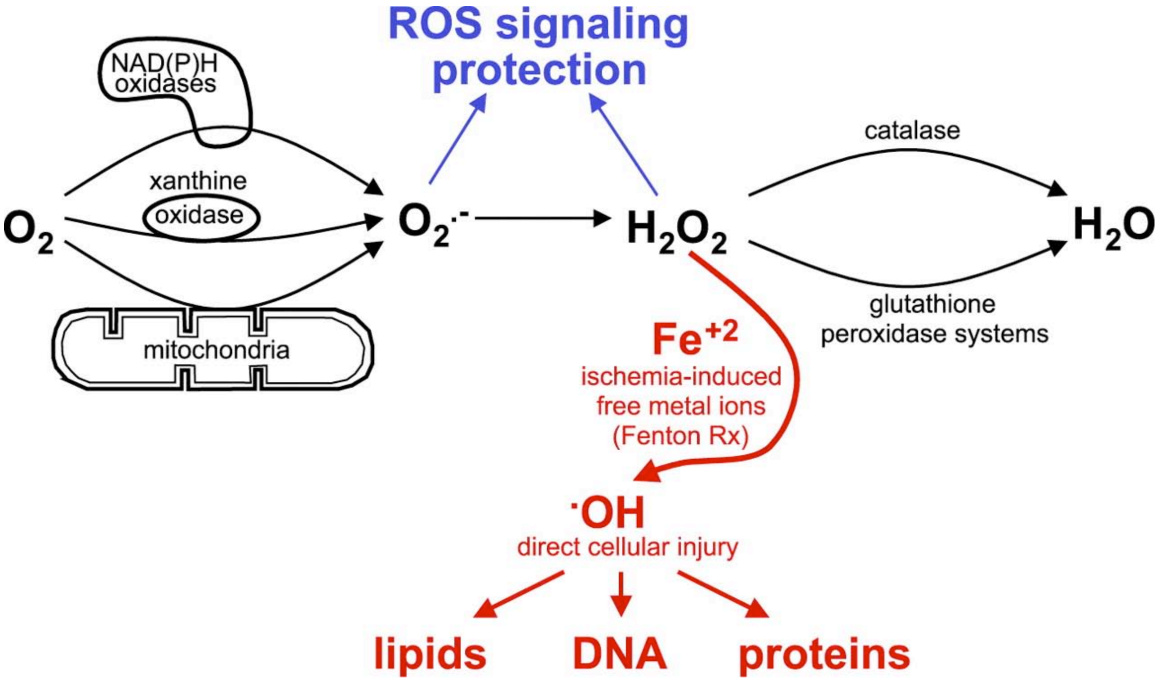
ROS signaling protection
NAD(P)H oxidases
xanthine oxidase
mitochondria
O_2
$O_2^{\cdot -}$
H_2O_2
catalase
H_2O
glutathione peroxidase systems
Fe^{+2}
ischemia-induced free metal ions (Fenton Rx)
$^\cdot OH$
direct cellular injury
lipids
DNA
proteins

Figure 4: Mitochondrial ROS generation via univalent pathway during ischemia reperfusion. H_2O_2 generated upon reduction of oxygen participates in ROS signaling. In ischemic conditions the presence of free metal ions converts H_2O_2 into more deleterious OH• that contributes directly to cell injury [21].

Other mitochondrial sources of ROS during IR are ubisemiquinone that contributes majorly to ROS generated during ischemia as shown in isolated mitochondria [32, 33], and monoamine oxidase as shown in vivo in rat brains [34].

2.2.1.3 NADPH oxidase

Nicotinamide adenine dinucleotide phosphate (NADPH) oxidase is a membrane bound enzyme found on many cells including cardiomyocytes, fibroblasts, smooth muscle and phagocytic cells. It is an electron transport system that transfers intracellular electrons to extracellular O_2 forming $O_2^{\cdot-}$. Reduced oxygen supply and presence of metabolites formed during IR like lactate induces cardiomyocytes to produce O_2^{-} via NADPH oxidase [35].

2.2.1.4 Arachidonic acid metabolites

One of the consequences of ROS is oxidation of lipids forming lipid peroxides. To remove the peroxide and replace with normal fatty acids the phospholipase enzyme comes into action and converts peroxides to arachidonic acid (AA) [36, 37]. The metabolism of AA further contributes to generation of ROS directly [38] and indirectly via NADPH oxidase [39]. However, the direct contribution of AA towards ROS during IR is yet to be elucidated in vivo.

2.2.2 Consequences of reactive oxygen species during ischemia reperfusion

2.2.2.1 Reactive oxygen species the bad guy

It is interesting to note that the different species of ROS vary in their degree of damage rendered to the tissue. Inhibition of hydroxyl radicals has more potential to attenuate tissue injury in isolated hearts rather than inhibition of superoxide anion or hydrogen peroxide [40]. The deleterious effects of ROS converge into cell apoptosis by directly inhibiting the anti-apoptotic Bcl-2 protein and indirectly as listed below.

- ***Oxidation of biomolecules***

  ROS as an oxidant oxidizes lipids constituting the cell membrane forming lipid peroxides and lipid aldehydes. They also alter the structure and function of DNA and RNA thereby highly affecting cell survival. ROS suppresses protease inhibitors and enhances elastase that works on tissue disruption.

- ***Contribution to inflammation and coagulation***

As mentioned earlier ROS leads to formation of AA. AA enhances leukocyte chemotaxis via synthesis of eicosanoids. Also, ROS activates NFkB and AP-1 signaling pathways that are involved in expression of leukocyte adhesion molecules and cytokines thereby contributing to inflammation. The activity of Kallikrein as an inhibitor of coagulation cascade is reduced by ROS, thereby contributing to clot formation.

- ***Membrane permeability***

The cell membrane permeability is compromised due to disruption of ion channels during IR resulting in cell edema. Opening of the mitochondrial permeability transition pore (mPTP) also compromises permeability of mitochondrial membrane. A detailed cause and consequence of mPTP opening has been reviewed. [41]. The deleterious consequences of mPTP opening in MI are supported by findings where infarct size was significantly reduced by use of mPTP inhibitors [42, 43]. Lastly, mPTP contributes to ROS generation by the phenomenon of ROS induced ROS release (RIRR). Inhibitors of mPTP dose dependently reduced ROS generation in cultured cardiomyocytes [44].

2.2.2.2 Reactive oxygen species the good guy (mechanism of pre- and post-conditioning)

The role of ROS as signaling molecules, also known as redox signaling, was first described in 1972 [45]. This introduced a non-detrimental view of ROS and became a platform of extensive research. Redox signaling by ROS is now known to participate in cell mitosis, and inflammatory response [46].

Mitochondria are increasingly accepted as a major contributor to cell death during IR via the opening of mPTP. RIRR is initiated by mPTP opening resulting in an immense increase in ROS. The excess of ROS prevents it from participating in redox signaling, which could aid cell survival [47]. Thus, prevention of mPTP opening would avoid excessive aggregation of ROS and the ROS generated during reperfusion would be optimal to allow redox signaling. This can be attained by maintaining cellular acidosis during reperfusion allowing only transient normalization of cellular pH and forms the backbone mechanism of pre- and post-conditioning [48]. Ischemic preconditioning is when repeated short periods of ischemia protects the myocardium upon a subsequent sustained ischemic insult and in postconditioning, the episodes of ischemia are induced during reperfusion. ROS generated under such controlled durations of ischemia, serves several protective mechanisms via the activation of signaling pathways [48]. For example, it activates protein kinase C signaling pathway, which among others prevents mPTP opening.

2.3 The role of antioxidants

Antioxidants like SOD, betacarotene and vitamin E have failed to show benefit in patients with acute MI [49]. Betacarotene was shown to induce oxidative stress in vitro by impairing mitochondrial respiration [50]. Toxic effects of the antioxidants could explain their failure in clinical trials. A much more widely applicable reasoning can be traced to the basic characteristic of these antioxidants. The water-soluble and lipid soluble antioxidants work synergistically. In isolated hypoxic-reoxygenated rat hearts synergistic effect of vitamin E and dihydrolipoic acid was confirmed by improved cardiac functional recovery [51]. Also antioxidants delivered in areas of normal cellular activity may hamper the protective activity of ROS. It is therefore essential to identify specific ROS species and their sites of generation to deliver appropriately targeted therapy as discussed by [21]. Supporting this concept is a study that showed antioxidant capacity of different rat tissues to vary depending on the type of tissue and age of the rat [52]. Some major antioxidants and their site of action are summarized in Table 2.

Table 2: Some major antioxidants and their sites of action in cardiomyocytes [53].

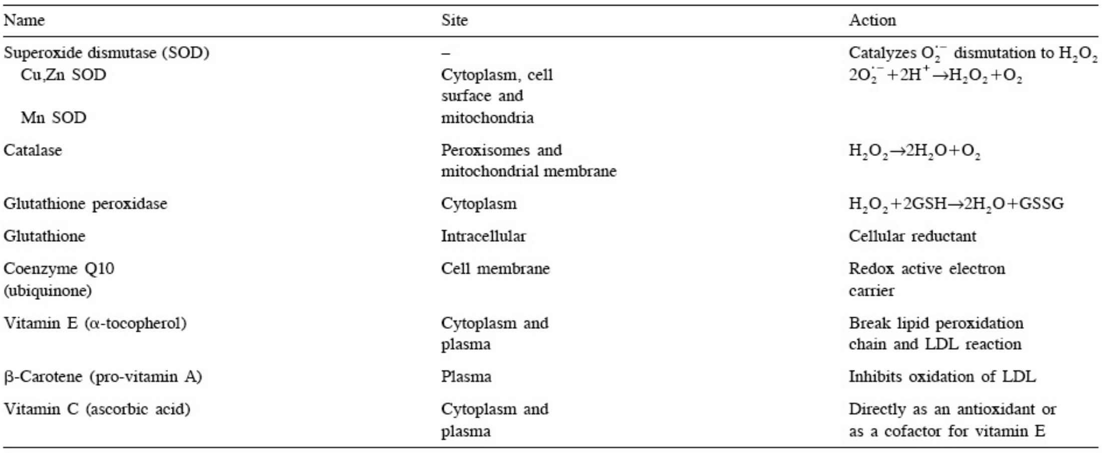

Name	Site	Action
Superoxide dismutase (SOD)	–	Catalyzes $O_2^{\cdot -}$ dismutation to H_2O_2
Cu,Zn SOD	Cytoplasm, cell surface and	$2O_2^{\cdot -} + 2H^+ \rightarrow H_2O_2 + O_2$
Mn SOD	mitochondria	
Catalase	Peroxisomes and mitochondrial membrane	$H_2O_2 \rightarrow 2H_2O + O_2$
Glutathione peroxidase	Cytoplasm	$H_2O_2 + 2GSH \rightarrow 2H_2O + GSSG$
Glutathione	Intracellular	Cellular reductant
Coenzyme Q10 (ubiquinone)	Cell membrane	Redox active electron carrier
Vitamin E (α-tocopherol)	Cytoplasm and plasma	Break lipid peroxidation chain and LDL reaction
β-Carotene (pro-vitamin A)	Plasma	Inhibits oxidation of LDL
Vitamin C (ascorbic acid)	Cytoplasm and plasma	Directly as an antioxidant or as a cofactor for vitamin E

2.4 Conclusion

ROS have been known to be harmful by-products of IR that damage the microenvironment adding to pathology of IR injury. In MI ROS are hypothesized as the cause for myocardial stunning [54]. However, detailed analysis of these dynamic molecules has revealed their importance in normal physiological processes. One step further, ROS is now confirmed to have substantial beneficial role during the pathology of IR injury. Myocardial infarction studies conducted in vivo in rabbits demonstrate that ROS is not only necessary but also sufficient for the heart to adapt defensive mechanisms [55]. The perception of ROS among scientists has therefore moved from the 'Bad guy' to the 'Good and bad guy'. The dual role of ROS also indicates the high level of specificity in its function based on the kind of ROS species, its concentration and localization in the cell. The effector function of ROS, driven by precision and sensitivity, explains the discordant results obtained in experiments implementing ROS scavengers to reduce infarct size. This concept has been extensively discussed in a book chapter written by Downey and Yellon [56].

2.5 Project in the context of reactive oxygen species

We tested the role of ROS during MI in a pig model with dexrazoxane treatment. Dexrazoxane is clinically used as an adjuvant in anti-cancer therapy and was shown to be cardioprotective for its metal chelating properties. Myocardial necrosis, cardiac function and extent of inflammation were analyzed. Results are summarized in Paper II. In conjunction with testing the effects of dexrazoxane, the infarcted hearts were scanned by magnetic resonance imaging (MRI). The MRI scans revealed regions of edema in the infarcted heart, which could be useful to identify an infarct in a forensic setting. Results of this study are summarized in Paper III.

3 Inflammation

3.1 Introduction

Inflammation is a biological response to a potentially harmful stimulus. During IR, the stimulus is generated endogenously to trigger an immune reaction in response to the non-physiological conditions. The inflammation during IR is therefore referred to as sterile inflammation the occurrence of which is necessary to regain homeostasis. However, the inflammatory process also destroys affected tissue, the extent of which largely depends on the type of tissue and duration of ischemia. This section introduces the different immune responses and dwells into their role during IR. In general, an immune response can be broadly classified into humoral or fluid phase and cellular response.

3.1.1 Humoral immune response

The humoral immune response basically consists of the non-cellular plasma proteins that elicit an immune reaction. Components of the humoral immune response, namely the complement system (including preformed natural antibodies) and cytokines are addressed.

3.1.1.1 The complement system

Hill and Ward were the first to show involvement of complement in IR injury [57]. The complement system is a cascade of blood borne and cell surface proteins that participate in identification and elimination of pathogens. Three different pathways can activate proteins of the complement system. Distally these pathways converge and follow a common cascade until termination. The complement cascade is a relatively well-understood system and is briefly explained below (Figure 5). For a detailed recent review please read [58, 59].

3.1.1.1.1 Pathways of complement activation

Alternative pathway of complement activation

The alternate pathway is also known as the amplification loop for its role in amplifying complement activation. C3 in blood plasma is prone to constant hydrolysis referred to as C3 tick over. In a healthy organism there are mechanisms to avoid this hydrolysis. However, in a pathogenic environment C3 hydrolyzes to form C3 (H_2O) which is functionally similar to C3b. Factor D cleaves the C3b associated Factor B resulting in formation of the C3bBb complex on the cell surface, which forms the alternate pathway C3 convertase. C3 convertase further splits up C3 to form more C3b and therefore amplifying the loop. The C3b generated may also bind to the alternate pathway C3 convertase to form C3bBb3b, which is the alternate pathway C5 convertase.

Classical pathway of complement activation

Complement activation occurs via the classical pathway mostly when the deposition of IgG and/or IgM antibodies trigger the process. Complement protein C1 is a complex formed from C1q, C1r and C1s. The Fc region of aggregated IgG and/or IgM forms an epitope for C1q domain of C1. The binding activates C1r and cleaves C1s. The released C1s triggers C4 to split into C4a and C4b. The latter binds to cell surface and activate C2 to form its split products C2b and C2a. The latter remains bound to C4b on the cell surface while C2b is released into the plasma. The C4b2a complex, also referred to as classical C3 convertase, splits C3 into C3a and C3b. C3a diffuses into the circulation and plays important role as an anaphylatoxin. C3b binds to the C3 convertase to form C4b2a3b complex, also known as the C5 convertase.

Lectin pathway of complement activation

The lectin pathway is initiated by binding of mannose binding lectin (MBL) to cell surface epitopes. MBL closely resembles C1q and is associated with two serine proteases MASP-1 and MASP-2, which resemble C1r and C1s, respectively. Following the binding of MBL on a cell surface, MASP-2 catalyzes the activation of C4 followed by C2. Subsequent reactions are the same as in the classical pathway ending with the C5 convertase.

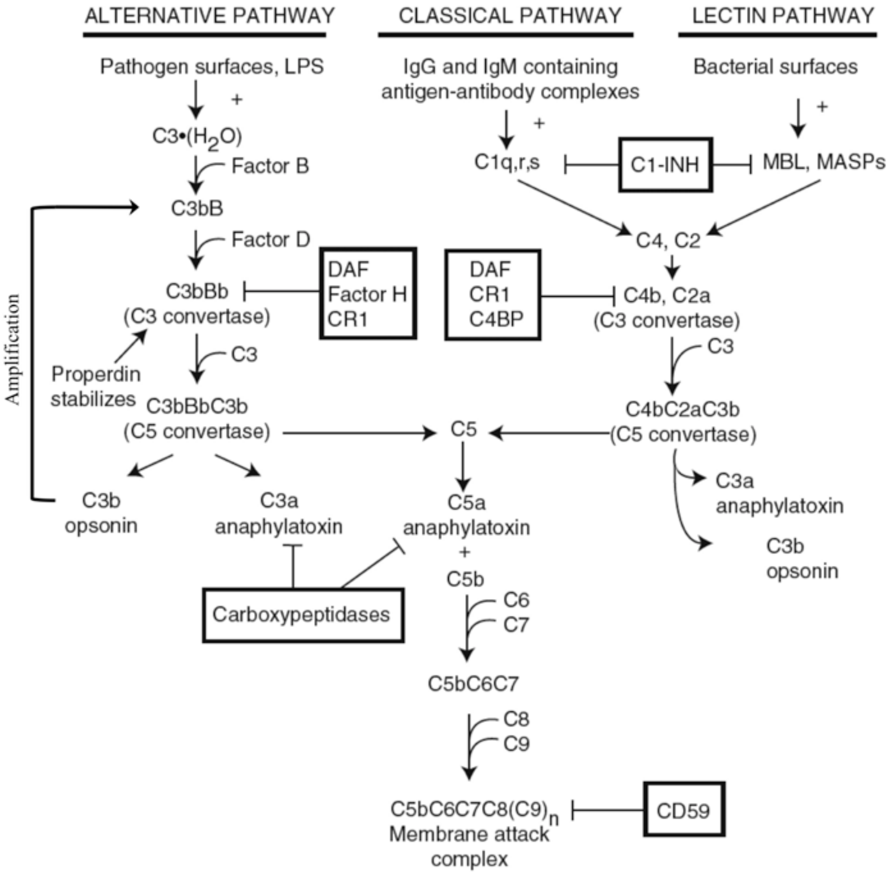
ALTERNATIVE PATHWAY
CLASSICAL PATHWAY
LECTIN PATHWAY
Pathogen surfaces, LPS
IgG and IgM containing antigen-antibody complexes
Bacterial surfaces
+
C3•(H2O)
Factor B
C3bB
Factor D
C3bBb
(C3 convertase)
DAF
Factor H
CR1
DAF
CR1
C4BP
C1q,r,s
C1-INH
MBL, MASPs
C4, C2
C4b, C2a
(C3 convertase)
C3
Properdin stabilizes
C3bBbC3b
(C5 convertase)
C4bC2aC3b
(C5 convertase)
C5
Amplification
C3b opsonin
C3a anaphylatoxin
C5a anaphylatoxin
+
C5b
C3a anaphylatoxin
C3b opsonin
Carboxypeptidases
C6
C7
C5bC6C7
C8
C9
C5bC6C7C8(C9)n
Membrane attack complex
CD59

Figure 5: The three main pathways of complement activation. The complement system can be activated via the alternative, classical or lectin pathway which converge distally to form the terminal membrane attack complex. The figure also shows proteins that regulate the complement system at different steps. Figure modified from [58].

The C5 convertase formed from all three pathways initiates a common cascade to form the terminal complement complex. Starting with C5 cleavage into C5a and C5b, the latter of which binds to cell membrane. C5a is an important anaphylatoxin during inflammation. The rest of the proteins in the cascade, namely C6, C7, C8 and C9, chronologically accrete to the bound C5b making the C5b-9 complex. This C5b-9 complex dwells holes into the cell membrane increasing its permeability and eventually resulting in cell death. The terminal C5b-9 complex is also known as the membrane attack complex or MAC.

3.1.1.1.2 Complement activation during ischemia/reperfusion

Complement activation during IR is explained below and summarized in Figure 6.

Antibody mediated classical pathway complement activation during ischemia/reperfusion

For the first time in 1975, involvement of the classical complement system was identified in patients after hospitalization for chest pain shown by decreased levels of C1, C4, and C3 [60]. Hind limb IR experiments conducted on mice deficient in C3 or C4 or serum immunoglobulins, all showed reduced injury when compared to wild type [61]. It was therefore concluded that immunoglobulins were involved in activation of complement and thus the participation of classical pathway. Further studies identified IgM as the major immunoglobulin involved as shown by an intestinal model of IR. This was demonstrated by reinstating injury when RAG-/- mice were reconstituted with IgM [62]. In the same model participation of a subset of natural IgG and IgM antibodies was identified in Cr2-/- mice [63, 64]. This subset of IgM was found to be the CM22 clone confirmed by mouse model of intestinal [65] and hind limb [66] IR injury. Subsequent experiments led to the finding that the antibodies recognized a specific epitope on the cell surface. This was a highly conserved protein region represented by N2 peptide within non-muscle heavy chain II protein (NMHC II) [67]. NMHC II belongs to the myosin family of proteins, and the authors of the study postulate that intrinsic changes during hypoxia cause the NMHC II protein to migrate to the cell surface exposing its N2 peptide to circulating natural IgM. Although the source of NMHC II needs further confirmation, it has become clear that it forms a major antigen for initiation of IgM dependent complement activation in IR, at least in mice. Other epitopes that could be possibly expressed during IR include phospholipid, β-2 glycoproteins [68, 69] and phosphorylcholine, which may synergistically influence antibody deposition. IgM mediated complement activation has been proved to hold true even during MI. IgM deficient mice illustrated reduced infarct size when compared to the IgM deficient mice that was reconstituted with wild type IgM [70].

During IR injury, classical pathway of complement system could also be activated independent of antibody deposition. Studies illustrating this are mentioned later in this chapter.

Lectin pathway of complement activation during ischemia/reperfusion

The lectin pathway is capable of antibody independent complement activation via binding of MBL to cell surface. Participation of lectin pathway in IR injury was first shown by immunostaining for MBL in reperfused areas of previously ischemic rat hearts [71] and kidneys [72]. MBL deposition was found on ischemic tissue only upon reperfusion. Furthermore, the use of monoclonal antibody against MBL [73] and elimination of MBL but not C1q [74] demonstrated attenuation of MI. Significant contribution of MBL to injury in IR was also shown in intestinal [75] and renal [76] models.

The involvement of classical and lectin pathway was conclusively shown in intestinal model of IR injury [77]. Here, the MBL-/- mice showed IgM deposition in the reperfused tissue and wild type mice showed colocalization of MBL and IgM. These results indicated the initial deposition of IgM followed by MBL. The recognition of IgM by MBL was supported by in vitro affinity chromatography studies conducted previously [78]. Although another in vitro study illustrated that MBL cannot bind to IgM that is already bound to an antigen [79].

A novel technique of triple knockout mice that lacked secreted IgM, MBL-A and MBL-C demonstrated the previously described co-functioning of IgM and MBL towards injury in a model of MI in mice [80]. From an intestinal model of IR the IgM immune complex was isolated and found to consist of MBL and C1q. Thereby demonstrating that the primary initiator of complement activation in IR is the IgM-MBL-C1q complex [81].

Alternative pathway of complement activation during ischemia/reperfusion

The alternate pathway is both an initiator and an amplifier system of complement activation. The involvement of alternative pathway in myocardial IR injury was shown in rats wherein necrosis was reduced by inhibiting alternative pathway just before reperfusion. The use of a classical pathway inhibitor in the same model suggested higher role of classical than alternative pathway in myocardial IR pathology [82]. Direct role of alternative pathway in intestinal IR was shown by attenuation of injury in Factor D deficient mice [83].

Other molecules that activate complement during ischemia/reperfusion

C-reactive protein (CRP) is an acute phase protein normally present in plasma in trace amounts and rises up to 1000 fold in inflammatory conditions. It is traditionally used as a marker for acute inflammatory response and is generally associated with cardiovascular diseases including MI [84]. To date, high sensitivity CRP measurement is one of the common clinical practices for examining cardiac patients [85], although speculations to use it as a target of therapy are ongoing [86]. IR alters the phospholipid molecules constituting the cell membrane [87]. CRP binds to these altered self molecules and the bound CRP forms an epitope for C1q [88] thereby activating the classical pathway of complement [89, 90]. Activation of complement system by CRP has been shown in patients with MI [91, 92] and the post mortem analysis revealed co-deposition of IgM with CRP [93]. Consequences of complement activation by CRP involves binding to leukocytes, modulating leukocyte function [94] and inducing the expression of adhesion molecules on endothelial cells [95]

Other than the traditional molecules involved in complement pathway activation, IR makes available several molecules that could be recognized by the components of the system and get activated. ROS oxidizes lipids, proteins, DNA and RNA of a cell causing necrosis. A necrotic cell releases sub cellular membrane constituents, which can trigger binding / activation of complement fragments C1, C2, C4 and C3 [60, 96]. C1q of the classical pathway is able to directly bind to apoptotic/necrotic cells independent of antibody deposition [97]. A mitochondrial membrane associated protein called cardiolipin was recognized as a C1q binding protein with sites also for C5 and C9. Cardiolipin was found to rise from baseline after ischemia to one hour of reperfusion in cardiac lymph of dogs [98]. A recent study also shows aggregated but not disrupted actin cytoskeleton to form binding sites for IgM in a murine model of intestinal IR injury [99]. Finally, the oxidative stress during IR is hypothesized to directly activate C3 and thereby activating the alternative pathway [100].

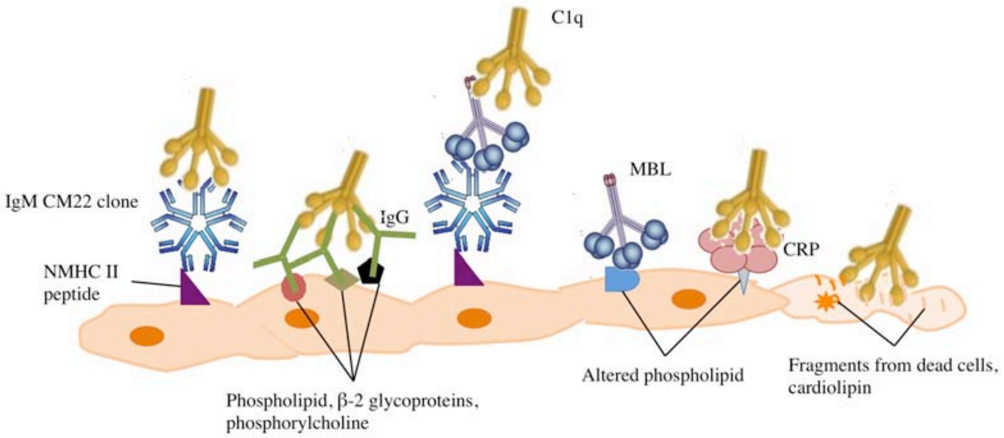
C1q
IgM CM22 clone
IgG
NMHC II peptide
MBL
CRP
Altered phospholipid
Fragments from dead cells, cardiolipin
Phospholipid, β-2 glycoproteins, phosphorylcholine

Figure 6: Mechanisms of complement activation during ischemia/reperfusion. Cellular protein modifications formed during IR along with components of apoptotic and necrotic cells form neoepitopes. These neoepitopes make binding sites for various molecules that could eventually activate the complement system (own illustration).

3.1.1.1.3 Consequences of complement activation

Major complement components that participate in effector functions of the system are MAC and the anaphylatoxins. Complement protein C6, a component of MAC was shown to disrupt endothelial cell integrity in a xenotransplant setting [101]. The terminal complex, MAC, apart from causing cell necrosis also participates in influencing neutrophil function. It triggers the cells to release ROS and matrix degrading enzymes. It further enhances production of leukotriene B4, prostaglandin E2 and thromboxane, thereby amplifying inflammatory response [102, 103]. MAC is also associated with platelet deposition and binding sites for FVa and FXa components of the coagulation cascade [104]

iC3b is formed as a cleavage product of C3b on the cell surface. Since it lacks the ability to react with Factor B it does not contribute to amplification of complement activation. Instead, iC3b participates in cell opsonization and is shown to induce IL-1 production by monocytes [105].

The major anaphylatoxins C3a and C5a are prominent during IR and are formed already during ischemia. C5a is found to be more deleterious than C3a as shown by a mouse model of MI [106] and treatment with C5a receptor antagonist reduced MI in pigs [107]. The anaphylatoxins and MAC complex formed during IR ensues expression of adhesion molecules and an array of inflammatory mediators. This was shown indirectly in rats where neutrophil mediated tissue injury was reduced by use of soluble complement receptor 1 [108]. Tissue injury was also reduced in a mesenteric IR model in mice by inhibiting complement [109]

3.1.1.2 Cytokine generation during ischemia/reperfusion and its consequences

Cytokines are signaling proteins produced in response to a stimuli and mediate/regulate immune reaction. During IR this stimuli could be recruited inflammatory cells and even ROS as shown for TNFα [110]. The synthesized cytokines activate NF-κB that regulates genes expressing cytokines, chemokines and adhesion molecules [111]. Cytokines therefore support the synthesis of more cytokines in a positive feedback mechanism. The different cytokines, their role in IR and the models they were tested in are summarized in Table 3.

3.1.1.3 Chemokine generation and consequences during ischemia/reperfusion

Chemokines are cytokines that participate in leukocyte extravasation. Many cells are able to produce chemokines among which endothelial cells and mononuclear phagocytes are special in the sense that they can produce an array of different chemokines concomitantly in inflammatory conditions. Apart from recruiting leukocytes, certain chemokines affect the function and activation of leukocytes, smooth muscle cells, neurons and endothelial cells [112, 113]. MCP-1 and IL-8 are a few chemokines that have been shown to be upregulated in ischemic myocardium and associated with injury and repair [114, 115]. A summary of the chemokines during IR injury, the experimental models in which they were tested, their role and localization, is given in Table 4 [116]

Table 3: Role of cytokines in myocardial infarction (own table).

	Source	Role in IR	In vivo models of MI
Pro-inflammatory			
TNFα	EC[1], fibroblasts, SMC, neutrophils [117], mononuclear cells, mast cells	Imbalance in Ca^{2+} homeostasis, apoptosis, Induction of coagulation, cardio protective (TNFα+TNFR2) ↑ oxidant stress, iNOS, IL-1beta ↓ cardiac function (TNFα+TNFR1)	Mice [118]
IL-1β	Myocardial cells and neutrophils induced by TNF [111, 119], EC, macrophages	Recruitment of inflammatory cells [120]	Murine [121]
IL-6	Mononuclear cells activated by TNFα and IL-1β, EC, neutrophils induced by TNFα [122]	Neutrophil recruitment [123]	Canine [123]
Anti-inflammatory			
IL-10	Monocytes and mast cells	Tissue remodeling ↓ NO [124], macrophage production of TNFα, IL-1α, IL-1β, IL-6, IL-8 [125], IL-8 from neutrophil, neutrophil recruitment.	Murine [124], human [126]
TGF-β	Induced by plasmin, myocytes [127] and/or non myocytes [128]	Tissue remodeling, endothelial-dependent coronary relaxation ↓ tissue plasminogen (anti-fibrinolytic), TNFα, H_2O_2, $O_2^{\cdot}$ - ↑ collagen synthesis, angiogenesis, myocardial hypertrophy.	Rat [129]

[1] Abbreviations: EC (endothelial cells), SMC (smooth muscle cell), ↑increase, ↓ decrease

Table 4: Chemokine expression during myocardial ischemia reperfusion [116][1].

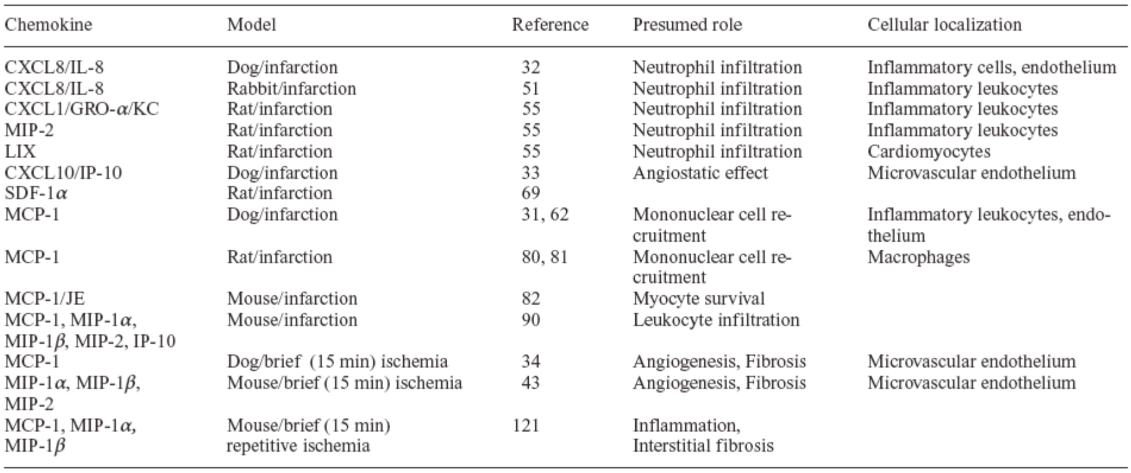

Chemokine	Model	Reference	Presumed role	Cellular localization
CXCL8/IL-8	Dog/infarction	32	Neutrophil infiltration	Inflammatory cells, endothelium
CXCL8/IL-8	Rabbit/infarction	51	Neutrophil infiltration	Inflammatory leukocytes
CXCL1/GRO-α/KC	Rat/infarction	55	Neutrophil infiltration	Inflammatory leukocytes
MIP-2	Rat/infarction	55	Neutrophil infiltration	Inflammatory leukocytes
LIX	Rat/infarction	55	Neutrophil infiltration	Cardiomyocytes
CXCL10/IP-10	Dog/infarction	33	Angiostatic effect	Microvascular endothelium
SDF-1α	Rat/infarction	69		
MCP-1	Dog/infarction	31, 62	Mononuclear cell recruitment	Inflammatory leukocytes, endothelium
MCP-1	Rat/infarction	80, 81	Mononuclear cell recruitment	Macrophages
MCP-1/JE	Mouse/infarction	82	Myocyte survival	
MCP-1, MIP-1α, MIP-1β, MIP-2, IP-10	Mouse/infarction	90	Leukocyte infiltration	
MCP-1	Dog/brief (15 min) ischemia	34	Angiogenesis, Fibrosis	Microvascular endothelium
MIP-1α, MIP-1β, MIP-2	Mouse/brief (15 min) ischemia	43	Angiogenesis, Fibrosis	Microvascular endothelium
MCP-1, MIP-1α, MIP-1β	Mouse/brief (15 min) repetitive ischemia	121	Inflammation, Interstitial fibrosis	

[1] Reference list in the table pertains to the referencing in respective article

The various sources for chemokine during IR are elaborated in a review by [130] and are summarized below.

- ROS is the main source of chemokine production during IR via activation of NFkB. It is however not clear if the effect of ROS is direct or indirect via myocardial necrosis.
- Cytokines and inflammatory mediators like TNFα, IL-1β, histamine, and tryptase, respectively, induce chemokine production post infarction.
- Complement C6 deficiency attenuates IL-8 chemokine in rabbit after MI [131]. C5a receptor antagonist reduces chemokine-mediated neutrophil infiltration in renal IR [132].
- TLR 2, 4 and 5 receptors are associated with chemokine production from cardiomyocytes and keratinocytes [133]. TLR 4 activated by hyaluronan fragments specifically regulates chemokine production based on hyaluronan size [134] in macrophages and endothelial cells [135]. Direct involvement of TLR4 was demonstrated in TLR4 deficient mice showing reduced inflammation after MI [136, 137]

3.1.2 Cellular immune response

Leukocytes are the blood cells with the highest capacity to generate ROS. The main leukocytes known to participate in IR are neutrophils, monocytes, platelets, mast cells, T cells and B cells and are listed below

- Neutrophils elicit both protective and deleterious effects during IR. A detailed review of how these molecules are recruited in an ischemic myocardium and their function during IR is given in [96].
- Monocytes are seen early in MI via the influence of MCP-1 chemokine and were identified as two distinct subsets that peak at days 3-5 in humans [138]. The subsets were further shown to have different roles during MI as one was shown to regulate myocardial recovery whereas the other not.
- Platelet recruitment in post-ischemic tissue requires leukocyte adhesion and P-selectin expression. A platelet-leukocyte complex is therefore formed on the vessel wall eliciting a negative synergistic effect.
- Mast cells that participate in IR are either resident in the myocardium or recruited during inflammation. Tryptase and chymase are factors specific to mast cells that are released upon degranulation via oxidants or anaphylatoxins [139]. Mast cell released factors interact with rennin system, help in leukocyte recruitment [139] and contribute to heart arrhythmia.
- T cells are resident in perivascular area and contribute to innate and adaptive immune response. During IR they are known be multifunctional by producing pro-inflammatory cytokines as well as aiding in tissue repair. Modulation in T cell response has been indentified during acute coronary syndrome. Also a specific T cell subset, the CD4+ cells, but not CD8+ cells were shown to contribute to MI in mice [140]. T cells are also known to interact with rennin system.
- B cells are predominantly pathogenic by generating IgM that activates classical pathway complement activation. However, non-peritoneal B cells elicit protective effects during IR. The IgM produced by them do not contribute to IR injury but instead generate the anti-inflammatory cytokine IL-10 during IR in mice kidney [141].

3.2 Consequences of inflammation

The role of various inflammatory molecules during IR makes it clear that the consequence of inflammation is both deleterious and protective. While inflammation mediates tissue destruction it also participates in myocardial scar formation and healing. Experimental and clinical studies have demonstrated diminished reduction in injury when the inflammatory system is completely inhibited. For an extensive review on the consequences of complete inhibition of inflammation read [142]. However, anti-inflammatory treatments have been tried in many clinical trials and are reviewed in [143]. The action of pro- and anti-inflammatory cytokines is both deleterious and protective in MI as shown in Figure 7 [144]. The effect is determined by the concentration, time of synthesis and type of receptors engaged by them. Both the effects of cytokines are explained and a potential therapeutic approach is suggested, which would be to regulate the activation of survival activating factor enhancement (SAFE) pathway [145]

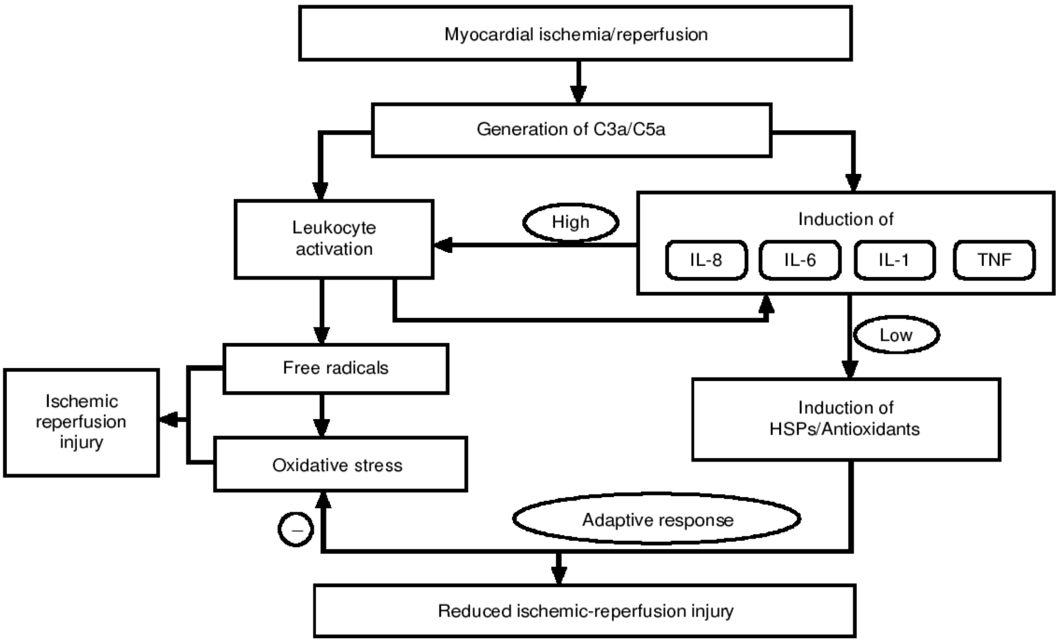
Myocardial ischemia/reperfusion
Generation of C3a/C5a
Leukocyte activation
High
Induction of
IL-8
IL-6
IL-1
TNF
Low
Free radicals
Ischemic reperfusion injury
Oxidative stress
Induction of HSPs/Antioxidants
Adaptive response
−
Reduced ischemic-reperfusion injury

Figure 7: Dual role of cytokines during ischemia reperfusion. Myocardial IR results in generation of anaphylatoxins that regulate the outcome of injury by inducing cytokine gene expression. At high concentrations of the pro-inflammatory cytokines, leukocytes are activated generating free radicals and oxidative stress terminating into tissue injury. At lower cytokine concentrations, however, heat shock proteins and antioxidants are induced that reduce the injury [144].

3.3 Projects in the context of inflammation

The involvement of different components of the inflammatory cascade and their possible role in IR injury has been studied extensively. With regard to the role of complement, mainly knockout mouse models were used. During my studies, we used a clinically relevant pig model of to study complement activation in acute MI. Two groups of 20 min ischemia and 60 min ischemia, followed by 6 hours reperfusion, were included in the study. In the group with 20 min ischemia no necrotic myocardium was found. The inflammatory molecules identified in this group were compared with the 60 min ischemia group, which rendered the myocardium partly necrotic. Results from this study are discussed in Paper IV.

4 Coagulation

4.1 Introduction

A primary consequence of IR injury is endothelial cell dysfunction resulting in a mutilated blood vessel. In response to the injured vessel, the coagulation system of the body is triggered. This occurs via a cascade of proteolyses that are broadly divided into the extrinsic pathway that mainly initiates the cascade and the intrinsic pathway that contributes to inflammation [146] along with propagation of clot formation. The two pathways terminally converge into the common pathway as discussed below.

Intrinsic (contact activation) pathway of coagulation activation

The intrinsic pathway is initiated by negatively charged molecules, which could be cholesterol sulfates, phospholipids, glycosaminoglycans, etc. in physiologic conditions. A hypothesis for initiation of coagulation via intrinsic pathway has been reviewed [147]. Briefly, high molecular weight kininogen (HK) circulates in plasma as a complex with prekallikrein (PK) and FXII. HK in the complex binds to a multiprotein kininogen receptor (majorly cyokeratin-1) found on endothelial cells, platelets and granulocytes. Interaction of complex with receptor activates PK to kallikrein, which in turn activates factor XII to XIIa (Figure 8). As a result, bradykinin is released from Kallikrein and factor XIIa propagates further proteolyses to form thrombin as shown in Figure 9.

Extrinsic (Tissue factor) pathway of coagulation activation

The extrinsic pathway is initiated on a breached endothelium that exposes tissue factor (TF) protein on its surface. TF is a 47KDa protein [148] that mediates the formation of thrombin and eventually fibrin [149] (Figure 9).

Common pathway

The extrinsic and intrinsic pathways converge at the formation of thrombin. Thrombin facilitates the conversion of fibrinogen to fibrin thereby forming clot. The coagulation cascade with both pathways is summarized in Figure 9.

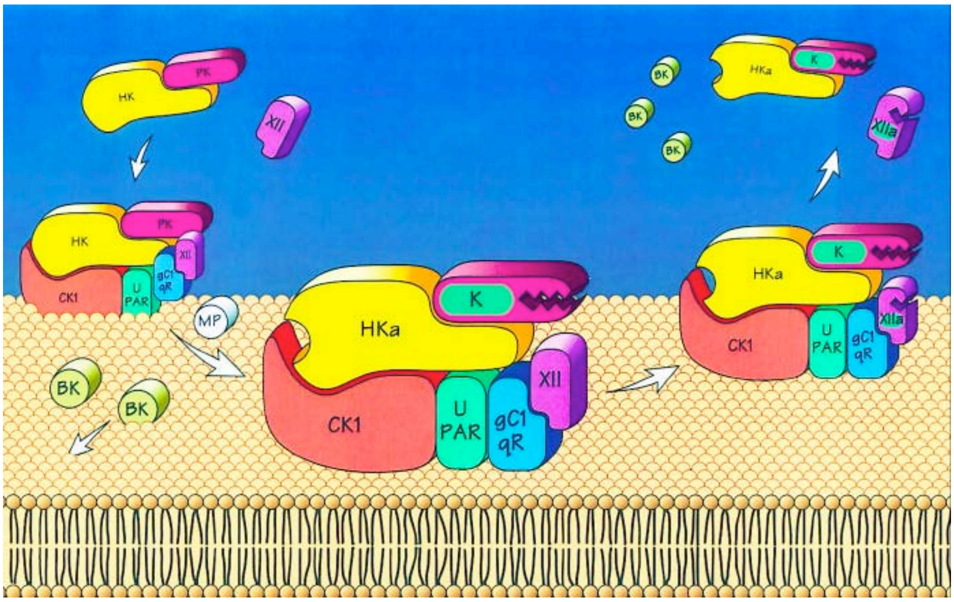
HK
PK
XII
HK
PK
CK1
U PAR
gC1 qR
XII
MP
BK
BK
HKa
K
CK1
U PAR
gC1 qR
XII
BK
BK
BK
HKa
K
XIIa
HKa
K
CK1
U PAR
gC1 qR
XIIa

Figure 8: Initiation of intrinsic pathway of coagulation. Complex of kininogen (HK), prekallikrein (PK) and FXII binds to cell surface kininogen receptors to activate FXII. **[147]**

4.2 Inhibitors of coagulation cascade

Any physiologic cascade needs to include certain regulatory molecules to maintain physiologic homeostasis. During coagulation it is the tissue factor pathway inhibitor (TFPI), Protein C and Antithrombin (AT) that regulate the system. TFPI forms a complex with TF, factor VIIa and Xa to inhibit the initiation of coagulation cascade. Protein C is converted to its activated form Protein Ca by binding of thrombin to endothelial cell membrane associated molecule thrombomodulin (also known as a proteoglycan). Activated protein Ca can then proteolytically inactivate factor Va and VIIIa thus controlling the formation of thrombin. AT has both anti-coagulant and anti-inflammatory effects.

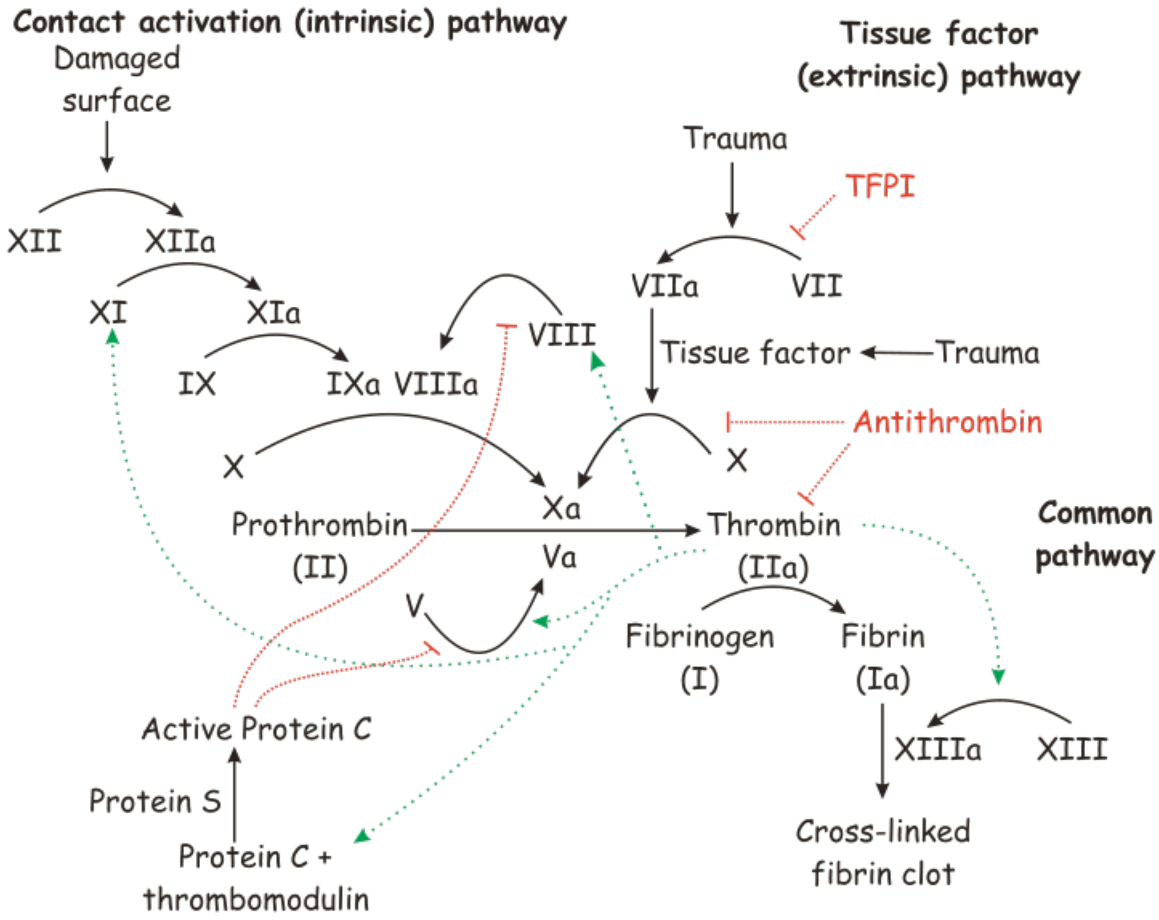
Contact activation (intrinsic) pathway
Damaged surface
XII
XIIa
XI
XIa
IX
IXa VIIIa
VIII
X
Xa
Va
V
Prothrombin (II)
Thrombin (IIa)
Active Protein C
Protein S
Protein C + thrombomodulin
Tissue factor (extrinsic) pathway
Trauma
TFPI
VIIa
VII
Tissue factor
Trauma
Antithrombin
X
Common pathway
Fibrinogen (I)
Fibrin (Ia)
XIIIa
XIII
Cross-linked fibrin clot

Figure 9: Pathways of coagulation system. Coagulation cascade can be activated by the Extrinsic or intrinsic pathway that result in formation of thrombin. The formation of clot from thrombin is common to both pathways. Red arrows show inhibition and green arrows show activation (Illustration by Joe D on Wikipedia, http://en.wikipedia.org/wiki/Coagulation).

4.3 Coagulation in ischemia reperfusion injury

The pro-coagulant phase of IR involves both intrinsic and extrinsic pathways. Involvement of the intrinsic pathway has been mainly studied in models of stroke where factor XII and XI deficient mice showed lower injury post IR [150]. Pertaining to heart, control of coagulation activation is of major interest in cardio pulmonary bypass due to the presence of external plastic surfaces through which the blood passes. The negatively charged polymer surfaces may activate the intrinsic pathway of coagulation as well as the complement system with deleterious effects. As an example, inhibition of kallikrein in such a model was shown to reduce coagulation and fibrinolysis [151]

Initiation of the extrinsic pathway occurs by the complex formed between expressed TF and Factor VIIa. Inhibition of this complex formation could therefore reduce the activation of coagulation pathway. This was achieved in a model of MI in rabbits by the use of recombinant human Factor VII blocked at its active site [152]

Various inflammatory mediators such as C5a, TNFα, IFNγ, IL-1, PAF induce TF expression on endothelial cells and cardiomyocytes [153, 154]. Infact, MI in rabbits has shown increased expression of TF on cardiomyocytes, possibly due to vascular leakage [155]. In this model, TF on myocytes co-localized with thrombin and fibrin, which terminally participate in clot formation. Inhibition of activation of the extrinsic pathway by administering antibodies against TF has therefore the potential to increase coronary blood flow and attenuate MI. According to this study, administration of anti TF antibody 15 min before ischemia (infarct size = 16%) was more beneficial when compared to treatment given after 30 min ischemia (infarct size = 47%) [155]

Thrombin deposition not only further progresses into fibrin and propagation of the coagulation pathway, but also works in amplification of the coagulation response by initiating more TF expression. Increase in TF mRNA expression by thrombin has been shown in EC [156]. Reduced TF expression was attained in a model of balloon angioplasty by using hirudin, which inhibits thrombin [157]. Thrombin is known to induce the expression of adhesion molecules and cytokines [158]. It induces expression of IL-8, E-selectin, P-selectin, ICAM-1 from endothelial cells [159, 160] and IL-6, MCP-1 from smooth muscle cells [161]

The effect of thrombin inhibition was shown by a decrease in IL-8 and MCP-1 [157] in an in vivo model. Thrombin also participates in recruitment of platelets, which adds to IR injury, further highlighting the importance on inhibiting thrombin [162].

4.4 Consequence of activation of coagulation during ischemia/reperfusion

Although the participation of TF, thrombin and fibrin has been shown in models of IR injury, their individual contributions to the injury is as yet unknown. In a rabbit model of cardiac IR injury, inhibition of TF and thrombin showed reduction in MI. In the same model depletion of fibrinogen did not reduce infarct size, suggesting that the TF-thrombin activity is independent of fibrin [163]. Instead, a mechanism involving a cell membrane G protein coupled receptor namely PAR-1 was postulated in TF-thrombin activity. This was confirmed in PAR-1 knock out mice with renal IR injury [164] and MI [165]. The latter study further indicated the extended damage caused by activation of inflammation via the involvement of PAR-1.

5 Vascular system

Apart from the preliminary IR responses taking place on the surface of the vasculature, the vascular system itself plays considerable role during IR. Vascular function comprising of vasodilation and vasoconstriction is regulated by vasoactive factors. The main factors include endothelium derived prostaglandins, thromboxane, ROS, molecules from the renin-angiotensin system, the endothelium derived nitric oxide (NO), endothelin (ET), and non endothelium-derived relaxing factors. Cellular changes occurring during IR affect the production of these factors and may lead to vascular dysfunction. The vasorelaxing factor NO and vasoconstricting factor ET play significant role in this respect and are discussed below

5.1 Vasoactive factors during ischemia/reperfusion

5.1.1 Nitric oxide

Nitric oxide executes the function of vasodilation, inhibition of platelet aggregation, and leukocyte adhesion [166]. Its presence in the vasculature is therefore important to avoid ‘No reperfusion’ due to vasoconstriction and blockage of vessels. Supporting this concept are several in vivo animal studies that show attenuation of MI by increasing availability of NO [166].

NO is generated by both enzymatic and non-enzymatic mechanisms [167]. The enzymes involved in NO generation are called nitric oxide synthases (NOS). They are a family of three isoforms namely neuronal (nNOS), inducible (iNOS) and endothelial (eNOS) NOS. nNOS and eNOS are found in the heart but their expression depends on location in the cell and the specie. NOS are located in endothelial cells and may also be present in platelets and leukocytes upon activation.

During ischemia the non-enzymatic mechanism plays a predominant role, wherein NO is generated either directly from nitrite or via XO [167, 168]. The generation of NO is not very straightforward and depends of various co factors and substrate availability. The cofactors include tetrahydrobiopterin, calcium, calmodulin, caveolin and others [169]. NO is also regulated by a diverse set of biomolecules including neurohumoral factor angiotensin II and cytokine TNFα [170, 171]. Taken together the NO availability is determined by several factors, most of which are affected during IR, and therefore NO abundance is misbalanced during IR.

The role of NO in myocardium is also not straightforward. Although NO is shown to protect the myocardium from IR as mentioned above, a lot of literature exists that indicates the opposite and is summarized in [166]. The conflicting role of NO is a result of its diverse functions in affecting different bio systems of vascular tone, inflammation, cardiac function, mitochondrial respiration and cell apoptosis. In principle NO is antioxidant, anti-apoptotic, anti-inflammatory and regulates vascular tone [172], thereby preserving blood flow during IR. In low concentrations it also enhances cardiac function. At high concentration NO reduces cardiac function, impairs mitochondrial respiration, triggers inflammation and myocyte apoptosis. NO is metabolized into peroxynitrile (ONOO-) and dinitrogen trioxide (N2O3) in the presence of superoxide anion and oxygen, respectively [166], thereby aggravating the tissue injury due to reactive radicals. It is therefore important to carefully adjust the concentrations of NO in order to attenuate the injury during IR.

5.1.2 Endothelin

Endothelin occurs in four isoforms namely ET-1, ET-2, ET-3 and ET-4. Among these, ET-1 is the major form of ET and the most potential vasoconstrictor. The function of ET is based on the receptor engaged by it. The ET-A receptor mediates vasoconstriction, cell proliferation and increased intracellular calcium concentration. The ET-B receptor is inhibitory by obstructing formation of ET-1 and mediating clearance of existing ET-1. It also engages vasodialatory effects by inducing NO and prostacyclin. ET-1 has been shown to participate in maintaining physiological vascular tone in humans via the ET-A receptor. It is therefore clear that ET-1 can have opposite effects and is probably determined by its concentration. This is supported by a study conducted in humans wherein ET-1 reduced cardiac contractility in healthy individuals but improved contractility in patients with advanced left ventricular dysfunction [173].

The concentration of ET-1 was measured to rise after 50 min ischemia in rats during MI. In the same study, ET-1 levels increased even more upon reperfusion [174]. ET-1 has also been shown to be elevated in patients with acute MI and is used a prognostic marker for the same [175]. During MI, ET-1 has both protective and deleterious actions. It is known to aggravate reperfusion injury and was shown to be associated with no reflow in the myocardium [176].

5.2 No-reflow: A cause and consequence of reperfusion injury

The effect of IR on vasculature depends on the size of the vessels. The arteries are less affected than arterioles and the venules are more affected that the arterioles. The effect of decreased NO and increased ET impair vasodilation thereby increasing vascular resistance in the arterioles. Constricted arterioles decrease the blood flow into capillaries rendering the area of the tissue served by them devoid of blood flow during reperfusion. This is called the ‘no–reflow‘ phenomenon leading to increased hydraulic conductivity and interstitial edema. Additionally, leukocyte adhesion and rolling is enhanced in capillaries and post-capillary venules that disrupt the endothelial junctions and increase vascular permeability. All the more, the recruited neutrophils release ROS adding to the oxidative burst and causing further destruction of the tissue. There is therefore capillary clogging followed by increased permeability and minimal tissue perfusion during reperfusion (Figure 10). It is due to this no-reflow phenomenon that at times, reperfusion injury is simply referred to as injury due to no perfusion.

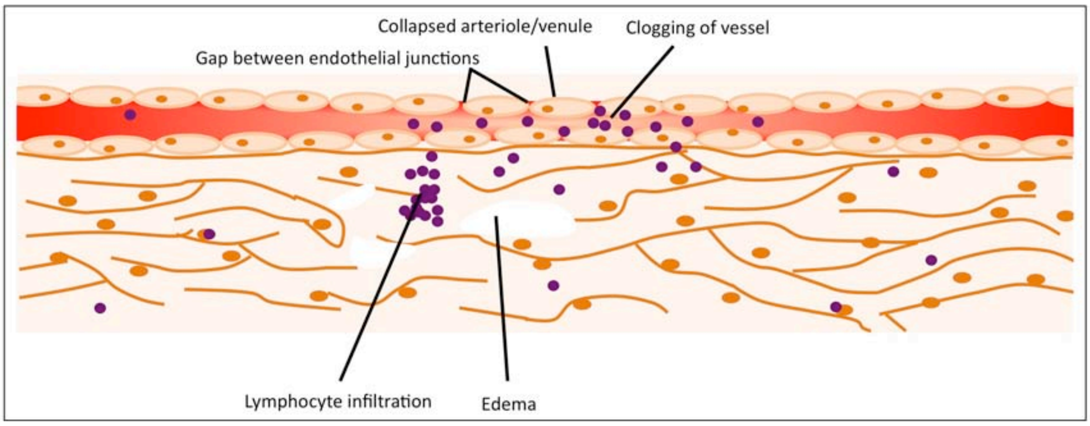

Figure 10: No-reflow phenomenon. Misbalance of the vasoactive factors during IR cause the smaller arteriole/venules to collapse. This increases interstitial edema with enhanced adhesion of immune cells and capillary plugging (own illustration).

5.3 Project to attenuate myocardial infarction by maintaining vascular tone

During myocardial IR, vascular function is necessary for myocardial function. Experimental studies have tested the attenuation of IR injury by modulating the vasoactive factors. Another approach to maintain the patency of cardiac microvasculature is by increasing pressure in the coronary sinus also known as intermittent coronary sinus occlusion (ICSO). Based on this technique we tested the effect of pressure controlled intermittent coronary sinus occlusion (PICSO) in our pig model. The study is summarized in Paper V.

6 Endothelial glycocalyx

6.1 Introduction – Glycocalyx as an endothelial fringe

Glycocalyx is a carbohydrate rich coating on the plasma membrane of every cell in the human body. IR is a form of vascular disease, the study of vascular/endothelial glycocalyx is therefore relevant to understand the participation of glycocalyx during IR.

The endothelial glycocalyx may be visualized as sea reef. Just as the sea reefs are firmly attached to the seabed with branches freely floating in water, the endothelial glycocalyx is attached to endothelial cells with its proximal parts floating in blood plasma (Figure 11). It forms a highly dynamic interface between the flowing blood and surrounding tissue forming the first line of defense that is continuously shed and replaced [177] in order to maintain homeostasis. In pathological conditions biosynthesis and shedding of the glycocalyx is highly regulated [178]

The backbone structure of the glycocalyx-'reef' is made of long proteoglycans (PGs) and relatively shorter glycoproteins, both of which attach the glycocalyx to the cell surface. Several polysaccharide chains known as glycosaminoglycans (GAGs) hang out from the proteoglycan structures, to float in the blood plasma and allow free interaction with plasma proteins (Figure 11). The PGs and GAGs are major constituents of endothelial glycocalyx and therefore will be discussed more in detail.

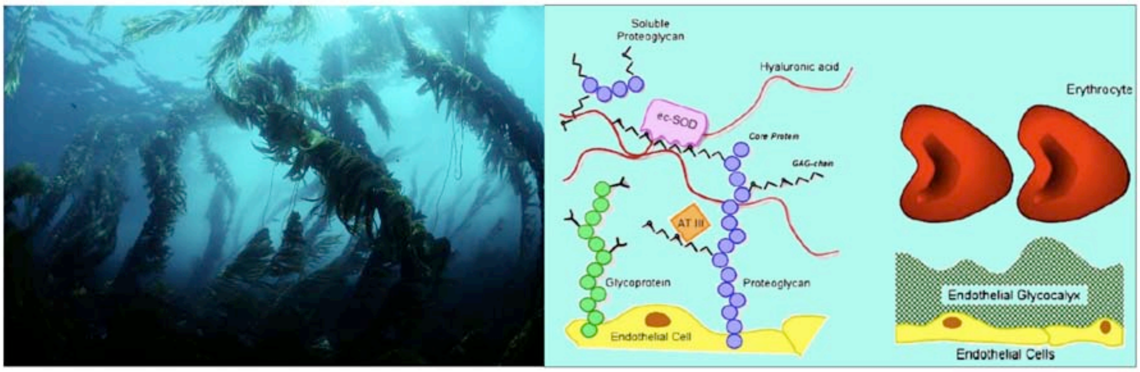

Figure 11: The endothelial glycocalyx. The endothelial glycocalyx can be visualized as sea reefs on the surface of the endothelium (left) (photography by Phillip Colla, CA). They extend from the surface of the endothelium and are freely floating in the vascular fluid (middle) [179]. Size of the glycocalyx relative to red blood cells (right) [179].

6.1.1 Proteoglycans- and the versatility in their nature

Proteoglycans consist of GAG chains spanning from a core protein that mediates its adherence to endothelial cells. The core proteins are a family of proteins namely syndecan, glypican, perlecan, versican, decorin, mimecan and biglycan. These proteins vary in their size, the number of GAGs bound to them and their ability to attach to the cell surface. However, what makes the core proteins versatile by themselves is that they need not always carry the same type and amount of GAGs. For instance syndecan on epithelial cells normally carry heparan sulfate and chondroitin sulfate GAG chains. But, the presence of TGF-β (cytokine involved in coagulation and tissue remodeling) promotes addition of chondroitin sulfate chains to syndecans [180]. Again, this may or may not hold true for syndecan on any other cell type. So a main function of the core protein is to regulate the site and amount of expression of a certain GAG on the surface of the cell, depending on the cell type and milieu. In this regard, it is suggested that certain domains of the core protein are evolutionarily conserved in order to carry out some important functions. It is based on the fact that syndecans possess regions that are hypervariable and regions that are highly conserved in the same molecule [181]. The dynamic nature of PGs is represented by its function that is highly driven by specificity for its location, molecular composition and ligand bound to it. Although the specificity of its attributes is ascertained in some cases there are several interactions where the prevalence of specificity is yet to be elucidated or may just not exist. The table below summarizes the structure and composition of PG family (Table 5).

Table 5: Proteoglycans of endothelial glycocalyx [179]

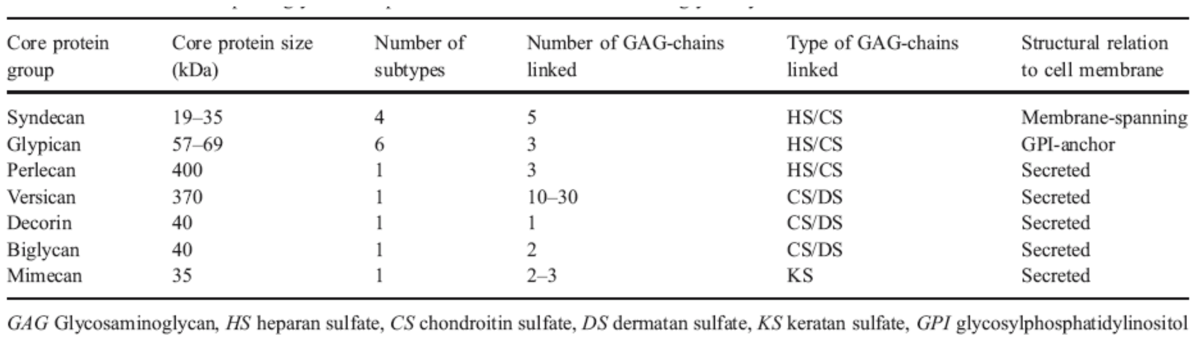

Core protein group	Core protein size (kDa)	Number of subtypes	Number of GAG-chains linked	Type of GAG-chains linked	Structural relation to cell membrane
Syndecan	19–35	4	5	HS/CS	Membrane-spanning
Glypican	57–69	6	3	HS/CS	GPI-anchor
Perlecan	400	1	3	HS/CS	Secreted
Versican	370	1	10–30	CS/DS	Secreted
Decorin	40	1	1	CS/DS	Secreted
Biglycan	40	1	2	CS/DS	Secreted
Mimecan	35	1	2–3	KS	Secreted

GAG Glycosaminoglycan, *HS* heparan sulfate, *CS* chondroitin sulfate, *DS* dermatan sulfate, *KS* keratan sulfate, *GPI* glycosylphosphatidylinositol

6.1.1.1 Proteoglycans during ischemia/reperfusion injury

6.1.1.1.1 Syndecans

Syndecans make 50-90% of the endothelial glycocalyx and therefore are widely studied in IR injury. There are four subtypes of syndecan namely syndecan 1–4 that have similar cytoplasmic and transmembrane domains. The extracellular domains however vary widely depending on site of expression, type and position of GAGs [182] (Table 6). Syndecan attached to the cell surface can be shed as an intact PG [181, 183], and is functional both in attached and shed forms [181, 184].

Table 6: Characteristics of syndecan (own table)

Syndecan	Distribution	Type of GAGs attached	Position of attached GAG
Syndecan-1	Epithelial and endothelial cells	CS, HS	Distal (HS), proximal (CS)
Syndecan-2	Fibroblast and endothelial cells	Majorly HS	Distal
Syndecan-3	Neural cells	Majorly HS	Distal and proximal
Syndecan-4	Epithelial and fibroblasts	Majorly HS	Distal

Syndecan-2 is expressed on normal endothelial cells but is replaced by syndecan-1 in response to an external stimulus that activates the endothelial cell. Syndecan-1 is shown to rise significantly in human patients during cardiopulmonary bypass [185]. The effect of cardiopulmonary bypass during surgery on syndecan shedding was tested and no difference was found in syndecan-1 shedding during coronary artery bypass grafting in patients undergoing on- or off-pump surgery [186]. Syndecan-1 expression is anti-inflammatory and reduces cardiac dilation and dysfunction after MI [187]. In angiotensin II treated rats, where the inflammation is reduced, syndecan-1 enhanced cardiac fibrosis [188]. The effect of syndecan-1 is therefore complex and context dependent. As mentioned before, the shed ectodomain is biologically active and may compete with the adherent syndecan-1. As a result of the competition the effector functions of various cytokines and growth factors that bind to cell surface syndecan-1 are largely affected [189]

Syndecan-4 is involved in mechanosensing of cardiomyocytes for their prevalence in costamers and z-disks in rats [190]. Rise in plasma levels of syndecan-4 was measured in patients after MI. The expression of syndecan-4 was restricted to infarcted zone indicating its role in remodeling [191]. In mice after MI syndecan 4 was shown to inhibit apoptosis, affect cardiac remodeling [192], and improve cardiac function [193].

To summarize, syndecan is a major component of the endothelial glycocalyx with specific responses to stimuli both in the membrane attached and fluid phase form. Since the endothelium is the primary port of interaction for the flowing blood, syndecan is extensively studied in IR injury.

6.1.1.1.2 Glypican, mimecan and biglycan

Glypicans are transmembrane proteoglycans, the expression of which is regulated by the cell type and milieu. The HS on glypicans and the core protein themselves interact with several growth factors and are important during development [194]. Mimecan and biglycan are soluble proteoglycans that are secreted by endothelial cells and are found in the glycocalyx [179]. Mimecan has recently come to light to be directly proportional to the left ventricular mass as shown in rats, mice and humans [195]. It is being considered as a marker for heart failure [196].

6.1.2 Glycosaminoglycan (Essentials of glycocalyx)

GAGs are the most copious unbranched heteropolysaccharides in the body. The polysaccharide chain is made of alternating units of uronic acid or galactose and hexosamine. To be more specific the uronic acid residue could be glucuronate or iduronate and the hexosamine could be N-acetylglucosamine or N-acetylgalactosamine. There are five types of GAGs, heparan sulfate, chondroitin sulfate, dermatan sulfate, keratan sulfate and hyaluronan. These GAGs differ in the type of uronic acid and hexosamine residues making up their disaccharide units. Different GAGs of the endothelial glycocalyx and their components are listed in Table 7. Along with different disaccharide units making up different GAGs, an additional layer of heterogeneity is added to the GAG chains, which makes the GAGs different from each other. This is the sulfation of disaccharide units at defined positions. Every GAG chain is varyingly sulfated, depending on a combination of factors. These include the milieu outside the cells they are expressed on, the core protein carrying them (if any), and the type and location of the GAG synthesizing cell [197]. The sulfation is defined during synthesis but can also be modified post synthesis.

A note on GAG sulfation

The biosynthesis of GAG chains occurs in the Golgi apparatus of the cell. As the chains are synthesized the N-deacetylase/N-sulphotransferase (NDST) enzymes add sulfate groups on the polymerized chains in a non-template driven fashion. Once expressed on the cell surface another set of enzymes known as Sulf enzymes have the capability to modulate extracellular GAG sulfation [198]. GAG sulfation plays a major role during inflammation, which is a potential mediator of IR injury. Human microvascular endothelial cells in the presence of pro-inflammatory cytokines like IFNγ and TNFα increasingly synthesize NDST and therefore increase sulfation of HS GAGs presented by the cells. The increased sulfation mediates the binding of other cytokines, like RANTES, on the treated cells and this in turn may facilitate leukocyte migration [199]. Also the sulfation pattern on a certain GAG chain could be regulated by the sulfation pattern of another GAG chain present in its vicinity. For example, over-sulfation of HS chains decreases sulfation on CS chains.

Table 7: Glycosaminoglycans of endothelial glycocalyx [179]

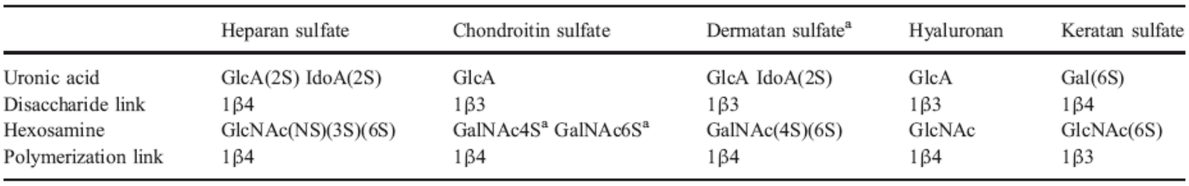

	Heparan sulfate	Chondroitin sulfate	Dermatan sulfate[a]	Hyaluronan	Keratan sulfate
Uronic acid	GlcA(2S) IdoA(2S)	GlcA	GlcA IdoA(2S)	GlcA	Gal(6S)
Disaccharide link	1β4	1β3	1β3	1β3	1β4
Hexosamine	GlcNAc(NS)(3S)(6S)	GalNAc4S[a] GalNAc6S[a]	GalNAc(4S)(6S)	GlcNAc	GlcNAc(6S)
Polymerization link	1β4	1β4	1β4	1β4	1β3

6.1.2.1 Glycosaminoglycans in ischemia/reperfusion injury

GAGs participate specifically in IR injury as discussed in the next section.

7 Glycocalyx are central to pathways involved in ischemia/reperfusion

Endothelial cells maintain themselves as an anti-coagulant and –inflammatory surface lining the vessels via the glycocalyx layer produced by them. The glycocalyx also acts as a sensory part of endothelial cells and activates them in presence of stimuli. In other words, an external stimulus is responded to by changes in the endothelial glycocalyx. The activated cell then responds specifically to the kind of stimuli.

Ischemia followed by reperfusion may also act as an external stimulus to cause changes in endothelial glycocalyx. As discussed further in the section, endothelial glycocalyx has the ability to bind to an array of biomolecules. Changes in the glycocalyx may in turn modulate binding and function of these molecules both autocrine and paracrine to the affected area. Although there is growing evidence adding to such modulator/effector behavior of the endothelial glycocalyx, a lot more investigation is required in this direction in the context of IR. It is therefore important for the reader to critically infer the message given out in this section considering the experimental conditions of studies mentioned.

7.1 Interaction of glycocalyx with other pathways in ischemia/reperfusion

7.1.1 Interaction with shear stress

Productions of vasoactive factors like NO and prostacyclin are induced by shear stress. At least in the case of NO, the glycocalyx behaves as the mediator transducing mechanical force (from shear stress) into cellular signal (producing NO). The glycocalyx therefore participates in regulating shear stress induced vascular tone.

Individual constituents of the glycocalyx have shown distinct roles in mechanotransduction of shear stress [200]. For instance HS and HA are involved in shear induced NO production but not CS. HS and glypicans-1 are also known to mediate flow-induced activation of endothelial nitric oxide synthase [201]. This indicates that the mechanotransduction function is mediated by specific components of the glycocalyx.

Shear stress and cell surface glycocalyx are in constant balance with each other. Studies have shown the differential effect of glycocalyx on fluid shear stress and shear rate based on its structure [202]. On the other hand, the glycocalyx composition is highly regulated by the shear stress imparted on it. In a recent study fluid shear stress was shown to regulate synthesis of HA by human endothelial cells [203]. In vivo studies conducted on rat mesenteric venules show clustering or elongation of GAGs during ischemia. Reperfusion of the previously ischemic venules led to profuse shedding of GAGs, mainly CS followed by HS [178]. Such responses may be partly due to the change in shear stress. The endothelium seems to modulate its glycocalyx to compensate for the change in shear stress and this compensation by means of structure and composition is pretty specific.

Vascular permeability is measured in terms of hydraulic conductivity and in capillaries hydraulic conductivity depends on shear stress as shown in frog mesenteric venules [204]. This response is mediated by HA and HS by NO induction and by CS probably by a mechanism downstream to NO induction [205]. This illustrates the permeability of vasculature based on the type of GAG expressed on its surface. The interaction of glycocalyx with shear stress is summarized in figure 12.

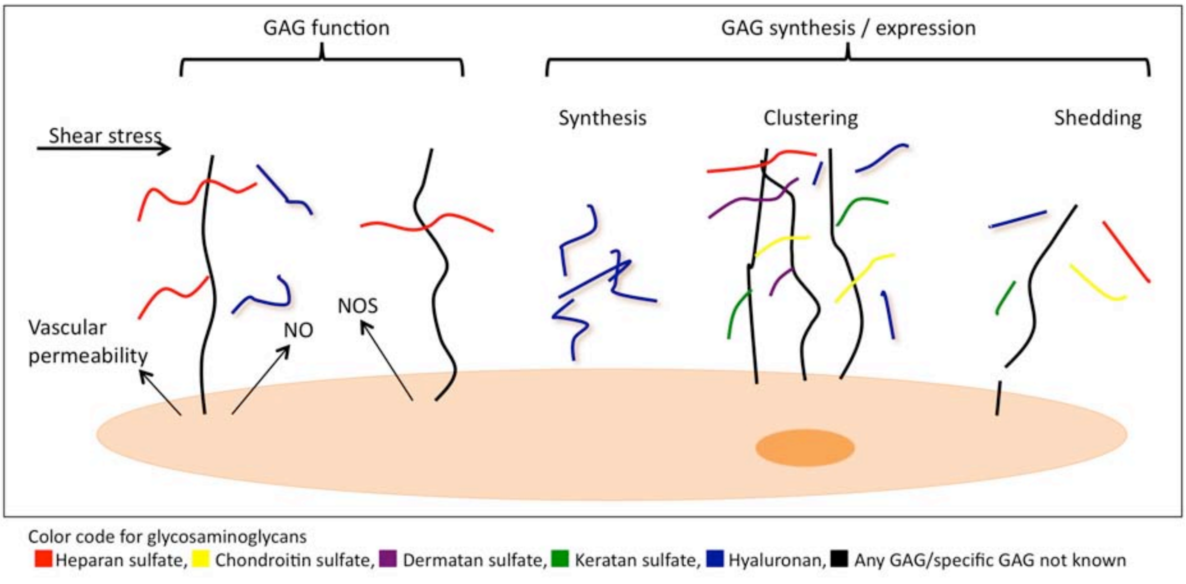
GAG function
GAG synthesis / expression
Synthesis
Clustering
Shedding
Shear stress
Vascular permeability
NO
NOS
Color code for glycosaminoglycans
🟥Heparan sulfate, 🟨Chondroitin sulfate, 🟪Dermatan sulfate, 🟩Keratan sulfate, 🟦Hyaluronan, ⬛Any GAG/specific GAG not known

Figure 12: Interaction of glycocalyx with shear stress. From left to right. Shear stress mediates GAG function by regulating vascular permeability and inducing nitric oxide (NO) via HS and HA GAGs. Via HS it mediates nitric oxide synthase (NOS) production. Shear stress also affects the synthesis, clustering and shedding (own illustration).

7.1.2 Interaction with ROS

An ischemic cell generates ROS, which increases many folds upon reperfusion of the cell. ROS and the glycocalyx influence each other to a great extent. Although not yet tested in endothelial cells, endogenous HA produced from fibroblasts in the presence of ROS, displays characteristics of an antioxidant by inhibiting lipid peroxidation among other antioxidant properties [206].

The participation of ROS in glycocalyx shedding is known and this process is highly regulated. Mouse cremaster muscle was subjected to IR injury and visualized by intravital microscopy. IR mediated ROS production reduced thickness vascular glycocalyx to permit the penetration of 70 kDa but not of 580 kDa macromolecule into the glycocalyx layer [207]. Such regulated shedding may be in part due to the selective modification of GAG structures by ROS. In vitro studies have shown ROS to depolymerize GAGs, with the non-sulfated GAGs more susceptible to depolymerization than the highly sulfated GAGs. ROS was also shown to chemically modify the uronic acid residue in GAGs to hexosamine [208]. Ex vivo studies on isolated kidneys have demonstrated decreased synthesis of proteoglycans in presence of ROS [209]. Under the influence of ROS, alveolar glycocalyx was prone to modification and was different for different species of ROS. While H_2O_2 degraded the core protein, OH• could break down both the core protein and the GAGs [210].

Glycocalyx harbors many enzymes including xanthine oxidase (XO) and extracellular superoxide dismutase (EC-SOD). The interaction between XO, SOD and glycocalyx is electrostatic and highly specific for the type of sulfation on GAG. Inhibition of XO by oxypurinol is limited when the XO is bound to GAGs [211]. In the case of bovine XO, they bind with high affinity to CS rather than to HS. This study, conducted on cultured bovine endothelial cells, also showed internalization of XO by the PG [24]. EC-SOD binds to HS with high affinity and one of its isoforms SOD-C has higher GAG affinity than the others. Such specific interaction between GAG and SOD was shown to extend the half-life of SOD in vivo in rats [212] and shedding of EC-SOD is proven to be pro-oxidant [213].

XO is a ROS generator and SOD a ROS scavenger. The preferential binding XO to CS and SOD to HS could play an important role during IR pathology when the glycocalyx composition is highly influential. For instance, if during the pathology CS expression on cells increases and at the same time if HS is shed, then there is increased availability of ROS leading to cell death. Interaction of glycocalyx with ROS is summarized in Figure 13.

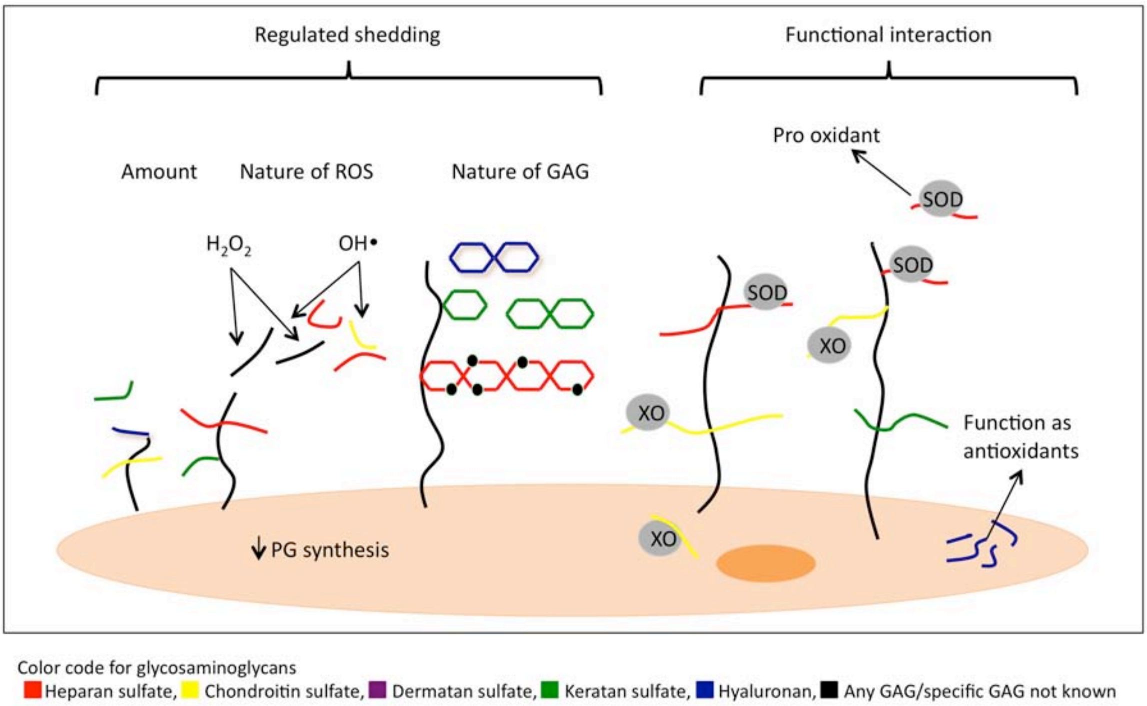
Regulated shedding
Functional interaction
Pro oxidant
Amount
Nature of ROS
Nature of GAG
SOD
H_2O_2
OH•
SOD
SOD
XO
XO
Function as antioxidants
XO
PG synthesis
Color code for glycosaminoglycans
🟥 Heparan sulfate, 🟨 Chondroitin sulfate, 🟪 Dermatan sulfate, 🟩 Keratan sulfate, 🟦 Hyaluronan, ⬛ Any GAG/specific GAG not known

Figure 13: Glycosaminoglycans and ROS. From left to right. ROS induces shedding of GAG chains. The amount is shedding highly regulated by the nature of ROS, with H_2O_2 acting on core proteins and OH• acting on GAGs and core proteins. Shedding also depends on GAG structure. Sulfated GAGs (sulfation shown by dark circles) are less prone to depolymerization than non sulfated GAGs. ROS producing enzyme xanthine oxidase (XO) and scavenging enzyme superoxide dismutase (SOD) functionally interact with their specific GAGs HS and CS respectively. Endogenous HA act as antioxidants (own illustration).

7.1.3 Interaction with complement system

Several modified structures are exposed on the surface of an ischemic cell, which are recognized by natural antibodies, MBL and CRP that trigger the activation of complement system by its different pathways (discussed in section 3.1.1.1.2). A connection between glycocalyx and the complement system also seems to exist. In vitro and in vivo studies of rats injected with CRP, showed a dose dependent shedding of HA and HS from the glycocalyx followed by endothelial dysfunction [214].

In vitro studies have shown GAG to minimize complement activation. Heparin is long known for it's anti-inflammatory effects by enhancing the activity of C1-inh by 15-35 fold [215]. Recently the enhanced activity of C1-inh was shown to be transient in rats in the presence of dextran sulfate, a GAG very similar to heparin [216]. Heparin also inhibits activation of C1q and formation of C3 convertase [217]. The complement inhibitory property of physiological GAGs like HS, CS-A, CS-C, DS have been shown by reduced deposition of C3 and C4 on aggregated IgG [218]. Another study nicely illustrates this activity of GAG to be specific to the size, orientation and degree of sulfation on GAG. Here, the complement inhibition of bound C3b by binding of factor H was enhanced by heparin and CS-A but not CS-C, KS and HA. N-desulfated or short chains of heparin reduced the enhanced binding of factor H [219]. Kazatchkine et al. showed N-substitution, O-sulfation, but not N-sulfation, of GAGs to be important for anti complementary activity [220]. Heparin and dextran sulfate showed no activity on factor H as a cofactor for Factor I or for its decay accelerating activity on C3bBb [221]. It is therefore clear that there are highly specific interactions of GAG with components of the complement system. These are summarized in Figure 14.

7.1.4 Interaction with cytokines

The cytokine TNFα has long been known to shed glycocalyx off the endothelial surface [222]. It reduces syndecan-1 expression on endothelial cells and simultaneously induces ICAM-1 expression. These in vitro results hold true in vivo in a mouse model of healing skin wounds [223]. HS binds to IFN-Y at its sulfated terminal sequences and its internal N-acetyl rich sequence links two IFN-Y molecules, thereby helping in molecule dimerization [224]. Similarly, all cytokines may have the possibility to bind to GAGs by forming ionic bonds between amino acid domains on the cytokines and sulfated domains on GAGs [224].

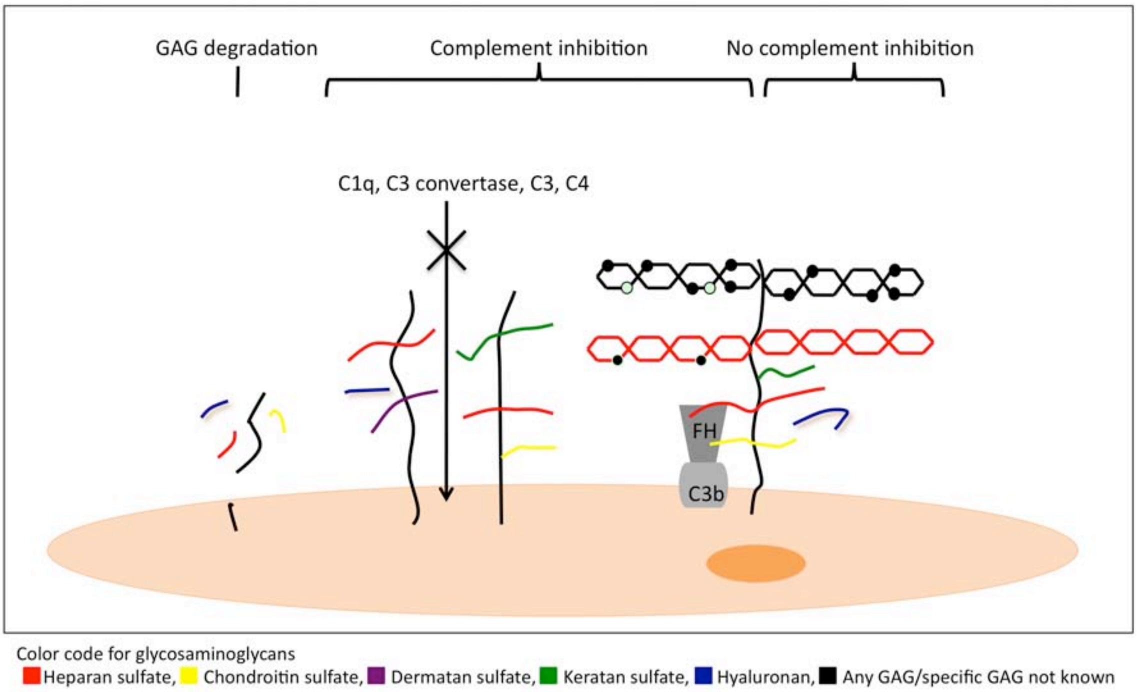
GAG degradation
Complement inhibition
No complement inhibition
C1q, C3 convertase, C3, C4
FH
C3b
Color code for glycosaminoglycans
🟥Heparan sulfate, 🟨 Chondroitin sulfate, 🟪 Dermatan sulfate, 🟩 Keratan sulfate, 🟦 Hyaluronan, ⬛ Any GAG/specific GAG not known

Figure 14: Glycosaminoglycans and complement. From left to right. Complement proteins mediate GAG degradation. GAG participates in complement inhibition by restricting the binding of C1q, C3 convertase, C3 and C4 complement proteins. Complement inhibition is highly regulated by GAG composition. N substitution (green circles) and O sulfation (black circles) of GAGs inhibit complement. N sulfated HS inhibits complement partly by binding to factor H (FH). CS also mediates FH binding and complement inhibition. N sulfated GAGs, non sulfated HS, KS, HA and CS-C do not inhibit complement (own illustration).

Interaction between GAGs and chemokines has been elucidated in much more detail than interaction with cytokines. Basically all chemokines can bind to GAGs and in most cases the binding is highly specific. Chemokine binding to GAG is specific for its chain length, degree and position of sulfation. Differential binding of RANTES to DS and CS indicate that the binding does not only depend on the amount of sulfation but also on the position of sulfation. Also, chemokines MIP1α, IL8, MCP1 and RANTES have higher affinity for O-sulfation rather than N-sulfation [225]. In the case of MIP 1α the HS binding site consists of two highly sulfated regions that are 12–14 monosaccharide units, separated by a N-acetylated region. This region supports binding of MIP-1α dimers rather than monomers or tetramers [226]. The specificity of GAG-chemokine interaction may play a role in making available certain chemokines at a specific location and instance and thereby regulating inflammation. Moreover, chemokines bound to cell surface GAGs may show different function from those bound to circulating GAGs. The later could restrict them from binding to cell surface receptors [225]. Decreased sulfation on endothelial cells reduces leukocyte extravasation in inflammatory conditions [227]. This may be due to the specific interactions of chemokines with GAGs carrying the sulfation.

A general paradigm of an inflammatory reaction is that the stimulus induces cytokine synthesis, which then triggers expression of chemokines. An interesting study connects the signaling system of cytokines and chemokines with GAG as a mediator. The study illustrates modification in composition of GAG triggered by pro-inflammatory cytokines. These modifications allow GAGs to bind to chemokines, which in turn facilitate leukocyte recruitment. The study used TNFα and IFN-Y as pro-inflammatory cytokines to enhance chemotactic response in human microvascular endothelial cells [199].

To summarize, GAGs participate in cytokine concentration at the target, polymerization, activation, signal transduction and protection from denaturation. They are therefore referred to as sophisticated model of cellular responses to cytokines [228]. Interaction of glycocalyx with cytokines are summarized in Figure 15.

7.1.5 Interaction with growth factors

The most extensively researched growth factor is basic fibroblast growth factor (bFGF) for its specific interactions with HS that richly populates the surface of endothelium. All 23 members of the FGF family have binding domains on HS that vary. bFGF binds to N-sulfate enriched and O-sulfate scarce domains on HS. It is however a prerequisite for the HS length to be deca- or dodecasaccharide with a 6-O sulfate group for biological activity of bFGF [229]. Different tissue types express characteristic HS sequences, which facilitate the binding and activity of specific FGF type [230]. HS regulates bFGF function by participation in its signaling. This requires very specific binding of HS to the bFGF [231]. Therefore modulating HS sulfation pattern could regulate FGF activity and signaling.

VEGF is responsible for angiogenesis and is important during IR. Every isoform of VEGF has an individual binding domain on GAG. Specific sequences in GAG facilitate interaction of the individual isoform with its receptor [232]. Similar to bFGF, VEGF binds to HS, which also regulates its signaling [233]

There are many other morphogens that are involved in vascular development and are altered during IR. However, these morphogens are less studied in the context of their interaction with GAGs. During vascular development a defective N-sulfation of heparan sulfate proteoglycans limits PDGF-BB binding and pericyte recruitment [234]. Interactions of glycocalyx with growth factors are summarized in Figure 15.

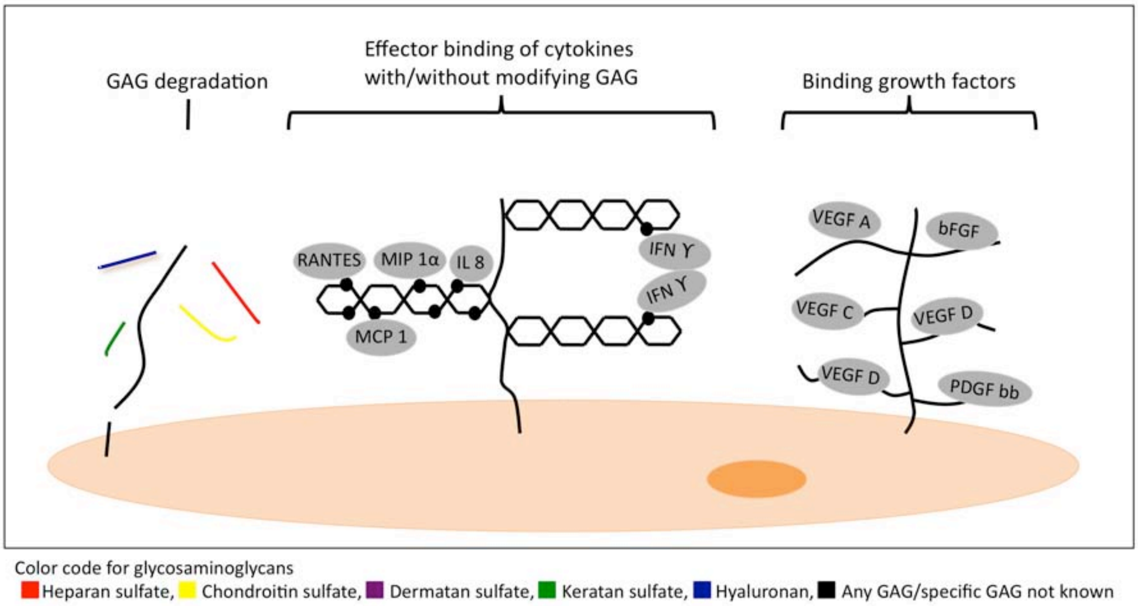
GAG degradation
Effector binding of cytokines with/without modifying GAG
Binding growth factors
RANTES
MIP 1α
IL 8
MCP 1
IFN γ
IFN γ
VEGF A
bFGF
VEGF C
VEGF D
VEGF D
PDGF bb
Color code for glycosaminoglycans
🟥Heparan sulfate, 🟨 Chondroitin sulfate, 🟪 Dermatan sulfate, 🟩 Keratan sulfate, 🟦 Hyaluronan, ⬛ Any GAG/specific GAG not known

Figure 15: Glycosaminoglycans with cytokines and growth factors. From left to right. Cytokines induce GAG degradation. Cytokines bind to specific patterns on GAG. GAG helps in dimerization of interferon gamma. Growth factors bind to specific domains on GAG (own illustration).

7.1.6 Interaction with coagulation cascade

The ability of sulfated polysaccharides to interact with coagulation was recognized by the anticoagulant nature of heparin. The sulfated polysaccharides in heparin form binding sites for many serine protease and their inhibitors thereby contributing as an effective anticoagulant. The participation of heparin as a catalyst is important in the case of antithrombin as mutation of AT in its heparin binding site results in thrombosis [235]. The binding of AT to heparin/HS is highly specific to a pentasaccharide sequence containing a unique 3-O sulfate group (Figure 5 in ref #233) [236-238]. Factor Xa mediated activation of protein C is directly proportional to the degree of sulfation on the heparin chain [239]. Full-length heparin increases binding to 3 fold and also adds to the antithrombin activity by accommodating the proteinase FXa and FIXa in the same chain forming a ternary complex [240]. The mechanism of interaction between AT and HS/heparin has been reviewed [241].

The endothelial layer also elicits anticoagulant property [242] partly by HS mediated activation of antithrombin [243, 244]. Another anticoagulant on EC surface is thrombomodulin that elicits its function via sulfated polysaccharide chains similar to CS [245, 246]. It is also known to bind to fibrinogen and accelerate thrombin inhibition by antithrombin [247]. Antithrombin regulates neutrophil migration via interaction with cell surface syndecan-4 [248].

Tissue factor pathway inhibitor is one of the major physiological anticoagulants and binds to heparin via its N terminal part [249]. Injection of heparin increases TFPI quantity in plasma due to its high affinity to heparin [250] and the heparin released TFPI is a stronger inhibitor than any other form of TFPI [251, 252]. TFPI binds to other GAG molecules with different affinities - heparin > DS > HS > CS-C without any affinities for CS-A and HA [253]. CSPG induced coagulation by inhibiting TFPI and activating FVII was confirmed in a mouse model of blood coagulation [254]. Another GAG able to interact with coagulation is DS, which inactivates thrombin [255] by binding to heparin cofactor II at sites that lack N-sulfation [256]. The role of GAGs in coagulation has been extensively reviewed in [249]. Interaction of glycocalyx with coagulation cascade is summarized in Figure 16.

7.2 Conclusion

The endothelial glycocalyx is a dynamic layer covering the lumen of vessels and is continuously modulated to maintain homeostasis. Ischemia changes the glycocalyx directly and indirectly by changing the milieu and tipping the different systems of ROS, complement, etc off the balance. The modified glycocalyx now bears a different structural composition defined by GAG length, degree and position of sulfation. These changes help to preferentially bind biomolecules and regulate the systems in return. Such regulation may cause more modifications and this cycle continues throughout reperfusion and remodeling, probably until homeostasis is achieved. Like this the glycocalyx is continuously responding to and regulating the pathology during IR (Figure17)

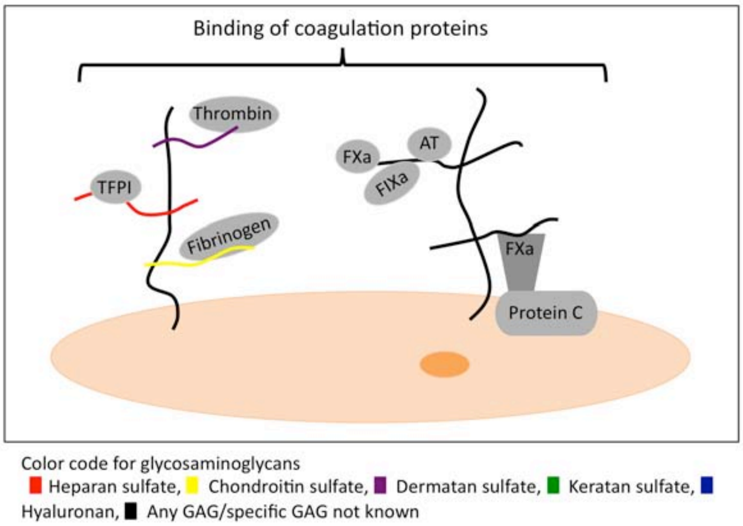
Binding of coagulation proteins
Thrombin
TFPI
Fibrinogen
FXa
AT
FIXa
FXa
Protein C
Color code for glycosaminoglycans
🟥 Heparan sulfate, 🟨 Chondroitin sulfate, 🟪 Dermatan sulfate, 🟩 Keratan sulfate, 🟦 Hyaluronan, ⬛ Any GAG/specific GAG not known

Figure 16: Glycosaminoglycans with coagulation. GAGs regulate the coagulation cascade by binding to proteins that propagate and inhibit the cascade (own illustration).

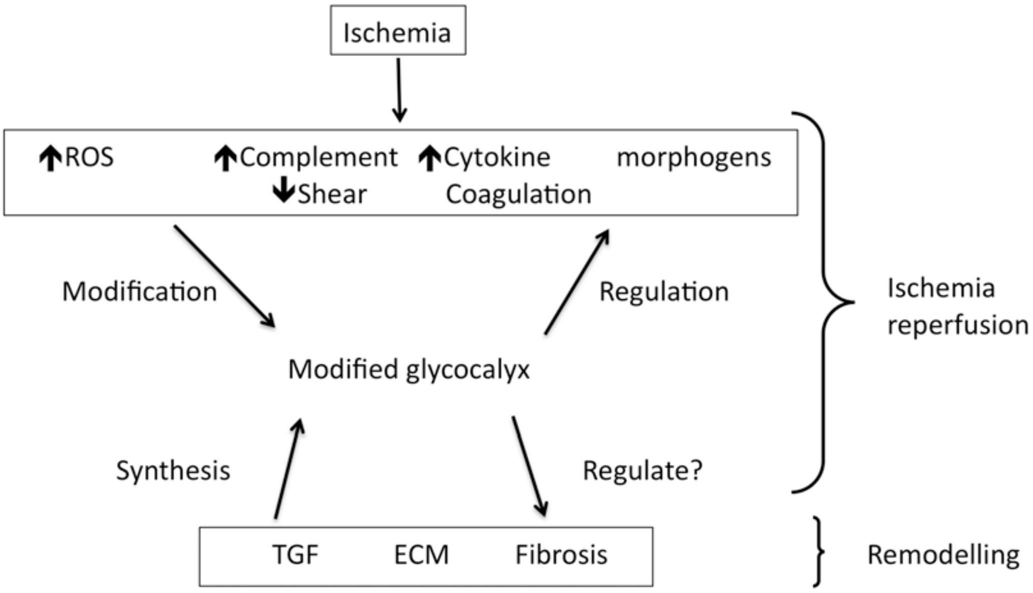
Ischemia
↑ROS
↑Complement
↑Cytokine
morphogens
↓Shear
Coagulation
Modification
Regulation
Modified glycocalyx
Synthesis
Regulate?
TGF
ECM
Fibrosis
Ischemia reperfusion
Remodelling

Figure 17: Modulator/regulator effect of endothelial glycocalyx during ischemia reperfusion. Ischemia induced activation of different pathways modifies the glycocalyx. Modified glycocalyx in turn regulates the specific components of the pathways. While this occurs during ischemia and reperfusion, at the stage of remodeling synthesis of glycocalyx occurs. The newly synthesized glycocalyx possibly may regulate tissue remodeling to restore homeostasis (own illustration).

A few general conclusions may be drawn from the interaction between these systems as seen in different experimental settings.

1. Both proteoglycans and GAGs are important. GAG mediates binding to proteins and PG serves in signal transduction.
2. HS expression on cell surface could be more protective than CS – as seen by NO production, SOD and XO binding.
3. Sulfation is better than non-sulfation – as it determines depolymerization by ROS and complement inhibition.
4. O-sulfation is better than N-sulfation – as seen by complement inhibition and chemokine binding.

In IR GAGs carrying the above characteristics have shown to attenuate injury during MI. Heparin and dextran sulfate are highly sulfated GAGs that have shown reduction in injury [257, 258].

Molecules belonging to the three major pathways ROS, inflammation and coagulation, cause IR injury. This section highlights the potential of glycocalyx to interact specifically and govern the function of these molecules. There is therefore a possibility for such interactions to also occur during IR injury, which could be important to better understand and modulate the pathology.

7.3 Project to study shed glycosaminoglycans during myocardial infarction

Considering the increasingly significant role of glycosaminoglycans during IR we studied the same in a pig model of MI. Blood samples were taken from the pigs at defined time points. The heparan sulfate GAGs were isolated and characterized for their disaccharides sulfated at different degree and positions. Differential shedding of the disaccharides were measured after a reperfusion period as short as 2 minutes (Paper VI).

8 Summary and discussion

This thesis summarizes ischemia reperfusion injury mainly as a cause of pathology during MI. It deals in detail with the major pathways engaged in the process. A booklet attached to the back of this thesis, illustrates these pathways and also indicates the interactions known between them. It has been out of the scope for this thesis to indicate other key processes that also contribute to the pathology. This would be the reactive nitrogen species that contributes to oxidation of biomolecules and adhesion molecules that mediate immune cell trafficking. The effects of IR are clearly seen on the cardiac function and have not been dealt with in this introduction. However, this was studied in one of the projects via a pressure-volume catheter placed in the left ventricle (Paper II). Finally, the different pathways mentioned terminate into necrosis of the cells. However, cell death may also occur due to apoptosis as reviewed by [259].

As an overview of the involvement of major pathways in IR the importance of ROS is controversial as until now, their contribution has been shown only in vitro or in isolated heart models. Such models lack the presence of whole blood, which carries other factors that may contribute to pathology in conjunction with ROS. For complement, its role in IR pathology is clear from in vivo models that show attenuation of MI by using complement inhibitory substances like Mirococept (APT070) and dextran sulfate. However, this does not bring us close to solving the problem as these substances have their own drawbacks, which in the case of DXS is its high anti-coagulant property. This work has not dealt with the role of coagulation pathways to the same extent as the other pathways. It is therefore not appropriate to speculate much about it in the discussion. Finally the endothelial glycocalyx is increasingly being appreciated for its significant role in IR pathology directly and indirectly by influencing other pathways.

9 References

1 Gourdin MJ, Bree B, De Kock M: The impact of ischaemia-reperfusion on the blood vessel. Eur J Anaesthesiol 2009;26:537-547.

2 Jennings RB, Murry CE, Steenbergen C, Jr., Reimer KA: Development of cell injury in sustained acute ischemia. Circulation 1990;82:II2-12.

3 Kloner RA, Jennings RB: Consequences of brief ischemia: Stunning, preconditioning, and their clinical implications: Part 2. Circulation 2001;104:3158-3167.

4 Jennings RB, Reimer KA: The cell biology of acute myocardial ischemia. Annu Rev Med 1991;42:225-246.

5 Opie LH, Sack MN: Metabolic plasticity and the promotion of cardiac protection in ischemia and ischemic preconditioning. J Mol Cell Cardiol 2002;34:1077-1089.

6 Ambrosio G, Zweier JL, Flaherty JT: The relationship between oxygen radical generation and impairment of myocardial energy metabolism following post-ischemic reperfusion. J Mol Cell Cardiol 1991;23:1359-1374.

7 Piper HM, Abdallah Y, Schafer C: The first minutes of reperfusion: A window of opportunity for cardioprotection. Cardiovasc Res 2004;61:365-371.

8 Varadarajan SG, An J, Novalija E, Smart SC, Stowe DF: Changes in [na(+)](i), compartmental [ca(2+)], and nadh with dysfunction after global ischemia in intact hearts. Am J Physiol Heart Circ Physiol 2001;280:H280-293.

9 Murphy E, Steenbergen C: Ion transport and energetics during cell death and protection. Physiology (Bethesda) 2008;23:115-123.

10 Inserte J, Garcia-Dorado D, Ruiz-Meana M, Padilla F, Barrabes JA, Pina P, Agullo L, Piper HM, Soler-Soler J: Effect of inhibition of na(+)/ca(2+) exchanger at the time of myocardial reperfusion on hypercontracture and cell death. Cardiovasc Res 2002;55:739-748.

11 Schlack W, Uebing A, Schafer M, Bier F, Schafer S, Piper HM, Thamer V: Regional contractile blockade at the onset of reperfusion reduces infarct size in the dog heart. Pflugers Arch 1994;428:134-141.

12 Sebbag L, Verbinski SG, Reimer KA, Jennings RB: Protection of ischemic myocardium in dogs using intracoronary 2,3-butanedione monoxime (bdm). J Mol Cell Cardiol 2003;35:165-176.

13 Jennings RB, Reimer KA, Steenbergen C: Myocardial ischemia revisited. The osmolar load, membrane damage, and reperfusion. J Mol Cell Cardiol 1986;18:769-780.

14 Lesnefsky EJ, Moghaddas S, Tandler B, Kerner J, Hoppel CL: Mitochondrial dysfunction in cardiac disease: Ischemia--reperfusion, aging, and heart failure. J Mol Cell Cardiol 2001;33:1065-1089.

15 Vanden Hoek TL, Shao Z, Li C, Zak R, Schumacker PT, Becker LB: Reperfusion injury on cardiac myocytes after simulated ischemia. Am J Physiol 1996;270:H1334-1341.

16 Vetterlein F, Schrader C, Volkmann R, Neckel M, Ochs M, Schmidt G, Hellige G: Extent of damage in ischemic, nonreperfused, and reperfused myocardium of anesthetized rats. Am J Physiol Heart Circ Physiol 2003;285:H755-765.

17 Droge W: Free radicals in the physiological control of cell function. Physiol Rev 2002;82:47-95.

18 Rubanyi GM, Vanhoutte PM: Superoxide anions and hyperoxia inactivate endothelium-derived relaxing factor. Am J Physiol 1986;250:H822-827.

19 Vanden Hoek TL, Li C, Shao Z, Schumacker PT, Becker LB: Significant levels of oxidants are generated by isolated cardiomyocytes during ischemia prior to reperfusion. J Mol Cell Cardiol 1997;29:2571-2583.

20 Zweier JL, Flaherty JT, Weisfeldt ML: Direct measurement of free radical generation following reperfusion of ischemic myocardium. Proc Natl Acad Sci U S A 1987;84:1404-1407.

21 Becker LB: New concepts in reactive oxygen species and cardiovascular reperfusion physiology. Cardiovasc Res 2004;61:461-470.

22 Tan S, Gelman S, Wheat JK, Parks DA: Circulating xanthine oxidase in human ischemia reperfusion. South Med J 1995;88:479-482.

23 Pandey NR, Kaur G, Chandra M, Sanwal GG, Misra MK: Enzymatic oxidant and antioxidants of human blood platelets in unstable angina and myocardial infarction. Int J Cardiol 2000;76:33-38.

24 Houston M, Estevez A, Chumley P, Aslan M, Marklund S, Parks DA, Freeman BA: Binding of xanthine oxidase to vascular endothelium. Kinetic characterization and oxidative impairment of nitric oxide-dependent signaling. J Biol Chem 1999;274:4985-4994.

25 Di Lisa F, Menabo R, Canton M, Petronilli V: The role of mitochondria in the salvage and the injury of the ischemic myocardium. Biochim Biophys Acta 1998;1366:69-78.

26 McCord JM: Free radicals and myocardial ischemia: Overview and outlook. Free Radic Biol Med 1988;4:9-14.

27 Petrosillo G, Ruggiero FM, Di Venosa N, Paradies G: Decreased complex iii activity in mitochondria isolated from rat heart subjected to ischemia and reperfusion: Role of reactive oxygen species and cardiolipin. FASEB J 2003;17:714-716.

28 Lesnefsky EJ, Tandler B, Ye J, Slabe TJ, Turkaly J, Hoppel CL: Myocardial ischemia decreases oxidative phosphorylation through cytochrome oxidase in subsarcolemmal mitochondria. Am J Physiol 1997;273:H1544-1554.

29 Turrens JF, Boveris A: Generation of superoxide anion by the nadh dehydrogenase of bovine heart mitochondria. Biochem J 1980;191:421-427.

30 Turrens JF: Mitochondrial formation of reactive oxygen species. J Physiol 2003;552:335-344.

31 Chen Q, Moghaddas S, Hoppel CL, Lesnefsky EJ: Ischemic defects in the electron transport chain increase the production of reactive oxygen species from isolated rat heart mitochondria. Am J Physiol Cell Physiol 2008;294:C460-466.

32 Nohl H, Koltover V, Stolze K: Ischemia/reperfusion impairs mitochondrial energy conservation and triggers o2.- release as a byproduct of respiration. Free Radic Res Commun 1993;18:127-137.

33 Becker LB, vanden Hoek TL, Shao ZH, Li CQ, Schumacker PT: Generation of superoxide in cardiomyocytes during ischemia before reperfusion. Am J Physiol 1999;277:H2240-2246.

34 Simonson SG, Zhang J, Canada AT, Jr., Su YF, Benveniste H, Piantadosi CA: Hydrogen peroxide production by monoamine oxidase during ischemia-reperfusion in the rat brain. J Cereb Blood Flow Metab 1993;13:125-134.

35 Mohazzab HK, Kaminski PM, Wolin MS: Lactate and po2 modulate superoxide anion production in bovine cardiac myocytes: Potential role of nadh oxidase. Circulation 1997;96:614-620.

36 Asai K, Hirabayashi T, Houjou T, Uozumi N, Taguchi R, Shimizu T: Human group ivc phospholipase a2 (cpla2gamma). Roles in the membrane remodeling and activation induced by oxidative stress. J Biol Chem 2003;278:8809-8814.

37 Balboa MA, Balsinde J: Oxidative stress and arachidonic acid mobilization. Biochim Biophys Acta 2006;1761:385-391.

38 Kim C, Kim JY, Kim JH: Cytosolic phospholipase a(2), lipoxygenase metabolites, and reactive oxygen species. BMB Rep 2008;41:555-559.

39 Kim C, Dinauer MC: Impaired nadph oxidase activity in rac2-deficient murine neutrophils does not result from defective translocation of p47phox and p67phox and can be rescued by exogenous arachidonic acid. J Leukoc Biol 2006;79:223-234.

40 Maxwell L, Gavin J: Anti-oxidant therapy improves microvascular ultrastructure and perfusion in postischemic myocardium. Microvasc Res 1992;43:255-266.

41 Di Lisa F, Bernardi P: Mitochondria and ischemia-reperfusion injury of the heart: Fixing a hole. Cardiovasc Res 2006;70:191-199.

42 Argaud L, Gateau-Roesch O, Muntean D, Chalabreysse L, Loufouat J, Robert D, Ovize M: Specific inhibition of the mitochondrial permeability transition prevents lethal reperfusion injury. J Mol Cell Cardiol 2005;38:367-374.

43 Nakagawa T, Shimizu S, Watanabe T, Yamaguchi O, Otsu K, Yamagata H, Inohara H, Kubo T, Tsujimoto Y: Cyclophilin d-dependent mitochondrial permeability transition regulates some necrotic but not apoptotic cell death. Nature 2005;434:652-658.

44 Zorov DB, Filburn CR, Klotz LO, Zweier JL, Sollott SJ: Reactive oxygen species (ros)-induced ros release: A new phenomenon accompanying induction of the mitochondrial permeability transition in cardiac myocytes. J Exp Med 2000;192:1001-1014.

45 Proctor P: Electron-transfer factors in psychosis and dyskinesia. Physiol Chem Phys 1972;4:349-360.

46 Finkel T: Signal transduction by reactive oxygen species. J Cell Biol 2001;194:7-15.

47 Das DK, Maulik N: Conversion of death signal into survival signal by redox signaling. Biochemistry (Mosc) 2004;69:10-17.

48 Perrelli MG, Pagliaro P, Penna C: Ischemia/reperfusion injury and cardioprotective mechanisms: Role of mitochondria and reactive oxygen species. World J Cardiol 2011;3:186-200.

49 Flaherty JT, Pitt B, Gruber JW, Heuser RR, Rothbaum DA, Burwell LR, George BS, Kereiakes DJ, Deitchman D, Gustafson N: Recombinant human superoxide dismutase (h-sod) fails to improve recovery of ventricular function in patients undergoing coronary angioplasty for acute myocardial infarction. Circulation 1994;89:1982-1991.

50 Siems W, Sommerburg O, Schild L, Augustin W, Langhans CD, Wiswedel I: Beta-carotene cleavage products induce oxidative stress in vitro by impairing mitochondrial respiration. FASEB J 2002;16:1289-1291.

51 Haramaki N, Assadnazari H, Zimmer G, Schepkin V, Packer L: The influence of vitamin e and dihydrolipoic acid on cardiac energy and glutathione status under hypoxia-reoxygenation. Biochem Mol Biol Int 1995;37:591-597.

52 Cao G, Giovanoni M, Prior RL: Antioxidant capacity in different tissues of young and old rats. Proc Soc Exp Biol Med 1996;211:359-365.

53 Dhalla NS, Elmoselhi AB, Hata T, Makino N: Status of myocardial antioxidants in ischemia-reperfusion injury. Cardiovasc Res 2000;47:446-456.

54 Heyndrickx GR: Myocardial stunning: An experimental act with a large clinical audience. Arch Mal Coeur Vaiss 2003;96:665-670.

55 Tang XL, Takano H, Rizvi A, Turrens JF, Qiu Y, Wu WJ, Zhang Q, Bolli R: Oxidant species trigger late preconditioning against myocardial stunning in conscious rabbits. Am J Physiol Heart Circ Physiol 2002;282:H281-291.

56 Downey J.M. YDM: Do free radicals contribute to myocardial cell death during ischemia-reperfusion? Myocardial protection.; in Yellon D.M. JRB (ed The pathophysiology of reperfusion and reperfusion injury, Raven Press, New York, 1992, pp 35–57.

57 Hill JH, Ward PA: The phlogistic role of c3 leukotactic fragments in myocardial infarcts of rats. J Exp Med 1971;133:885-900.

58 Sarma JV, Ward PA: The complement system. Cell Tissue Res 2011;343:227-235.

59 Ehrnthaller C, Ignatius A, Gebhard F, Huber-Lang M: New insights of an old defense system: Structure, function, and clinical relevance of the complement system. Mol Med 2011;17:317-329.

60 Pinckard RN, Olson MS, Giclas PC, Terry R, Boyer JT, O'Rourke RA: Consumption of classical complement components by heart subcellular membranes in vitro and in patients after acute myocardial infarction. J Clin Invest 1975;56:740-750.

61 Weiser MR, Williams JP, Moore FD, Jr., Kobzik L, Ma M, Hechtman HB, Carroll MC: Reperfusion injury of ischemic skeletal muscle is mediated by natural antibody and complement. J Exp Med 1996;183:2343-2348.

62 Williams JP, Pechet TT, Weiser MR, Reid R, Kobzik L, Moore FD, Jr., Carroll MC, Hechtman HB: Intestinal reperfusion injury is mediated by igm and complement. J Appl Physiol 1999;86:938-942.

63 Fleming SD, Shea-Donohue T, Guthridge JM, Kulik L, Waldschmidt TJ, Gipson MG, Tsokos GC, Holers VM: Mice deficient in complement receptors 1 and 2 lack a tissue injury-inducing subset of the natural antibody repertoire. J Immunol 2002;169:2126-2133.

64 Reid RR, Woodcock S, Shimabukuro-Vornhagen A, Austen WG, Jr., Kobzik L, Zhang M, Hechtman HB, Moore FD, Jr., Carroll MC: Functional activity of natural antibody is altered in cr2-deficient mice. J Immunol 2002;169:5433-5440.

65 Zhang M, Austen WG, Jr., Chiu I, Alicot EM, Hung R, Ma M, Verna N, Xu M, Hechtman HB, Moore FD, Jr., Carroll MC: Identification of a specific self-reactive igm antibody that initiates intestinal ischemia/reperfusion injury. Proc Natl Acad Sci U S A 2004;101:3886-3891.

66 Austen WG, Jr., Zhang M, Chan R, Friend D, Hechtman HB, Carroll MC, Moore FD, Jr.: Murine hindlimb reperfusion injury can be initiated by a self-reactive monoclonal igm. Surgery 2004;136:401-406.

67 Zhang M, Alicot EM, Chiu I, Li J, Verna N, Vorup-Jensen T, Kessler B, Shimaoka M, Chan R, Friend D, Mahmood U, Weissleder R, Moore FD, Carroll MC: Identification of the target self-antigens in reperfusion injury. J Exp Med 2006;203:141-152.

68 Fleming SD, Egan RP, Chai C, Girardi G, Holers VM, Salmon J, Monestier M, Tsokos GC: Anti-phospholipid antibodies restore mesenteric ischemia/reperfusion-induced injury in complement receptor 2/complement receptor 1-deficient mice. J Immunol 2004;173:7055-7061.

69 Fleming SD, Monestier M, Tsokos GC: Accelerated ischemia/reperfusion-induced injury in autoimmunity-prone mice. J Immunol 2004;173:4230-4235.

70 Zhang M, Michael LH, Grosjean SA, Kelly RA, Carroll MC, Entman ML: The role of natural igm in myocardial ischemia-reperfusion injury. J Mol Cell Cardiol 2006;41:62-67.

71 Collard CD, Vakeva A, Morrissey MA, Agah A, Rollins SA, Reenstra WR, Buras JA, Meri S, Stahl GL: Complement activation after oxidative stress: Role of the lectin complement pathway. Am J Pathol 2000;156:1549-1556.

72 de Vries B, Walter SJ, Peutz-Kootstra CJ, Wolfs TG, van Heurn LW, Buurman WA: The mannose-binding lectin-pathway is involved in complement activation in the course of renal ischemia-reperfusion injury. Am J Pathol 2004;165:1677-1688.

73 Jordan JE, Montalto MC, Stahl GL: Inhibition of mannose-binding lectin reduces postischemic myocardial reperfusion injury. Circulation 2001;104:1413-1418.

74 Walsh MC, Bourcier T, Takahashi K, Shi L, Busche MN, Rother RP, Solomon SD, Ezekowitz RA, Stahl GL: Mannose-binding lectin is a regulator of inflammation that accompanies myocardial ischemia and reperfusion injury. J Immunol 2005;175:541-546.

75 Hart ML, Ceonzo KA, Shaffer LA, Takahashi K, Rother RP, Reenstra WR, Buras JA, Stahl GL: Gastrointestinal ischemia-reperfusion injury is lectin complement pathway dependent without involving c1q. J Immunol 2005;174:6373-6380.

76 Moller-Kristensen M, Wang W, Ruseva M, Thiel S, Nielsen S, Takahashi K, Shi L, Ezekowitz A, Jensenius JC, Gadjeva M: Mannan-binding lectin recognizes structures on ischaemic reperfused mouse kidneys and is implicated in tissue injury. Scand J Immunol 2005;61:426-434.

77 Zhang M, Takahashi K, Alicot EM, Vorup-Jensen T, Kessler B, Thiel S, Jensenius JC, Ezekowitz RA, Moore FD, Carroll MC: Activation of the lectin pathway by natural igm in a model of ischemia/reperfusion injury. J Immunol 2006;177:4727-4734.

78 Nevens JR, Mallia AK, Wendt MW, Smith PK: Affinity chromatographic purification of immunoglobulin m antibodies utilizing immobilized mannan binding protein. J Chromatogr 1992;597:247-256.

79 Arnold JN, Wormald MR, Suter DM, Radcliffe CM, Harvey DJ, Dwek RA, Rudd PM, Sim RB: Human serum igm glycosylation: Identification of glycoforms that can bind to mannan-binding lectin. J Biol Chem 2005;280:29080-29087.

80 Busche MN, Pavlov V, Takahashi K, Stahl GL: Myocardial ischemia and reperfusion injury is dependent on both igm and mannose-binding lectin. Am J Physiol Heart Circ Physiol 2009;297:H1853-1859.

81 Lee H, Green DJ, Lai L, Hou YJ, Jensenius JC, Liu D, Cheong C, Park CG, Zhang M: Early complement factors in the local tissue immunocomplex generated during intestinal ischemia/reperfusion injury. Mol Immunol 2009;47:972-981.

82 Murohara T, Guo JP, Delyani JA, Lefer AM: Cardioprotective effects of selective inhibition of the two complement activation pathways in myocardial ischemia and reperfusion injury. Methods Find Exp Clin Pharmacol 1995;17:499-507.

83 Stahl GL, Xu Y, Hao L, Miller M, Buras JA, Fung M, Zhao H: Role for the alternative complement pathway in ischemia/reperfusion injury. Am J Pathol 2003;162:449-455.

84 Pietila KO, Harmoinen AP, Jokiniitty J, Pasternack AI: Serum c-reactive protein concentration in acute myocardial infarction and its relationship to mortality during 24 months of follow-up in patients under thrombolytic treatment. Eur Heart J 1996;17:1345-1349.

85 Windgassen EB, Funtowicz L, Lunsford TN, Harris LA, Mulvagh SL: C-reactive protein and high-sensitivity c-reactive protein: An update for clinicians. Postgrad Med 2011;123:114-119.

86 Oh J, Teoh H, Leiter LA: Should c-reactive protein be a target of therapy? Diabetes Care 2011;34 Suppl 2:S155-160.

87 van der Vusse GJ, van Bilsen M, Reneman RS: Ischemia and reperfusion induced alterations in membrane phospholipids: An overview. Ann N Y Acad Sci 1994;723:1-14.

88 Volanakis JE, Narkates AJ: Interaction of c-reactive protein with artificial phosphatidylcholine bilayers and complement. J Immunol 1981;126:1820-1825.

89 Volanakis JE: Complement activation by c-reactive protein complexes. Ann N Y Acad Sci 1982;389:235-250.

90 Wolbink GJ, Brouwer MC, Buysmann S, ten Berge IJ, Hack CE: Crp-mediated activation of complement in vivo: Assessment by measuring circulating complement-c-reactive protein complexes. J Immunol 1996;157:473-479.

91 Beranek JT: C-reactive protein and complement in myocardial infarction and postinfarction heart failure. Eur Heart J 1997;18:1834-1836.

92 Nijmeijer R, Lagrand WK, Lubbers YT, Visser CA, Meijer CJ, Niessen HW, Hack CE: C-reactive protein activates complement in infarcted human myocardium. Am J Pathol 2003;163:269-275.

93 Lagrand WK, Niessen HW, Wolbink GJ, Jaspars LH, Visser CA, Verheugt FW, Meijer CJ, Hack CE: C-reactive protein colocalizes with complement in human hearts during acute myocardial infarction. Circulation 1997;95:97-103.

94 Mortensen RF, Zhong W: Regulation of phagocytic leukocyte activities by c-reactive protein. J Leukoc Biol 2000;67:495-500.

95 Pasceri V, Willerson JT, Yeh ET: Direct proinflammatory effect of c-reactive protein on human endothelial cells. Circulation 2000;102:2165-2168.

96 Frangogiannis NG, Smith CW, Entman ML: The inflammatory response in myocardial infarction. Cardiovasc Res 2002;53:31-47.

97 Nauta AJ, Trouw LA, Daha MR, Tijsma O, Nieuwland R, Schwaeble WJ, Gingras AR, Mantovani A, Hack EC, Roos A: Direct binding of c1q to apoptotic cells and cell blebs induces complement activation. Eur J Immunol 2002;32:1726-1736.

98 Rossen RD, Michael LH, Hawkins HK, Youker K, Dreyer WJ, Baughn RE, Entman ML: Cardiolipin-protein complexes and initiation of complement activation after coronary artery occlusion. Circ Res 1994;75:546-555.

99 Shi T, Moulton VR, Lapchak PH, Deng GM, Dalle Lucca JJ, Tsokos GC: Ischemia-mediated aggregation of the actin cytoskeleton is one of the major initial events resulting in ischemia-reperfusion injury. Am J Physiol Gastrointest Liver Physiol 2009;296:G339-347.

100 Chakraborti T, Mandal A, Mandal M, Das S, Chakraborti S: Complement activation in heart diseases. Role of oxidants. Cell Signal 2000;12:607-617.

101 Saadi S, Platt JL: Transient perturbation of endothelial integrity induced by natural antibodies and complement. J Exp Med 1995;181:21-31.

102 Campbell AK, Morgan BP: Monoclonal antibodies demonstrate protection of polymorphonuclear leukocytes against complement attack. Nature 1985;317:164-166.

103 Seeger W, Suttorp N, Hellwig A, Bhakdi S: Noncytolytic terminal complement complexes may serve as calcium gates to elicit leukotriene b4 generation in human polymorphonuclear leukocytes. J Immunol 1986;137:1286-1293.

104 Wiedmer T, Esmon CT, Sims PJ: On the mechanism by which complement proteins c5b-9 increase platelet prothrombinase activity. J Biol Chem 1986;261:14587-14592.

105 Couturier C, Haeffner-Cavaillon N, Weiss L, Fischer E, Kazatchkine MD: Induction of cell-associated interleukin 1 through stimulation of the adhesion-promoting proteins lfa-1 (cd11a/cd18) and cr3 (cd11b/cd18) of human monocytes. Eur J Immunol 1990;20:999-1005.

106 Busche MN, Stahl GL: Role of the complement components c5 and c3a in a mouse model of myocardial ischemia and reperfusion injury. Ger Med Sci 2010;8

107 van der Pals J, Koul S, Andersson P, Gotberg M, Ubachs JF, Kanski M, Arheden H, Olivecrona GK, Larsson B, Erlinge D: Treatment with the c5a receptor antagonist adc-1004 reduces myocardial infarction in a porcine ischemia-reperfusion model. BMC Cardiovasc Disord 2010;10:45.

108 Eror AT, Stojadinovic A, Starnes BW, Makrides SC, Tsokos GC, Shea-Donohue T: Antiinflammatory effects of soluble complement receptor type 1 promote rapid recovery of ischemia/reperfusion injury in rat small intestine. Clin Immunol 1999;90:266-275.

109 Rehrig S, Fleming SD, Anderson J, Guthridge JM, Rakstang J, McQueen CE, Holers VM, Tsokos GC, Shea-Donohue T: Complement inhibitor, complement receptor 1-related gene/protein y-ig attenuates intestinal damage after the onset of mesenteric ischemia/reperfusion injury in mice. J Immunol 2001;167:5921-5927.

110 Gilles S, Zahler S, Welsch U, Sommerhoff CP, Becker BF: Release of tnf-alpha during myocardial reperfusion depends on oxidative stress and is prevented by mast cell stabilizers. Cardiovasc Res 2003;60:608-616.

111 Onai Y, Suzuki J, Kakuta T, Maejima Y, Haraguchi G, Fukasawa H, Muto S, Itai A, Isobe M: Inhibition of ikappab phosphorylation in cardiomyocytes attenuates myocardial ischemia/reperfusion injury. Cardiovasc Res 2004;63:51-59.

112 Gerszten RE, Garcia-Zepeda EA, Lim YC, Yoshida M, Ding HA, Gimbrone MA, Jr., Luster AD, Luscinskas FW, Rosenzweig A: Mcp-1 and il-8 trigger firm adhesion of monocytes to vascular endothelium under flow conditions. Nature 1999;398:718-723.

113 Strieter RM, Polverini PJ, Arenberg DA, Walz A, Opdenakker G, Van Damme J, Kunkel SL: Role of c-x-c chemokines as regulators of angiogenesis in lung cancer. J Leukoc Biol 1995;57:752-762.

114 Kumar AG, Ballantyne CM, Michael LH, Kukielka GL, Youker KA, Lindsey ML, Hawkins HK, Birdsall HH, MacKay CR, LaRosa GJ, Rossen RD, Smith CW, Entman ML: Induction of

monocyte chemoattractant protein-1 in the small veins of the ischemic and reperfused canine myocardium. Circulation 1997;95:693-700.

115 Kukielka GL, Smith CW, LaRosa GJ, Manning AM, Mendoza LH, Daly TJ, Hughes BJ, Youker KA, Hawkins HK, Michael LH: Interleukin-8 gene induction in the myocardium after ischemia and reperfusion in vivo. J Clin Invest 1995;95:89-103.

116 Frangogiannis NG: Chemokines in the ischemic myocardium: From inflammation to fibrosis. Inflamm Res 2004;53:585-595.

117 Wei S, Blanchard DK, Liu JH, Leonard WJ, Djeu JY: Activation of tumor necrosis factor-alpha production from human neutrophils by il-2 via il-2-r beta. J Immunol 1993;150:1979-1987.

118 Maekawa N, Wada H, Kanda T, Niwa T, Yamada Y, Saito K, Fujiwara H, Sekikawa K, Seishima M: Improved myocardial ischemia/reperfusion injury in mice lacking tumor necrosis factor-alpha. J Am Coll Cardiol 2002;39:1229-1235.

119 Marucha PT, Zeff RA, Kreutzer DL: Cytokine-induced il-1 beta gene expression in the human polymorphonuclear leukocyte: Transcriptional and post-transcriptional regulation by tumor necrosis factor and il-1. J Immunol 1991;147:2603-2608.

120 Bochner BS, Peachell PT, Brown KE, Schleimer RP: Adherence of human basophils to cultured umbilical vein endothelial cells. J Clin Invest 1988;81:1355-1364.

121 Hayward R, Nossuli TO, Scalia R, Lefer AM: Cardioprotective effect of interleukin-10 in murine myocardial ischemia-reperfusion. Eur J Pharmacol 1997;334:157-163.

122 Cicco NA, Lindemann A, Content J, Vandenbussche P, Lubbert M, Gauss J, Mertelsmann R, Herrmann F: Inducible production of interleukin-6 by human polymorphonuclear neutrophils: Role of granulocyte-macrophage colony-stimulating factor and tumor necrosis factor-alpha. Blood 1990;75:2049-2052.

123 Kukielka GL, Smith CW, Manning AM, Youker KA, Michael LH, Entman ML: Induction of interleukin-6 synthesis in the myocardium. Potential role in postreperfusion inflammatory injury. Circulation 1995;92:1866-1875.

124 Yang Z, Zingarelli B, Szabo C: Crucial role of endogenous interleukin-10 production in myocardial ischemia/reperfusion injury. Circulation 2000;101:1019-1026.

125 Fiorentino DF, Zlotnik A, Mosmann TR, Howard M, O'Garra A: Il-10 inhibits cytokine production by activated macrophages. J Immunol 1991;147:3815-3822.

126 Shibata M, Endo S, Inada K, Kuriki S, Harada M, Takino T, Sato N, Arakawa N, Suzuki T, Aoki H, Hiramori K: Elevated plasma levels of interleukin-1 receptor antagonist and interleukin-10 in patients with acute myocardial infarction. J Interferon Cytokine Res 1997;17:145-150.

127 Thompson NL, Bazoberry F, Speir EH, Casscells W, Ferrans VJ, Flanders KC, Kondaiah P, Geiser AG, Sporn MB: Transforming growth factor beta-1 in acute myocardial infarction in rats. Growth Factors 1988;1:91-99.

128 Eghbali M: Cellular origin and distribution of transforming growth factor-beta in the normal rat myocardium. Cell Tissue Res 1989;256:553-558.

129 Chen H, Li D, Saldeen T, Mehta JL: Tgf-beta 1 attenuates myocardial ischemia-reperfusion injury via inhibition of upregulation of mmp-1. Am J Physiol Heart Circ Physiol 2003;284:H1612-1617.

130 Frangogiannis NG: Chemokines in ischemia and reperfusion. Thromb Haemost 2007;97:738-747.

131 Kilgore KS, Park JL, Tanhehco EJ, Booth EA, Marks RM, Lucchesi BR: Attenuation of interleukin-8 expression in c6-deficient rabbits after myocardial ischemia/reperfusion. J Mol Cell Cardiol 1998;30:75-85.

132 de Vries B, Kohl J, Leclercq WK, Wolfs TG, van Bijnen AA, Heeringa P, Buurman WA: Complement factor c5a mediates renal ischemia-reperfusion injury independent from neutrophils. J Immunol 2003;170:3883-3889.

133 Boyd JH, Mathur S, Wang Y, Bateman RM, Walley KR: Toll-like receptor stimulation in cardiomyoctes decreases contractility and initiates an nf-kappab dependent inflammatory response. Cardiovasc Res 2006;72:384-393.

134 McKee CM, Penno MB, Cowman M, Burdick MD, Strieter RM, Bao C, Noble PW: Hyaluronan (ha) fragments induce chemokine gene expression in alveolar macrophages. The role of ha size and cd44. J Clin Invest 1996;98:2403-2413.

135 Taylor KR, Trowbridge JM, Rudisill JA, Termeer CC, Simon JC, Gallo RL: Hyaluronan fragments stimulate endothelial recognition of injury through tlr4. J Biol Chem 2004;279:17079-17084.

136 Oyama J, Blais C, Jr., Liu X, Pu M, Kobzik L, Kelly RA, Bourcier T: Reduced myocardial ischemia-reperfusion injury in toll-like receptor 4-deficient mice. Circulation 2004;109:784-789.

137 Arslan F, Smeets MB, O'Neill LA, Keogh B, McGuirk P, Timmers L, Tersteeg C, Hoefer IE, Doevendans PA, Pasterkamp G, de Kleijn DP: Myocardial ischemia/reperfusion injury is mediated by leukocytic toll-like receptor-2 and reduced by systemic administration of a novel anti-toll-like receptor-2 antibody. Circulation 2010;121:80-90.

138 Tsujioka H, Imanishi T, Ikejima H, Kuroi A, Takarada S, Tanimoto T, Kitabata H, Okochi K, Arita Y, Ishibashi K, Komukai K, Kataiwa H, Nakamura N, Hirata K, Tanaka A, Akasaka T: Impact of heterogeneity of human peripheral blood monocyte subsets on myocardial salvage in patients with primary acute myocardial infarction. J Am Coll Cardiol 2009;54:130-138.

139 Kubes P, Granger DN: Leukocyte-endothelial cell interactions evoked by mast cells. Cardiovasc Res 1996;32:699-708.

140 Yang Z, Day YJ, Toufektsian MC, Xu Y, Ramos SI, Marshall MA, French BA, Linden J: Myocardial infarct-sparing effect of adenosine a2a receptor activation is due to its action on cd4+ t lymphocytes. Circulation 2006;114:2056-2064.

141 Renner B, Strassheim D, Amura CR, Kulik L, Ljubanovic D, Glogowska MJ, Takahashi K, Carroll MC, Holers VM, Thurman JM: B cell subsets contribute to renal injury and renal protection after ischemia/reperfusion. J Immunol 2010;185:4393-4400.

142 Wim K. Lagrand RN, Paul A.J. Krijnen, Hans W.M. Niessen, Cees A. Visser, C. Erik Hack: Anti-inflammatory interventions: A promising pathophysiological approach in the treatment of acute myocardial infarction? Heart and Metabolism 2001:6 - 15.

143 Banz Y, Rieben R: Role of complement and perspectives for intervention in ischemia-reperfusion damage. Ann Med 2011

144 Sharma HS, Das DK: Role of cytokines in myocardial ischemia and reperfusion. Mediators Inflamm 1997;6:175-183.

145 Lecour S, James RW: When are pro-inflammatory cytokines safe in heart failure? Eur Heart J 2011;32:680-685.

146 Levi M, Keller TT, van Gorp E, ten Cate H: Infection and inflammation and the coagulation system. Cardiovasc Res 2003;60:26-39.

147 Schmaier AH, Rojkjaer R, Shariat-Madar Z: Activation of the plasma kallikrein/kinin system on cells: A revised hypothesis. Thromb Haemost 1999;82:226-233.

148 Morrissey JH, Fakhrai H, Edgington TS: Molecular cloning of the cdna for tissue factor, the cellular receptor for the initiation of the coagulation protease cascade. Cell 1987;50:129-135.

149 Nemerson Y: Tissue factor and hemostasis. Blood 1988;71:1-8.

150 Kleinschnitz C, Stoll G, Bendszus M, Schuh K, Pauer HU, Burfeind P, Renne C, Gailani D, Nieswandt B, Renne T: Targeting coagulation factor xii provides protection from pathological thrombosis in cerebral ischemia without interfering with hemostasis. J Exp Med 2006;203:513-518.

151 Dietrich W: Reducing thrombin formation during cardiopulmonary bypass: Is there a benefit of the additional anticoagulant action of aprotinin? J Cardiovasc Pharmacol 1996;27 Suppl 1:S50-57.

152 Golino P, Ragni M, Cirillo P, Scognamiglio A, Ravera A, Buono C, Guarino A, Piro O, Lambiase C, Botticella F, Ezban M, Condorelli M, Chiariello M: Recombinant human, active site-blocked factor viia reduces infarct size and no-reflow phenomenon in rabbits. Am J Physiol Heart Circ Physiol 2000;278:H1507-1516.

153 Boyle EM, Jr., Verrier ED, Spiess BD: Endothelial cell injury in cardiovascular surgery: The procoagulant response. Ann Thorac Surg 1996;62:1549-1557.

154 Osterud B: Tissue factor expression by monocytes: Regulation and pathophysiological roles. Blood Coagul Fibrinolysis 1998;9 Suppl 1:S9-14.

155 Erlich JH, Boyle EM, Labriola J, Kovacich JC, Santucci RA, Fearns C, Morgan EN, Yun W, Luther T, Kojikawa O, Martin TR, Pohlman TH, Verrier ED, Mackman N: Inhibition of the tissue

factor-thrombin pathway limits infarct size after myocardial ischemia-reperfusion injury by reducing inflammation. Am J Pathol 2000;157:1849-1862.

156 Wang HJ, Huang H, Chuang YC, Huang HC: Paclitaxel induces up-regulation of tissue factor in human aortic endothelial cells. Int Immunopharmacol 2009;9:144-147.

157 Gertz SD, Fallon JT, Gallo R, Taubman MB, Banai S, Barry WL, Gimple LW, Nemerson Y, Thiruvikraman S, Naidu SS, Chesebro JH, Fuster V, Sarembock IJ, Badimon JJ: Hirudin reduces tissue factor expression in neointima after balloon injury in rabbit femoral and porcine coronary arteries. Circulation 1998;98:580-587.

158 Coughlin SR: Thrombin signalling and protease-activated receptors. Nature 2000;407:258-264.

159 Kaplanski G, Fabrigoule M, Boulay V, Dinarello CA, Bongrand P, Kaplanski S, Farnarier C: Thrombin induces endothelial type ii activation in vitro: Il-1 and tnf-alpha-independent il-8 secretion and e-selectin expression. J Immunol 1997;158:5435-5441.

160 Sugama Y, Tiruppathi C, offakidevi K, Andersen TT, Fenton JW, 2nd, Malik AB: Thrombin-induced expression of endothelial p-selectin and intercellular adhesion molecule-1: A mechanism for stabilizing neutrophil adhesion. J Cell Biol 1992;119:935-944.

161 Kranzhofer R, Clinton SK, Ishii K, Coughlin SR, Fenton JW, 2nd, Libby P: Thrombin potently stimulates cytokine production in human vascular smooth muscle cells but not in mononuclear phagocytes. Circ Res 1996;79:286-294.

162 Kupatt C, Habazettl H, Hanusch P, Wichels R, Hahnel D, Becker BF, Boekstegers P: C7e3fab reduces postischemic leukocyte-thrombocyte interaction mediated by fibrinogen. Implications for myocardial reperfusion injury. Arterioscler Thromb Vasc Biol 2000;20:2226-2232.

163 Mackman N: The role of the tissue factor-thrombin pathway in cardiac ischemia-reperfusion injury. Semin Vasc Med 2003;3:193-198.

164 Sevastos J, Kennedy SE, Davis DR, Sam M, Peake PW, Charlesworth JA, Mackman N, Erlich JH: Tissue factor deficiency and par-1 deficiency are protective against renal ischemia reperfusion injury. Blood 2007;109:577-583.

165 Chong AJ, Pohlman TH, Hampton CR, Shimamoto A, Mackman N, Verrier ED: Tissue factor and thrombin mediate myocardial ischemia-reperfusion injury. Ann Thorac Surg 2003;75:S649-655.

166 Schulz R, Kelm M, Heusch G: Nitric oxide in myocardial ischemia/reperfusion injury. Cardiovasc Res 2004;61:402-413.

167 Zweier JL, Samouilov A, Kuppusamy P: Non-enzymatic nitric oxide synthesis in biological systems. Biochim Biophys Acta 1999;1411:250-262.

168 Godber BL, Doel JJ, Sapkota GP, Blake DR, Stevens CR, Eisenthal R, Harrison R: Reduction of nitrite to nitric oxide catalyzed by xanthine oxidoreductase. J Biol Chem 2000;275:7757-7763.

169 Stuehr DJ: Mammalian nitric oxide synthases. Biochim Biophys Acta 1999;1411:217-230.

170 Mollnau H, Wendt M, Szocs K, Lassegue B, Schulz E, Oelze M, Li H, Bodenschatz M, August M, Kleschyov AL, Tsilimingas N, Walter U, Forstermann U, Meinertz T, Griendling K, Munzel T: Effects of angiotensin ii infusion on the expression and function of nad(p)h oxidase and components of nitric oxide/cgmp signaling. Circ Res 2002;90:E58-65.

171 Sanders DB, Larson DF, Hunter K, Gorman M, Yang B: Comparison of tumor necrosis factor-alpha effect on the expression of inos in macrophage and cardiac myocytes. Perfusion 2001;16:67-74.

172 Phillips L, Toledo AH, Lopez-Neblina F, Anaya-Prado R, Toledo-Pereyra LH: Nitric oxide mechanism of protection in ischemia and reperfusion injury. J Invest Surg 2009;22:46-55.

173 MacCarthy PA, Grocott-Mason R, Prendergast BD, Shah AM: Contrasting inotropic effects of endogenous endothelin in the normal and failing human heart: Studies with an intracoronary et(a) receptor antagonist. Circulation 2000;101:142-147.

174 Watanabe T, Suzuki N, Shimamoto N, Fujino M, Imada A: Contribution of endogenous endothelin to the extension of myocardial infarct size in rats. Circ Res 1991;69:370-377.

175 Omland T, Lie RT, Aakvaag A, Aarsland T, Dickstein K: Plasma endothelin determination as a prognostic indicator of 1-year mortality after acute myocardial infarction. Circulation 1994;89:1573-1579.

176 Niccoli G, Lanza GA, Shaw S, Romagnoli E, Gioia D, Burzotta F, Trani C, Mazzari MA, Mongiardo R, De Vita M, Rebuzzi AG, Luscher TF, Crea F: Endothelin-1 and acute myocardial infarction: A no-reflow mediator after successful percutaneous myocardial revascularization. Eur Heart J 2006;27:1793-1798.

177 Lipowsky HH: Microvascular rheology and hemodynamics. Microcirculation 2005;12:5-15.

178 Mulivor AW, Lipowsky HH: Inflammation- and ischemia-induced shedding of venular glycocalyx. Am J Physiol Heart Circ Physiol 2004;286:H1672-1680.

179 Reitsma S, Slaaf DW, Vink H, van Zandvoort MA, oude Egbrink MG: The endothelial glycocalyx: Composition, functions, and visualization. Pflugers Arch 2007;454:345-359.

180 Rapraeger A: Transforming growth factor (type beta) promotes the addition of chondroitin sulfate chains to the cell surface proteoglycan (syndecan) of mouse mammary epithelia. J Cell Biol 1989;109:2509-2518.

181 Bernfield M, Gotte M, Park PW, Reizes O, Fitzgerald ML, Lincecum J, Zako M: Functions of cell surface heparan sulfate proteoglycans. Annu Rev Biochem 1999;68:729-777.

182 Elenius K, Jalkanen M: Function of the syndecans--a family of cell surface proteoglycans. J Cell Sci 1994;107 (Pt 11):2975-2982.

183 Kim CW, Goldberger OA, Gallo RL, Bernfield M: Members of the syndecan family of heparan sulfate proteoglycans are expressed in distinct cell-, tissue-, and development-specific patterns. Mol Biol Cell 1994;5:797-805.

184 Tkachenko E, Rhodes JM, Simons M: Syndecans: New kids on the signaling block. Circ Res 2005;96:488-500.

185 Rehm M, Bruegger D, Christ F, Conzen P, Thiel M, Jacob M, Chappell D, Stoeckelhuber M, Welsch U, Reichart B, Peter K, Becker BF: Shedding of the endothelial glycocalyx in patients undergoing major vascular surgery with global and regional ischemia. Circulation 2007;116:1896-1906.

186 Svennevig K, Hoel T, Thiara A, Kolset S, Castelheim A, Mollnes T, Brosstad F, Fosse E, Svennevig J: Syndecan-1 plasma levels during coronary artery bypass surgery with and without cardiopulmonary bypass. Perfusion 2008;23:165-171.

187 Vanhoutte D, Schellings MW, Gotte M, Swinnen M, Herias V, Wild MK, Vestweber D, Chorianopoulos E, Cortes V, Rigotti A, Stepp MA, Van de Werf F, Carmeliet P, Pinto YM, Heymans S: Increased expression of syndecan-1 protects against cardiac dilatation and dysfunction after myocardial infarction. Circulation 2007;115:475-482.

188 Schellings MW, Vanhoutte D, van Almen GC, Swinnen M, Leenders JJ, Kubben N, van Leeuwen RE, Hofstra L, Heymans S, Pinto YM: Syndecan-1 amplifies angiotensin ii-induced cardiac fibrosis. Hypertension 2010;55:249-256.

189 Alexopoulou AN, Multhaupt HA, Couchman JR: Syndecans in wound healing, inflammation and vascular biology. Int J Biochem Cell Biol 2007;39:505-528.

190 VanWinkle WB, Snuggs MB, De Hostos EL, Buja LM, Woods A, Couchman JR: Localization of the transmembrane proteoglycan syndecan-4 and its regulatory kinases in costameres of rat cardiomyocytes: A deconvolution microscopic study. Anat Rec 2002;268:38-46.

191 Kojima T, Takagi A, Maeda M, Segawa T, Shimizu A, Yamamoto K, Matsushita T, Saito H: Plasma levels of syndecan-4 (ryudocan) are elevated in patients with acute myocardial infarction. Thromb Haemost 2001;85:793-799.

192 Echtermeyer F, Harendza T, Hubrich S, Lorenz A, Herzog C, Mueller M, Schmitz M, Grund A, Larmann J, Stypmann J, Schieffer B, Lichtinghagen R, Hilfiker-Kleiner D, Wollert KC, Heineke J, Theilmeier G: Syndecan-4 signalling inhibits apoptosis and controls nfat activity during myocardial damage and remodelling. Cardiovasc Res 2011

193 Matsui Y, Ikesue M, Danzaki K, Morimoto J, Sato M, Tanaka S, Kojima T, Tsutsui H, Uede T: Syndecan-4 prevents cardiac rupture and dysfunction after myocardial infarction. Circ Res 2011;108:1328-1339.

194 Song HH, Filmus J: The role of glypicans in mammalian development. Biochim Biophys Acta 2002;1573:241-246.

195 Petretto E, Sarwar R, Grieve I, Lu H, Kumaran MK, Muckett PJ, Mangion J, Schroen B, Benson M, Punjabi PP, Prasad SK, Pennell DJ, Kiesewetter C, Tasheva ES, Corpuz LM, Webb MD, Conrad GW, Kurtz TW, Kren V, Fischer J, Hubner N, Pinto YM, Pravenec M, Aitman TJ, Cook

SA: Integrated genomic approaches implicate osteoglycin (ogn) in the regulation of left ventricular mass. Nat Genet 2008;40:546-552.

196 Block D AS, Hess G, Huedig H, Liu P, Wienhues-Thelen U: Use of mimecan in the assessment of heart failure; in GmbH RD (ed: THE GOVERNING COUNCIL OF THE UNIVERSITY OF TORONTO ARAB, Sara, 2011, WO/2011/012268 ,

197 Kato M, Wang H, Bernfield M, Gallagher JT, Turnbull JE: Cell surface syndecan-1 on distinct cell types differs in fine structure and ligand binding of its heparan sulfate chains. J Biol Chem 1994;269:18881-18890.

198 Lamanna WC, Kalus I, Padva M, Baldwin RJ, Merry CL, Dierks T: The heparanome--the enigma of encoding and decoding heparan sulfate sulfation. J Biotechnol 2007;129:290-307.

199 Carter NM, Ali S, Kirby JA: Endothelial inflammation: The role of differential expression of n-deacetylase/n-sulphotransferase enzymes in alteration of the immunological properties of heparan sulphate. J Cell Sci 2003;116:3591-3600.

200 Pahakis MY, Kosky JR, Dull RO, Tarbell JM: The role of endothelial glycocalyx components in mechanotransduction of fluid shear stress. Biochem Biophys Res Commun 2007;355:228-233.

201 Eno Essien Ebong DCS, John M Tarbell: The endothelial glycocalyx in vitro: Its structure and the role of heparan sulfate and glypican-1 in enos activation by flow. FASEB J 2010;24

202 Wang W: Change in properties of the glycocalyx affects the shear rate and stress distribution on endothelial cells. J Biomech Eng 2007;129:324-329.

203 Maroski J, Vorderwuelbecke B, Fiedorowicz K, Da Silva-Azevedo L, Siegel G, Marki A, Pries A, Zakrzewicz A: Shear stress increases endothelial hyaluronan synthase 2 and hyaluronan synthesis especially in regard to an atheroprotective flow profile. Exp Physiol 2011

204 Williams DA: Intact capillaries sensitive to rate, magnitude, and pattern of shear stress stimuli as assessed by hydraulic conductivity (lp). Microvasc Res 2003;66:147-158.

205 Lopez-Quintero SV, Amaya R, Pahakis M, Tarbell JM: The endothelial glycocalyx mediates shear-induced changes in hydraulic conductivity. Am J Physiol Heart Circ Physiol 2009;296:H1451-1456.

206 Campo GM, Avenoso A, Campo S, D'Ascola A, Traina P, Sama D, Calatroni A: The antioxidant effect exerted by tgf-1beta-stimulated hyaluronan production reduced nf-kb activation and apoptosis in human fibroblasts exposed to feso4 plus ascorbate. Mol Cell Biochem 2008;311:167-177.

207 Rubio-Gayosso I, Platts SH, Duling BR: Reactive oxygen species mediate modification of glycocalyx during ischemia-reperfusion injury. Am J Physiol Heart Circ Physiol 2006;290:H2247-2256.

208 Moseley R, Waddington R, Evans P, Halliwell B, Embery G: The chemical modification of glycosaminoglycan structure by oxygen-derived species in vitro. Biochim Biophys Acta 1995;1244:245-252.

209 Kashihara N, Watanabe Y, Makino H, Wallner EI, Kanwar YS: Selective decreased de novo synthesis of glomerular proteoglycans under the influence of reactive oxygen species. Proc Natl Acad Sci U S A 1992;89:6309-6313.

210 Moseley R, Waddington RJ, Embery G, Rees SG: The modification of alveolar bone proteoglycans by reactive oxygen species in vitro. Connect Tissue Res 1998;37:13-28.

211 Kelley EE, Trostchansky A, Rubbo H, Freeman BA, Radi R, Tarpey MM: Binding of xanthine oxidase to glycosaminoglycans limits inhibition by oxypurinol. J Biol Chem 2004;279:37231-37234.

212 Karlsson K, Sandstrom J, Edlund A, Marklund SL: Turnover of extracellular-superoxide dismutase in tissues. Lab Invest 1994;70:705-710.

213 Maczewski M, Duda M, Pawlak W, Beresewicz A: Endothelial protection from reperfusion injury by ischemic preconditioning and diazoxide involves a sod-like anti-o2- mechanism. J Physiol Pharmacol 2004;55:537-550.

214 Devaraj S, Yun JM, Adamson G, Galvez J, Jialal I: C-reactive protein impairs the endothelial glycocalyx resulting in endothelial dysfunction. Cardiovasc Res 2009;84:479-484.

215 Hortin GL, Trimpe BL: C1 inhibitor: Different mechanisms of reaction with complement component c1 and c1s. Immunol Invest 1991;20:75-82.

216 Bos IG, van Mierlo GJ, Bleeker WK, Rigter GM, te Velthuis H, Dickneite G, Hack CE: The potentiation of human c1-inhibitor by dextran sulphate is transient in vivo: Studies in a rat model. Int Immunopharmacol 2001;1:1583-1595.

217 Strunk R, Colten HR: Inhibition of the enzymatic activity of the first component of complement (c1) by heparin. Clin Immunol Immunopathol 1976;6:248-255.

218 Wuillemin WA, te Velthuis H, Lubbers YT, de Ruig CP, Eldering E, Hack CE: Potentiation of c1 inhibitor by glycosaminoglycans: Dextran sulfate species are effective inhibitors of in vitro complement activation in plasma. J Immunol 1997;159:1953-1960.

219 Meri S, Pangburn MK: Regulation of alternative pathway complement activation by glycosaminoglycans: Specificity of the polyanion binding site on factor h. Biochem Biophys Res Commun 1994;198:52-59.

220 Kazatchkine MD, Fearon DT, Metcalfe DD, Rosenberg RD, Austen KF: Structural determinants of the capacity of heparin to inhibit the formation of the human amplification c3 convertase. J Clin Invest 1981;67:223-228.

221 Koistinen V: Effects of sulphated polyanions on functions of complement factor h. Mol Immunol 1993;30:113-118.

222 Chappell D, Hofmann-Kiefer K, Jacob M, Rehm M, Briegel J, Welsch U, Conzen P, Becker BF: Tnf-alpha induced shedding of the endothelial glycocalyx is prevented by hydrocortisone and antithrombin. Basic Res Cardiol 2009;104:78-89.

223 Kainulainen V, Nelimarkka L, Jarvelainen H, Laato M, Jalkanen M, Elenius K: Suppression of syndecan-1 expression in endothelial cells by tumor necrosis factor-alpha. J Biol Chem 1996;271:18759-18766.

224 Lortat-Jacob H, Turnbull JE, Grimaud JA: Molecular organization of the interferon gamma-binding domain in heparan sulphate. Biochem J 1995;310 (Pt 2):497-505.

225 Kuschert GS, Coulin F, Power CA, Proudfoot AE, Hubbard RE, Hoogewerf AJ, Wells TN: Glycosaminoglycans interact selectively with chemokines and modulate receptor binding and cellular responses. Biochemistry 1999;38:12959-12968.

226 Stringer SE, Forster MJ, Mulloy B, Bishop CR, Graham GJ, Gallagher JT: Characterization of the binding site on heparan sulfate for macrophage inflammatory protein 1alpha. Blood 2002;100:1543-1550.

227 Wang L, Fuster M, Sriramarao P, Esko JD: Endothelial heparan sulfate deficiency impairs l-selectin- and chemokine-mediated neutrophil trafficking during inflammatory responses. Nat Immunol 2005;6:902-910.

228 Tanaka Y, Kimata K, Adams DH, Eto S: Modulation of cytokine function by heparan sulfate proteoglycans: Sophisticated models for the regulation of cellular responses to cytokines. Proc Assoc Am Physicians 1998;110:118-125.

229 Lundin L, Larsson H, Kreuger J, Kanda S, Lindahl U, Salmivirta M, Claesson-Welsh L: Selectively desulfated heparin inhibits fibroblast growth factor-induced mitogenicity and angiogenesis. J Biol Chem 2000;275:24653-24660.

230 Allen BL, Filla MS, Rapraeger AC: Role of heparan sulfate as a tissue-specific regulator of fgf-4 and fgf receptor recognition. J Cell Biol 2001;155:845-858.

231 Jastrebova N, Vanwildemeersch M, Lindahl U, Spillmann D: Heparan sulfate domain organization and sulfation modulate fgf-induced cell signaling. J Biol Chem 2010;285:26842-26851.

232 Soker S, Goldstaub D, Svahn CM, Vlodavsky I, Levi BZ, Neufeld G: Variations in the size and sulfation of heparin modulate the effect of heparin on the binding of vegf165 to its receptors. Biochem Biophys Res Commun 1994;203:1339-1347.

233 Ashikari-Hada S, Habuchi H, Kariya Y, Kimata K: Heparin regulates vascular endothelial growth factor165-dependent mitogenic activity, tube formation, and its receptor phosphorylation of human endothelial cells. Comparison of the effects of heparin and modified heparins. J Biol Chem 2005;280:31508-31515.

234 Abramsson A, Kurup S, Busse M, Yamada S, Lindblom P, Schallmeiner E, Stenzel D, Sauvaget D, Ledin J, Ringvall M, Landegren U, Kjellen L, Bondjers G, Li JP, Lindahl U, Spillmann D, Betsholtz C, Gerhardt H: Defective n-sulfation of heparan sulfate proteoglycans limits pdgf-bb binding and pericyte recruitment in vascular development. Genes Dev 2007;21:316-331.

235 van Boven HH, Lane DA: Antithrombin and its inherited deficiency states. Semin Hematol 1997;34:188-204.

236 Petitou M, Casu B, Lindahl U: 1976-1983, a critical period in the history of heparin: The discovery of the antithrombin binding site. Biochimie 2003;85:83-89.

237 Olson ST, Bjork I, Bock SC: Identification of critical molecular interactions mediating heparin activation of antithrombin: Implications for the design of improved heparin anticoagulants. Trends Cardiovasc Med 2002;12:198-205.

238 Olson ST, Bjork I, Sheffer R, Craig PA, Shore JD, Choay J: Role of the antithrombin-binding pentasaccharide in heparin acceleration of antithrombin-proteinase reactions. Resolution of the antithrombin conformational change contribution to heparin rate enhancement. J Biol Chem 1992;267:12528-12538.

239 McRae SJ, Stafford AR, Fredenburgh JC, Weitz JI: In the presence of phospholipids, glycosaminoglycans potentiate factor xa-mediated protein c activation by modulating factor xa activity. Biochemistry 2007;46:4195-4203.

240 Olson ST, Bjork I: Predominant contribution of surface approximation to the mechanism of heparin acceleration of the antithrombin-thrombin reaction. Elucidation from salt concentration effects. J Biol Chem 1991;266:6353-6364.

241 Olson ST, Richard B, Izaguirre G, Schedin-Weiss S, Gettins PG: Molecular mechanisms of antithrombin-heparin regulation of blood clotting proteinases. A paradigm for understanding proteinase regulation by serpin family protein proteinase inhibitors. Biochimie 2010;92:1587-1596.

242 Colburn P, Buonassisi V: Anti-clotting activity of endothelial cell cultures and heparan sulfate proteoglycans. Biochem Biophys Res Commun 1982;104:220-227.

243 Marcum JA, Atha DH, Fritze LM, Nawroth P, Stern D, Rosenberg RD: Cloned bovine aortic endothelial cells synthesize anticoagulantly active heparan sulfate proteoglycan. J Biol Chem 1986;261:7507-7517.

244 de Agostini AI, Watkins SC, Slayter HS, Youssoufian H, Rosenberg RD: Localization of anticoagulantly active heparan sulfate proteoglycans in vascular endothelium: Antithrombin binding on cultured endothelial cells and perfused rat aorta. J Cell Biol 1990;111:1293-1304.

245 Bourin MC: [thrombomodulin: A new proteoglycan. Structure-function relation]. Ann Biol Clin (Paris) 1991;49:199-207.

246 Bourin MC, Lundgren-Akerlund E, Lindahl U: Isolation and characterization of the glycosaminoglycan component of rabbit thrombomodulin proteoglycan. J Biol Chem 1990;265:15424-15431.

247 Esmon CT: Thrombomodulin as a model of molecular mechanisms that modulate protease specificity and function at the vessel surface. FASEB J 1995;9:946-955.

248 Kaneider NC, Egger P, Dunzendorfer S, Wiedermann CJ: Syndecan-4 as antithrombin receptor of human neutrophils. Biochem Biophys Res Commun 2001;287:42-46.

249 Bourin MC, Lindahl U: Glycosaminoglycans and the regulation of blood coagulation. Biochem J 1993;289 (Pt 2):313-330.

250 Sandset PM, Abildgaard U, Larsen ML: Heparin induces release of extrinsic coagulation pathway inhibitor (epi). Thromb Res 1988;50:803-813.

251 Hansen JB, Huseby KR, Huseby NE, Sandset PM, Hanssen TA, Nordoy A: Effect of cholesterol lowering on intravascular pools of tfpi and its anticoagulant potential in type ii hyperlipoproteinemia. Arterioscler Thromb Vasc Biol 1995;15:879-885.

252 Lindahl AK, Jacobsen PB, Sandset PM, Abildgaard U: Tissue factor pathway inhibitor with high anticoagulant activity is increased in post-heparin plasma and in plasma from cancer patients. Blood Coagul Fibrinolysis 1991;2:713-721.

253 Valentin S, Larnkjer A, Ostergaard P, Nielsen JI, Nordfang O: Characterization of the binding between tissue factor pathway inhibitor and glycosaminoglycans. Thromb Res 1994;75:173-183.

254 Zheng PS, Reis M, Sparling C, Lee DY, La Pierre DP, Wong CK, Deng Z, Kahai S, Wen J, Yang BB: Versican g3 domain promotes blood coagulation through suppressing the activity of tissue factor pathway inhibitor-1. J Biol Chem 2006;281:8175-8182.

255 Tollefsen DM, Maimone MM, McGuire EA, Peacock ME: Heparin cofactor ii activation by dermatan sulfate. Ann N Y Acad Sci 1989;556:116-122.

256 Sarilla S, Habib SY, Tollefsen DM, Friedman DB, Arnett DR, Verhamme IM: Glycosaminoglycan-binding properties and kinetic characterization of human heparin cofactor ii expressed in escherichia coli. Anal Biochem 2010;406:166-175.

257 Thourani VH, Brar SS, Kennedy TP, Thornton LR, Watts JA, Ronson RS, Zhao ZQ, Sturrock AL, Hoidal JR, Vinten-Johansen J: Nonanticoagulant heparin inhibits nf-kappab activation and attenuates myocardial reperfusion injury. Am J Physiol Heart Circ Physiol 2000;278:H2084-2093.

258 Banz Y, Hess OM, Robson SC, Mettler D, Meier P, Haeberli A, Csizmadia E, Korchagina EY, Bovin NV, Rieben R: Locally targeted cytoprotection with dextran sulfate attenuates experimental porcine myocardial ischaemia/reperfusion injury. Eur Heart J 2005;26:2334-2343.

259 Krijnen PA, Nijmeijer R, Meijer CJ, Visser CA, Hack CE, Niessen HW: Apoptosis in myocardial ischaemia and infarction. J Clin Pathol 2002;55:801-811.

Paper I

Endothelial cell activation, Complement and Cytokines at the onset of Reperfusion after Tourniquet Application in Hand Surgery

Pranitha Kamat, MSc[1], Bettina Juon, MD[2], Brigitte Jossen, BMA[1], Thusitha Gajanayake, PhD[2], Robert Rieben, PhD[1, 2*], Esther Vögelin, MD[2]

[1]University of Bern, Department of Clinical Research, Bern, Switzerland, [2]Clinic of Plastic- and Hand Surgery, University Hospital, Bern, Switzerland

Activation of the endothelium, complement activation and generation of cytokines are known events during ischemia/reperfusion that mediate tissue injury.

Aim: To elucidate the roles of endothelium, complement and cytokines at the onset of reperfusion after ischemia of less than 2 hours.

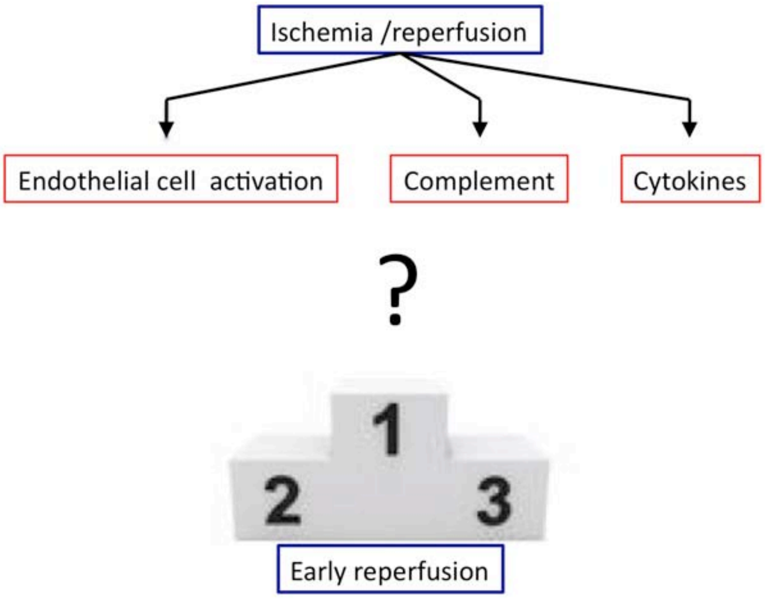

Model: Tourniquet induced ischemia reperfusion injury in upper arm of human patients.

Conclusion: Tourniquet induced ischemia in skeletal muscle stimulates secretion of cytokines as the preliminary event at 10 minutes after reperfusion. There is no complement deposition, heparan sulfate shedding or endothelial cell activation at this early phase of reperfusion.

Endothelial cell activation, complement and cytokines at the onset of reperfusion after tourniquet application in hand surgery

Pranitha Kamat[1], Bettina Juon[2], Brigitte Jossen[1], Thusitha Gajanayake[2], Robert Rieben[1, 2,]*, Esther Vögelin[2]

[1]University of Bern, Department of Clinical Research, Bern, Switzerland, [2]Clinic for Plastic- and Hand Surgery, Inselspital, Bern University Hospital, Bern, Switzerland

pranitha.kamat@dkf.unibe.ch, bettina.juon@insel.ch, brigittej@gmx.ch, thusitha.gajanayake@dkf.unibe.ch, robert.rieben@dkf.unibe.ch, esther.voegelin@insel.ch

*Corresponding author
Robert Rieben
University of Bern
Department of Clinical Research
Murtenstrasse 50
3008 Bern, Switzerland
Tel: +41 31 632 9669
Fax: +41 31 632 7594
E-mail: robert.rieben@dkf.unibe.ch

Abstract

Background: Tourniquet application in hand surgery causes short-term ischemia, followed by reperfusion. Activation of the endothelium, complement activation and generation of cytokines are known events during ischemia-reperfusion (I/R) that mediate tissue injury. Aim of this study was to elucidate their respective participation at the onset of the reperfusion phase after less than 2 hours of ischemia. The study was conducted with patients admitted for routine hand surgery.

Methods: Ten patients were included in the study after obtaining informed consent. A tourniquet was placed on the upper arm and inflated to 250 mmHg for 116±16 min, during which the surgery was performed. Venous blood and tissue samples from the surgical area were taken at baseline as well as 0, 2, and 10 min after reperfusion.

Results: Markers for endothelial integrity and/or activation like heparan sulfate, CD31, vWF, and syndecan-1 showed no significant changes until 10 min reperfusion. Tissue deposition of antibodies and complement did not show significant changes from baseline during early reperfusion. Stable plasma levels of C1-inhibitor, C3a and C4d confirmed minimal complement activation. However, IL-6, IL-7, IL-17, TNFα, GM-CSF, VEGF, and PDGF bb were all significantly increased at 10 min reperfusion with respect to baseline. Skeletal muscle creatine kinase showed a rise from baseline at the onset of reperfusion ($p<0.001$) and dropped again at 2 min ($p<0.01$) reperfusion, suggesting ischemic muscle damage.

Conclusions: In this clinical setting no changes on the endothelium, antibody deposition or complement activation were observed during early reperfusion. The increase of pro-inflammatory cytokines and growth factors during the first 10 min of reperfusion suggests a contribution of these molecules in the early stages of I/R injury.

Keywords: Tourniquet, hand surgery, ischemia / reperfusion injury, cytokines, complement, endothelium, glycocalyx

Background

Ischemia / reperfusion (I/R) injury is a common source of pathology in many vascular diseases. Mechanisms underlying I/R injury have been studied extensively and are known to engage a spectrum of pathways. Elucidating the key molecules involved in triggering the entire process of injury is important to help develop targeted therapy to attenuate I/R injury in its early stages.

In any vascularized organ or tissue, a monolayer of endothelial cells (EC) forms the interface between blood and the surrounding tissue. Among other factors, the glycocalyx covering the endothelium, plays a critical role in maintaining the homeostasis of the blood vessel wall [1]. The conditions during I/R cause this glycocalyx layer to partly shed [2], which occurs already during ischemia and more significantly during reperfusion [3]. Glycocalyx shedding activates the endothelium by transforming it into a pro-inflammatory and pro-coagulant phenotype [4], thereby propagating injury. Moreover, the glycocalyx acts as an interface between blood and tissue, forms receptors for many inflammatory molecules including cytokines and therefore participates in inflammation [5, 6]. Shedding of the glycocalyx after 2 min of reperfusion has been shown in humans [7], but the respective study was based on large vessels and data on I/R induced shedding of the glycocalyx in smaller, peripheral blood vessels are lacking.

Complement activation leads directly to tissue necrosis and trafficking of immune cells. Various knockout animal models have illustrated the participation of natural antibodies and complement in propagation of I/R injury [8, 9]. The importance of complement in I/R injury has been reviewed [10]. Complement thus has the potential to significantly contribute to early reperfusion injury.

The model used in this study was that of tourniquet-induced I/R injury. Tourniquet application in extremity surgery is a prerequisite to provide a blood-less environment during surgery. The blood flow in the ischemic limb is restored after surgery by releasing the tourniquet. Use of the tourniquet thereby comes with the risk of I/R injury. Clinically, this manifests as pain, swelling, tissue necrosis along with systemic effects, which the surgeons try to avoid by limiting tourniquet times to a maximum of 2 hours [11-15]. Several studies in humans have been dedicated to understanding I/R injury due to tourniquet application in upper and lower limbs. These studies have shown the involvement of radical oxygen species (ROS) [16], expression of adhesion molecules [17], recruitment of activated leukocytes [18] and thereby progression of inflammation. The process of I/R injury in skeletal muscle has been extensively studied [19] and reviewed [20]. However, the role of cytokines during early reperfusion is still unclear and yet to be investigated in upper limb I/R injury. This would be important, as cytokines apart from trafficking immune cells are known to cause shedding of the endothelial glycocalyx [21].

Based on the above cited literature, including our own studies, we hypothesized that natural antibodies, complement and the endothelial glycocalyx, together with a number of pro-inflammatory cytokines and growth factors, would be involved in the very early reperfusion phase. The involvement and relative contribution of these different factors in the initial phase of reperfusion injury was therefore assessed in this study.

Methods

All patients (n = 10) underwent elective hand surgery under tourniquet application and gave informed consent for participation in the study, which was approved by the ethical committee of the Canton of Bern, Switzerland. Exclusion criteria were trauma, anticoagulation, age under sixteen years and diabetes.

In four cases with traumatic or non-traumatic arthrosis an arthroplasty (3 x first carpometacarpal and 1x distal radioulnar joint) was done. There was one procedure for scaphoid non union. Three patients underwent tenolysis and arthrolysis after complex trauma. In two cases a decompression and submuscular transposition of the ulnar nerve at the elbow was performed.

The tourniquet device was the A.T.S. 2000 automatic Tourniquet System (Zimmer, Inc. Warsaw, IL, USA) with a low profile cuff and accurate pressure monitoring. Before the cuff was applied on the upper arm a cuff sleeve to reduce shearing of soft tissue was used. After standardized disinfection with 0.5% chlorhexidin and sterile dressing surgery, samples were collected for the study.

Sample collection

Blood was collected from veins immediately leaving the surgical area with a sterile syringe. Collected blood was immediately transferred into vacutainers containing EDTA (1.6 mg/ml) to obtain EDTA-plasma, and to tubes containing a clotting activator (glass pearls) to obtain serum. Samples were collected before application of tourniquet (baseline), immediately after release of tourniquet (ischemia sample / 0 min reperfusion), 2 minutes (2 min reperfusion) and 10 minutes (10 min reperfusion) after release of tourniquet. Samples were kept on ice until centrifugation at 3000 rpm for 10 min. Serum and EDTA-plasma were then stored at –80°C until use.

Tissue biopsies were taken immediately after the application of tourniquet (baseline), just before releasing the tourniquet (end ischemia) and 10 minutes after release of tourniquet (10 min reperfusion). They were fixed in 2% formaldehyde for 24 hours and then transferred into 18% sucrose for 15 hours. The biopsies were embedded in Shandon M1 embedding matrix (Thermo Scientific, Inc., Geneva, Switzerland) and stored at –20°C until sectioned.

Markers for EC integrity/activation and detection of complement activation on tissue

Free float technique was used for immunostaining of tissue samples. In brief, 30 µm thick cryosections were cut from each sample and treated with TBS-Triton X100 for 15 min. EC integrity/activation were assessed by mouse anti-human heparan sulfate proteoglycan (HSPG) (Abcam plc., Cambridge, UK), mouse anti-human von Willebrand factor (vWF) (DAKO), mouse anti-human CD31 (eBioscience, Inc., San Diego, CA, USA). As secondary antibodies we used Dylight 488 labeled donkey anti-mouse (Jackson ImmunoResearch Laboratories, Inc., West Grove, PA, USA), Cy3-labeled donkey anti-mouse (Jackson ImmunoResearch) and FITC labeled rabbit anti-mouse (DAKO).

The following antibodies were used to determine natural antibody binding and complement activation: Cy3 labeled goat anti-human IgG (KPL, Inc., Gaithersburg, MD, USA), allophycocyanin labeled goat anti-human IgM (Open Biosystems / Thermo Scientific), FITC labeled rabbit anti-human C3b/c (DAKO, Glostrup, Denmark), and FITC-labeled rabbit anti-human C4b/c (DAKO).

Scoring of stained tissue sections.

Sections of skeletal muscle from the hand of a healthy human were used as common control in every staining batch. Images of a representative blood vessel were taken under the confocal microscope from all sections including the common control. With Imaris software (Bitplane AG, Zurich, Switzerland), the area of the vessel was calculated from the image, and a histogram of the color channel of interest for the same area was obtained. The histogram of the common control was used to normalize histograms of other tissues from the same batch. This enabled sections from different batches to be comparable. Area under the curve (AUC) values were obtained from the normalized histogram for each tissue and divided by the area of the vessel to obtain a final score for the section. Sections were then compared with their final scores, which considered the size of the vessel and the intensity of staining within that vessel. Sections were blinded at all times.

Analysis of EC integrity/activation and complement activation in venous blood

ELISA kits were used to determine the concentrations of heparan sulfate (HS) and syndecan-1 as markers of EC activation. To study complement activation ELISA for C3a, C4d and C1-inhibitor were used. The assays were performed according to manufacturers' protocols and samples were analyzed in duplicates for each time point. Concentrations were determined by comparing with standards provided with the kit. HS (Seikagaku Corp., Tokyo, Japan) and syndecan-1 (Diaclone, Gene-Probe Inc., San Diego, CA, USA) were measured in blood serum samples. C3a, C4d (Quidel Corp., San Diego, CA, USA) and C1-inhibitor (USCN Life Sciences, Inc., Wuhan, China) were measured in EDTA plasma samples.

Analysis of cytokines in circulation

A multiplex immunoassay, consisting of fluorescent microspheres conjugated with a monoclonal antibody specific for a target protein, was used to detect an array of cytokines. Kits for IL-5, IL-6, IL-7, IL-8, IL-10, IL-17, G-CSF, GM-CSF, MCP-1, TNFα, VEGF, and PDGF bb were purchased from Bio-Rad (Bio-Rad Laboratories, Inc., Hercules, CA, USA) and multiplex analysis was performed on a Bio-Plex 100 system (Bio-Rad). Assays were performed according to manufacturer’s instructions. Briefly, plasma was diluted 1:2 and incubated with antibody-coupled beads. Complexes were washed and then incubated with biotinylated detection antibody followed by streptavidin-phycoerythrin prior to assessing titers of cytokine concentration. Recombinant cytokines were used to establish standard curves. Analyte concentrations were calculated using the Bio-Plex Manager 4.0 Software (Bio-Rad).

Measurement of skeletal muscle injury

An ELISA kit for measuring skeletal muscle creatine kinase (CK-MM, from USCN Life Sciences) was used to measure skeletal muscle injury. The assay was performed according to the manufacturers' protocol and samples were analyzed in duplicates for each time point. Concentrations were determined by comparing with standards provided with the kit.

Statistical Analysis

For measurements of HSPG, syndecan-1, C1-inhibitor and CK-MM by ELISA, time dependent changes were tested by Friedman’s non-parametric test for related samples with confidence interval set to 95%. For comparing immunostained samples, one-way ANOVA with 95% confidence interval was used. Dunn’s multiple comparison test was used as a post test. When only two time points had to be statistically compared, two tailed paired t-test was used with the level of significance set to 95%

Results

The average tourniquet time for the 10 patients was 116 ± 16 minutes.

Shedding of glycocalyx and EC integrity/activation

Heparan sulfates and syndecan-1 were measured in the venous blood before and after tourniquet application by ELISA. There was no time dependent change in the levels of HS measured at baseline (6.5 ± 1.9 µg/ml), 0 min reperfusion (5.6 ± 1.9 µg/ml), 2 min reperfusion (5.5 ± 2.1 µg/ml) and 10 min reperfusion (6.2 ± 1.8 µg/ml). Similarly, syndecan-1 levels showed no time dependent changes from baseline (196.4 ± 28.4 ng/ml) to 0 min reperfusion (196.5 ± 35.8 ng/ml), 2 min reperfusion (196.0 ± 18.6 ng/ml), and until 10 min reperfusion (102.7 ± 27.5 ng/ml) (Figure 1).

The endothelial lining of blood vessels was studied by immunostaining the tissue sections for HSPG, vWF and CD31 as markers of EC integrity/activation. Table 2 shows mean values ± standard deviations for each marker at the different time points for all 10 patients. Analysis of the data by Friedman’s non-parametric test for repeated measurements showed no significant differences in staining intensity, confirming no loss of endothelial integrity or activation of the EC until 10 min reperfusion. Representative pictures for HSPG at the different time points are shown in Figure 2.

Binding of antibodies and activation of complement system

Products of complement activation were measured by ELISA at baseline and after 10 min of reperfusion in EDTA plasma samples. The paired t-test showed no significant differences between the levels of C3a at baseline (247.0 ± 221.5) and at 10 min reperfusion (144.7 ± 161.1). Also the values for the classical pathway complement activation marker C4d showed no significant difference between baseline (42.47 ± 35.93) and 10 min reperfusion (67.58 ± 78.43, Figure 3). In line with the C3a and C4d results, also no significant differences were found for the levels of C1-inhibitor at the different time points (Figure 4).

In the tissue samples, deposition of IgM, IgG, C3b/c and C4b/c were analyzed by immunostaining. Immunofluorescence scores for staining intensity of the respective antigens within blood vessels are shown in Table 2. Statistical analysis by one-way ANOVA revealed no significant differences for antibody- or complement deposition in tissue between baseline and 10 min reperfusion, Pictures representative for C3b/c and C4b/c deposition are shown in Figure 5.

Cytokine levels

An array of cytokines and growth factors, namely IL-5, IL-6, IL-7, IL-8, IL10, IL17, G-CSF, GM-CSF MCP-1, TNFα, VEGF and PDGF bb, were measured by Bio-Plex assay. Because several of the measurements revealed low values outside of the range of the standard curves, raw fluorescence intensity values were used for statistical analysis, rather than the calculated concentrations of the respective cytokines. As shown in Figure 6, the 10 min reperfusion samples were significantly higher than baseline for IL-6 ($p=0.0243$), IL-7 ($p=0.0058$), IL-17 ($p=0.0344$), GM-CSF ($p=0.0169$), VEGF ($p=0.0071$), TNFα ($p=0.0465$), and PDGF bb ($p=0.0001$).

Skeletal muscle injury

Creatine kinase-MM was measured in plasma samples as a marker for skeletal muscle injury (Figure 7). CK-MM values were increased significantly from 2066 ± 1122 U/L at baseline to 5908 ± 1843 U/L at 0 min reperfusion ($p<0.001$). At 2 min reperfusion the levels dropped again significantly to 3504 ± 1855 U/L ($p<0.05$). However, also at 10 min reperfusion, CK-MM levels (4296 ± 1894 U/L) were still higher than at baseline ($p<0.05$).

Discussion

Endothelial cells form the interface between blood and tissue and serve as the first line of defense against microorganisms invading through the blood stream. It is therefore not difficult to consider the EC to react immediately to pathology occurring during I/R. The first morphological change of an EC during any pathology is the loss of its native, anticoagulant and anti-inflammatory surface layer, the glycocalyx [22]. The latter is composed mainly of heparan sulfate proteoglycans, among which syndecans as core proteins [7]. We therefore measured the levels of shed syndecan-1, which did not show any changes from baseline to 10 min reperfusion. In line with this finding, the concentration of free HS in serum did not increase from baseline until 10 min reperfusion, and also the vascular expression of HSPG in the tissue biopsies did not show any changes over time. Together, these data support the notion that no significant activation of EC occurred in our setting of tourniquet-induced ischemia and reperfusion. This finding is in contrast to earlier reports, for example on patients undergoing coronary artery bypass grafting under extracorporeal circulation, where increased serum levels of syndecan-1 and HS were found as early as after 2 min of reperfusion [7]. In the latter study, however, the tubings and filters in the extracorporeal circulation circuit, which are known to lead to complement activation, may account for at least part of the observed EC activation.

However, composition of endothelial glycocalyx should not be completely excluded from undergoing any change during early reperfusion. The HS is a polymer of disaccharide units that are sulfated at different positions. The sulfation pattern on these disaccharides is highly regulated and may be modified during pathology [23]. Such modifications in return can drastically affect the outcome of other events during pathology as the sulfation pattern on HS allows it to specifically interact with various proteins [24]. The antibody we used for detection of HS does not specifically identify a certain sulfation pattern but binds in general to sulfated HS. Detection of the more subtle changes in HS sulfation patterns would require the use of sulfation-specific antibodies.

Other markers of EC activation documented previously are CD31 and vWF [25, 26], and we included detection of these antigens in the analysis of our tissue biopsies by immunostaining. Earlier studies by Huhges et al. [27, 28], showed no significant increase in vWF plasma levels after 10 min and 30 min of ischemia and 15 min and 30 min reperfusion, respectively. Our study confirms this finding on the tissue level, where we found no significant changes in vWF and CD31 expression in biopsies, which further support that in human upper limb tourniquet induced ischemia for 116 ± 16 min there is only minimal EC activation or damage until 10 min reperfusion.

Previous studies on murine skeletal muscle I/R injury models have identified natural IgM antibodies as a major initiator of the activation of the complement system, which was also shown to be causally related to the observed tissue injury [8]. We therefore analyzed deposition of IgM as well as IgG in the tissue. However, no significant differences between ischemia and reperfusion samples were found for these antibody isotypes. In line with the absence of antibody deposition also the presence of the complement activation markers C3a and C4d, did not change in the plasma until 10 min reperfusion. This suggests that no significant activation of the complement system occurs during the early phase of our tourniquet-induced ischemia and reperfusion setting. Also the levels of C1-inhibitor, which is the only known physiologic inhibitor of classical complement pathway activation [29], showed no changes from baseline to 10 min reperfusion. Absence of activation of the complement system was also confirmed by no changes in the deposition of activated complement components C3b/c and C4b/c in tissue.

Several studies have been dedicated to the use of a tourniquet on the upper extremities of humans. These studies have helped to determine its optimal position, pressure and duration of use on the upper arm [15]. A lot of work has also been done on the biomolecular changes, which occur due to I/R injury and application of the tourniquet by itself.

One of these studies has shown a steep increase in xanthine oxidase levels in the ischemic limb immediately after reperfusion [30]. Xanthine oxidase is a major source of reactive oxygen species, which promote expression of adhesion molecules on both leukocytes and EC [31]. This has also been demonstrated in a human tourniquet induced model of I/R injury wherein a decrease in shed CD62L, increase in CD11b and leukocyte extravasation was shown [27, 28]. In our study, we went further to analyze inflammatory cytokines, which may be released during early stages of I/R injury. Pro-inflammatory cytokines are secreted to preserve immune integrity and stimulate repair mechanisms to counteract the ongoing tissue damage [32, 33]. The pro-inflammatory cytokines IL-1 and TNFα in particular are released by monocytes and macrophages during the acute phase of I/R injury. These two in turn stimulate the production of IL-6 [34]. In our study we found that TNFα and IL-6 were significantly elevated in serum at 10 min reperfusion as compared to baseline. This result is in line with two reports of tourniquet application in lower limb surgery, where also a rise in IL-6 was shown at 2 h and 4 h reperfusion, respectively, in the draining blood of the ischemic limbs [19, 35] We also found a significant rise in the levels of IL-17 from baseline, highlighting the involvement of another pro-inflammatory molecule, which is known to induce EC to secrete cytokines.

Among the cytokines known to be secreted by EC, IL-7 showed a significant rise in the 10 minutes reperfusion sample, but this was not the case for IL-8. Predominantly anti-inflammatory cytokines like IL-10 and IL-5 did not show any significant changes at 10 min reperfusion.

To our knowledge, the role of MCP-1 has as yet not been studied in human skeletal muscle I/R injury. Studies on MCP-1 in other models have shown its involvement in both inflammation [36] and muscle regeneration [37]. Our data show no significant changes in the levels of MCP-1 until 10 min of reperfusion. On the other hand, an increased level of GM-CSF, but not of G-CSF, was found, probably due to the recruitment of monocytes at the site of ischemia. VEGF [38] and PDGF bb [39] are growth factors that help in angiogenesis and formation of new blood vessels and are induced as a response to ischemia. In the present study we could also show this type of vascular responses to ischemia by significantly higher plasma levels of VEGF and PDGF bb at 10 min reperfusion.

In addition to the above described assessment of EC activation and -damage, CK-MM was measured as a marker for skeletal muscle injury [40]. The observed significant rise of the enzyme levels at end of ischemia (0 min reperfusion) as well as at 10 min reperfusion when compared to baseline indicates that a certain level of skeletal muscle injury is occurring in our model, despite the apparent absence of activation of complement and EC.

Conclusions and limitations

In our study with 116 ±1 6 min ischemia and a follow-up until 10 min after reperfusion, the aim was to analyze molecules participating in the early stages of reperfusion. We show an active involvement of the inflammatory cascade with a rise in pro-inflammatory cytokines TNFα, IL-6 and IL-17, which stimulate production of chemokines apart from mediating extravasation of leukocytes. In addition, the observed increase in GM-CSF and IL-7 further supports leukocyte extravasation. We could also show a rise in angiogenic factors PDGF bb and VEGF induced by hypoxia. Finally, the rise of CK-MM points towards a certain degree of skeletal muscle injury post surgery, whereas, in contrast to our original hypothesis, no significant activation of EC or the complement system could be observed until 10 min reperfusion. For the formation of edema, which may lead to the feared compartment syndrome, EC activation and damage are key events. Their absence during the very early reperfusion phase may offer a window of opportunity to protect the endothelium and thus to prevent further reperfusion injury, for example by local use of endothelial cell protective substances which proved to be effective to prevent I/R injury in experimental myocardial infarction [41, 42].

The short follow-up of only 10 min during the reperfusion phase is an obvious limitation of the study. Clinically, edema becomes apparent only several hours after surgery and additional studies with analyses of plasma samples after reperfusion times of 6 h or more need to be done. Another limitation of the study is the ischemia period with a rather wide standard deviation. Studies of tissue samples after fixed ischemia times and prolonged reperfusion periods will have to be carried out in animals.

The authors declare that they have no completing interests

Author Contributions

Designed the experiments / the study: PK, BJU, RR, EV

Analyzed and interpreted the data: PK, BJ, TG, RR

Collected data / did experiments for the study: PK, BJ

Enrolled patients/conducted the surgery: BJU, EV

Contributed to the writing of the paper: PK, BJU, TG, RR, EV

Agree with manuscript's results and conclusions: all authors

Acknowledgements

This study was supported by the Inselspital, Bern University Hospital (study no. 1711) and the Swiss National Science Foundation (3200B0-116618 and 32003B-135272). We would like to thank Prof. Hans Imboden, University of Bern, for support with the free float staining technique, Dr. Mathias Traub for his help with patient-related work and Mrs. Katja Matozan for technical support in the project.

Table 1: Immunofluorescence staining for markers of EC integrity / activation. Values are mean ± standard deviation of immunofluorescence scores (quantitation by Imaris software).

Markers of EC integrity / activation	Baseline	End ischemia	10 min reperfusion	P value
HSPG	0.45 ± 0.16	0.44 ± 0.14	0.58 ± 0.11	n.s.
vWF	0.34 ± 0.37	0.64 ± 0.64	0.60 ± 0.49	n.s.
CD31	2.20 ± 3.99	0.61 ± 0.83	0.51 ± 0.57	n.s.

Table 2: Immunofluorescence staining for markers of complement activation. Values are mean ± standard deviation of immunofluorescence scores (quantitation by Imaris software).

Antibody and complement deposition in tissue	Baseline	End ischemia	10 min reperfusion	P value
IgG	1.03 ± 9.60	0.81 ± 0.60	0.50 ± 0.40	n.s.
IgM	0.02 ± 0.02	0.06 ± 0.08	0.03 ± 0.03	n.s.
C3b/c	0.12 ± 0.13	0.12 ± 0.22	0.13 ± 0.22	n.s.
C4b/c	0.16 ± 0.10	0.29 ± 0.46	0.22 ± 0.31	n.s.

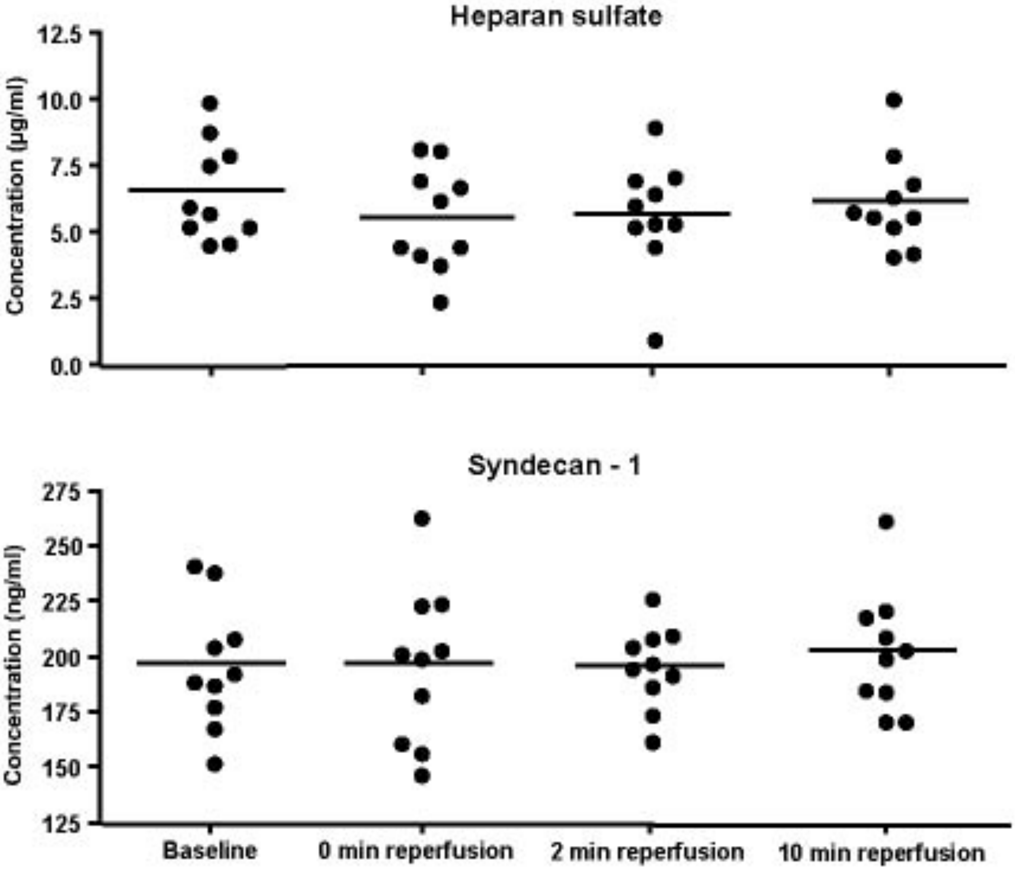

Figure 1. Serum levels of Heparan sulfate and Syndecan-1.

Serum levels of HS and syndecan-1 were measured by ELISA. Samples from baseline were compared with 0, 2, and 10 min reperfusion. No significant changes between time points were found by Friedman's non-parametric test for related samples.

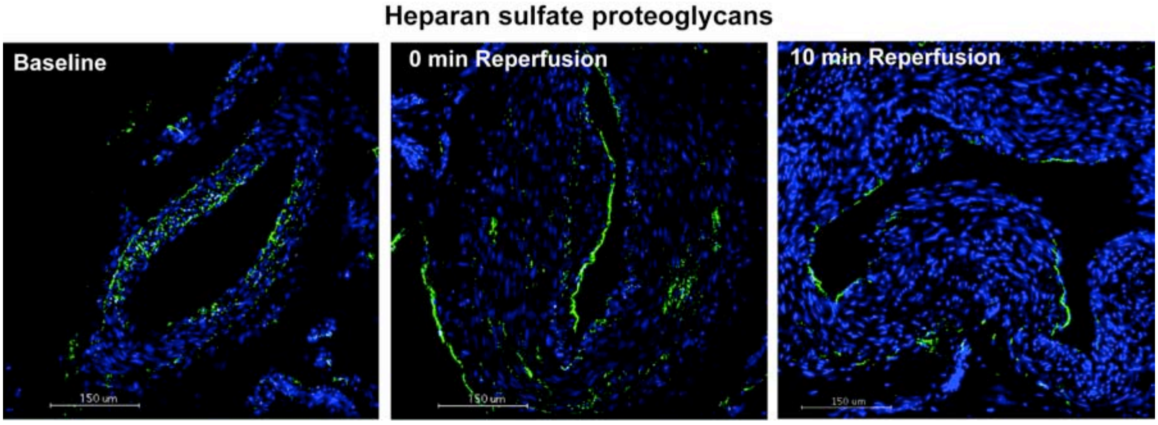
Heparan sulfate proteoglycans
Baseline
0 min Reperfusion
10 min Reperfusion
150 um
150 um
150 um

Figure 2: Immunofluorescence staining for HSPG.

Tissue samples from baseline, end ischemia and 10min reperfusion were analyzed by Immunofluorescence for HSPG. Pictures are representative for the shown time points. No statistical differences in HSPG expression were found by one-way ANOVA. Scale bars = 150µm.

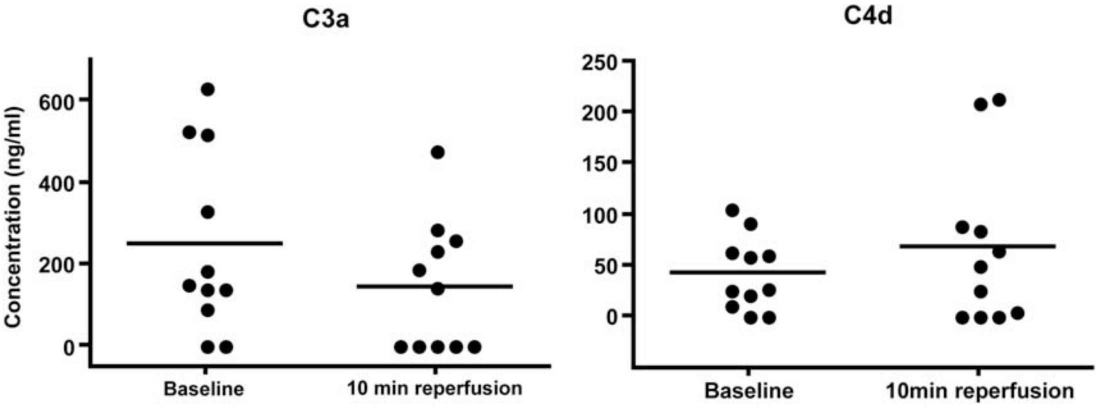

Figure 3: Plasma levels of C3a and C4d.

Plasma levels of the complement activation markers C3a and C4d were measured by ELISA. Values at baseline and after 10 min reperfusion were not statistically different (one-way ANOVA).

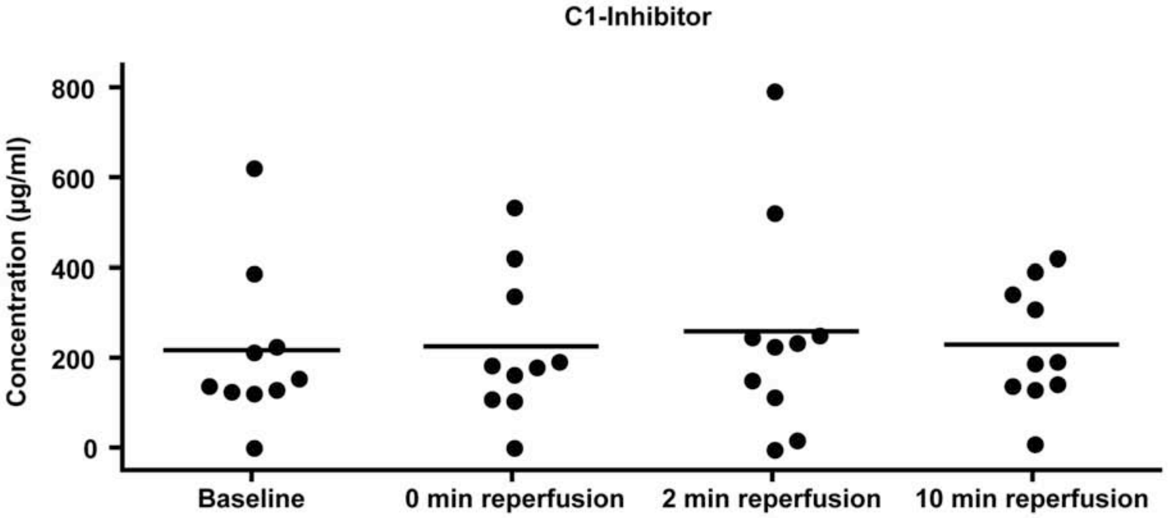

Figure 4: C1-Inhibitor in plasma.

C1-inhibitor levels in plasma were measured by ELISA. Values were not significantly different between time points (Friedman's non-parametric test for related samples).

Deposition of complement component C3b/c

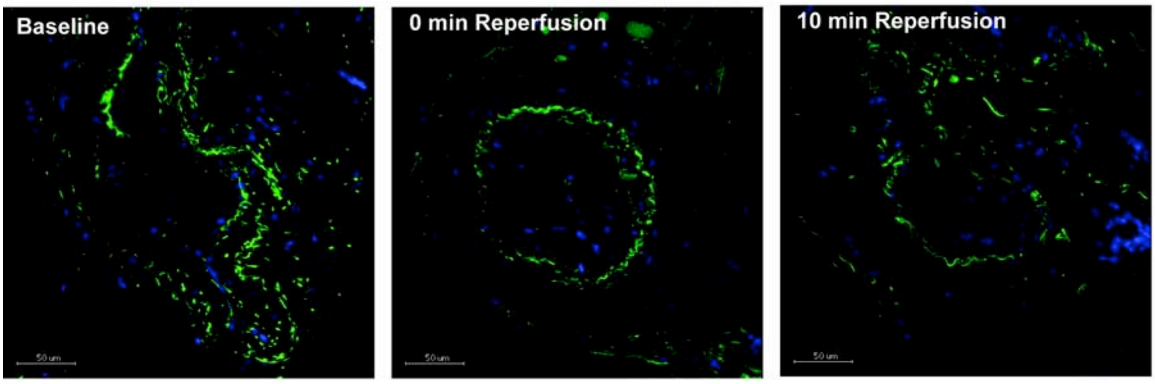
Baseline
0 min Reperfusion
10 min Reperfusion
50 um
50 um
50 um

Deposition of complement component C4b/c

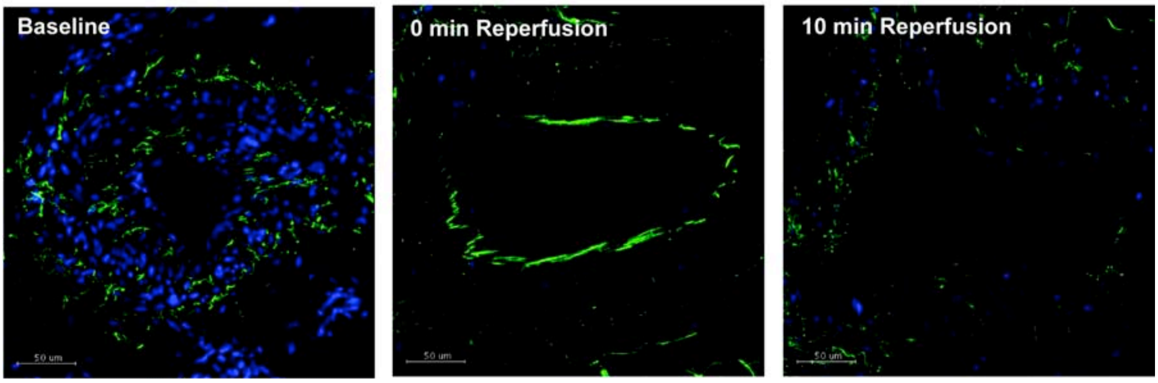
Baseline
0 min Reperfusion
10 min Reperfusion
50 um
50 um
50 um

Figure 5: Immunofluorescence staining for C3b/c and C4b/c.

Tissue samples from baseline, end ischemia and 10 min reperfusion were analyzed by Immunofluorescence for deposition of the complement components C3b/c and C4b/c. Pictures are representative for the time points and no significant differences were found by one-way ANOVA. Scale bars = 50µm.

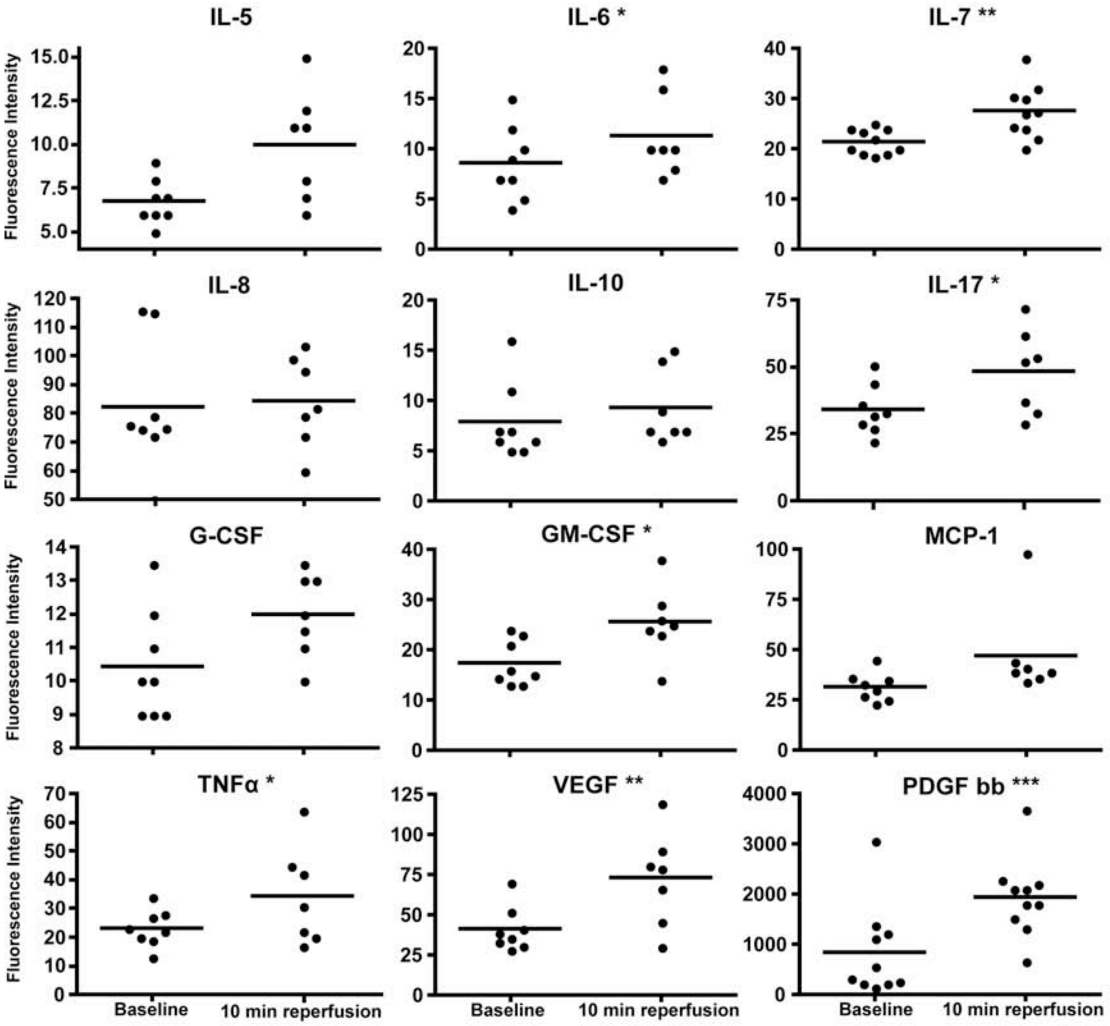

Figure 6: Measurement of cytokines and growth factors in serum.

The cytokines IL-5, IL-6, IL-7, IL-8, IL-10, IL-17, G-CSF, GM-CSF MCP-1, TNFα, VEGF and PDGF bb were measured by Bio-Plex assay. Baseline samples were compared with 10 min reperfusion samples for each cytokine. *p<0.05, **p<0.005, ***p<0.0005 (two-tailed Student's t-test).

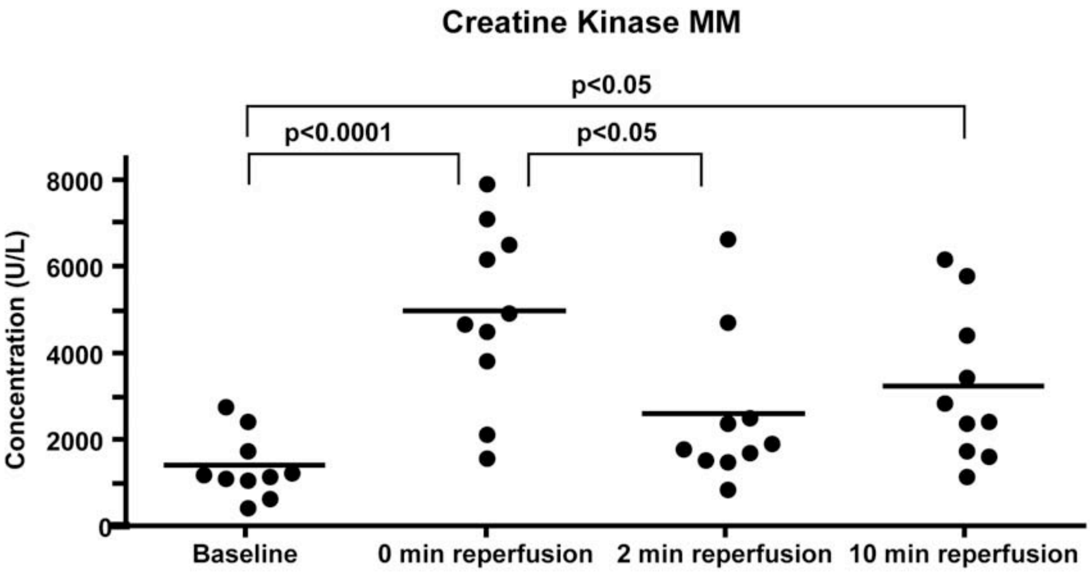

Figure 7: Plasma levels of creatine kinase MM.

CK-MM was measured by ELISA and found to be significantly higher at the end of ischemia (0 min reperfusion) as compared to baseline. Levels dropped again during the reperfusion phase, but were still higher than baseline after 10 min reperfusion (Friedman’s non-parametric test for related samples).

References

1. Van Teeffelen JW, Brands J, Stroes ES, Vink H: **Endothelial glycocalyx: sweet shield of blood vessels.** *Trends Cardiovasc Med* 2007, **17:**101-105.
2. Mulivor AW, Lipowsky HH: **Inflammation- and ischemia-induced shedding of venular glycocalyx.** *Am J Physiol Heart Circ Physiol* 2004, **286:**H1672-1680.
3. Ward BJ, Donnelly JL: **Hypoxia induced disruption of the cardiac endothelial glycocalyx: implications for capillary permeability.** *Cardiovasc Res* 1993, **27:**384-389.
4. Shibata S, Sasaki T, Harpel P, Fillit H: **Autoantibodies to vascular heparan sulfate proteoglycan in systemic lupus erythematosus react with endothelial cells and inhibit the formation of thrombin-antithrombin III complexes.** *Clin Immunol Immunopathol* 1994, **70:**114-123.
5. Wang L, Fuster M, Sriramarao P, Esko JD: **Endothelial heparan sulfate deficiency impairs L-selectin- and chemokine-mediated neutrophil trafficking during inflammatory responses.** *Nat Immunol* 2005, **6:**902-910.
6. Tanaka Y, Kimata K, Adams DH, Eto S: **Modulation of cytokine function by heparan sulfate proteoglycans: sophisticated models for the regulation of cellular responses to cytokines.** *Proc Assoc Am Physicians* 1998, **110:**118-125.
7. Rehm M, Bruegger D, Christ F, Conzen P, Thiel M, Jacob M, Chappell D, Stoeckelhuber M, Welsch U, Reichart B, et al: **Shedding of the endothelial glycocalyx in patients undergoing major vascular surgery with global and regional ischemia.** *Circulation* 2007, **116:**1896-1906.
8. Austen WG, Jr., Zhang M, Chan R, Friend D, Hechtman HB, Carroll MC, Moore FD, Jr.: **Murine hindlimb reperfusion injury can be initiated by a self-reactive monoclonal IgM.** *Surgery* 2004, **136:**401-406.
9. Zhang M, Alicot EM, Chiu I, Li J, Verna N, Vorup-Jensen T, Kessler B, Shimaoka M, Chan R, Friend D, et al: **Identification of the target self-antigens in reperfusion injury.** *J Exp Med* 2006, **203:**141-152.
10. Banz Y, Rieben R: **Role of complement and perspectives for intervention in ischemia-reperfusion damage.** *Ann Med* 2011.
11. Mohler LR, Pedowitz RA, Lopez MA, Gershuni DH: **Effects of tourniquet compression on neuromuscular function.** *Clin Orthop Relat Res* 1999**:**213-220.
12. Lin LN, Wang LR, Wang WT, Jin LL, Zhao XY, Zheng LP, Jin LD, Jiang LM, Xiong XQ: **Ischemic preconditioning attenuates pulmonary dysfunction after unilateral thigh tourniquet-induced ischemia-reperfusion.** *Anesth Analg*, **111:**539-543.
13. Smith TO, Hing CB: **The efficacy of the tourniquet in foot and ankle surgery? A systematic review and meta-analysis.** *Foot Ankle Surg*, **16:**3-8.
14. Girardis M, Milesi S, Donato S, Raffaelli M, Spasiano A, Antonutto G, Pasqualucci A, Pasetto A: **The hemodynamic and metabolic effects of tourniquet application during knee surgery.** *Anesth Analg* 2000, **91:**727-731.
15. Sapega AA, Heppenstall RB, Chance B, Park YS, Sokolow D: **Optimizing tourniquet application and release times in extremity surgery. A biochemical and ultrastructural study.** *J Bone Joint Surg Am* 1985, **67:**303-314.

16. Lindsay T, Romaschin A, Walker PM: **Free radical mediated damage in skeletal muscle.** *Microcirc Endothelium Lymphatics* 1989, **5:**157-170.
17. Germann G, Drucke D, Steinau HU: **Adhesion receptors and cytokine profiles in controlled tourniquet ischaemia in the upper extremity.** *J Hand Surg Br* 1997, **22:**778-782.
18. Sutter PM, Spagnoli GC, Marx A, Gurke L, Troeger H, Fricker R, Harder F, Heberer M: **Increased surface expression of CD18 and CD11b in leukocytes after tourniquet ischemia during elective hand surgery.** *World J Surg* 1997, **21:**179-184; discussion 185.
19. Huda R, Solanki DR, Mathru M: **Inflammatory and redox responses to ischaemia/reperfusion in human skeletal muscle.** *Clin Sci (Lond)* 2004, **107:**497-503.
20. Gute DC, Ishida T, Yarimizu K, Korthuis RJ: **Inflammatory responses to ischemia and reperfusion in skeletal muscle.** *Mol Cell Biochem* 1998, **179:**169-187.
21. Chappell D, Hofmann-Kiefer K, Jacob M, Rehm M, Briegel J, Welsch U, Conzen P, Becker BF: **TNF-alpha induced shedding of the endothelial glycocalyx is prevented by hydrocortisone and antithrombin.** *Basic Res Cardiol* 2009, **104:**78-89.
22. Morgan MR, Humphries MJ, Bass MD: **Synergistic control of cell adhesion by integrins and syndecans.** *Nat Rev Mol Cell Biol* 2007, **8:**957-969.
23. Lamanna WC, Kalus I, Padva M, Baldwin RJ, Merry CL, Dierks T: **The heparanome--the enigma of encoding and decoding heparan sulfate sulfation.** *J Biotechnol* 2007, **129:**290-307.
24. Gandhi NS, Mancera RL: **The structure of glycosaminoglycans and their interactions with proteins.** *Chem Biol Drug Des* 2008, **72:**455-482.
25. Woodfin A, Voisin MB, Imhof BA, Dejana E, Engelhardt B, Nourshargh S: **Endothelial cell activation leads to neutrophil transmigration as supported by the sequential roles of ICAM-2, JAM-A, and PECAM-1.** *Blood* 2009, **113:**6246-6257.
26. Datta YH, Ewenstein BM: **Regulated secretion in endothelial cells: biology and clinical implications.** *Thromb Haemost* 2001, **86:**1148-1155.
27. Hughes SF, Hendricks BD, Edwards DR, Bastawrous SS, Roberts GE, Middleton JF: **Mild episodes of tourniquet-induced forearm ischaemia-reperfusion injury results in leukocyte activation and changes in inflammatory and coagulation markers.** *J Inflamm (Lond)* 2007, **4:**12.
28. Hughes SF, Hendricks BD, Edwards DR, Middleton JF: **Tourniquet-applied upper limb orthopaedic surgery results in increased inflammation and changes to leukocyte, coagulation and endothelial markers.** *PLoS One* 2010, **5:**e11846.
29. Storini C, Rossi E, Marrella V, Distaso M, Veerhuis R, Vergani C, Bergamaschini L, De Simoni MG: **C1-inhibitor protects against brain ischemia-reperfusion injury via inhibition of cell recruitment and inflammation.** *Neurobiol Dis* 2005, **19:**10-17.
30. Friedl HP, Smith DJ, Till GO, Thomson PD, Louis DS, Ward PA: **Ischemia-reperfusion in humans. Appearance of xanthine oxidase activity.** *Am J Pathol* 1990, **136:**491-495.
31. Yung LM, Leung FP, Yao X, Chen ZY, Huang Y: **Reactive oxygen species in vascular wall.** *Cardiovasc Hematol Disord Drug Targets* 2006, **6:**1-19.
32. Ferencik M: **[Molecular and cellular mechanisms in inflammatory reactions].** *Bratisl Lek Listy* 1995, **96:**509-519.

33. Ferencik M, Stvrtinova V: **Endogenous control and modulation of inflammation.** *Folia Biol (Praha)* 1996, **42:**47-55.

34. Akira S, Isshiki H, Nakajima T, Kinoshita S, Nishio Y, Natsuka S, Kishimoto T: **Regulation of expression of the interleukin 6 gene: structure and function of the transcription factor NF-IL6.** *Ciba Found Symp* 1992, **167:**47-62; discussion 62-47.

35. Clementsen T, Reikeras O: **Cytokine patterns after tourniquet-induced skeletal muscle ischaemia reperfusion in total knee replacement.** *Scand J Clin Lab Invest* 2008, **68:**154-159.

36. Lu B, Rutledge BJ, Gu L, Fiorillo J, Lukacs NW, Kunkel SL, North R, Gerard C, Rollins BJ: **Abnormalities in monocyte recruitment and cytokine expression in monocyte chemoattractant protein 1-deficient mice.** *J Exp Med* 1998, **187:**601-608.

37. Shireman PK, Contreras-Shannon V, Ochoa O, Karia BP, Michalek JE, McManus LM: **MCP-1 deficiency causes altered inflammation with impaired skeletal muscle regeneration.** *J Leukoc Biol* 2007, **81:**775-785.

38. Cherwek DH, Hopkins MB, Thompson MJ, Annex BH, Taylor DA: **Fiber type-specific differential expression of angiogenic factors in response to chronic hindlimb ischemia.** *Am J Physiol Heart Circ Physiol* 2000, **279:**H932-938.

39. Iihara K, Sasahara M, Hashimoto N, Uemura Y, Kikuchi H, Hazama F: **Ischemia induces the expression of the platelet-derived growth factor-B chain in neurons and brain macrophages in vivo.** *J Cereb Blood Flow Metab* 1994, **14:**818-824.

40. Wu AH, Perryman MB: **Clinical applications of muscle enzymes and proteins.** *Curr Opin Rheumatol* 1992, **4:**815-820.

41. Banz Y, Hess OM, Robson SC, Mettler D, Meier P, Haeberli A, Csizmadia E, Korchagina EY, Bovin NV, Rieben R: **Locally targeted cytoprotection with dextran sulfate attenuates experimental porcine myocardial ischaemia/reperfusion injury.** *Eur Heart J* 2005, **26:**2334-2343.

42. Banz Y, Hess OM, Robson SC, Csizmadia E, Mettler D, Meier P, Haeberli A, Shaw S, Smith RA, Rieben R: **Attenuation of myocardial reperfusion injury in pigs by Mirococept, a membrane-targeted complement inhibitor derived from human CR1.** *Cardiovasc Res* 2007, **76:**482-493.

Paper II

Testing Dexrazoxane as an Attenuator of Ischemia/Reperfusion Injury in a Closed-Chest Porcine Model of Myocardial Infarction

Pranitha J Kamat, MSc[1]; Stijn Vandenberghe, PhD[2]; Stephan Christen, PhD[3]; Olgica Beslac[1]; Daniel Mettler, DVM[1];
Bernhard Meier, MD[4]; Otto M Hess, MD[4]; Robert Rieben, PhD[1]; Ahmed A Khattab, MD.[4]

[1] Department of Clinical Research, University of Bern, [2] ARTORG Center, University of Bern, [3]Department of Infectious Diseases, University of Bern, [4]Department of Cardiology, Bern University Hospital, Bern, Switzerland

During ischemia/reperfusion there is an overload of calcium and iron metal ions within the cell. Calcium overload induces cardiomyocyte death through hypercontracture, while iron catalyses generation of reactive oxygen species (ROS).

Aim: To attenuate ischemia/reperfusion injury by using a potent intracellular metal chelator, dexrazoxane.

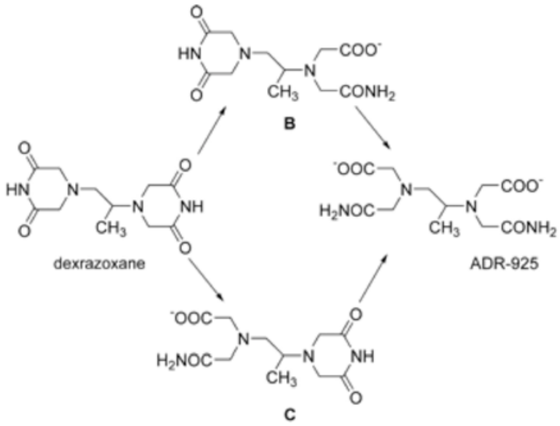

Dexrazoxane is hydrolyzed in vivo. B and C are its one-ring open hydrolysis intermediates. ADR 925 is its complete hydrolysis product which has metal chelating properties.

Model: Myocardial infarction in pigs with 1 hour ischemia and 2 hours reperfusion.

Conclusion: Dexrazoxane favorably reduces endothelial cell activation (analyzed by CD 31), leukocyte recruitment (analyzed by MCP-1) and cardiac function (increased stroke volume) but has no effects on reduction of infarct size and complement deposition.

Testing Dexrazoxane as an Attenuator of Ischemia/Reperfusion Injury in a Closed-Chest Porcine Model of Myocardial Infarction

Pranitha J Kamat, MSc[1]; Stijn Vandenberghe, PhD[2]; Stephan Christen, PhD[3] Olgica Beslac[1];
Daniel Mettler, DVM[1]; Bernhard Meier, MD[4]; Otto M Hess, MD[4]; Robert Rieben, PhD[1];
Ahmed A Khattab, MD.[4]

[1] Department of Clinical Research, University of Bern, [2] ARTORG Center, University of Bern, [3]Depatment of Infectious Diseases, University of Bern, [4]Department of Cardiology, Bern University Hospital, Bern, Switzerland

(Manuscript in process of submission)

No conflicts of interest to be disclosed

Address for correspondence

Ahmed A Khattab, MD

Department of Cardiology

Swiss Cardiovascular Center

University Hospital

3010 Bern, Switzerland

Tel: +41-31-6324714

E-mail: ahmed.khattab@insel.ch

Abstract

Background: The mechanism of ischemia reperfusion (IR) injury during myocardial infarction (MI) is not fully elucidated although calcium and iron overload may play a central role in this deleterious process. Calcium overload induces cardiomyocyte death through hypercontracture, while iron catalyses generation of reactive oxygen species (ROS). We hypothesized that dexrazoxane, a potent intracellular metal chelator, would attenuate IR injury.

Methods: MI was induced by balloon occlusion of left anterior descending artery for 1 hour followed by 2 hours reperfusion in a closed-chest porcine model. 30 min before reperfusion either 400mg/80ml dexrazoxane (n=5) or 80ml placebo (n=5) was infused intravenously in a randomized and blinded fashion. The left ventricular function was recorded at all times. Myocardial necrosis was determined after sacrificing the animals by staining the ischemic myocardium with triphenyl tetrazolium chloride and by measuring serum troponin-I levels. Inflammation and vascular damage were assessed in the tissue and blood samples.

Results: Significantly higher stroke volumes (p=0.03) and lower MCP-1 (inflammatory cytokine induced by ROS; p=0.007) and CD31 (marker for endothelial dysfunction; p=0.049) levels were noticed in the dexrazoxane group. Necrotic area was similar as was troponin-I level in both groups. Inflammation analyzed by C3c and C5b9 on tissue and in serum was also similar between groups.

Conclusions: Dexrazoxane attenuated IR injury favorably and preserved stroke volume by reducing MCP1 and CD31 levels. This may be attributed to the metal chelating property of dexrazoxane.

Keywords: ischemia reperfusion injury, ROS, Dexrazoxane, cardiac function, inflammation

Introduction

Although mortality rates of acute myocardial infarction have considerably declined over the past decades [43,44,45] yet the risk of heart failure and death remains high [43]. Prompt recanalization of the infarct-related artery, preferably by percutaneous coronary intervention (PCI) to re-establish myocardial perfusion comprises the state-of-art treatment. Myocardial reperfusion however, can paradoxically induce injury and thereby contribute to the adverse outcome after myocardial infarction. This phenomenon is termed ischemia/reperfusion (IR) injury.

The exact mechanism of IR injury is not fully elucidated, yet a multifactorial etiology is likely. Tissue necrosis, which is an end result of inflammation, is triggered by three synergistic pathways during IR. Shedding of the endothelial glycocalyx rendering the endothelial surface pro-inflammatory and pro-coagulative is one of the primary pathways. Recognition of neoepitopes by natural antibodies, activating the complement system and resulting in inflammation is the second pathway. Last not least, is the generation of reactive oxygen species (ROS) [46,47].

ROS are generated by sequential breakdown of oxygen during reperfusion [48] and in the heart by anaerobic mitochondrial respiration [49,50], activated neutrophils [51,52] and enzymes [53]. In short, reperfusion reintroduces oxygen to the previously ischemic i.e. oxygen deprived tissue which results in a sudden deleterious burst of ROS including hydroxyl radical, superoxide anion and hydrogen peroxide [54]. Generation of ROS has been detected during myocardial infarction in humans and some antioxidants have shown to attenuate myocardial infarction in vivo in animals [55,56]. Among the different ROS generated, hydroxyl radical is a strong oxidant that is not scavenged by any of the available biological scavengers, and leads to peroxidation of lipid membranes [57]. In biological systems it is formed in the presence of transition metals like iron that act as catalysts [58]. Since iron propagates the effects of ROS, shielding or neutralizing it may be effective in reducing tissue damage during IR [59]. Previous study has shown reduction in myocardial infarct size by either replacing or chelating the iron [60].

Calcium paradox defines an abrupt increase of intracellular calcium during reperfusion, resulting in cardiac cell death due to hypercontracture and mitochondrial permeability transition pore opening [61,62].

Dexrazoxane is clinically approved to reduce anthracyclin-induced cardiotoxicity [63,64,65,66]. It is a bis-dioxopiperazine that is intracellularly hydrolyzed to ADR-925 [67,68] and has proven to reduce redox activity of iron by chelating it [68,69]. The free iron binding capacities of Dexrazoxane has also been shown in hypoxic conditions [70]. As an anion binding to dicationic iron, it even preferentially binds to calcium in its presence [71]. We therefore hypothesized that Dexrazoxane would favorably attenuate myocardial infarction and tested it in a pig model, for its similarity to human heart [72].

Material and methods

Care and use of animals in the present study were in compliance with the Guide for the Care and Use of Laboratory Animals (NIH publication no. 85-23, revised 1996) as well as Swiss National Guidelines. The local ethical committee for animal research (Amt für Landwirtschaft und Natur des Kantons Bern) approved the conduction of this study.

Closed-chest porcine model of myocardial infarction

Ten medium-sized house pigs (30 ± 2 kg) were pre-medicated with ketamine (20 mg/kg), midazolam (0.5 mg/kg) and atropine (0.05 mg/kg), intubated, and mechanically ventilated with a Draeger respirator (O_2/N_2O 1:3, isoflurane 1–1.5 vol.%). Continuous infusions of pancuronium bromide (1 mg/kg/h i.v) and fentanyl (10 µ g/kg/h i.v.) were given throughout the procedure. ECG, mean arterial pressure were recorded throughout with a Hewlett-Packard CMS patient monitor.

A single bolus of unfractionated heparin (5000 IU) was administered intravenously before starting the procedure. Heparin (2500 IU) was administered intravenously every two hours after then.

The left anterior descending (LAD) artery was occluded just distally of the first large diagonal branch with a semi-compliant conventional PCI balloon catheter (balloon length 20 mm, diameter 3.0 mm). The balloon was inflated to completely occlude the vessel (used pressure 4–6 atm) for 60 min. Localization of the balloon and state of inflation was controlled angiographically on a regular basis using a BV PULSERA digital mobile C-arm fluoroscopy system (Philips Medical System).

Thirty minutes after the onset of ischemia 80ml of 5mg/ml Dexrazoxane (Cardoxane®, Novartis, Switzerland, hereafter Dex), (n=5) or 80ml saline (n=5) was infused intravenously. Then the balloon was deflated (and removed) to allow for 2 hours of reperfusion. Following 2 hours reperfusion, the balloon was re-introduced and re-inflated at the same place in the LAD and 60 ml Evan's Blue (2% wt/vol solution) was injected intravenously. The pigs were sacrificed with an intravenous 10ml bolus of 20% potassium chloride just after Evan's Blue injection and the heart excised for further analysis.

All experimenters were blinded with regard to treatment assignment. Randomization of the animals into the 2 groups was done using a randomization code with a random number generator prior to the experiment. The 80 ml samples were prepared according to the randomization output on the morning of each experiment by an independent laboratory technician. Sample size was determined in advance, estimated from previous experience and not by formal sample size calculations.

In the case of ventricular fibrillation during the experiment, a biphasic defibrillator (150 J) was used for cardioconversion.

Myocardial area at risk and necrosis

The excised heart was cut perpendicular to the septum from the apex to the base into 3 mm slices until the mitral valve. For every slice the Evan's Blue unstained parts within the left ventricle were separated, weighed and expressed as a percentage of the left ventricle. This gave the myocardial area at ischemic risk (AAR) as percentage of the left ventricle. The AAR from all slices were then treated with 1% triphenyl tetrazolium chloride (TTC, Sigma, pH 7.4) for 20 min at 37°C. Viable myocardium [viable ischemic tissue (VIT)] was stained bright red while the infarcted tissue [necrotic ischemic tissue (NIT)], remained unstained. High dynamic range images of the slices were taken after the TTC staining. The TTC unstained areas within the AAR was marked by ImageJ software and expressed as percentage of the AAR to obtain the myocardial necrosis/infarct size. Tissue samples were taken from the Evan's Blue stained areas, which were not at ischemic risk (ANR), NIT and VIT for immunostaining.

Measurement of left ventricular function using pressure-volume loops

A conductance catheter (Scisense ADVantage system) was placed in the left ventricle that measured the left ventricular pressure and volume. The catheter was calibrated for individual pigs based on the blood conductance. The catheter was positioned so that left ventricular pressure-volume loops displayed stable rectangular shapes and the admittance phase and magnitude signals showed pulsatile signals. Data was recorded at all times during the experiment. Data acquisition and analysis was done with the Chart5 software. The analyzed parameters were end systolic pressure (ESP), end diastolic pressure (EDP), ejection fraction (EF), stroke volume (SV) and stroke work (SW). Time points of analysis were at baseline, 50 min after ischemia, 1 hour and 2 hour after reperfusion. Value at each time point was expressed as a percentage of baseline and the area under the curve (AUC) were obtained for every pig. Both groups were then compared based on the AUC.

Soluble markers for myocardial necrosis, inflammation and vascular damage

Serum samples collected at baseline, 50 min after ischemia, 10 min, 1 hour and 2 hour after reperfusion were analyzed. Commercially available antibodies specific for porcine CD31 (mAb, R&D), cardiac Troponin (cTn)-I (mAb, HyTest), MCP-1 (pAb, Peprotech), C3c (pAb, Dako), and C5b-9 (mAb, Diatec) were used as capture antibodies. Each antibody was coupled to different fluorescently labeled polystyrene COOH Luminex-beads by using Bio-Plex amine coupling kit (Bio-Rad). The amount of captured analytes was then measured by using biotinylated detection antibodies, followed by streptavidin-PE.

Calibration curves from recombinant protein standards were prepared with threefold dilution steps in antibody diluent containing 0.5% polyvinyl alcohol and 0.8% polyvinylpyrrolidone. Standards were measured, and blank values were subtracted from all readings. A mixture containing 2500 coupled beads per antibody (50 µl/well) was incubated with the standards, sample and blank in a final volume of 50 µl/well. The mix was incubated for 60 min at room temperature. Beads were washed thrice, and incubated together with a cocktail of biotinylated antibodies: anti PECAM-1 (pAb, R&D), anti cTn-I (pAb, HyTest), anti MCP-1 (pAb, Peprotech), anti C3c (pAb, Dako) and anti C5b-9 (mAb, Quidel) in a final volume 25 µl/well. After 30 min incubation with biotinylated antibody, streptavidin-PE (50 µl/well) was added. Measurement and data analysis were performed with the Bio-Plex system and Bio-Plex Manager software.

Markers for inflammation on tissue

Immunofluorescence staining was done by the free float technique in tissue samples obtained from three regions of the excised heart. The samples, ANR, VIT and NIT were fixed in 2% formaldehyde for 24 hours followed by overnight incubation in 18% sucrose at 4°C. Samples were then embedded in Shandon M1 embedding matrix and stored at - 20°C until staining.

Tissues were sectioned to 30 µm thickness and permeablized with triton-X-100 for 15min at room temperature. Sections were then incubated with the directly labeled primary antibodies, goat anti porcine IgG FITC and goat anti porcine IgM FITC (Southern Biotech and Serotec respectively) for 90 min at room temperature. The unlabelled primary antibodies sheep anti human C3b/c (Dako A0062) and sheep anti human C5b9 (Dako) were incubated overnight at 4°C. The secondary antibodies used was rabbit anti sheep Cy3 (Sigma) for both C3b/c and C5b9 and was incubated for 90 min at room temperature.

A normal pigs heart was used as common sample in every batch of staining. Representative images were taken with a confocal microscope from the stained sections. Histogram for the images were obtained with ImageJ software and normalized with histogram from their corresponding common sample. Area under the curve (AUC) value was then obtained from the normalized histograms. Sections were finally compared based on the AUC values thereby avoiding errors between staining batches. Sections were blinded at all times regarding treatment groups.

Statistical analysis

AUC values for parameters of heart function were compared by one tailed Mann-Whitney test. Myocardial necrosis and soluble markers in the serum at each time point between the groups were compared by two-tailed T-test. One-Way ANOVA and Bonferroni's post test compared different tissue samples from both groups.

Results

Myocardial area at risk and necrosis

The area of the left ventricle subjected to ischemic risk (AAR) was comparable in both groups. This was expressed as a percentage of the left ventricle and was 44 ± 4% for the Dex group and 48.8 ± 11% for the saline group (Figure 1A). The myocardial necrosis was also on an average similar in both the groups (Figure 1B). This was expressed as percentage of the AAR and was 77.2 ± 18% for Dex group and 76.4 ± 14% for the saline group.

Left ventricular function

Figure 2 shows an average of the percentage baseline values with standard deviation. At 2 hours after reperfusion, the ESP and EDP were higher in the saline group and EF, SW and SV were higher in the Dex group. The overall performance of the heart indicated by AUC value was significantly higher in the Dex group for SV ($p=0.03$).

Soluble markers for myocardial necrosis, inflammation and vascular damage

Serum samples were analyzed for cTn-I, MCP-1, CD31, C3b/c and C5b9. Serum levels of all these proteins were similar in both groups until 10 min reperfusion. However at the end of 2 hours reperfusion, C3b/c, C5b9, MCP-1 and CD31 levels were lower in the Dex group compared to the saline group. This was significant for MCP-1 and CD31 with $p=0.007$ and $p=0.049$, respectively.

Markers of inflammation on tissue

The deposition of natural antibodies IgG and IgM were almost similar on the ANR, VIT and NIT in both groups. Although IgG on NIT of Dex group was slightly higher than NIT of saline group, this increase was not significant. The ANR and VIT for both groups had comparable deposition of C3b/c with higher deposition on the NIT from Dex group. Complement end product C5b9 was similar in ANR and NIT of both groups with slightly higher deposition on VIT from Dex group.

Discussion

The findings of this study indicate a favorable effect of Dexrazoxane, a potent intracellular chelating agent, during reperfusion therapy for acute myocardial infarction probably by reducing IR injury caused by calcium overload and ROS. The experimental model used and the mode of drug application (intravenously 30min before the onset of reperfusion) and its dosage (5mg/ml which is clinically approved), make the setting very similar to a clinical scenario. An in vivo model was further essential as the activity of ROS is known to differ between in vivo and ex vivo models [73].

Myocardial IR is characterized by calcium overload that ultimately suppresses myocardial function, the so-called calcium paradox that is secondary to sarcolemmal membrane damage and oxidative stress-induced dysfunction of the sarcoplasmic reticulum [74,75]. Dex chelates free and bound iron but preferentially binds to calcium in its presence [71]. In our study, we demonstrated a significant preservation of stroke volume in the hearts of Dex treated pigs. This effect of Dex has been previously shown in rats [76,77].

To our knowledge only one study has been conducted to test Dex in a model of myocardial infarction in vivo [76]. This study has shown significant reduction in myocardial necrosis after intraperitonial injection of Dex in rats. Our study with pigs however showed no reduction in the myocardial infarct size upon treatment with Dex, measured both histologically, and chemically using cardiac troponin–I (cTN-I) levels in the circulation.

Upon reperfusion after a prolonged period of ischemia, the affected endothelium takes on a pro-coagulant and pro-inflammatory phenotype, with upregulation of pro-coagulant tissue factor and vascular adhesion molecules, as well as stimulation of cytokine production [61,62,78,79]. Importantly, reperfusion appears to be critical for injury to the luminal surface coating of the endothelium, the glycocalyx [4]. A direct marker for endothelial dysfunction is platelet endothelial cell adhesion molecule-1 (CD31) [80,81]. We therefore measured soluble CD31 in serum to account for any protective effect of Dex in diminishing ROS mediated endothelial dysfunction. The circulating CD31 levels in Dex treated pigs were significantly lower at the end of 2 hours reperfusion when compared to the saline treated pigs. This indicates that Dex reduces reperfusion-induced endothelial damage probably by reducing the availability of ROS.

Monocyte chemotactic protein-1 (MCP-1) is an oxy-sensitive chemokine that participates in recruiting leukocytes [82]. Its expression by the myocardial cells and endothelial cells during early reperfusion is induced by ROS [83,84,85]. Infact, the production of ROS is necessary for the activation of MCP-1 even in the absence of infarction [86]. The infusion of Dex during myocardial infarction in our model significantly reduced the circulating levels of MCP-1. This may again indicate the reduction of ROS by Dex that in turn resulted in a decrease in MCP-1. A study conducted by Chen et al. supports this concept as it shows reduced expression of MCP-1 in the absence of ROS and iron [87].

The necrosis in myocardial infarction is an end result of inflammation in the tissue. Apart from ROS, there are other inflammatory molecules that play important roles during reperfusion. Deposition of natural antibodies on the ischemic myocardium activates the complement system at the onset of reperfusion. We therefore looked for IgG and IgM natural antibody deposition on the tissue at the end of 2hours of reperfusion. IgG deposition was almost similar on the ANR and VIT in both the groups. The NIT from Dex treated pigs was non-significantly higher than NIT from saline treated pigs. IgM deposition on ANR, VIT and NIT were similar in both groups. Rather interesting was the fact that IgM deposition was lowest on the necrotic (NIT) tissue, where one would expect highest deposition. This may be related to the time point during reperfusion.

Markers for complement activation C3b/c and C5b9 were analyzed both on the tissue sample and in the serum. On the tissue, C3b/c complement deposition was similar in the ANR and VIT between the groups. In the NIT, the deposition was higher in Dex than in saline group. For C5b9, the deposition was similar on ANR and NIT in both groups. But the deposition was higher in Dex than in saline for VIT. In the serum, circulating C3c and C5b9 were higher in the Dex group than in the saline group by the end of 2hours reperfusion. C3c is a byproduct in the complement cascade and C5b9 the end product. C5b9, also known as the membrane attack complex punches holes into the cell membrane turning them necrotic. Higher C3b/c and C5b9 in the Dex group underline the multiple pathways responsible for IR injury.

Conclusion: In a clinically relevant model of myocardial infarction and 2 hours reperfusion, Dexrazoxane ameliorated IR injury as reflected by preserved stroke volume and reduced MCP-1 and CD31 levels. However, there was no reduction in myocardial infarct size and complement activation. A chronic animal model is needed in a next step to demonstrate differences such as long-term effects on left ventricular function and death.

Acknowledgement

We would like to thank Anjan Bongoni for analyzing the serum samples in Bioplex. Also, Katja Matozan for support in conducting the pig experiments.

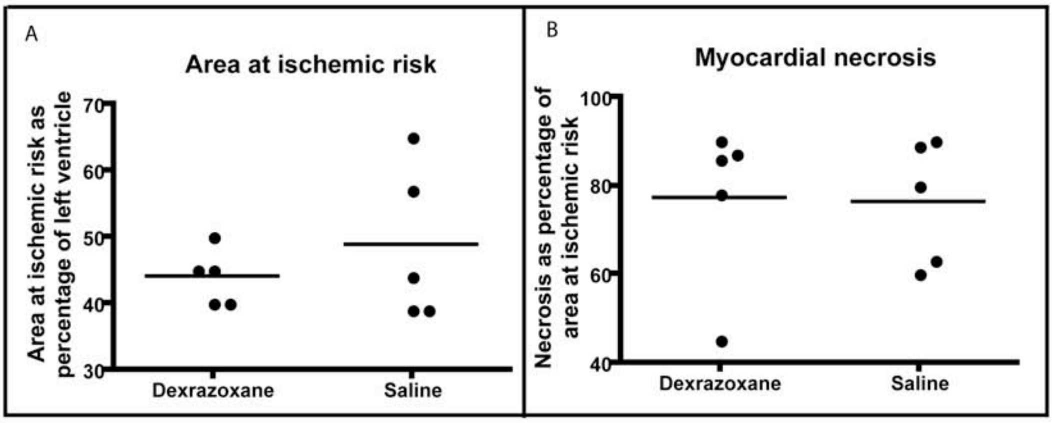

Figure 1: Myocardial area at risk and necrosis

The area at ischemic risk expressed as percentage of the left ventricle (A). The myocardial necrosis expressed as percentage of the ischemic area at risk within the left ventricle (B).

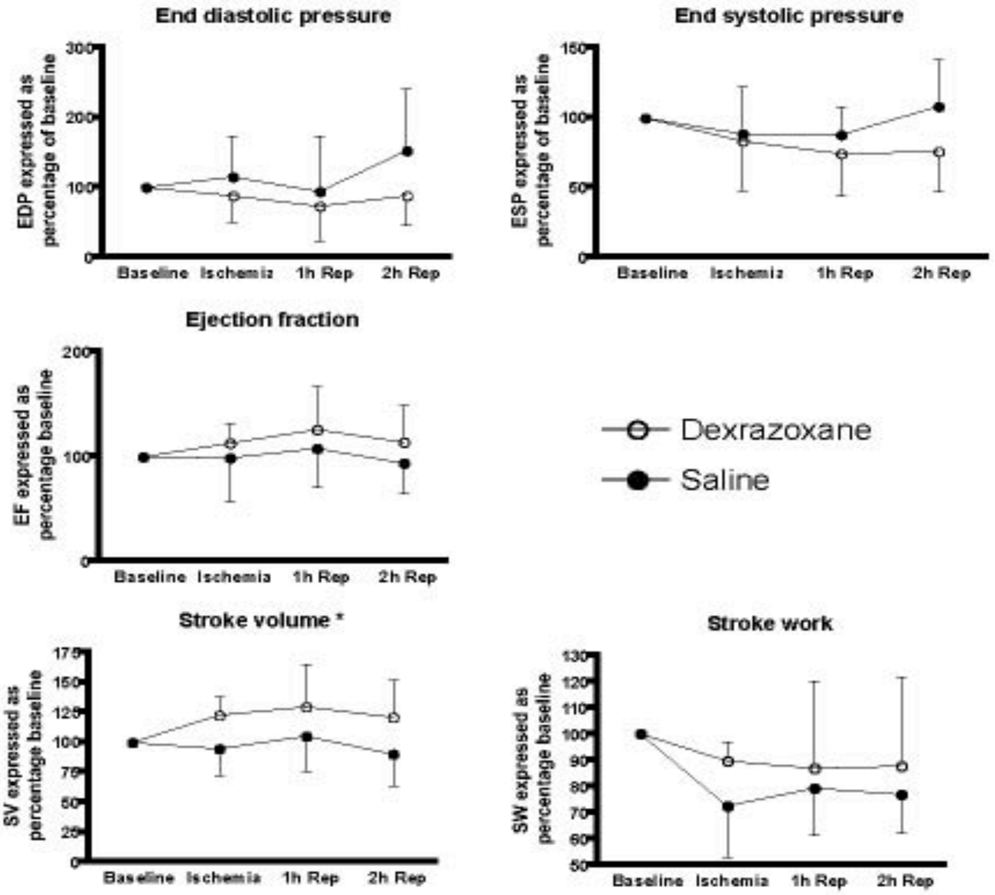

Figure 2: Measurement of left ventricular function using pressure-volume loops

Figure shows end systolic pressure (ESP), end diastolic pressure (EDP), ejection fraction (EF), stroke volume (SV) and stroke work (SW). Values at baseline, 50 min after ischemia (ischemia), 1 hour and 2 hours after reperfusion (1h Rep and 2h Rep respectively) are represented as percentage of baseline.

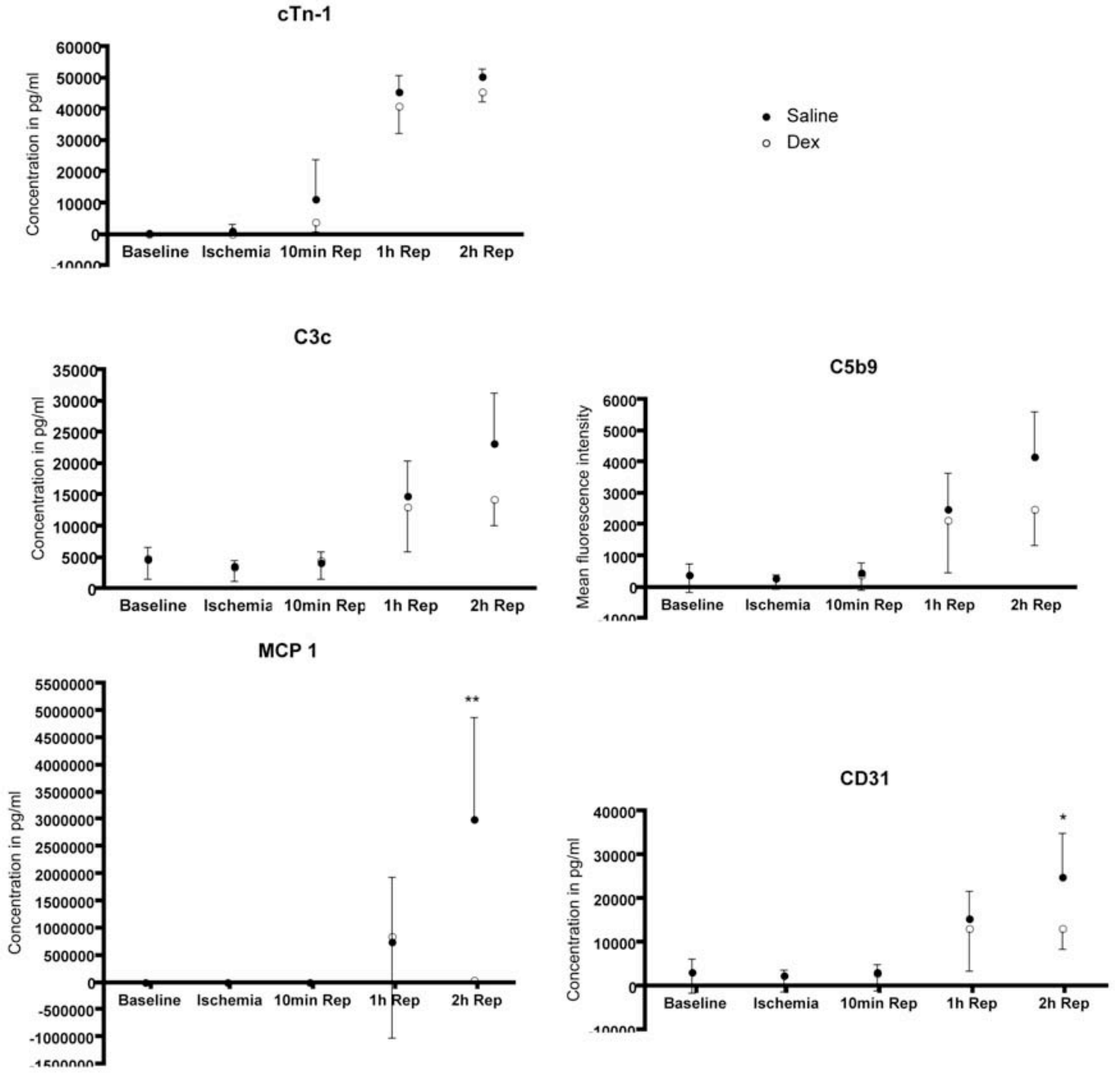

Figure 3: Soluble markers for myocardial necrosis, inflammation and vascular damage

Cardiac Troponin I, complement product C5b9 (C5b9), monocytes chemotactic protein 1 (MCP-1), complement product C3c (C3c) and platelet endothelial cell adhesion molecule 1 (CD31) were measured at baseline, 50 min after ischemia (ischemia), 10 min, 1 hour and 2 hour after reperfusion (10min Rep, 1h Rep and 2h Rep respectively).

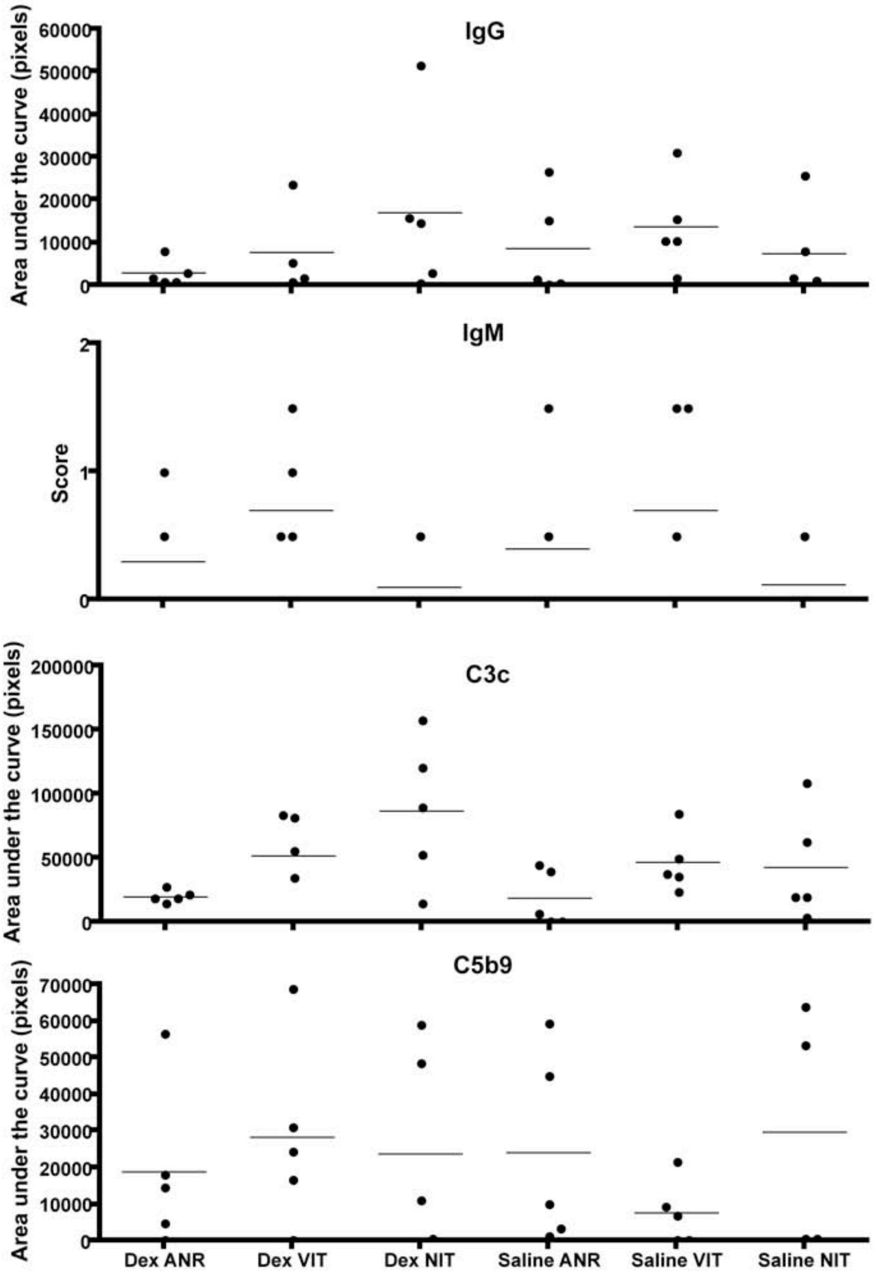

Figure 4: Markers for inflammation on tissue

Deposition of natural antibodies (IgG, IgM) and complement products (C3b/c, C5b9) were analyzed on tissue samples. ANR (area not at ischemic risk), VIT (viable ischemic tissue) and NIT (necrotic ischemic tissue).

References

1 Lloyd-Jones D, Adams RJ, Brown TM, Carnethon M, Dai S, De Simone G, Ferguson TB, Ford E, Furie K, Gillespie C, Go A, Greenlund K, Haase N, Hailpern S, Ho PM, Howard V, Kissela B, Kittner S, Lackland D, Lisabeth L, Marelli A, McDermott MM, Meigs J, Mozaffarian D, Mussolino M, Nichol G, Roger VL, Rosamond W, Sacco R, Sorlie P, Thom T, Wasserthiel-Smoller S, Wong ND, Wylie-Rosett J: Heart disease and stroke statistics--2010 update: A report from the american heart association. Circulation;121:e46-e215.

2 Fox KA, Steg PG, Eagle KA, Goodman SG, Anderson FA, Jr., Granger CB, Flather MD, Budaj A, Quill A, Gore JM: Decline in rates of death and heart failure in acute coronary syndromes, 1999-2006. JAMA 2007;297:1892-1900.

3 Krumholz HM, Wang Y, Chen J, Drye EE, Spertus JA, Ross JS, Curtis JP, Nallamothu BK, Lichtman JH, Havranek EP, Masoudi FA, Radford MJ, Han LF, Rapp MT, Straube BM, Normand SL: Reduction in acute myocardial infarction mortality in the united states: Risk-standardized mortality rates from 1995-2006. JAMA 2009;302:767-773.

4 Bolli R: Mechanism of myocardial "Stunning". Circulation 1990;82:723-738.

5 Powell SR, Tortolani AJ: Recent advances in the role of reactive oxygen intermediates in ischemic injury. I. Evidence demonstrating presence of reactive oxygen intermediates; ii. Role of metals in site-specific formation of radicals. J Surg Res 1992;53:417-429.

6 Bolli R, Jeroudi MO, Patel BS, DuBose CM, Lai EK, Roberts R, McCay PB: Direct evidence that oxygen-derived free radicals contribute to postischemic myocardial dysfunction in the intact dog. Proc Natl Acad Sci U S A 1989;86:4695-4699.

7 Tompkins AJ, Burwell LS, Digerness SB, Zaragoza C, Holman WL, Brookes PS: Mitochondrial dysfunction in cardiac ischemia-reperfusion injury: Ros from complex i, without inhibition. Biochim Biophys Acta 2006;1762:223-231.

8 Hess ML, Manson NH: Molecular oxygen: Friend and foe. The role of the oxygen free radical system in the calcium paradox, the oxygen paradox and ischemia/reperfusion injury. J Mol Cell Cardiol 1984;16:969-985.

9 Duilio C, Ambrosio G, Kuppusamy P, DiPaula A, Becker LC, Zweier JL: Neutrophils are primary source of o2 radicals during reperfusion after prolonged myocardial ischemia. Am J Physiol Heart Circ Physiol 2001;280:H2649-2657.

10 Mitsos SE, Askew TE, Fantone JC, Kunkel SL, Abrams GD, Schork A, Lucchesi BR: Protective effects of n-2-mercaptopropionyl glycine against myocardial reperfusion injury after neutrophil depletion in the dog: Evidence for the role of intracellular-derived free radicals. Circulation 1986;73:1077-1086.

11 Szocs K: Endothelial dysfunction and reactive oxygen species production in ischemia/reperfusion and nitrate tolerance. Gen Physiol Biophys 2004;23:265-295.

12 Kloner RA, Przyklenk K, Whittaker P: Deleterious effects of oxygen radicals in ischemia/reperfusion. Resolved and unresolved issues. Circulation 1989;80:1115-1127.

13 McCormick J, Barry SP, Sivarajah A, Stefanutti G, Townsend PA, Lawrence KM, Eaton S, Knight RA, Thiemermann C, Latchman DS, Stephanou A: Free radical scavenging inhibits stat phosphorylation following in vivo ischemia/reperfusion injury. FASEB J 2006;20:2115-2117.

14 Sukmawan R, Yada T, Toyota E, Neishi Y, Kume T, Shinozaki Y, Mori H, Ogasawara Y, Kajiya F, Yoshida K: Edaravone preserves coronary microvascular endothelial function after ischemia/reperfusion on the beating canine heart in vivo. J Pharmacol Sci 2007;104:341-348.

15 Bagchi M, Prasad MR, Engelman RM, Das DK: Effects of free radicals on the fluidity of myocardial membranes. Free Radic Res Commun 1989;7:375-380.

16 Liochev SI: The mechanism of "Fenton-like" Reactions and their importance for biological systems. A biologist's view. Met Ions Biol Syst 1999;36:1-39.

17 Berenshtein E, Mayer B, Goldberg C, Kitrossky N, Chevion M: Patterns of mobilization of copper and iron following myocardial ischemia: Possible predictive criteria for tissue injury. J Mol Cell Cardiol 1997;29:3025-3034.

18 Karck M, Tanaka S, Berenshtein E, Sturm C, Haverich A, Chevion M: The push-and-pull mechanism to scavenge redox-active transition metals: A novel concept in myocardial protection. J Thorac Cardiovasc Surg 2001;121:1169-1178.

19 Minezaki KK, Suleiman MS, Chapman RA: Changes in mitochondrial function induced in isolated guinea-pig ventricular myocytes by calcium overload. J Physiol 1994;476:459-471.

20 Mochizuki S, Jiang C: Na+/ca++ exchanger and myocardial ischemia/reperfusion. Jpn Heart J 1998;39:707-714.

21 Herman EH, Ferrans VJ: Reduction of chronic doxorubicin cardiotoxicity in dogs by pretreatment with (+/-)-1,2-bis(3,5-dioxopiperazinyl-1-yl)propane (icrf-187). Cancer Res 1981;41:3436-3440.

22 Cvetkovic RS, Scott LJ: Dexrazoxane : A review of its use for cardioprotection during anthracycline chemotherapy. Drugs 2005;65:1005-1024.

23 Kane RC, McGuinn WD, Jr., Dagher R, Justice R, Pazdur R: Dexrazoxane (totect): Fda review and approval for the treatment of accidental extravasation following intravenous anthracycline chemotherapy. Oncologist 2008;13:445-450.

24 Hasinoff BB, Hellmann K, Herman EH, Ferrans VJ: Chemical, biological and clinical aspects of dexrazoxane and other bisdioxopiperazines. Curr Med Chem 1998;5:1-28.

25 Hasinoff BB: The hydrolysis activation of the doxorubicin cardioprotective agent icrf-187 [+)-1,2-bis(3,5-dioxopiperazinyl-1-yl)propane). Drug Metab Dispos 1990;18:344-349.

26 Hasinoff BB: Pharmacodynamics of the hydrolysis-activation of the cardioprotective agent (+)-1,2-bis(3,5-dioxopiperazinyl-1-yl)propane. J Pharm Sci 1994;83:64-67.

27 Hasinoff BB: Chemistry of dexrazoxane and analogues. Semin Oncol 1998;25:3-9.

28 Hasinoff BB: Dexrazoxane (icrf-187) protects cardiac myocytes against hypoxia-reoxygenation damage. Cardiovasc Toxicol 2002;2:111-118.

29 Hasinoff BB, Schroeder PE, Patel D: The metabolites of the cardioprotective drug dexrazoxane do not protect myocytes from doxorubicin-induced cytotoxicity. Mol Pharmacol 2003;64:670-678.

30 Crick SJ, Sheppard MN, Ho SY, Gebstein L, Anderson RH: Anatomy of the pig heart: Comparisons with normal human cardiac structure. J Anat 1998;193 (Pt 1):105-119.

31 Coudray C, Boucher F, Pucheu S, De Leiris J, Favier A: Relationship between severity of ischemia and oxidant scavenger enzyme activities in the isolated rat heart. Int J Biochem Cell Biol 1995;27:61-69.

32 Tamareille S, Achour H, Amirian J, Felli P, Bick RJ, Poindexter B, Geng YJ, Barry WH, Smalling RW: Left ventricular unloading before reperfusion reduces endothelin-1 release and calcium overload in porcine myocardial infarction. J Thorac Cardiovasc Surg 2008;136:343-351.

33 Vassalle M, Lin CI: Calcium overload and cardiac function. J Biomed Sci 2004;11:542-565.

34 Zhou L, Sung RY, Li K, Pong NH, Xiang P, Shen J, Ng PC, Chen Y: Cardioprotective effect of dexrazoxane in a rat model of myocardial infarction: Anti-apoptosis and promoting angiogenesis. Int J Cardiol

35 Ramu E, Korach A, Houminer E, Schneider A, Elami A, Schwalb H: Dexrazoxane prevents myocardial ischemia/reperfusion-induced oxidative stress in the rat heart. Cardiovasc Drugs Ther 2006;20:343-348.

36 Chong AJ, Pohlman TH, Hampton CR, Shimamoto A, Mackman N, Verrier ED: Tissue factor and thrombin mediate myocardial ischemia-reperfusion injury. Ann Thorac Surg 2003;75:S649-655.

37 Carden DL, Granger DN: Pathophysiology of ischaemia-reperfusion injury. J Pathol 2000;190:255-266.

38 Shibata S, Sasaki T, Harpel P, Fillit H: Autoantibodies to vascular heparan sulfate proteoglycan in systemic lupus erythematosus react with endothelial cells and inhibit the formation of thrombin-antithrombin iii complexes. Clin Immunol Immunopathol 1994;70:114-123.

39 Sinning JM, Losch J, Walenta K, Bohm M, Nickenig G, Werner N: Circulating cd31+/annexin v+ microparticles correlate with cardiovascular outcomes. Eur Heart J

40 Werner N, Wassmann S, Ahlers P, Kosiol S, Nickenig G: Circulating cd31+/annexin v+ apoptotic microparticles correlate with coronary endothelial function in patients with coronary artery disease. Arterioscler Thromb Vasc Biol 2006;26:112-116.

41 Loetscher P, Seitz M, Clark-Lewis I, Baggiolini M, Moser B: Monocyte chemotactic proteins mcp-1, mcp-2, and mcp-3 are major attractants for human cd4+ and cd8+ t lymphocytes. FASEB J 1994;8:1055-1060.

42 Kumar AG, Ballantyne CM, Michael LH, Kukielka GL, Youker KA, Lindsey ML, Hawkins HK, Birdsall HH, MacKay CR, LaRosa GJ, Rossen RD, Smith CW, Entman ML: Induction of monocyte chemoattractant protein-1 in the small veins of the ischemic and reperfused canine myocardium. Circulation 1997;95:693-700.

43 Lakshminarayanan V, Beno DW, Costa RH, Roebuck KA: Differential regulation of interleukin-8 and intercellular adhesion molecule-1 by h2o2 and tumor necrosis factor-alpha in endothelial and epithelial cells. J Biol Chem 1997;272:32910-32918.

44 Seino Y, Ikeda U, Sekiguchi H, Morita M, Konishi K, Kasahara T, Shimada K: Expression of leukocyte chemotactic cytokines in myocardial tissue. Cytokine 1995;7:301-304.

45 Lakshminarayanan V, Lewallen M, Frangogiannis NG, Evans AJ, Wedin KE, Michael LH, Entman ML: Reactive oxygen intermediates induce monocyte chemotactic protein-1 in vascular endothelium after brief ischemia. Am J Pathol 2001;159:1301-1311.

46 Chen XL, Zhang Q, Zhao R, Medford RM: Superoxide, h2o2, and iron are required for tnf-alpha-induced mcp-1 gene expression in endothelial cells: Role of rac1 and nadph oxidase. Am J Physiol Heart Circ Physiol 2004;286:H1001-1007.

Paper III

Detection of acute myocardial infarction by postmortem magnetic resonance imaging

Thomas Ruder[1], Pranitha Kamat[2], Ahmed Aziz Khattab[3], Michael Thali[1], Robert Rieben[2], Lars Ebert[1]

[1]Virtopsy, Institute of Forensic Medicine, University of Zurich, [2]Department of Clinical Research, University of Bern, [3] Department of Cardiology, Bern University Hospital

Magnetic resonance imaging (MRI) is one of the high-tech imaging techniques used by forensic scientists to investigate body structures by a minimally invasive procedure. In forensics, recognition of acute myocardial infarction by routine histology examinations is difficult, particularly when death has occurred within a few hours after the onset of symptoms.

Aim: To assess if early acute myocardial infarction can be detected with post-mortem cardiac MRI.

Model: Myocardial infarction in pigs under controlled conditions of 1 hour ischemia and 2 hours reperfusion.

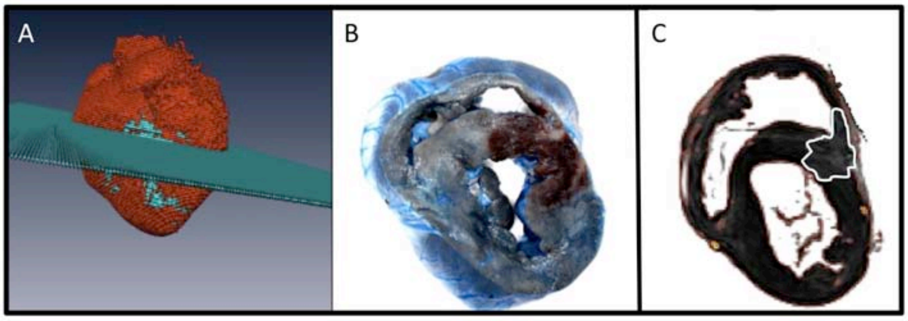

3D rendering of a pig heart scanned by MR, with the green plane showing the scan axis (A). Slice of the same heart stained blue for the non ischemic area and non-blue for the ischemic area (B). Approximately the same slice scanned by MR showing the ischemic area within the white boundary (C).

Conclusion: Post-mortem cardiac MRI is able to detect early acute myocardial infarction wherein dark central zones on the MRI correspond to necrotic tissue and the bright zones indicate ischemic but not yet infarcted areas.

Detection of acute myocardial infarction by postmortem magnetic resonance imaging

Thomas Ruder[1], Pranitha Kamat[2], Ahmed Aziz Khattab[3], Michael Thali[1], Robert Rieben[2], Lars Ebert[1, *]

[1]Virtopsy, Institute of Forensic Medicine, University of Zurich, [2]Department of Clinical Research, University of Bern, [3] Department of Cardiology, Bern University Hospital

Address for correspondence

Lars Ebert, PhD

Virtopsy Group

Institute for Forensic Medicine

University of Zurich

8057 Zurich, Switzerland

Tel: +41-44-6355611

E-mail: lars.ebert@irm.uzh.ch

Abstract

Background: Myocardial infarcts lesser than 4 hours old are usually unapparent on both, gross examination and routine histology examination. It was the goal of this study to assess if early acute myocardial infarction can be detected with post-mortem cardiac magnetic resonance imaging (MR) under controlled conditions in a porcine model.

Material and Methods: Twenty three pigs underwent selective catheterization and occlusion of the left coronary artery distal to the first diagonal branch for 60 min, followed by reperfusion for 120 min. Evan's Blue was injected intravenously after re-occlusion of the artery at the same place to demarcate areas at ischemic risk from the rest of the heart. Only 16 animals completed the entire procedure. The other seven animals died prior to occlusion (n = 4); during occlusion (occlusion time < 30 min n = 2); or during reperfusion (reperfusion time 7 min n = 1). Each heart was excised immediately after death, placed in iced 0.9% saline solution and scanned by MR. MR protocol followed was one isotropic short axis turbo spin echo T2-weighted sequence with a slice thickness of 2.2 mm. After MR imaging, each heart was sliced in axial slices of 15 mm, orientated correspondingly to the short-axis view from cardiac MR and photographed digitally. Slices were then stained with triphenyltetrazolium chloride solution that allows for the macroscopic distinction between healthy and infarcted myocardial tissue.

Results: Radio-morphologic correlation revealed a very high consistency between the macroscopically visible ischemic area and the changes on MR. Six cases where MR had not displayed any findings corresponded to cases where death had occurred prior to or during occlusion and yielded no findings at autopsy. All 16 cases featuring a dark cetral zone with hyperintense rim corresponded to cases with complete occlusion and reperfusion

Discussion: Our findings suggest that the dark central zones on post-mortem cardiac MR correspond to tissue edema and the bright zones indicate ischemic but not yet infarcted areas. The absence of MR findings in the two cases with occlusion times < 30 min suggest, that an occlusion time of less than 30 min is too short to induce any signal changes on MR. To conclude, in this study we show that post-mortem MR is able to visualize acute myocardial infarction at an earlier stage.

Introduction

“Approximately every 25 seconds, an American will have a new coronary attack and approximately every minute, someone will die of one.” [1]

Sudden cardiac death is an important issue of public health [2] and a large portion of the cases referred to our institute for medico-legal autopsy have died from cardiac death with previously undiagnosed cardio-vascular disease. Recognition of acute myocardial infarction at autopsy can be difficult, particularly when death has occurred within a few hours after the onset of symptoms [3]. Myocardial infarcts fewer than 4 hours old are usually unapparent on both, gross examination and routine histology examination.

In living patients, acute chest pain is routinely assessed with electrocardiogram, lab tests and diagnostic/therapeutic coronary angiography [4]. Cardiac MR is rarely used in the acute setting but it provides detailed information regarding the extent of an infarct [5]. MR is also able to visualize myocardial edema, which is a rapid tissue reaction to ischemic injury [5-7]. Myocardial edema may be present for up to a year after its first occurrence in an acute myocardial infarct, and its decrease can be monitored on T2-weighted (T2W) sequences during the follow-up of a myocardial infarction.

In the last decade, cardiac MR has been introduced to post-mortem investigations [8-14]. Preliminary studies have provided promising results regarding radio-morphologic correlation between post-mortem cardiac MR images and macroscopic findings in the myocardium at autopsy [8, 10]. Occasionally, investigators were confronted to cases, where case history and MR findings were suggestive for myocardial infarction but neither macroscopic nor microscopic examination of the heart revealed any pathological changes [11, 13]. Such cases led to the hypothesis that MR may be able to diagnose acute myocardial infarction at an earlier stage than traditional autopsy [11, 13, 14].

It was the goal of this study to assess if early acute myocardial infarction can be detected by post-mortem cardiac MR under controlled conditions in an animal model with porcine hearts.

Material and Methods

Subjects

The responsible local justice department and the ethics committee of the university both approved this study. The study was a joint research project between the Institute of Clinical Research at University of Bern and the Institute of Forensic Medicine at the University of Bern and Zurich respectively. The subjects for this prospective study consisted of 23 pigs. The 23 animals included in this study were selected during a period from 6th January and 19th November 2010 in function of logistical capacity of both institutes involved, including the availability of MR scan time.

Standard study protocol

The standard study protocol included the following procedure for each animal [15]: general anesthesia, fluoroscopy guided selective catheterization of the left coronary artery, complete occlusion of the left coronary artery distal to the first diagonal branch for 60 min, reperfusion for 120 min, and re-occlusion (< 5 min). During re-occlusion, 60 ml of Evan's Blue (Sigma-Aldrich, E2129) were injected intravenously, staining all organs blue except the myocardial tissue supplied by the occluded vessel.

Only 16 animals completed the entire procedure. Seven animals died prematurely: prior to occlusion (n = 4); during occlusion (occlusion time 15 min n = 1, occlusion time 30 min n = 1); or during reperfusion (reperfusion time 7 min = 1). Evan's Blue staining was not possible in these cases. The heart was excised Immediately after death, rinsed, placed in container with iced 0.9% saline solution, and transported to the MR suite.

Imaging protocol

MR imaging was performed using a 1.5 Tesla MR unit (Magnetom Avanto/Symphony, Siemens, Erlangen, Germay). Each heart was re-placed in a saline filled container (1.0 l volume, temperature: 21° C) and positioned in the head coil. Due to time constraints, MR protocol was limited to one isotropic short axis T2-weighted (T2W) turbo spin echo (TSE) sequence using the following parameters: repetition time (TR): 3860 ms; echo time (TE): 100 ms; slice thickness: 2.2 mm; field of view (FoV): 300 mm; matrix size: 512 x 512 mm; total scan duration: 16 min. Each heart was returned to the laboratory in iced 0.9% saline solution after imaging. Transportation time for each way: 7-12 min.

Documentation, staining and fixation of the heart

Each heart was cut in slices of 15 mm from the apex to the mitral valve. Slices were orientated correspondingly to the short-axis view from cardiac MR. Each slice was photographed digitally before being immersed in a staining solution with 2,3,4-triphenyltetrazolium chloride (TTC). TTC staining was done for 20 min at 37°C and allows for the macroscopic distinction between healthy and infarcted myocardial tissue [16]. TTC staining is based on the activity of the enzyme dehydrogenase, which is higher in healthy myocardium than in infarcted myocardium [15, 16]. TTC staining must commence within 45 min of explanation of the heart in order to allow for the differentiation between viable and infarcted myocardium. Otherwise normal post-mortem tissue degradation processes will annihilate the initial difference of enzyme activity between infarcted myocardium and the remainder tissue.

MR interpretation and radio-morphologic correlation

All 23 cardiac MR datasets were stored in a digital picture archive and communication system (PACS) and interpreted on a PACS workstation (IDS7, Sectra, Linköping, Sweden). Reporting was performed in a blinded fashion by a radiologist with 5 years of experience. MR findings were described in relation/relative to the healthy myocardial tissue. For radio-morphologic correlation, MR images were reconstructed using multiplanar reformatting (MPR) to match the slice orientation of the heart specimen. Macroscopic findings were compared to MR image findings in a consensus reading.

Results

MR findings

MR displayed no findings in 6/23 cases. In 16/23 cases MR revealed a hyperintense signal at the margin and no signal change in the center of the ischemic tissue. The signal intensity and width of the hyperintense rim varied considerably between these 16 cases. Finally, there was a homogenous hyperintense signal within the ischemic area in 1/23 cases.

Radio-morphologic correlation

Radio-morphologic correlation revealed excellent agreement between MR and autopsy findings. All six cases where MR had not displayed any findings corresponded to cases where death had occurred prior to or during occlusion and yielded no findings at autopsy. All 16 cases featuring a hyperintense rim corresponded to cases with complete occlusion and reperfusion. MR and autopsy findings showed good correlation: the hyperintese rim on MR corresponded to the margin of the infarcted tissue. TTC staining revealed that these zones contain still viable, non-necrotic myocardial tissue, whereas the necrotic tissue was more centrally located within the ischemic area. Both, non-hemorrhagic and hemorrhagic infarction produced an equally dark MR signal. It is interesting to note that MR revealed no difference between the necrotic myocardium within the hyperintense rim and the healthy myocardium outside the rim. The single case displaying a homogenous bright MR signal within the ischemic tissue corresponded to the one case with complete occlusion but incomplete reperfusion time.

Discussion

In this study we showed, that acute myocardial infarction can be detected by post-mortem cardiac MR within 4 hours after the onset of ischemia in porcine hearts; and that myocardial edema is a characteristic MR finding of acute infarcts. These findings provide strong evidence that MR is able to detect acute cardiac infarction at an earlier stage than traditional autopsy and routine histology, thereby confirming the hypothesis of Thali, Jackowski et Shiotani [11, 13, 14].

We have found that an occlusion time of 60 min, followed by a reperfusion time of 120 min, results in a characteristic signal increase on post-mortem T2W cardiac MR images. Overall, our results stand in agreement with the results of Tscholakoff et al. who found an increase in signal intensity on T2W MR images of in vivo dogs three hours after coronary artery occlusion in an experimental study in 1986 [17]. In our cases we found a hyperintense signal at the margin of the ischemic tissue, which corresponds to the still viable area at risk. The center of the ischemic area with the necrotic tissue proved to be dark compared its bright rim MR. This pattern matches the findings of clinical imaging in cardiac infarction and stands in agreement with the findings of previous post-mortem studies [8-11]

It is interesting to note that both, non-hemorrhagic and hemorrhagic infarction produced an equally dark MR signal. This observation concurs with the general image properties of hemoglobin on T2W MR images. Importantly, MR reveald no difference between the necrotic myocardium within the hyperintense rim and the healthy myocardium outside the rim.

Nevertheless our findings differ from the findings of previous studies in two points. First, in our population the dark central zones were isointense compared to the healthy myocardium and only hypointense compared to myocardial edema. Other authors have reported a decrease of MR signal in the necrotic center of the infarction not only relative to edema, but also relative to healthy myocardium, resulting in a hypointese region in what was thought to be the infarcted myocardium. This difference may be explained by the temperature dependence of MR signal resulting in an overall lower signal from the healthy myocardium in the cooled extracted heart specimen in our population [18]. Second according to our results, edema represents the first tissue reaction to ischemia resulting in an early signal increase in the affected area. The dark central zones appeared only later, after reperfusion. This observation differs from the results of Jackowski at al. [8-11]. According to their publications, a focal hypointensity within the myocardium was the first sign on post-mortem cardiac MR to indicate possible ischemia in a population of eight and 20 forensic routine cases in a non-controlled setting [8, 10].

Our findings in the cases with occlusion times of 15 min and 30 min respectively suggest, that an occlusion time of less than 30 min is too short to induce any signal changes on MR. This observation is supported by the pathophysiological pathway of infarction where ischemia of less than 30 min causes reversible damage only [3].

Reperfusion injury is a well-known issue in patients with myocardial infarction. In our population, one animal died during the early reperfusion phase. It is interesting to note, that here the entire ischemic area of the myocardium featured a hyperintense signal on post-mortem MR. This finding may be the result of (nearly) absent reperfusion, however since it occurred in one case only, it is not possible to draw any conclusions from this observation.

Edema is known to be an early response to ischemia [6]. In our study we have found that edema is already present in the early acute phase of a myocardial infarct. However, it is important to note that myocardial edema is an unsuitable MR finding to date myocardial infarction: after its formation in the acute phase of myocardial ischemia, edema may remain present on imaging for several month. Myocardial edema may be present for up to a year after its first occurrence in an acute myocardial infarct, and its decrease can be monitored on T2-weighted (T2W) sequences during the follow-up of a myocardial infarction.

Importantly, the occurrence of multiple non-simultaneous minor ischemic incidents in the pre-history of cardiac death might cause overlapping edema mimicking the image of one single extensive acute myocardial infarction. Physicians involved in post-mortem investigations should be very careful with the diagnosis of acute myocardial infarction based on one single post-mortem cardiac MR. Based on our findings and the work of other authors on this subject we consider MR to be an adequate tool for the detection of myocardial ischemia, however the diagnosis of acute myocardial ischemia should always be made in conjunction with autopsy findings.

Limitations

A few limitations of this study deserve discussion. First, the exclusion of histology may be criticized. However, the use of TTC staining allows for *macroscopic* detection of myocardial infarction. In addition MR is an imaging modality with a resolution in the range of millimeters. In order to assess the capability of MR to detect the early acute myocardial infarction, a macroscopic radio-morphologic correlation was more suitable to the objective of the study. Second, the exclusive use of a single T2W MR sequence in this study may seem to be insufficient. The authors agree, that myocardial infarcts are best investigated using a larger set of sequences, including T1-weighted as well as susceptibility weighted sequences. However, to assess the occurrence of edema, T2W-sequences are most suitable and due to time-constraints we were forced to limit MR imaging to one single sequence. In order to achieve optimal radio-morphologic correlation we decided to use an isotropic sequence, which allows reconstructing images in all three planes a higher quality of MPR images.

Finally, the setting of our study should be discussed. The controlled setting does not reflect the variety of findings in real cases of sudden cardiac death. This may appear to be a limitation. However, *because* of the complexity of real cases, it is elementary to first assess the capability of MR to detect acute myocardial infarcts under controlled conditions.

Conclusions

Early acute myocardial infarcts are usually unapparent at autopsy and on routine histology examination and their recognition is difficult for pathologist. In this study we have shown that post-mortem cardiac MR is able to detect early acute myocardial infarction. Based on the results of this study we suggest relying on post-mortem MR to diagnose early acute myocardial infarction when findings on traditional autopsy and histology are absent.

However, post-mortem cardiac MR is still in its infancy. Premature conclusions on the capability of MR for the assessment of myocardial infarcts would be harmful to the growing acceptance and credibility of cross sectional imaging modalities in the post-mortem setting. Therefore we strongly recommend using MR exclusively as an adjunct to autopsy and always attempt to perform radio-morphologic correlation in order to improve the knowledge on the post-mortem MR image properties of myocardial infarcts.

.

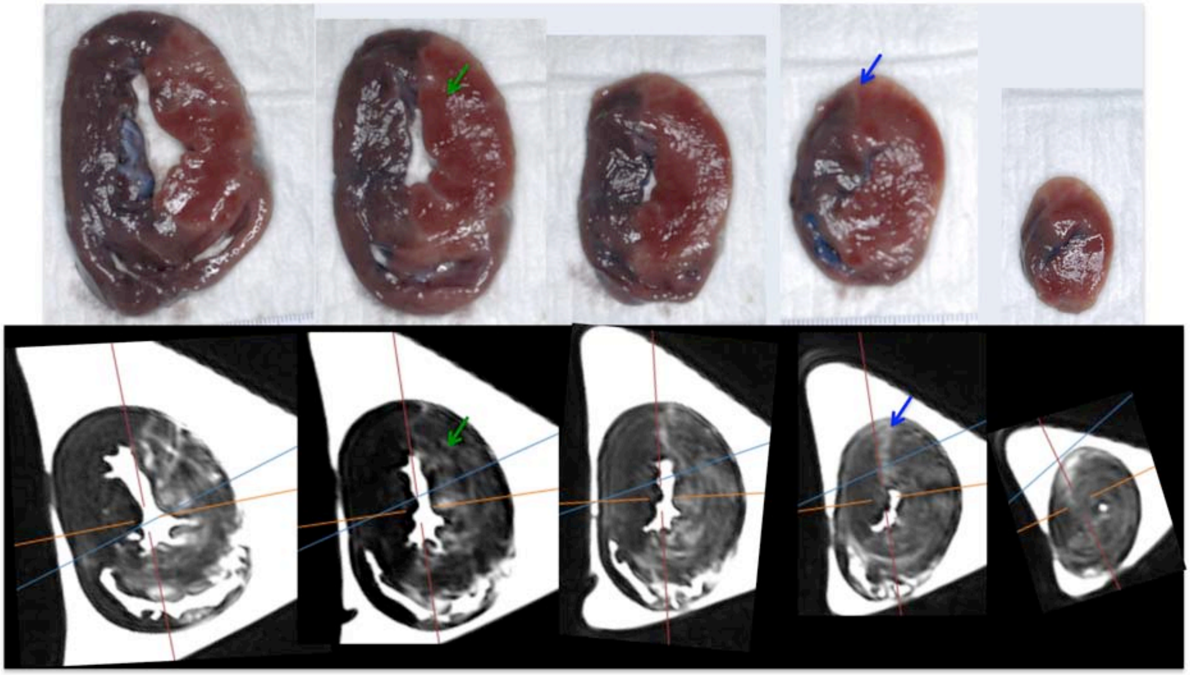

Figure 18: MR findings. Images of heart slices were taken before TTC staining (above panel) and compared with scan images from the MR (below panel). Ischemic areas in the freshly cut heart slice corresponded to dark zones in the MR (green arrows). The border zone of infarcted area was seen as very bright rim on the MR (blue arrows).

References

1 Lloyd-Jones D, Adams RJ, Brown TM, Carnethon M, Dai S, De Simone G, Ferguson TB, Ford E, Furie K, Gillespie C, Go A, Greenlund K, Haase N, Hailpern S, Ho PM, Howard V, Kissela B, Kittner S, Lackland D, Lisabeth L, Marelli A, McDermott MM, Meigs J, Mozaffarian D, Mussolino M, Nichol G, Roger VL, Rosamond W, Sacco R, Sorlie P, Thom T, Wasserthiel-Smoller S, Wong ND, Wylie-Rosett J: Heart disease and stroke statistics--2010 update: A report from the american heart association. Circulation 2010;121:e46-e215.

2 Adabag AS, Luepker RV, Roger VL, Gersh BJ: Sudden cardiac death: Epidemiology and risk factors. Nat Rev Cardiol 2010;7:216-225.

3 Schoen F: The heart; in Cotran RS KV, Collins T (ed Robbins pathologic basis of disease, Philadelphia PA: W.B. Saunders Company, 1999, pp 543-600.

4 Schulte B BA, Beyer D. Myokardinfarkt: Mrt des herzens und der gefässe, ed 1st. Berlin, Germany: Springer, 2005.

5 Jürgens KU LM, Maintz DC. Herz: Ganzkörper mr-tomographie, ed 2nd. Stuttgart, Germany: Georg Thieme Verlag, 2006.

6 Cury RC, Shash K, Nagurney JT, Rosito G, Shapiro MD, Nomura CH, Abbara S, Bamberg F, Ferencik M, Schmidt EJ, Brown DF, Hoffmann U, Brady TJ: Cardiac magnetic resonance with t2-weighted imaging improves detection of patients with acute coronary syndrome in the emergency department. Circulation 2008;118:837-844.

7 Herfkens RJ, Sievers R, Kaufman L, Sheldon PE, Ortendahl DA, Lipton MJ, Crooks LE, Higgins CB: Nuclear magnetic resonance imaging of the infarcted muscle: A rat model. Radiology 1983;147:761-764.

8 Jackowski C, Christe A, Sonnenschein M, Aghayev E, Thali MJ: Postmortem unenhanced magnetic resonance imaging of myocardial infarction in correlation to histological infarction age characterization. Eur Heart J 2006;27:2459-2467.

9 Jackowski C, Schweitzer W, Thali M, Yen K, Aghayev E, Sonnenschein M, Vock P, Dirnhofer R: Virtopsy: Postmortem imaging of the human heart in situ using msct and mri. Forensic Sci Int 2005;149:11-23.

10 Jackowski C, Warntjes MJ, Berge J, Bar W, Persson A: Magnetic resonance imaging goes postmortem: Noninvasive detection and assessment of myocardial infarction by postmortem mri. Eur Radiol 2010;21:70-78.

11 Jackowski C TM: Cardiac pathology; in Thali MJ DR, Vock P (ed The virtopsy approach, Boca Raton FL: CRC Press, 2009, pp 230-249.

12 Ruder TD, Bauer-Kreutz R, Ampanozi G, Rosskopf AB, Pilgrim TM, Weber OM, Thali MJ, Hatch GM: Assessment of coronary artery disease by post-mortem cardiac mr. Eur J Radiol 2011

13 Shiotani S, Yamazaki K, Kikuchi K, Nagata C, Morimoto T, Noguchi Y, Suzuki M, Atake S, Kohno M, Ohashi N: Postmortem magnetic resonance imaging (pmmri) demonstration of reversible injury phase myocardium in a case of sudden death from acute coronary plaque change. Radiat Med 2005;23:563-565.

14 Thali MJ, Yen K, Schweitzer W, Vock P, Boesch C, Ozdoba C, Schroth G, Ith M, Sonnenschein M, Doernhoefer T, Scheurer E, Plattner T, Dirnhofer R: Virtopsy, a new imaging horizon in forensic pathology: Virtual autopsy by postmortem multislice computed tomography (msct) and magnetic resonance imaging (mri)--a feasibility study. J Forensic Sci 2003;48:386-403.

15 Banz Y, Hess OM, Robson SC, Mettler D, Meier P, Haeberli A, Csizmadia E, Korchagina EY, Bovin NV, Rieben R: Locally targeted cytoprotection with dextran sulfate attenuates experimental porcine myocardial ischaemia/reperfusion injury. Eur Heart J 2005;26:2334-2343.

16 Khalil PN, Siebeck M, Huss R, Pollhammer M, Khalil MN, Neuhof C, Fritz H: Histochemical assessment of early myocardial infarction using 2,3,5-triphenyltetrazolium chloride in blood-perfused porcine hearts. J Pharmacol Toxicol Methods 2006;54:307-312.

17 Tscholakoff D, Higgins CB, McNamara MT, Derugin N: Early-phase myocardial infarction: Evaluation by mr imaging. Radiology 1986;159:667-672.

18 Ruder TD, Hatch GM, Siegenthaler L, Ampanozi G, Mathier S, Thali MJ, Weber OM: The influence of body temperature on image contrast in post mortem mri. Eur J Radiol 2011

Paper IV

Antibodies and complement are deposited in viable myocardium in a porcine model of acute coronary syndrome

Pranitha Kamat[1], Anne Broillet[2], Alexandre Helbert[2], Thierry Bettinger[2],Otto Martin Hess[3], Michel Schneider[2], Robert Rieben[1,3]

[1]University of Bern, Department of Clinical Research, Bern, Switzerland, [2]Bracco Research SA, Geneva, Switzerland, [3] Plastic- and Hand Surgery, University Hospital, Bern, Switzerland

Activation of the complement cascade in conjunction with other inflammatory molecules contributes significantly to ischemia reperfusion injury. Ischemia exposes neo-epitopes on the cells surface that can be recognized by various complement activating proteins. Once activated the complement cascade propagates during ischemia and reperfusion into formation of the terminal complex and release of anaphylatoxins.

Aim: To assess the role of complement and inflammatory molecules in ischemia/reperfusion.

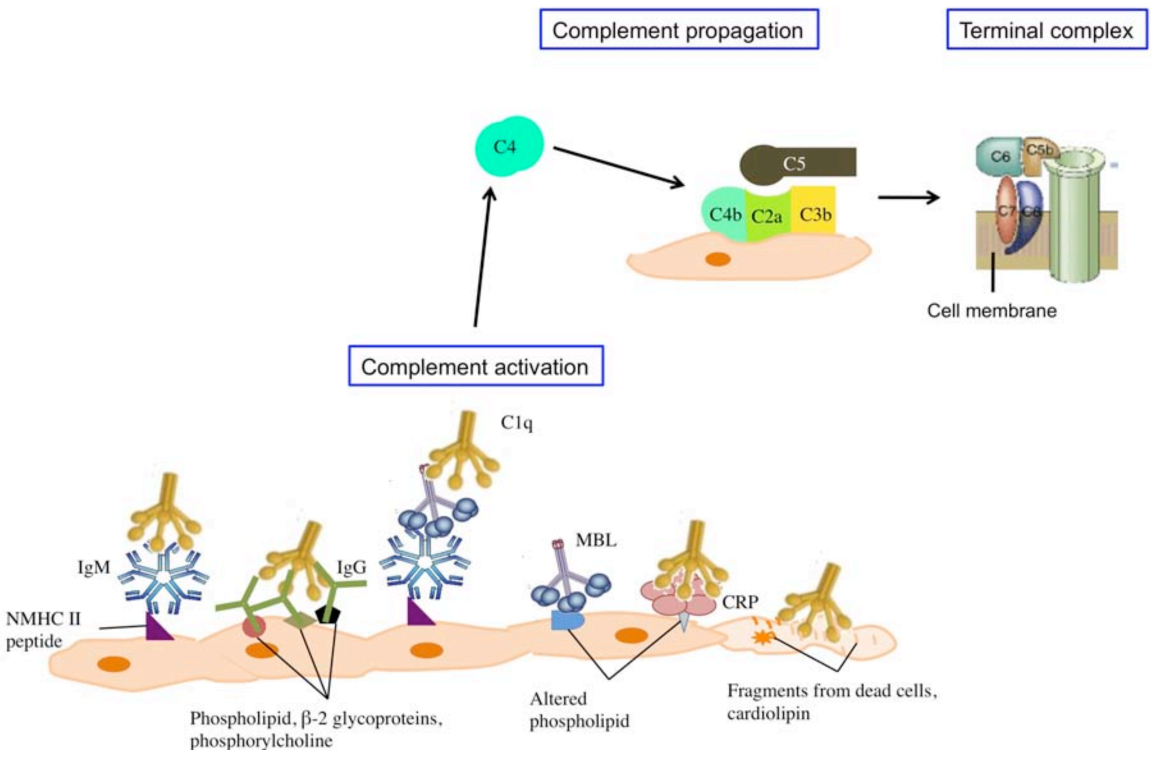
Complement propagation
Terminal complex
C4
C5
C4b
C2a
C3b
C6
C5b
C7
C8
Cell membrane
Complement activation
C1q
IgM
IgG
MBL
CRP
NMHC II peptide
Phospholipid, β-2 glycoproteins, phosphorylcholine
Altered phospholipid
Fragments from dead cells, cardiolipin

Model: Myocardial infarction in pigs with 60 minutes or 20 minutes ischemia and 6 hours reperfusion.

Conclusion: Tissue necrosis was seen after ischemic duration of 60 minutes and not after 20 minutes. But deposition of IgM and C3b/c was observed also within the ischemic myocardium after 20 minutes ischemia. Natural antibody deposition and complement activation may therefore be essential players in ischemia/reperfusion.

Antibodies and complement are deposited in viable myocardium in a porcine model of acute coronary syndrome

Pranitha Kamat[1], Anne Broillet[2], Alexandre Helbert[2], Thierry Bettinger[2], Otto Martin Hess[3], Michel Schneider[2], Robert Rieben[1,3*]

[1]University of Bern, Department of Clinical Research, Bern, Switzerland, [2]Bracco Research SA, Geneva, Switzerland, [3] Plastic and Hand Surgery, University Hospital, Bern, Switzerland

*Corresponding author
Robert Rieben
University of Bern
Department of Clinical Research
Murtenstrasse 50
3008 Bern, Switzerland
Tel: +41 31 632 9669
Fax: +41 31 632 7594
E-mail: robert.rieben@dkf.unibe.ch

Abstract

Background: In mice, recognition of ischemia-induced neoepitopes by IgM, followed by complement activation, was proposed as pathophysiological mechanism in reperfusion injury. We now assessed their role, as well as the one of proinflammatory molecules, in a porcine model of acute coronary syndrome.

Method: 30Kg piglets were used to induce coronary occlusion by balloon catheter for 60 minutes (group 1) (n=12) and 20 minutes (group 2) (n=5), followed by 6 hours of reperfusion. The myocardial ischemic area at risk was demarcated by Evan's blue and Triphenyl tetrazolium chloride was used to discriminate between vital and necrotic tissue. IgM, IgG, C3b/c, C1q, C5b9 and neutrophil infiltration were detected by immunofluorescence. Cytokine and Troponin I levels were analyzed in blood samples taken at different time points.

Results: Myocardial necrosis and a rise of Troponin-I were observed for group 1 but not for group 2. The necrotic tissue from group 1 also showed increased neutrophil recruitment ($p<0.01$) when compared to the non-ischemic tissue. However, increased deposition of IgM ($P=0.0494$) and C3b/c ($P=0.0298$) in ischemic as compared to non-ischemic myocardium, was found also for group 2 after 20 minutes of ischemia. The total amount of IL-6 secreted was higher for group 1 than for group 2 but not significant. Levels of IL-8, IL-10, IL-1β C3a and C5a were similar in both groups.

Discussion: Tissue necrosis was seen after ischemic duration of 60 minutes and not after 20 minutes. But deposition of IgM and C3b/c was observed also within the ischemic myocardium after 20 minutes ischemia. Natural antibody deposition and complement activation may therefore be essential players in ischemia/reperfusion injury. However, additional factors seem to be decisive for tissue injury, among which is neutrophil infiltration mediated by cytokines like IL-6 and possibly other chemotactic molecules secreted by endothelial cells.

Introduction

Ischemia reperfusion (IR) is a common phenomenon contributing to pathology in many diseases especially concerning the vasculature. Mechanisms driving the injury due to ischemia followed by reperfusion involves the complement system among others.

Several knockout models in mice and rats have been used to elucidate the pathway of complement activation during IR. Ischemia and reperfusion prompts cellular changes generating neo epitopes on the cell surface [105,106]. The natural antibody, IgM recognizes these neo epitopes and activates the complement system via the classical pathway [9,107]. Complement activation is also shown to occur via the lectin pathway by MBL that can deposit itself directly [108] or via IgM [109]. A novel technique of triple knockout mice that lacked secreted IgM, MBL-A and MBL-C demonstrated the complement - initiating molecule to be a complex of IgM-MBL and C1q [110]. Direct role of alternative pathway in intestinal IR was shown by attenuation of injury in Factor D deficient mice [111]. It is therefore clear the initiation of complement during IR that occurs already during ischemia and continues during reperfusion.

Contribution of complement system in pathology during IR naturally instigated studies that aimed to attenuate injury by suppressing the complement system. Several of such studies have been successful in large animals by the use of complement inhibitory drugs like APT070, DXS, sCR1and also in human clinical trials [10].

An immune response during IR is inevitable resulting in tissue damage. However, at the same time it plays an effective role in mending the damaged tissue. A controlled level of inflammatory response is therefore a requisite to regulate injury during IR. This was confirmed by a study that shows increased damage due to IR by completely inhibiting inflammation [112]. Complement plays an important role in initiation of an immune response. It could therefore be possible that initiation of complement system also elicits a protective effect during IR.

To test this hypothesis we subjected pig hearts to ischemia reperfusion injury i.e. a pig model of myocardial infarction. It is known that an ischemic duration of 20 minutes or lesser does not result in any tissue necrosis after reperfusion. We therefore induced ischemia for 20 min in the pigs and studied for complement activation after 6 hours reperfusion. As a control we induced 60 min ischemia in another group of pigs and let them reperfuse also for 6 hours. In our study we could show significant amount of antibody and complement deposition in the viable myocardium after short ischemic duration of 20 min. Thereby indicating a non-deleterious effect of complement initiation.

Material and methods

Animal experiments

Large white pigs weighing approximately 30Kg were anesthetized and subjected to myocardial infarction as described previously [41]. Briefly, with a balloon catheter the anterior descending artery after the first diagonal branch was occluded. For group 1 the occlusion or ischemic duration was 60 min (n=12) and for group 2 the duration was 20 min (n=5). The balloon was then deflated to reperfuse the previously ischemic area for 6 hours in both groups. At end of reperfusion, 60 ml Evan's blue was given intravenously after re-occluding the artery at the same position. This helped to demarcate the ischemic area from the area not at ischemic risk. The pigs were then sacrificed by injecting KCl intravenously and the heart excised for further analysis.

Detection of myocardial viability

Myocardial viability was determined as described previously [41]. Briefly, hearts were sliced perpendicular to the axis and right ventricle removed. From the left ventricle the Evan's blue unstained parts were treated with 2,3,5- triphenlytetrazolium chloride (TTC) solution for 20 min at 37°C. The TTC stained red part represented the viable ischemic tissue (VIT) and the unstained part represented the necrotic ischemic tissue (NIT).

Sampling

Tissue samples were taken from area not at ischemic risk (ANR), VIT and NIT. Tissue samples taken were treated with 2% formaldehyde overnight at 4°C. They were then transferred into 18% sucrose solution and left at 4°C for 15 hours. Samples were then embedded in M1 shandon embedding matrix and stored at 20°C. As a control, heart sample from a normal pig was also processed and stained with the test samples.

Blood samples were taken in vacutainers containing EDTA (1.6 mg/ml) to obtain EDTA-plasma, and to tubes containing a clotting activator (glass pearls) to obtain serum. Samples were taken at baseline, 10 min before reperfusion (ischemia), 2 min, 5 min, 10 min, 20 min, 1 hour and 6 hours after reperfusion. Blood samples were centrifuged at 4°C for 5min under 3000 rpm. The supernatant was aliquoted and stored at -80°C until used.

Immunofluorescence staining

Samples were sectioned to 30μm thickness and permeablized by TBS containing Triton X-100 for 15 min at room temperature. Primary antibody incubation was conducted overnight at 4°C and secondary antibody incubation for 90 min at room temperature. In case of directly labeled primary antibody, the incubation was conducted at room temperature for 90 min. After every antibody, sections were washed with TBS containing Triton X-100. Sections were finally mounted onto slides coated with glycerin.

Staining for antibody deposition, complement and neutrophil infiltration

To stain for deposition of natural antibodies directly labeled antibodies goat anti porcine IgG FITC and goat anti porcine IgM FITC (Southern Biotech and Serotec respectively) were used. Activation of complement by C1q was analyzed with help of rabbit anti human polyclonal C1q antibody (Dako A0136). Complement activation was detected by staining for C3b/c with rabbit anti human polyclonal antibody (Dako A0062). Terminal complex of complement activation was detected by using rabbit anti human C5b9 (Callbiochem 204903). Neutrophil infiltration was detected by using an antibody against myeloperoxidase, rabbit anti human (Dako A0398). The secondary antibody used for all was sheep anti rabbit Cy3 (Sigma C2306).

ELISA for complement activation in plasma

C3a and C5a were measured by sandwich ELISA as described previously [42]. Microtiter plates were coated with a monoclonal antibody (IgG2b) against porcine C3a/C3a (desArg) or rabbit anti-mouse IgG (Dako, Glostrup, Denmark) followed by a monoclonal antibody (IgG1) against porcine C5a. After washing with PBS–Tween, plasma sam- ples were incubated at a 1:50 (C3a ELISA) or 1:2 (C5a ELISA) dilution in PBS/Tween/EDTA for 2 h. Biotinylated monoclonal anti-C3/C3a antibody or rabbit anti-C5a, fol- lowed by streptavidin-alkaline phosphatase conjugate (Amersham Pharmacia Biotech, Bucks, UK) and 4-nitrophe- nyl phosphate substrate (Sigma) were used to detect bound C3a and C5a (all non-commercial antibodies were obtained from the Georg-August University, Goettingen — Science- bridge GmbH, Germany).

Multiplex assay for detection of cardiac Troponin and cytokines in serum

A singleplex assay was used to detect cardiac Troponin I levels in serum as described previously [42]. Briefly, mouse anti-human Troponin I (Abcam Ltd, clone 19C7), biotinylated using the EZ-Link NHS-PEO Solid Phase Biotinylation Kit mini spin columns from Pierce (Pierce, Rockford, IL, USA), was used as the detection antibody and mouse anti-human troponin I, cross-reactive with porcine troponin I (Abcam Ltd., Cambridge, UK, clone 16A11), was used as the capture antibody. Covalent coupling of the capture antibody to the region-specific microspheres was performed using the Bio-Plex Amine Coupling Kit (Bio- Rad). For the cytokines tested commercial kits were bought from R&D systems and run together as a multiplex assay. The cytokines tested were IL-1β (DuoSet DY681), IL-6 (DuoSet DY686), IL-8 (DuoSet DY535), IL-10 (DuoSet DY693). Analysis was done with the Bio-Plex system and Bio- Plex Manager version 4.0 software (Bio-Rad) with five- parametric curve fitting. Assay conditions were derived from those of commercial tests.

Statistics

To compare staining on the tissue types within group 1, One way ANOVA was used with Bonferroni's post test. Since group 2 had only two tissue types, students t-test was used to compare samples within the group. The soluble markers in blood at different time points were expressed as percentage of baseline. Area under the curve was calculated for every pig and used to compare the groups with the Mann Whitney test.

Results

Myocardial viability

Staining with TTC identified the viable myocardium in the excised heart. Viability was represented as percentage of the area at risk (AAR) within the left ventricle. For group 1 the percentage viability ranged from 25% to 75% with a mean of 50%. For group 2 all pigs showed 100% viable myocardium (Figure 1).

Sampling

Since there was no necrosis of the ischemic area for group 2, the group contains samples only from the area not at risk (ANR) and viable ischemic tissue (VIT). For group 1 however, there was considerable necrosis within the ischemic area. The group therefore contains samples taken from ANR, VIT and necrotic ischemic tissue (NIT).

Antibody deposition on tissue

Tissue samples from ANR, VIT and NIT were stained for deposition of natural antibody IgG and IgM. Antibody deposition on ANR from both groups was similar to that on normal tissue (Figure 2). Significant rise in IgG deposition was observed on NIT when compared to ANR for group 1 ($p<0.05$). Similar rise for group 1 was seen for IgM ($p<0.01$), which was also higher in the VIT for group 2 when compared to its ANR ($p=0.0494$). Figure 4 shows representative images of IgM deposition on ischemic myocardium for both groups.

Complement deposition

Complement activation was analyzed by staining tissues for C1q deposition. All tissue samples from group 1 and group 2 showed similar levels of C1q deposition, which was comparable to normal tissue (Figure 3). Complement component C3b/c deposition was similar in ANR from both groups and the normal tissue (Figure 3). It was significantly higher in NIT when compared to ANR for group 1 ($p<0.05$) and in VIT when compared to ANR from group 2 ($p=0.0148$). Deposition of the terminal complement complex C5b9 was similar in all tissues and were comparable to normal tissue (Figure 3). Figure 4 shows representative images of C3b/c deposition on ischemic myocardium for both groups

Anaphylatoxins and cytokine level in circulation

Anaphylatoxins C3a and C5a were measured at different time points. The values were expressed as percentage of baseline and the area under the curve was compared between groups. The total C3a and C5a levels were similar for group 1 and 2 (Table 1).

In a similar way, cytokine levels were compared between the groups. Pro-inflammatory cytokines measured were IL-6 and IL-1β (Table 1). Although IL-1β did not show a difference between the groups, IL-6 was higher for group 1 than for group 2 although not significant. Anti-inflammatory cytokine IL-10 and chemokine IL-8 were similar in both groups (Table 1)

Neutrophil infiltration in tissue

Myeloperoxidase (MPO) staining allowed for analysis of infiltrated neutrophils in the tissue samples. The staining was very minimal in ANR from both groups and the normal tissue (Figure 5). Neutrophil infiltration was significantly higher for group 1 in the NIT when compared to ANR ($p<0.01$) and VIT ($p<0.05$). For group 2, neutrophil infiltration into the ischemic myocardium (VIT) was minimal as in the ANR in the same group. Figure 6 shows representative images of MPO on ischemic myocardium of both groups.

Cardiac troponin levels in circulation

Cardiac troponin-I levels in blood samples taken at different time points were measured by the multiplex system. Cardiac troponin remained at baseline levels until 5 min reperfusion in both groups (Figure 7). However from 10 min until 6 hours of reperfusion there was a continuous rise in troponin-I levels for group 1 and not for group 2. The rise was significant when analyzed by the Mann Whitney test ($p=0.0019$).

Discussion

In this study, pigs were subjected to myocardial infarction with ischemia for 60 min (group 1) and 20 min (group 2), both followed by 6 hours reperfusion. The excised hearts were analyzed for percentage of viable tissue within the ischemic area of the left ventricle (Figure 1). The viability varied from 25% – 75% for group 1 probably due to the physiology of the heart, which is different in every animal. The hearts from group 2 were 100% viable as expected with a short ischemic duration of 20 min.

Immunostaining on tissue samples was compared with tissue sample from a normal pigs heart as control. The ANR was in range with the normal for all parameters tested. Tissue samples were stained for deposition of natural antibodies to analyze the activation of complement by the classical pathway. Group 1 showed a significant deposition of IgG and IgM in the NIT when compared to ANR (Figure 2). This is in conjunction with previous studies where IgM was indentified to specifically target epitopes on ischemic cells and mediate tissue injury [107]. An increased deposition of IgM but not IgG was observed in VIT for group 2. The presence of IgM in the ischemic myocardium in absence of necrosis identifies complement to mediate functions other than necrosis during IR. Experiments conducted with only 20 min ischemia and without reperfusion in mouse model of intestinal IR injury, show traces of deposits of IgM [113]. This may indicate that most of the IgM deposition occurs upon reperfusion.

An early component of complement activation is C1q and was found to be at normal levels in all tissues from both groups (Figure 3). Another marker used for complement activation was C3b/c. (Figure 3). C3b/c deposition was similar to that of IgM. It was higher in the NIT for group 1 and VIT for group 2. Complement activation in both groups was therefore confirmed. It is definitely more interesting to have deposition of activated complement component in the viable myocardium after IR. Previous studies have shown deposition of C3 two hours after ischemia only. It was suggested that reactive oxygen species produced during ischemia might activate complement via the alternative pathway [114]. In another study after a short ischemic duration of 20 min, there were only traces of C3 observed[113]. It could therefore be that much of the complement activation via deposition of IgM and C3b/c for group 2 occurred during reperfusion.

C5b9 is the terminal complex downstream to complement activation, the main function of which is to drill holes into the cell membrane causing cell necrosis. C5b9 is shown to be deposited early upon reperfusion in rabbit hearts [115]. It was also shown in human infarcted myocardium [116] and is a specific marker for identifying infarcted myocardium in forensics [117]. In our study, we did not observe increased deposition of C5b9 in the infarcted myocardium for group 1 (Figure 3). This may suggest degradation of the complex at the end of prolonged reperfusion of 6 hours. Results from group 2 do coincide with previous studies by showing no deposition of C5b9 in the ischemic myocardium that was viable. However, the prolonged reperfusion time of 6 hours also applies to group2. The results obtained would need further confirmation probably by measuring soluble C5b9 at time points during the course of reperfusion.

In conjunction to tissue analysis, complement activation was also analyzed in blood plasma by measuring the anaphylatoxins C3a and C5a. The total C3a and C5a in circulation of pigs during course of the experiment were compared and found to be almost similar between the groups (Table 1). There was therefore same level of C3a and C5a generated by 60 min and 20 min ischemia followed by 6 hours reperfusion.

Inflammatory cytokines have shown to be generated during myocardial infarction as shown in humans and animal models [118]. We also compared the two groups in our study based on total cytokine in the circulation. This was determined by measuring cytokine levels at different time points, calculating the percentage baseline values and finally the area under the curve. Levels of pro-inflammatory cytokine IL-6 and IL-1β, anti-inflammatory cytokine IL-10 and chemokine IL-8 levels were similar in both groups. IL-6 showed much higher value for group 1 than for group 2 but was not significant.

Neutrophil infiltration was detected in tissue samples by MPO staining. It was significantly higher in the NIT when compared to the ANR for group 1 (Figure 5). This is in accordance to previous study in humans where neutrophil infiltration was shown to be associated with myocardial infarction [119]. The tissue necrosis observed for group 1 could be well mediated by the infiltrated neutrophils as they have the potential to degrade the surrounding tissue by producing enzymes and reactive oxygen species. For it has been shown in a model similar to this study but with 1hour ischemia and 2 hour reperfusion, a reduction in infract size by reducing neutrophil adhesion to endothelial cells [120]. Further more the result for group 2 supports the above data with no increase in neutrophil infiltration corresponding to no tissue necrosis.

Cardiac troponin is used in diagnostics as marker for myocardial necrosis. Its significant rise for group 1 is in accordance with the tissue necrosis in this group (Figure 7). For group 2, baseline level of cardiac troponin -1 supports the 100% viability of ischemic tissue.

To summarize, in our study we show that a short ischemic duration of 20 min followed by 6 hours reperfusion results in no tissue necrosis. However there is significant amount of antibody and complement deposition in the area at ischemic risk, which is viable. Thereby implying the activation of complement without deleterious effect on the tissue.

We also show a significant rise of neutrophil infiltration for group 1 but no significant rise in any of the chemotactic molecules (C3a, C5a, IL-8) measured. A rise in IL-6 was noticed for group 2, although not significant. IL-6 is known to mediate neutrophil trafficking and is also produced by recruited neutrophils. This may partly explain the results incurred. Also, it could be that in our model of pig myocardial infarction other chemotactic cytokines like TNFα and IFNγ play a bigger role in neutrophil trafficking.

IgM and C3c deposition is noticed in the viable myocardium even after long reperfusion period of 6 hours. Traditional markers for myocardial infarction like C5b9, cTn-I, CRP requires considerable amount of tissue necrosis. IgM and C3b/c may be used as a diagnostic marker in case of absence of tissue necrosis due to short ischemic period.

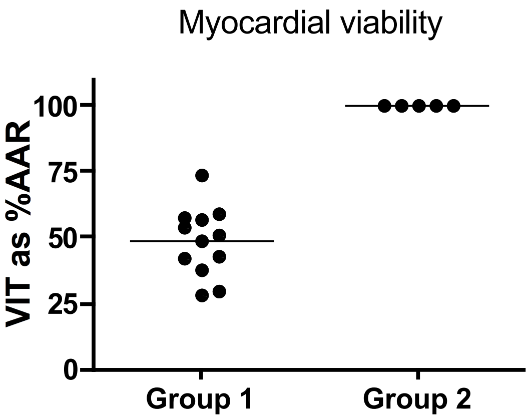

Figure 1: Myocardial viability. The myocardial viability after 60 min ischemia and 6 hour reperfusion (group 1) ranged from 25% - 75% with the ischemic area in the left ventricle. For group 2 with only 20 min ischemia followed by 6 hours reperfusion, this was 100%.

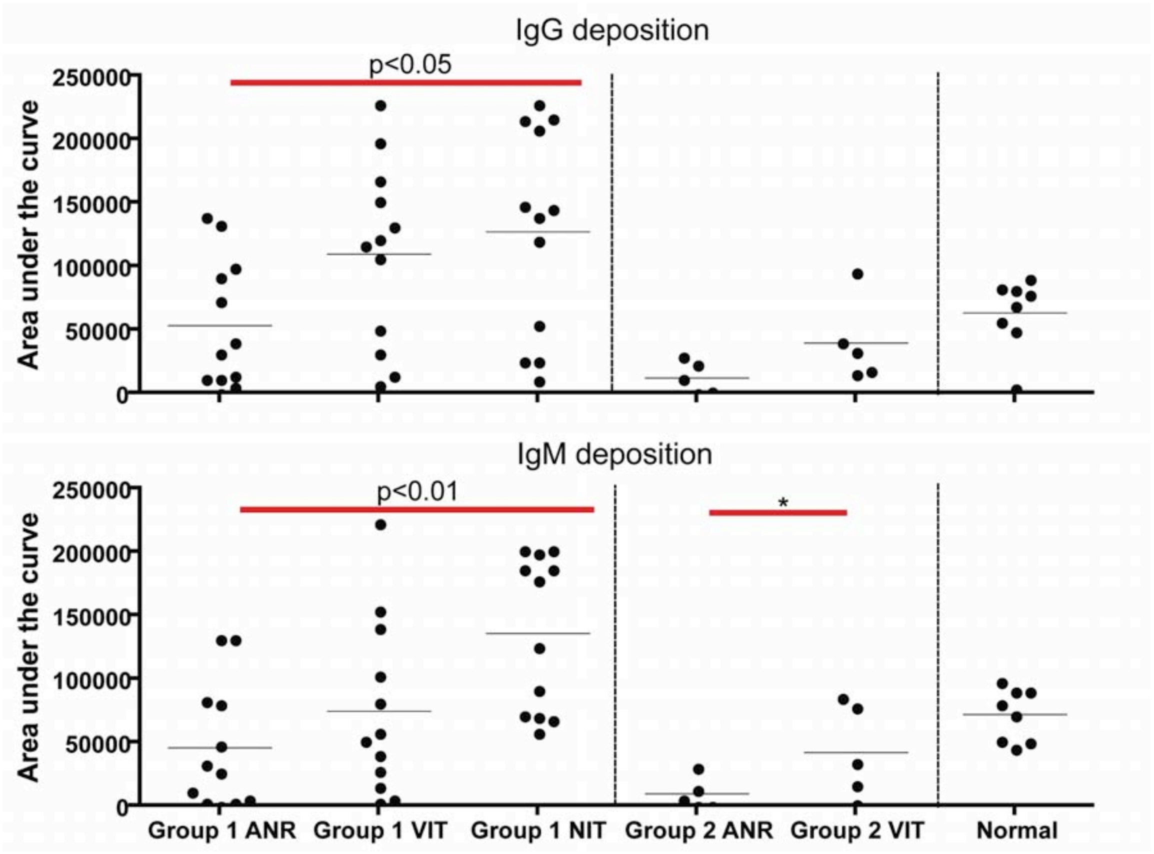

Figure 2: Antibody deposition on tissue. Natural antibody IgG and IgM deposition was significantly higher in NIT than ANR for group 1. This was not the case for group 2 with regard to IgG deposition. But for IgM, the VIT had significantly higher deposition of IgM than ANR

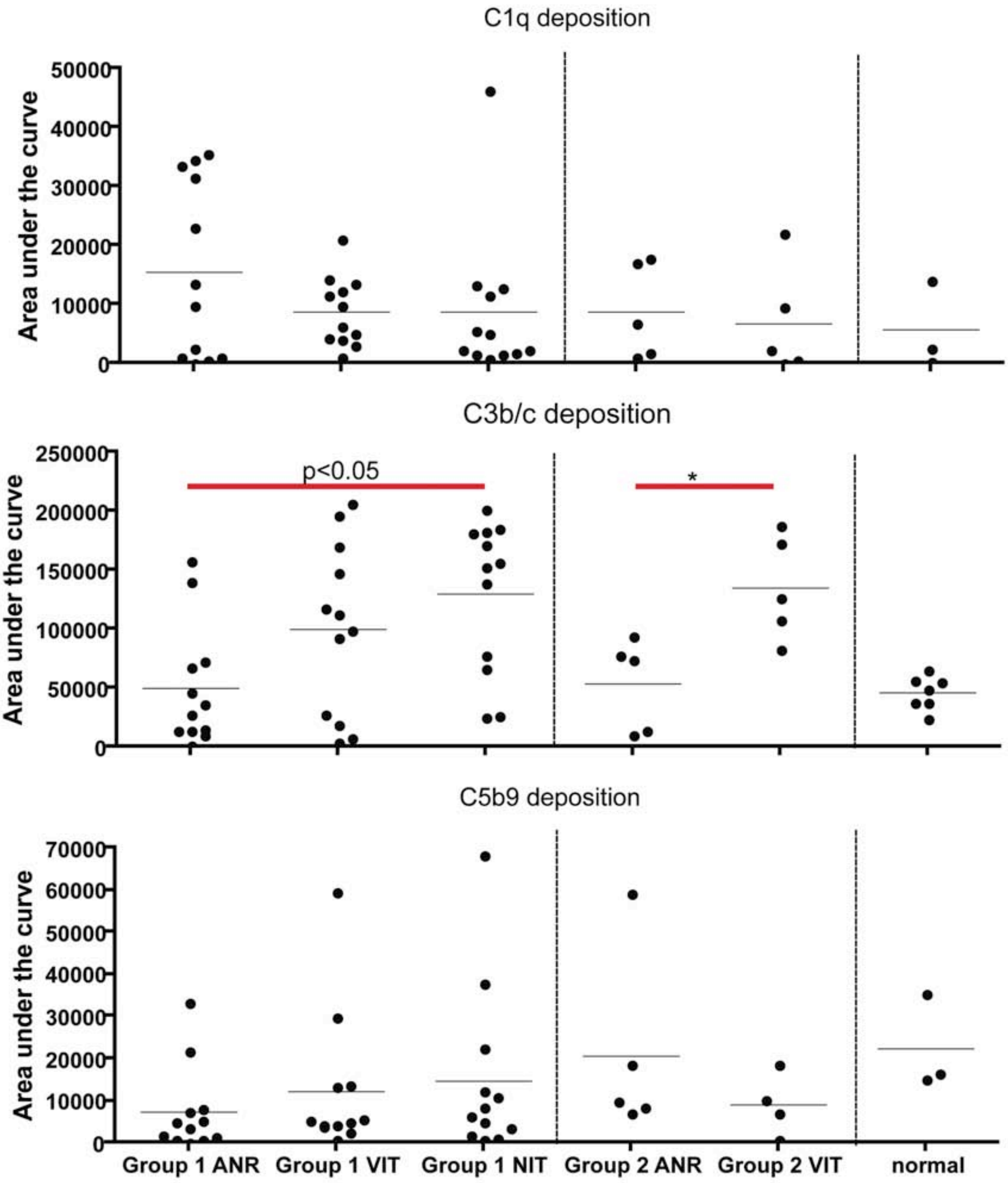

Figure 3: Complement deposition. Deposition of complement components C1q and C5b9 in tissues from both groups were similar to that in normal tissue. For C3b/c, the deposition was significantly higher in NIT for group 1 and VIT for group 2 when compared to their respective ANR.

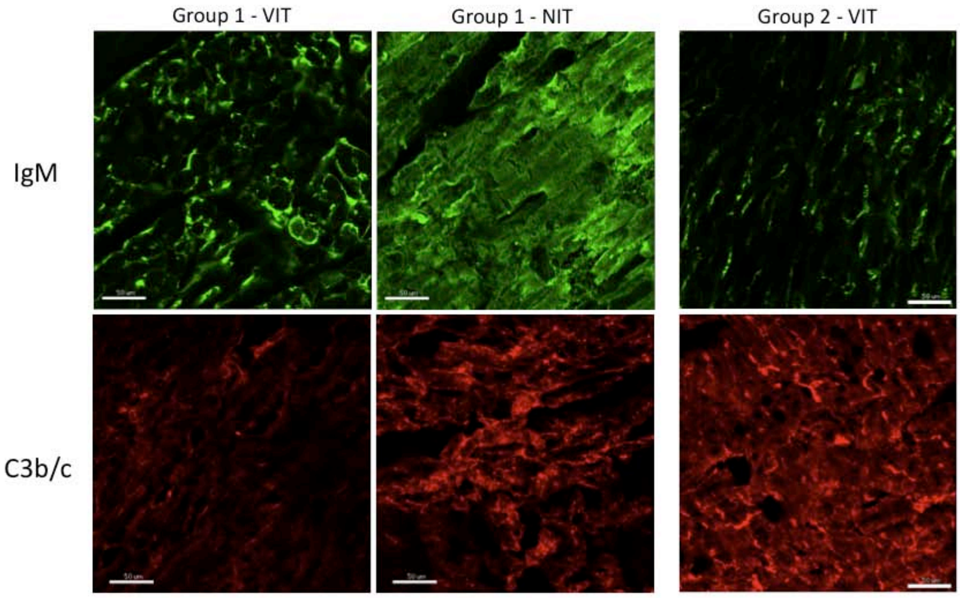

Figure 4: Deposition of IgM and C3b/c on tissue. Representative images of IgM and C3b/c deposition on the ischemic myocardium are shown. Scale = 50μm

Table 1: Anaphylatoxin and cytokine levels in circulation

		Group 1	Group 2
Anaphylatoxins	C3a	354 ± 116	319 ± 68
	C5a	298 ± 56	317 ± 57
Pro-inflammatory cytokine	IL-6	808 ± 275	289 ± 497
	IL-1β	47883 ± 9507	54037 ± 11685
Anti-inflammatory cytokine	IL-10	40644 ± 16856	54037 ± 11685
Chemokine	IL-8	156681 ± 30549	152839 ± 24785

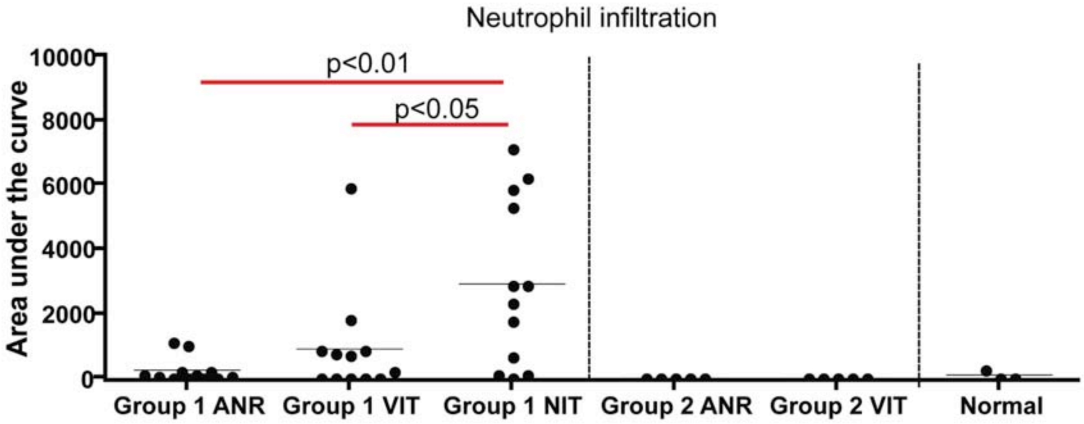

Figure 5: Neutrophil infiltration. For group 1 that showed tissue necrosis after infarction significant increase in infiltrated neutrophils was observed in the NIT when compared to ANR and VIT. For group 2 with no tissue necrosis the ischemia myocardium (VIT) had no infiltrated neutrophils similar to its ANR and normal tissue.

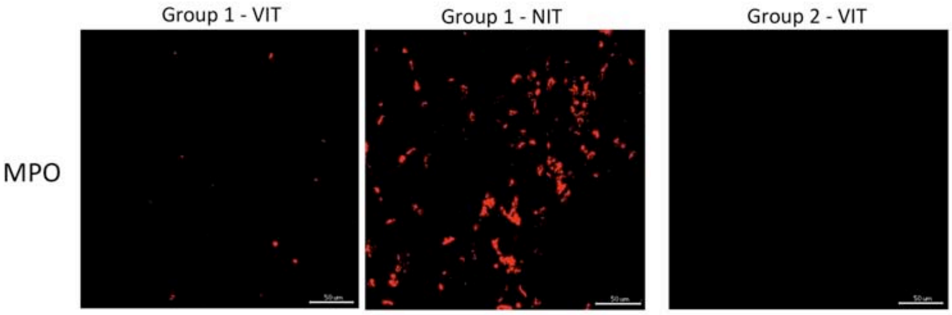

Figure 6: Myeloperoxidase staining. Representative images of myeloperoxidase (MPO) staining on the ischemic myocardium are shown. Scale = 50μm.

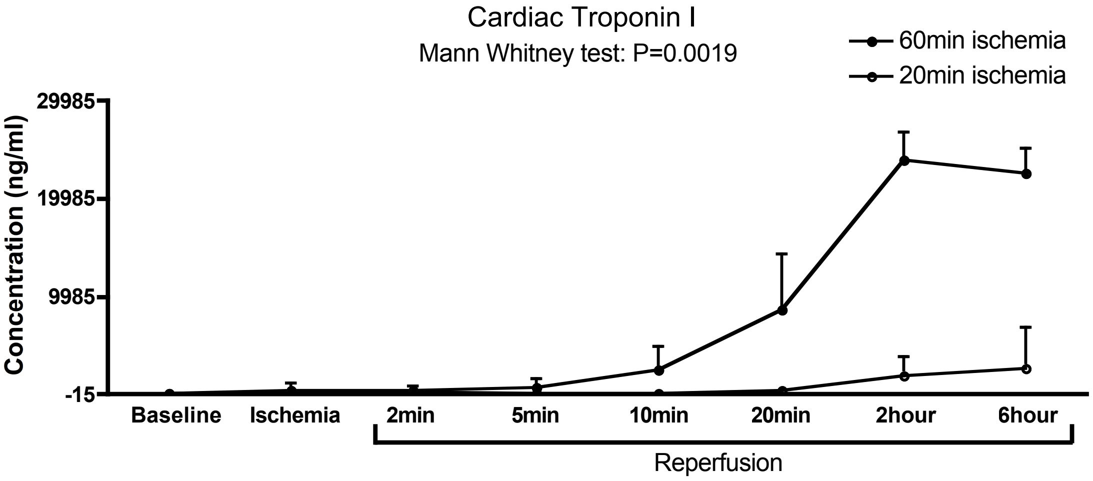

Figure 7: Cardiac troponin -I levels. No significant changes from baseline in cardiac troponin-1 were observed until 5 min reperfusion in both groups. From 10 min reperfusion until 6 hours reperfusion, a continuous and significant rise was seen for group 1 when compared to group 2.

References

1 Fleming SD, Egan RP, Chai C, Girardi G, Holers VM, Salmon J, Monestier M, Tsokos GC: Anti-phospholipid antibodies restore mesenteric ischemia/reperfusion-induced injury in complement receptor 2/complement receptor 1-deficient mice. J Immunol 2004;173:7055-7061.

2 Fleming SD, Monestier M, Tsokos GC: Accelerated ischemia/reperfusion-induced injury in autoimmunity-prone mice. J Immunol 2004;173:4230-4235.

3 Zhang M, Alicot EM, Chiu I, Li J, Verna N, Vorup-Jensen T, Kessler B, Shimaoka M, Chan R, Friend D, Mahmood U, Weissleder R, Moore FD, Carroll MC: Identification of the target self-antigens in reperfusion injury. J Exp Med 2006;203:141-152.

4 Zhang M, Michael LH, Grosjean SA, Kelly RA, Carroll MC, Entman ML: The role of natural igm in myocardial ischemia-reperfusion injury. J Mol Cell Cardiol 2006;41:62-67.

5 Walsh MC, Bourcier T, Takahashi K, Shi L, Busche MN, Rother RP, Solomon SD, Ezekowitz RA, Stahl GL: Mannose-binding lectin is a regulator of inflammation that accompanies myocardial ischemia and reperfusion injury. J Immunol 2005;175:541-546.

6 Zhang M, Takahashi K, Alicot EM, Vorup-Jensen T, Kessler B, Thiel S, Jensenius JC, Ezekowitz RA, Moore FD, Carroll MC: Activation of the lectin pathway by natural igm in a model of ischemia/reperfusion injury. J Immunol 2006;177:4727-4734.

7 Lee H, Green DJ, Lai L, Hou YJ, Jensenius JC, Liu D, Cheong C, Park CG, Zhang M: Early complement factors in the local tissue immunocomplex generated during intestinal ischemia/reperfusion injury. Mol Immunol 2009;47:972-981.

8 Stahl GL, Xu Y, Hao L, Miller M, Buras JA, Fung M, Zhao H: Role for the alternative complement pathway in ischemia/reperfusion injury. Am J Pathol 2003;162:449-455.

9 Banz Y, Rieben R: Role of complement and perspectives for intervention in ischemia-reperfusion damage. Ann Med 2011

10 Wim K. Lagrand RN, Paul A.J. Krijnen, Hans W.M. Niessen, Cees A. Visser, C. Erik Hack: Anti-inflammatory interventions: A promising pathophysiological approach in the treatment of acute myocardial infarction? Heart and Metabolism 2001:6 - 15.

11 Banz Y, Hess OM, Robson SC, Mettler D, Meier P, Haeberli A, Csizmadia E, Korchagina EY, Bovin NV, Rieben R: Locally targeted cytoprotection with dextran sulfate attenuates experimental porcine myocardial ischaemia/reperfusion injury. Eur Heart J 2005;26:2334-2343.

12 Banz Y, Hess OM, Robson SC, Csizmadia E, Mettler D, Meier P, Haeberli A, Shaw S, Smith RA, Rieben R: Attenuation of myocardial reperfusion injury in pigs by mirococept, a membrane-targeted complement inhibitor derived from human cr1. Cardiovasc Res 2007;76:482-493.

13 Shi T, Moulton VR, Lapchak PH, Deng GM, Dalle Lucca JJ, Tsokos GC: Ischemia-mediated aggregation of the actin cytoskeleton is one of the major initial events resulting in ischemia-reperfusion injury. Am J Physiol Gastrointest Liver Physiol 2009;296:G339-347.

14 Vakeva A, Morgan BP, Tikkanen I, Helin K, Laurila P, Meri S: Time course of complement activation and inhibitor expression after ischemic injury of rat myocardium. Am J Pathol 1994;144:1357-1368.

15 Mathey D, Schofer J, Schafer HJ, Hamdoch T, Joachim HC, Ritgen A, Hugo F, Bhakdi S: Early accumulation of the terminal complement-complex in the ischaemic myocardium after reperfusion. Eur Heart J 1994;15:418-423.

16 Schafer H, Mathey D, Hugo F, Bhakdi S: Deposition of the terminal c5b-9 complement complex in infarcted areas of human myocardium. J Immunol 1986;137:1945-1949.

17 Thomsen H, Held H: Immunohistochemical detection of c5b-9(m) in myocardium: An aid in distinguishing infarction-induced ischemic heart muscle necrosis from other forms of lethal myocardial injury. Forensic Sci Int 1995;71:87-95.

18 Stangl V, Baumann G, Stangl K, Felix SB: Negative inotropic mediators released from the heart after myocardial ischaemia-reperfusion. Cardiovasc Res 2002;53:12-30.

19 Bell D, Jackson M, Nicoll JJ, Millar A, Dawes J, Muir AL: Inflammatory response, neutrophil activation, and free radical production after acute myocardial infarction: Effect of thrombolytic treatment. Br Heart J 1990;63:82-87.

20 Curtis WE, Gillinov AM, Wilson IC, Bator JM, Burch RM, Cameron DE, Gardner TJ: Inhibition of neutrophil adhesion reduces myocardial infarct size. Ann Thorac Surg 1993;56:1069-1072; discussion 1072-1063.

Paper V

Effect of Pressure-Controlled Intermittent Coronary Sinus Occlusion (PICSO) on Myocardial Ischemia and Reperfusion in a Closed-Chest Porcine Model

Ahmed A Khattab, MD[1]; Stephan Stieger, MSc[1]; Pranitha J Kamat, MSc[2]; Stijn Vandenberghe, PhD[3]; Christian Seiler, MD[1]; Bernhard Meier, MD[1]; Otto M Hess, MD[1]; Robert Rieben, PhD[2]

[1] Department of Cardiology, Bern University Hospital, [2] Department of Clinical Research (DKF), University of Bern, [3] Artificial Organ (ARTORG) Center for Biomedical Engineering Research, University of Bern, Bern, Switzerland

Imbalance in vasoactive factors occurs during ischemia reperfusion, which causes a collapse in the microcirculation. This results in reduced or no reperfusion in parts of the previously ischemic myocardium, also known as the no-reflow phenomenon, contributing to myocardial infarct size.

Aim: To use a pressure-controlled intermittent coronary sinus occlusion (PICSO) catheter in the coronary sinus during myocardial infarction. It was hypothesized that by doing so the microvascular perfusion could be improved.

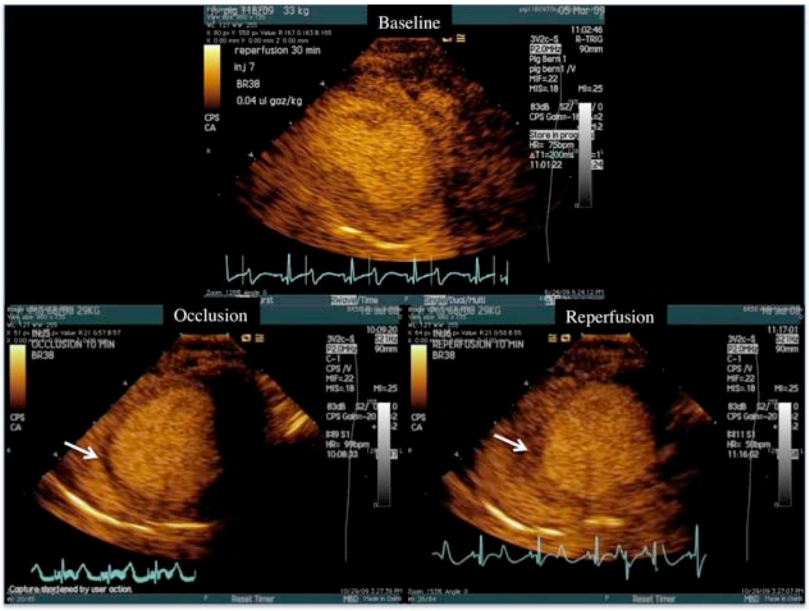

Snapshot of sonograph videos taken during pig myocardial infarction experiment. Baseline image shows clear perfusion of the left ventricle. At occlusion the is no perfusion of part of the ventricular wall (white arrow). Upon reperfusion, the left ventricluar wall was still not perfused (white arrow) probably due to the no-reflow phenomenon.

Model: Myocardial infarction in pigs with 1 hour ischemia and 3 hours reperfusion.

Conclusion: PICSO was effective in reducing microvascular obstruction as determined by a decrease in perfusion pressure gradient and the diastolic pressure deceleration slope.

Effect of Pressure-Controlled Intermittent Coronary Sinus Occlusion (PICSO) on Myocardial Ischemia and Reperfusion in a Closed-Chest Porcine Model

Ahmed A Khattab, MD[1]; Stephan Stieger, MSc[1]; Pranitha J Kamat, MSc[2]; Stijn Vandenberghe, PhD[3]; Christian Seiler, MD[1]; Bernhard Meier, MD[1]; Otto M Hess, MD[1]; Robert Rieben, PhD[2]

[1] Department of Cardiology, Bern University Hospital, [2] Department of Clinical Research (DKF), University of Bern, [3] Artificial Organ (ARTORG) Center for Biomedical Engineering Research, University of Bern, Bern, Switzerland

Total word count: Abstract: Figures: References:

Short title: PICSO in ischemia and reperfusion

(Manuscript in process of submission)

Address for correspondence

Ahmed A Khattab, MD

Department of Cardiology, University Hospital

3010 Bern, Switzerland

Tel: +41-31-632 4714

Fax: +41-31-632 4770

E-mail: ahmed.khattab@insel.ch

Abstract

Background: Despite the high success rate of percutaneous coronary intervention in restoring coronary artery patency in the setting of acute myocardial infarction, reperfusion at myocardial level remains markedly impaired. As a consequence, venous retroperfusion has recently regained attention.

Methods and results: We investigated a Pressure-Controlled Intermittent Coronary Sinus Occlusion (PICSO) system in a closed-chest porcine ischemia/reperfusion model, assigning randomly 18 adult pigs objected to 60 minutes of myocardial ischemia by left anterior descending coronary balloon occlusion to PICSO (n=12, groups A and B) or to controls (n=6, group C). PICSO started 10 minutes before (group A), or 10 minutes after (group B) reperfusion and was maintained till 180 minutes of reperfusion. Distal coronary pressure measurements were used to assess microvascular obstruction and post-mortem tissue samples were stained with Hematoxylin and Eosin and triphenyl tetrazolium chloride for assessing hemorrhagic lesions and the necrotic area, respectively.

At 180 minutes of reperfusion, diastolic coronary pressure was significantly lower in the control group than in the treatment groups (p=0.02), and mean coronary pressure was significantly lower than the mean systemic arterial pressure in that group (p=0.02). Myocardial perfusion pressure gradient was significantly lower in group A (p=0.03) and the diastolic pressure deceleration slope was steeper (p=0.03), compared to group C. Significantly more hemorrhagic lesions were seen in the ischemic myocardium of group C (p=0.002), compared to groups A and B, while the necrotic area was non-significantly different between groups. Immunofluorescence staining of tissue also revealed no significant differences between groups.

Conclusion: PICSO was effective in reducing microvascular obstruction in this ischemia/reperfusion model which is naturally deficient in collaterals, besides being safe and feasible.

Keywords: myocardial infarction; ischemia and reperfusion; microvascular obstruction; myocardial salvage

Introduction:

Prompt recanalization of the infarct-related artery (IRA) by either thrombolysis or percutaneous coronary intervention (PCI) to reperfuse the jeopardized myocardium is considered the cornerstone of therapy in acute ST-elevation myocardial infarction (STEMI) aiming to reduce morbidity and mortality.[1] Despite the proven ability to restore epicardial coronary blood flow, adequate reperfusion on the myocardial level cannot be accomplished in about 50% of patients with STEMI, which itself has adverse prognostic implications[2-5]. This relates to the development of myocardial microvascular dysfunction, due to mechanical or functional obstruction, as a consequence of the primary epicardial event and/or of the reperfusion itself.[6-8]

Due to the grave impact of microvascular dysfunction on patients outcome after STEMI, and the lack of effective preventive and therapeutic strategies, new developments are called for. Intermittent coronary sinus occlusion (ICSO) is a concept introduced several decades ago, based on intermittent pressure increase in the coronary sinus and was evaluated in animal models[9-11] and small clinical observations.[12,13] Pressure-controlled intermittent coronary sinus occlusion (PICSO) is a modification of the original time-dependent technology, and is applied through a dedicated catheter system (Miracor Medical Systems GmbH, Vienna, Austria). Potential indications have been suggested, particularly STEMI to improve regional myocardial function of the ischemic/reperfused myocardium. The proposed mechanisms of action are an intermittent pressure increase in the coronary venous circulation leading to (1) a suction effect, which may enhance wash-out of noxious and embolic material across the microvascular bed[14], and (2) retrograde perfusion via the distal IRA and an augmented collateral inflow from non-IRAs supplying the border zone of the myocardium at stake.[15]

We sought to investigate a PICSO device system in a closed-chest porcine ischemia/reperfusion model with respect to: (1) safety and feasibility of PICSO application in the setting of STEMI, (2) hemodynamic effects of PICSO during ischemia and reperfusion of STEMI , and (3) differential effects related to time of onset of PICSO application.

Methods:

Study design

Prospective, randomized controlled large animal experiment (house swine, average weight = 60 – 70 kg) investigating PICSO in the setting of ischemia (60 minutes) and subsequent reperfusion (190 minutes). 18 animals were divided into 3 groups, 12 PICSO (groups A and B) and 6 controls (group C). The PICSO group was divided into 2 equal arms depending on the starting time of PICSO intervention in relation to reperfusion. Randomization was done by sealed opaque envelopes including equally distributed groups. Care and use of animals in this study were according to the *Guide for the Care and Use of Laboratory Animals* published by the US National Institutes of Health (NIH Publication No. 85-23, revised 1996) and in agreement with the Swiss Animal Welfare Law. The local ethical committee for animal research (Amt für Landwirtschaft und Natur des Kantons Bern) approved the study.

Device under investigation

The PICSO system used (PICSO Impulse System, Miracor Medical Systems GmbH, Vienna, Austria) is composed of a console controlled by a menu and a balloon catheter connected to the console (Figure 1). The catheter contains four lumens, a 15.5mm in diameter x 20mm long balloon at the distal end, a soft tip and connectors on the proximal end for shuttle gas supply to the balloon and for the coronary sinus pressure measurement. By pressing the START button, the device starts with a pressure set up and baseline ICSO. This takes approximately 3 to 5 minutes. PICSO then starts automatically and continues for 30 minutes. Every 30 minutes, the device exchanges the shuttle gas (Helium) circuit and restarts automatically. Every PICSO cycle starts with controlled balloon inflation and is triggered by the QRS complex and depends on the pressure reached in the coronary sinus. It is limited to a maximum occlusion time of 30 seconds. The balloon is inflated until the desired balloon pressure has reached a plateau; the occlusion is intermittently released by balloon deflation. The deflation phase between two occlusions lasts at least 3 seconds (or 4 heart beats) and is controlled by the ECG module in the console. Then the next occlusion cycle starts. Several safety functions are integrated into the device: detection of balloon rupture, limitation of helium escape in case of balloon rupture, detection of balloon dislodgement, detection of power supply failure and switch to battery operation and, if the battery also fails, assuring balloon deflation and catheter removal from the coronary sinus. Moreover, the system warns when the balloon catheter remains in the sinus for too long time without function, which might lead to thrombotic complications. According to the assigned group, PICSO application was installed in group A, 10 minutes before and in group B, 10 minutes after the onset of reperfusion (i.e., after 50 minutes of ischemia or 10 minutes after the end of ischemia, respectively). PICSO was applied till 180 minutes of reperfusion in both groups. The remaining 10 minutes of reperfusion (till 190 minutes) were without PICSO. For group C reperfusion occurred after 60 minutes of ischemia for 190 minutes without PICSO application.

Closed-chest porcine ischemia/reperfusion model

Animals were pre-medicated with ketamine (20 mg/kg), midazolam (1mg/kg), and atropine (0.05 mg/kg) before intubation, induction of anesthesia by isofluran inhalation (1 – 1.5 vol.%) and mechanical ventilation with a Draeger respirator (O_2/N_2O 1:3) maintained till end of experiment. During ischemia and the placement of the PICSO device the animals received fentanyl (10mcg/kg/h). Bilateral common carotid artery and internal jugular vein exposure was done by surgical cut down, followed by direct puncture using Seldinger's technique. PICSO catheter was placed in the coronary sinus in all animals (sham procedure) using a C-arm X-ray unit and contrast dye. The PICSO catheter was introduced via a special pre-shaped 9F sheath, long enough to reach from the right jugular vein to the right atrium and coronary sinus ostium. The PICSO catheter was guided using its two radiopaque markers on both ends of the balloon into the coronary sinus, with the proximal marker situated close to the ostium of the coronary sinus. The use of a guide wire (up to 0.025”) was required in some cases to enter the coronary sinus and was followed by an over-the-wire delivery of the PICSO catheter. Through a standard 6F Judkins left guiding catheter a pressure wire (RADI, St. Jude Medical, Saint Paul, MN, USA) was introduced into the distal left anterior descending coronary artery (LAD) after successful calibration. To create ischemia as the first stage of the model, the LAD was occluded just distal to the first large diagonal branch by a conventional over-the-wire (3.5x15mm) angioplasty balloon for 60 minutes. The occlusion was confirmed by distal pressure measurements as well as angiographic control at the beginning and before the end of the occlusion. At the end of the experiment (after completion of the reperfusion period), LAD re-occlusion and intravenous injection of 120 mL Evan’s Blue (2% wt/vol. solution) were done, leaving all but the area at risk of infarction (AAR) stained blue. The animals were then sacrificed using 20 ml potassium chloride (20%) intravenous injection under deep anesthesia. Immediate thoracotomy via median sternotomy and cardiac explantation was done for further analysis. Coagulation status was monitored throughout the experiment (every 30 min.) and after a baseline activated clotting time (ACT) measurement and intravenous administration of 10000 IU heparin, a target ACT value of more than three times baseline was maintained by additional heparin injections. In case of ventricular fibrillation during the experiments, a biphasic defibrillator (150 J) was used for cardioversion.

Test system justification

The healthy large-swine model was chosen as the experimental species for this study because the size and anatomy of the cardiovascular system is clinically adequate for the purpose of testing such a medical device. The PICSO device was inserted percutaneously and directed under radioscopic guidance to the right atrium and inserted into the coronary sinus, which internal diameter (for this weight group) closely resembles that of humans, enabling us to use the commercially available PICSO balloon catheter. Nevertheless, there is one notable difference in coronary venous drainage between species, namely that the left azygous vein draining the left thoracic cavity directly joins into the coronary sinus in the pig’s heart, which renders placement of the balloon catheter distal to its anastomosis in the coronary sinus essential to generate sufficient pressure in the coronary venous circulation. Furthermore, the coronary arterial circulation in swine is deficient of collaterals, where each area of myocardium is supplied by a single coronary artery, therefore collateral flow contribution to the border zone of the area at risk of necrosis, which is an important mechanism of limiting infarct size in humans, cannot be examined in such model. Additionally, pigs like humans are both right dominant in 80-90% of cases. Last not least there is considerable experience of the research group with this experimental model.

Hemodynamics

Left ventricular function: A 7F admittance pigtail catheter connected to an ADVantage system (Scisense Inc., London, Ontario, Canada), was inserted via the right carotid artery into the left ventricle to acquire left ventricular pressure-volume (PV) loops. The catheter was positioned so that loops displayed stable rectangular shapes and the admittance phase and magnitude signals showed pulsatile signals. All signals were exported to a data acquisition device (model 416, iWorx, Dover, NH), digitized and recorded at 200Hz. The following LV parameters were then derived for each beat and averaged: endsystolic pressure (ESP), enddiastolic pressure (EDP), endsystolic volume (ESV), enddiastolic volume (EDV), maximum (dP/dt max) and minimum pressure change over time (dP/dt min), ejection fraction (EF), stroke volume (SV), and stroke work (SW). The data were analyzed with Labscribe2 software (iWorx) by selecting 30 sequential beats at each time point.

Myocardial perfusion: during the whole experiment surface ECG, rectal temperature, invasive arterial blood pressure, LAD pressure via the pressure wire, central venous pressure and coronary sinus pressure via the PICSO catheter were also recorded via the iWorx system. All pressures were calibrated with a PXCAL pressure calibrator (Edwards Lifesciences) before the experiment. The following parameters were derived to assess microvascular dysfunction[16]: coronary pressure measured during balloon occlusion of the LAD at 10 and 50 minutes of ischemia and at end of reperfusion. Pressure-derived collateral flow index (CFI) = coronary wedge pressure – coronary sinus pressure / mean arterial pressure – coronary sinus pressure, is used to correct for venous and arterial pressure effects on coronary wedge pressure. We measured instead the myocardial perfusion pressure gradient = coronary wedge pressure – coronary sinus pressure was calculated. Finally, the diastolic pressure deceleration slope was drawn between the diastolic pressure at 180 minutes reperfusion and the coronary wedge pressure at 190 minutes.

Staining for myocardial infarct size

The heart was cut perpendicular to the septum from the apex to the base into 3 mm slices until the mitral valve. Entire slices were stained with 1% triphenyl tetrazolium chloride (TTC, Sigma, pH 7.4) for 20 minutes at 37°C. Viable myocardium [viable ischemic tissue (VIT)] was stained bright red while the infarcted tissue [necrotic ischemic tissue (NIT)] remained unstained. High dynamic range images of the slices were taken before and after the TTC staining. Evan's Blue unstained areas of the left ventricle were marked by ImageJ software (NIH, USA) and expressed as a percentage of the left ventricle. This gave a measure of the percentage area at risk (AAR) of the left ventricle. The TTC stained and unstained areas within the AAR were marked and expressed as percentage of the AAR to obtain the amount of viable tissue and myocardial infarct size, respectively. The analysis was conducted in a blinded manner regarding the assigned treatment. Samples were taken from the Evan's blue stained area not at risk (ANR), VIT and NIT for histological analysis.

Immunofluorescence staining of the tissue

Free float technique was adapted for immunostaining of the tissue. In brief, 30μm thick sections were cut from each sample and treated with TBS-TritonX100 for 15 minutes.

Sections were incubated with primary antibody overnight and with secondary antibody for 90 minutes. In case directly labeled primary antibody, the incubation was done at room temperature for 90 minutes. Complement deposition was assessed using rabbit anti-human polyclonal C3c antibody (Sigma), and with sheep anti-rabbit Cy3 (Sigma) as secondary antibody. Natural antibody deposition was assessed with help of goat anti- porcine IgG FITC and IgM FITC antibodies (Southern Biotech and Serotec, respectively). After staining, sections were mounted on a glass slide and taken under the confocal microscope. Section of a healthy pig heart was taken as common control in every staining batch. Image representative of the staining was captured under the confocal microscope from all sections including the common control. With Imaris software (company?), a histogram of the channel of interest was obtained from the captured image. Histogram of the common control was used to normalize histograms of other tissues from the same batch. This enabled sections from different batches to be comparable. Area under the curve (AUC) value was obtained from the normalized histogram to derive a final score for the section. Sections were then compared with their final scores. Sections were blinded at all times.

Hematoxylin and Eosin (H&E) staining of myocardial tissue

Scores were given to H&E stained slides from each tissue type (ANR, VIT, NIT). The scores were given from 1-4 where 1 is the least and 4 the maximum. Analysis included myocytic damage determined by presence of contraction bands and cell necrosis, tissue edema and hemorrhagic lesions. Sections were blinded at all times.

Soluble markers measured in coronary sinus blood

Coronary sinus blood serum samples were taken before LAD occlusion, 50 minutes after, and every 30 minutes of reperfusion. Commercially available antibodies specific for porcine CD31 (R&D), cardiac Troponin (cTn-I) (HyTest), MCP-1 (Peprotech) were used as capture antibodies by coupling them to different fluorescent signatures of polystyrene COOH Luminex-beads by using Bio-Plex amine coupling kit (Bio-Rad). The amount of captured analytes was then measured by using biotinylated detection antibodies, followed by streptavidin-PE. Calibration curves from recombinant protein standards were prepared with threefold dilution steps in antibody diluents containing 0.5% polyvinyl alcohol and 0.8% polyvinylpyrrolidone. Standards were measured, and blank values were subtracted from all readings. Beads coupled with the capture antibody were mixed together in a total volume of 50µl/well containing 2500 beads from each antibody. The bead mix was then incubated with standards or plasma samples from pig (1:3 dilution) or blank to make a final volume of 50 µl/well. Incubation was done at room temperature on a shaker for 60 minutes. Beads were then washed 3 times, and incubated together with a cocktail of biotinylated antibodies: anti CD31 (R&D), anti cTn-I (HyTest), anti MCP-1 (Peprotech) in a final volume 25 µl/well for 30 min. Incubation with streptavidin-PE (50 µl/well) then followed. Measurement and data analysis were performed with the Bio-Plex system and Bio-Plex Manager software.

Statistical analysis

Infarct size data was compared using one-way analysis of variance (ANOVA). For hemodynamic and blood parameter data one-way analysis of variance (ANOVA) was used to detect significant differences between the 3 treatment groups for a certain time point whereas two-way repeated-measures ANOVA for repeated measures was applied to determine the significance of effect of time and treatment as fixed parameters. For direct comparison between two treatment groups for a certain time point two-sample t-tests assuming unequal variances was used. Differences were considered statistically significant at a p-value < 0.05. All p-values are results of two-tailed tests. Microsoft Office Excel 2007 version 12.0 (Microsoft Corp., Redmond, WA, USA) software was used for all analyses. Data, unless otherwise specified, are presented as mean ± standard deviation in tables and figures. There was random assignment of 18 pigs into 3 equal groups (n=6, each). However, in one pig allocated to group B, PICSO was erroneously started 10 minutes before reperfusion. Therefore and since data analysis is based on actual treatment received, this pig was included for group A.

Results

PICSO safety and feasibility

Coronary sinus pressure recorded across the tip of the PICSO catheter reflected the onset and course of PICSO application as per designated treatment group and compared to the control group, in which no notable changes in coronary sinus pressure throughout the experiment were seen (Figure 2). At autopsy, the coronary sinus which was longitudinally opened showed no macroscopic evidence of thrombi, intimal erosions, mural hematomas, or perforations in all animals.

Hemodynamics

Left ventricular function: there were no significant differences in any of the PV loops-derived parameters between groups at any time points. Table 1 displays the absolute values of the measured parameters at selected time points.

Myocardial perfusion: LAD pressure acquired by the pressure wire continuously declined among group C during reperfusion to become significantly lower at end of reperfusion compared to groups A and B. This pressure drop separately involved the diastolic (p=0.02), systolic (p=0.03) and mean (p=0.05) pressure at 180 minutes reperfusion. Figure 3 plots the LAD pressure changes across the time course of the experiments among all groups. These differences in LAD pressure were witnessed in spite of a constant systemic mean arterial blood pressure in all groups throughout the experiments. During reperfusion, LAD pressure was not significantly lower in regards to mean arterial pressure in all groups till 60 minutes, after which LAD pressure sloped in group C to become significantly lower than arterial blood pressure till end of reperfusion (p=0.02); (Figure 4). Exemplary real-time pressure tracings from the 3 groups at different time points are shown in Figure 5. The coronary wedge pressure was low at 10 minutes ischemia (4.5 vs. 4.8 vs. 5.2mmHg, for groups A, B and C, respectively), reflecting the absence of collateral inflow, while at 50 minutes ischemia, i.e. at PICSO onset in group A, there was a significant rise in wedge pressure in this group (15.7 vs. 5.7 vs. 6.6mmHg, for groups A, B and C, respectively) indicating retrograde LAD perfusion. At end of reperfusion, the wedge pressure was higher in groups C and B (9.6 and 10.4mmHg, respectively) compared to A (6.2mmHg), resulting in greater mean difference to that measured at 10 minutes ischemia (4.4 vs. 5.5 vs. 1.7mmHg, respectively). Accordingly, the derived myocardial perfusion pressure gradient was significantly higher in group C compared to group A at end of reperfusion (p=0.03), reflecting a higher grade microvascular obstruction (Figure 6A). This was again evident in the significant difference in diastolic pressure deceleration slope between groups, (Figure 6B).

Soluble markers measured in coronary sinus blood

There were no significant differences in troponin I, CD31, nor MCP-1 among the 3 study groups at any time point of analysis.

Myocardial area at risk and necrosis

The area of the left ventricle subjected to ischemic risk (AAR) was comparable between groups. This was expressed as a percentage of the left ventricle as illustrated in Figure 7A. The myocardial necrosis was also on an average similar among groups. The VIT was expressed as percentage of the AAR (Figure 7B).

Immunofluorescence staining of myocardial tissue

AUC were non-significantly different for IgG, IgM and C3c between groups in the ischemic tissue.

H&E staining of myocardial tissue

Significantly more hemorrhagic lesions were seen in the ischemic myocardium of group C (p=0.002; Figure 8). Otherwise no significant differences were seen in tissue edema and myocytic necrosis.

Discussion

The principal and novel finding of this study is that PICSO application in the setting of a closed-chest porcine myocardial ischemia/reperfusion model significantly reduced myocardial microvascular obstruction, particularly when applied before reperfusion.

Late mortality after acute myocardial infarction is attributed to two distinct yet interrelated etiologies: chronic heart failure and/or malignant arrhythmias. While left ventricular systolic dysfunction is determinant for developing heart failure[17], and mainly dependent on infarct size, electrical instability is not.[18,19] Markers indicative of electrical instability such as blunted heart rate turbulence and altered QT dynamicity are independent predictors of late mortality after acute myocardial infarction. Both were found to be directly related to the presence of myocardial microvascular obstruction after primary PCI largely independent of left ventricular function.[20,21]

Some decades ago, the concept of coronary sinus interventions gained wide interest and became an attractive subject for research. ICSO is a simple method that occludes the coronary sinus intermittently through inflation and deflation of a balloon-tipped catheter that is positioned in the orifice of the coronary sinus. PICSO is a modification of the original time-dependent technology, depending instead on the coronary sinus pressure achieved, as a feedback control for balloon inflation/deflation. Both technologies result in a redistribution of coronary sinus blood flow within the venous compartment to the ischemic myocardium through changes in pressure gradients throughout the coronary venous system.[11] The following mechanisms of anti-ischemic action were suggested: a functional venous microcirculation,[22] less blockade of the microcirculation, washout of reactive oxygen species, diminished granulocyte trapping, and improvement of cellular/interstitial edema.[22,23] Importantly, it is very likely that the extent of coronary collaterals plays a crucial role for the efficacy of (P)ICSO in reducing infarct size, as evident in a series of experimental studies.[24-29] This may also explain the discrepancy of results between studies examining the myocardial salvage potential of these interventions in animal models (initially dogs[30-31] and later on pigs[23,32-35]). It is widely known, that extensive coronary collateral networks can be seen in normal dog hearts[36,37] and that these are almost exclusively located at the epicardial surface, while in pigs, if collaterals are present at all, they are subendocardially.[38] These anatomic differences between species result in an overestimation or underestimation of the infarct size reduction potential of PICSO in humans, respectively. A meta-analysis of theses 7 studies analyzing the effect of ICSO revealed a significant reduction in infarct size of 29% in the treatment group compared with that in the placebo group ($p<0.001$; 95% CI, -40.9 to -17.7)[39]. The magnitude of coronary collateral flow is indeed one of the principal determinants of infarct size in humans.[40,41] Some collaterals are seen in nearly 40% of patients with an acute total coronary occlusion and more begin to appear soon after total occlusion occurs.[42] The function of coronary collaterals is primarily related to the severity of stenotic lesions, but there are functioning anastomoses between coronary supply areas even in the absence of atherosclerotic stenoses.

In 1986, Toggart et al[28] evaluated the efficacy of ICSO in preserving mechanical ventricular function during acute ischemia in swine heart preparations. The authors concluded from their results, that in an animal model lacking collateral circulation, ICSO is incapable of restoring regional or global left ventricular function during conditions of acute ischemia. Although they managed to verify the “wash-out” hypothesis of ICSO, they interpreted their data at that time as negative, which would not be the case with our current knowledge and understanding of the deleterious effects of acute myocardial infarction. Beside infarct size as a determinant of outcome, electrical restitution irrespective of ventricular function is now considered as important. The “wash-out” hypothesis of salvage or “suction effect” focuses on removing metabolic end-products, with augmented myocytic metabolic performance, and improved energy production ultimately enhancing myocardial contractile function and limiting infarct size. Today, a distinct pathologic entity, namely myocardial microvascular dysfunction has been recognized as an independent adverse prognostic marker after acute myocardial infarction irrespective of infarct size. Our data demonstrate the ability of PICSO to reduce myocardial microvascular obstruction as assessed by coronary pressure measurements which is an established tool in this respect.[16,43-45] The non-significant difference in infarct size between groups, and the overall large necrotic areas are referred to the intrinsic limitation of the used animal model, namely its deficiency of collaterals. It was previously shown in a canine ischemia/reperfusion model that collateral flow to TTC-positive regions was greater than flow to TTC-negative regions (P=0.01), underlining the role of collaterals in preserving the viability of tissue in the AAR.[46] Although our histological analysis showed also no significant difference in amount of myocytic damage and tissue edema between groups, a significantly higher amount of hemorrhage was seen in the ischemic myocardium of the control group. Intra myocardial hemorrhage in STEMI is associated with larger myocardial infarction and worse clinical outcome in humans.[47]

Already in 1898, the experimental work of Pratt suggested that venous retroperfusion may provide nutritional delivery to the myocardium,[48] however, attempts to introduce coronary sinus interventions clinically by interventional cardiologists have not prevailed. Although the myocardial salvage potential of ICSO was repeatedly shown in the 1970ies, 80ies and 90ies, yet these results were probably superseded by the simultaneous introduction of thrombolytics, and later on mechanical recanalization techniques which both form undoubtedly the breakthrough technology in modern myocardial infarction management. Today, with contemporary primary PCI practice for acute myocardial infarction, including thrombus aspiration, stent implantation and aggressive antithrombotic/antiplatelet treatment, a considerable amount of patients still experience microvascular obstruction, in spite of a patent IRA. As a consequence, the long pursued strategy of venous retroperfusion has again gained attention during recent years, as an adjunctive therapy to improve outcome after acute myocardial infarction.

We were able to show in an experimental work, that PICSO can effectively reduce microvascular obstruction using coronary flow measurements. Although the clinical and the experimental setting of ischemia-reperfusion share important underlying pathophysiologic aspects of microvascular obstruction, distal coronary microembolization of atherosclerotic debris or thrombotic material which might be responsible for a substantial part of clinically observed microvascular obstruction, cannot be simulated in standard animal models of ischemia and reperfusion.[49] Since left coronary blood flow is purely diastolic, the low distal coronary diastolic pressure expresses a diminished flow due to a maximally raised downstream resistance in the damaged microcirculation in the necrotic myocardium. According to Ohm’s law, coronary flow to the infarcted area must be reduced out of proportion relative to resistance, because a linear change of resistance and flow would result in a constant and preserved distal pressure. PICSO reduced microvascular resistance and hence improved coronary flow as reflected by the preserved distal pressure.

In conclusion, the commercially available PICSO study device was safe and feasible in its application as well as effective in reducing microvascular obstruction in this closed-chest porcine ischemia/reperfusion model. The next logic steps are to study more robust endpoints in animals such as long-term effects on left ventricular function and death, and to initiate clinical studies to determine the effect of PICSO on the level of myocardial ischemia and the influence of the collateral circulation on this effect.

Acknowledgements

The authors are grateful to Olgica Beslac and Daniel Mettler, Experimental Surgery Institute, and Katja Matozen and Carmen Fleurkens, Department of Clinical Research, both University of Bern for their assistance during the experiments.

Source of funding

Miracor Medical Systems GmbH, Vienna, Austria.

Disclosure

Ahmed A Khattab serves as a consultant for Miracor.

Table 1: Left ventricular function indices as derived from pressure-volume loops among pigs subjected to ischemia/reperfusion

Variable	**Baseline**				**10 Minutes Reperfusion**				**180 Minutes Reperfusion**			
	PICSO A (n=7)	**PICSO B (n=5)**	**Control (n=6)**	**p**	**PICSO A (n=7)**	**PICSO B (n=5)**	**Control (n=6)**	**p**	**PICSO A (n=7)**	**PICSO B (n=5)**	**Control (n=6)**	**p**
HR, beats/min	111±21	91±13	99±6	0.10	105±12	110±22	98±9	0.37	123±20	139±33	110±15	0.15
ESP, mmHg	106±18	91±21	104±18	0.39	95±20	83±10	90±27	0.60	86±15	77±8	80±12	0.47
EDP, mmHg	15±9	11±4	12±5	0.48	20±7	12±7	16±5	0.14	20±8	13±4	15±6	0.17
dP/dt max, mmHg/s	1541±336	1213±415	1485±320	0.10	1258±275	1117±154	1129±268	0.54	1240±417	1000±129	1061±169	0.34
dP/dt min, mmHg/s	-1952±451	-1761±415	-1977±320	0.64	-1530±570	-1486±192	-1485±496	0.98	-1361±264	-1284±130	-1332±204	0.83
ESV, mL	45±23	53±15	60±20	0.45	38±28	47±20	50±13	0.60	52±29	62±19	62±4	0.66
EDV, mL	95±27	105±14	111±20	0.41	76±41	93±27	104±27	0.33	92±37	99±31	114±15	0.45
SV, mL	50±7	52±4	52±4	0.64	37±16	46±11	54±17	0.18	40±10	38±13	51±12	0.12
EF, %	54±9	51±8	48±9	0.51	52±16	51±8	51±5	0.98	46±11	38±5	45±5	0.22
SW, mmHg. ml	4610±898	3948±628	4826±835	0.22	3082±1636	3371±982	3924±1891	0.64	2986±869	2404±1105	3498±1240	0.27

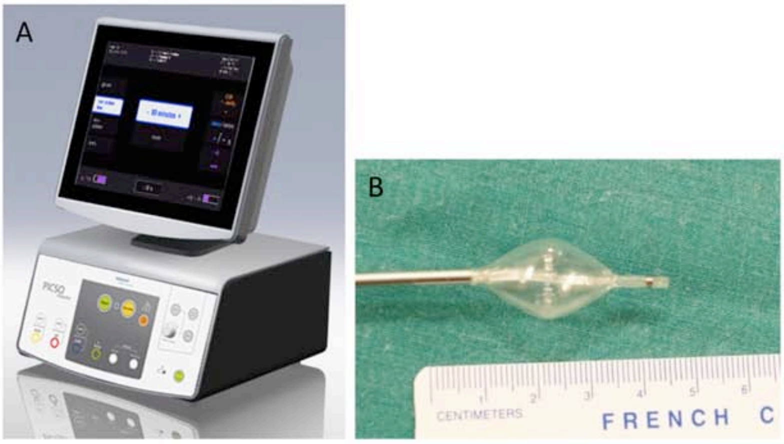
A
B
CENTIMETERS
FRENCH C

Figure 1: The CE-Mark approved Miracor PICSO device system (A) console, (B) inflated catheter balloon tip.

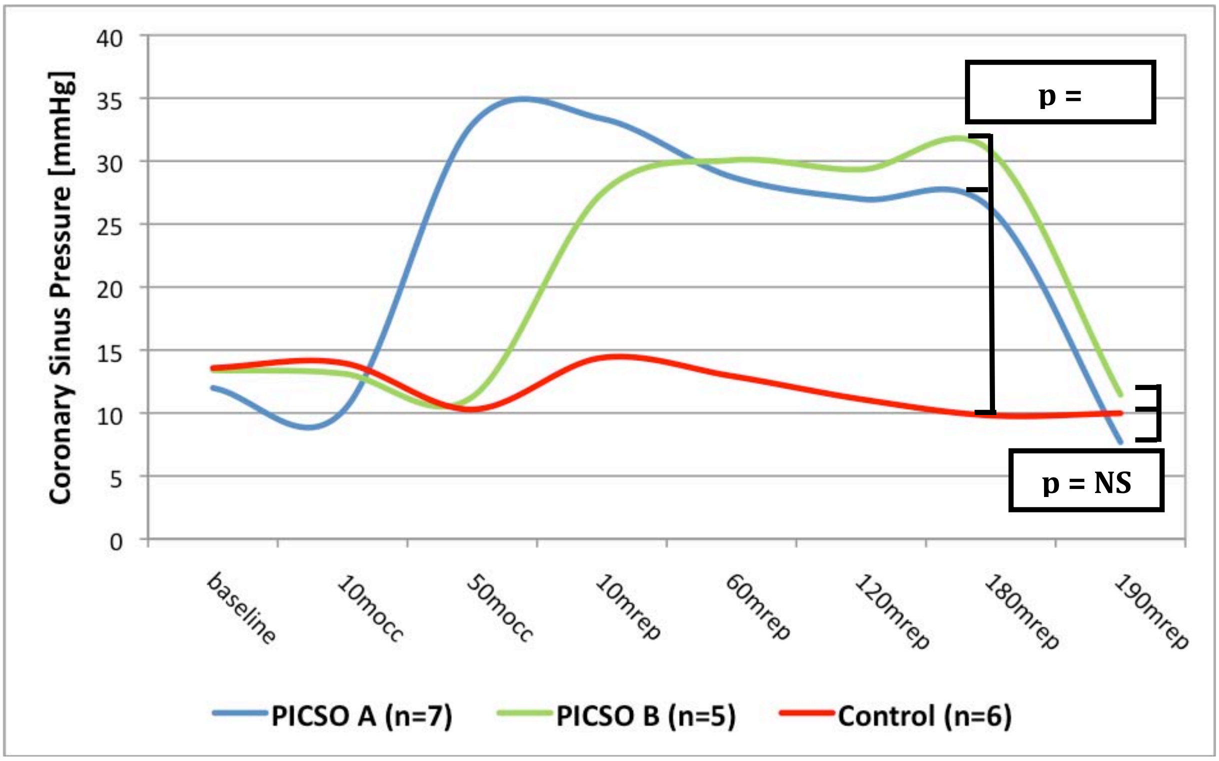

Figure 2: Coronary sinus pressure changes over the time course of the experiments in the 3 study groups.

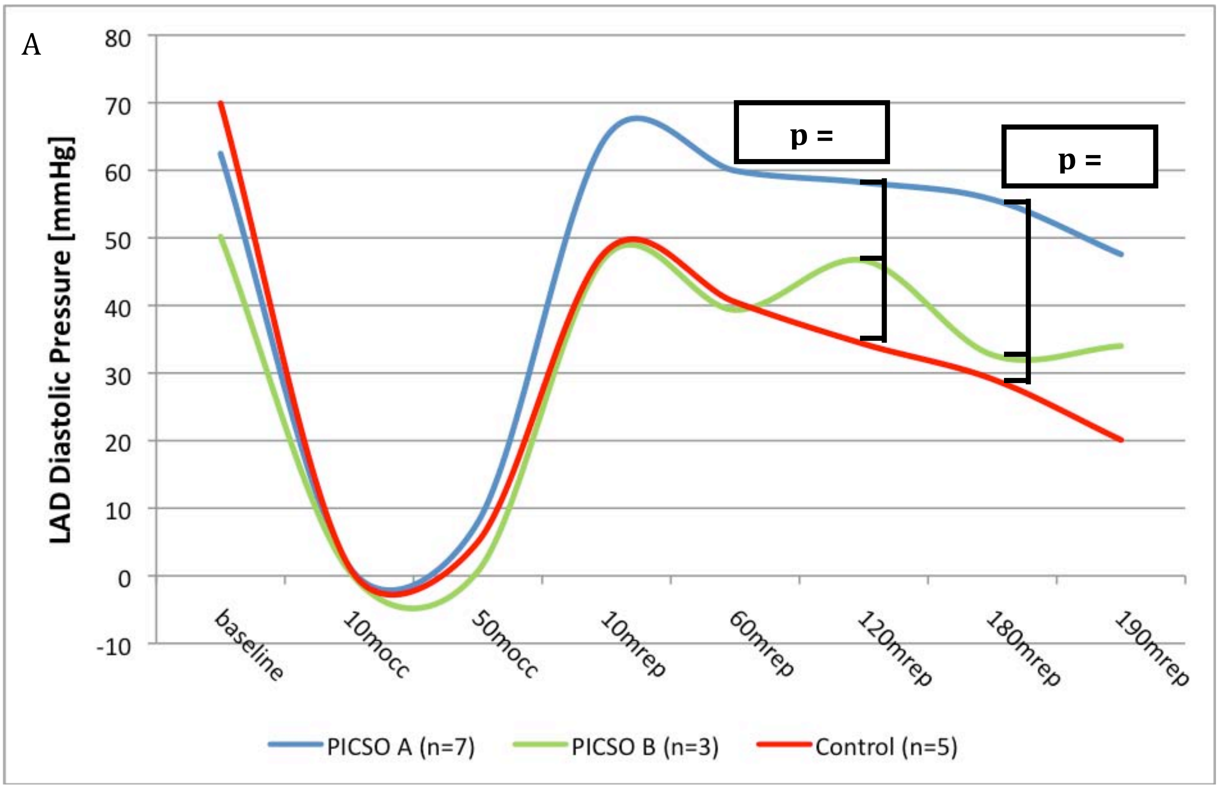
A
LAD Diastolic Pressure [mmHg]
80
70
60
50
40
30
20
10
0
-10
baseline
10mocc
50mocc
10mrep
60mrep
120mrep
180mrep
190mrep
p =
p =
PICSO A (n=7)
PICSO B (n=3)
Control (n=5)

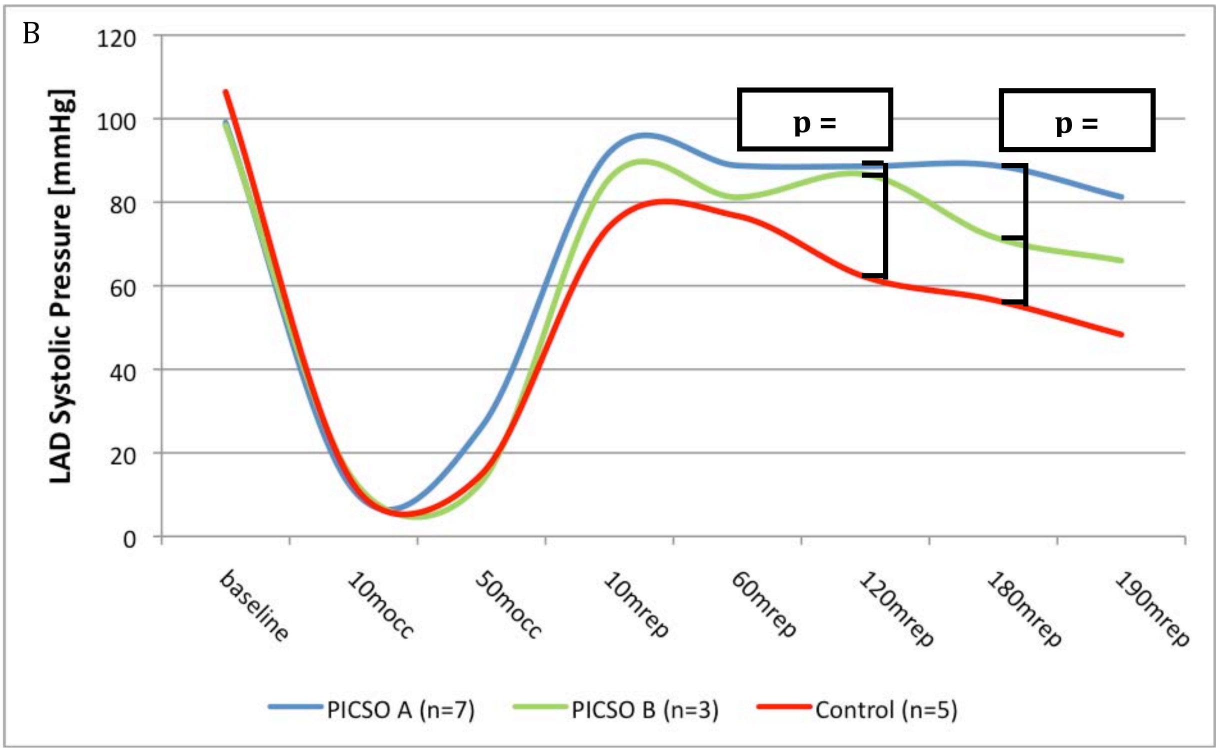
B
LAD Systolic Pressure [mmHg]
120
100
80
60
40
20
0
baseline
10mocc
50mocc
10mrep
60mrep
120mrep
180mrep
190mrep
p =
p =
PICSO A (n=7)
PICSO B (n=3)
Control (n=5)

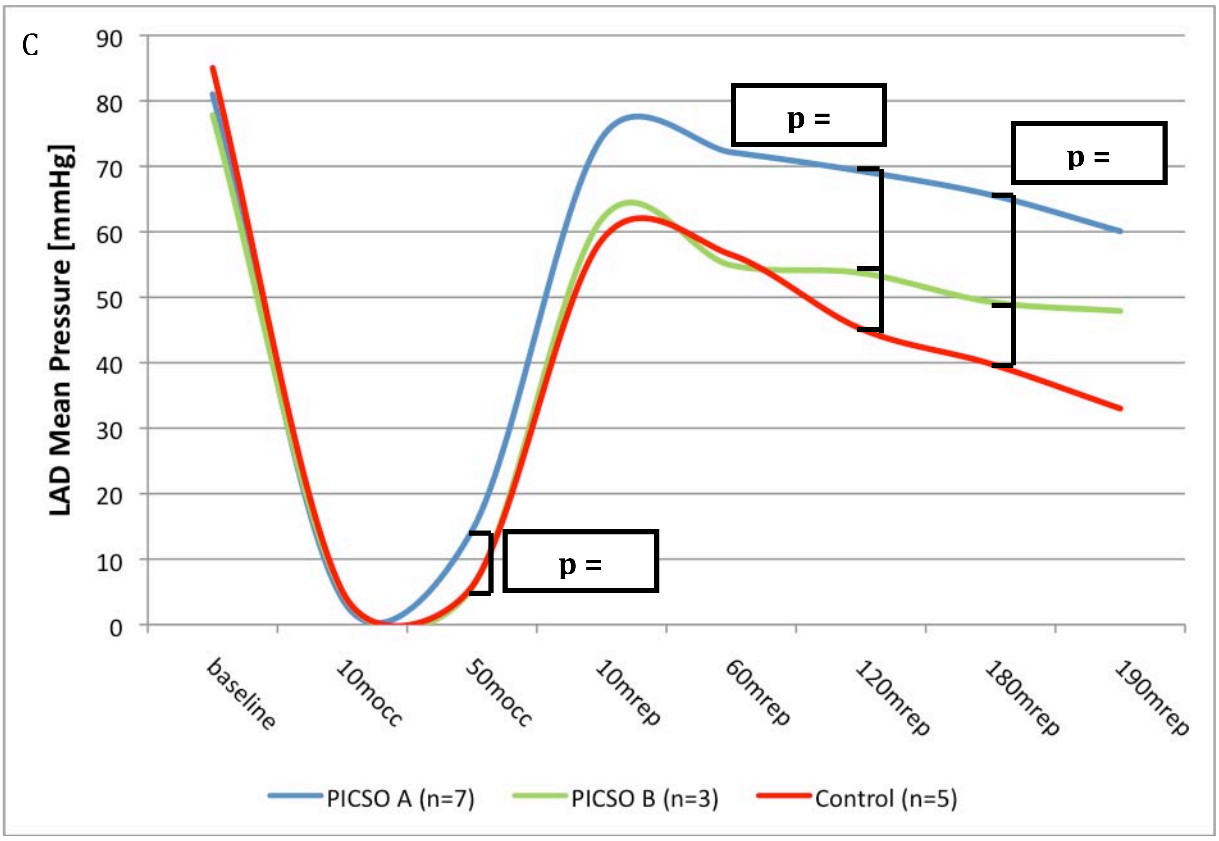

Figure 3: Distal left anterior descending coronary artery (LAD) pressure recordings across a pressure wire along the course of the experiments in the 3 study groups; (A) diastolic pressure, (B) systolic pressure, and (C) mean pressure.

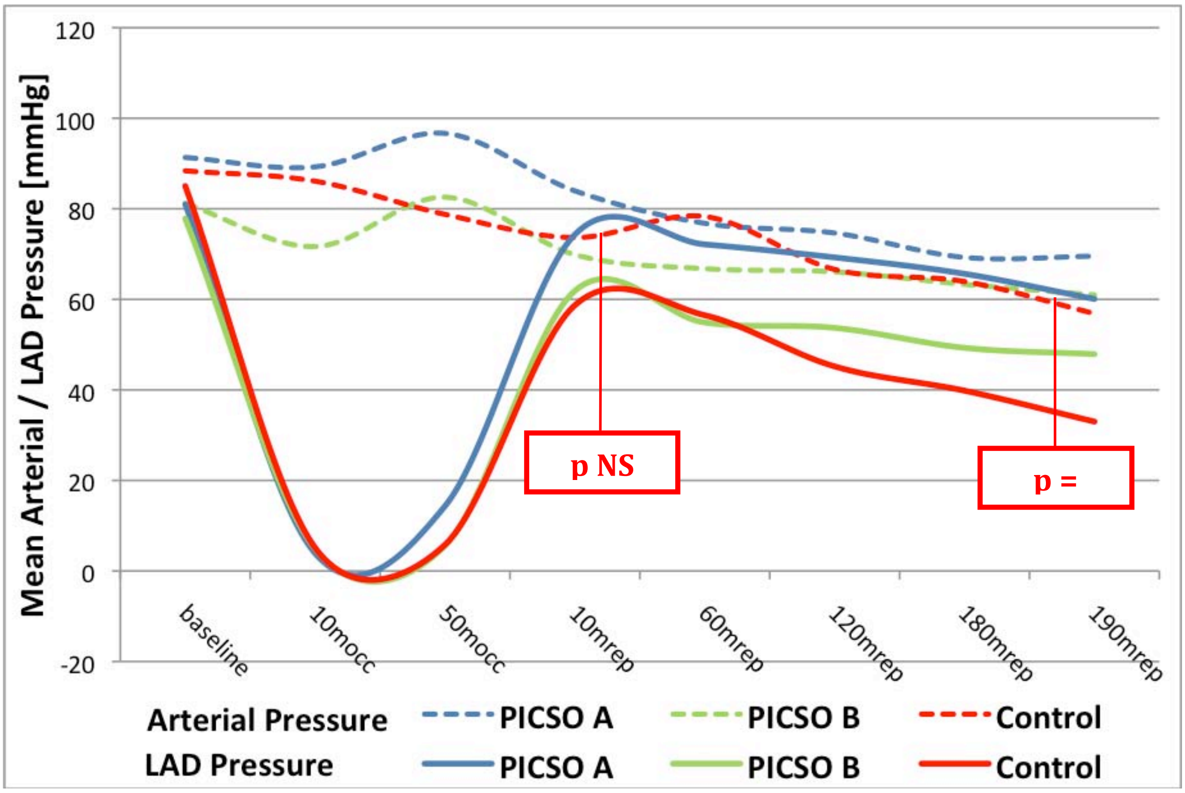

Figure 4: Distal left anterior descending coronary artery (LAD) pressure (mean pressure) plotted against mean systemic arterial blood pressure along the course of the experiments in the 3 study groups. The p-values indicated refer to the differences seen for group C. All differences in groups A and B were non-significant.

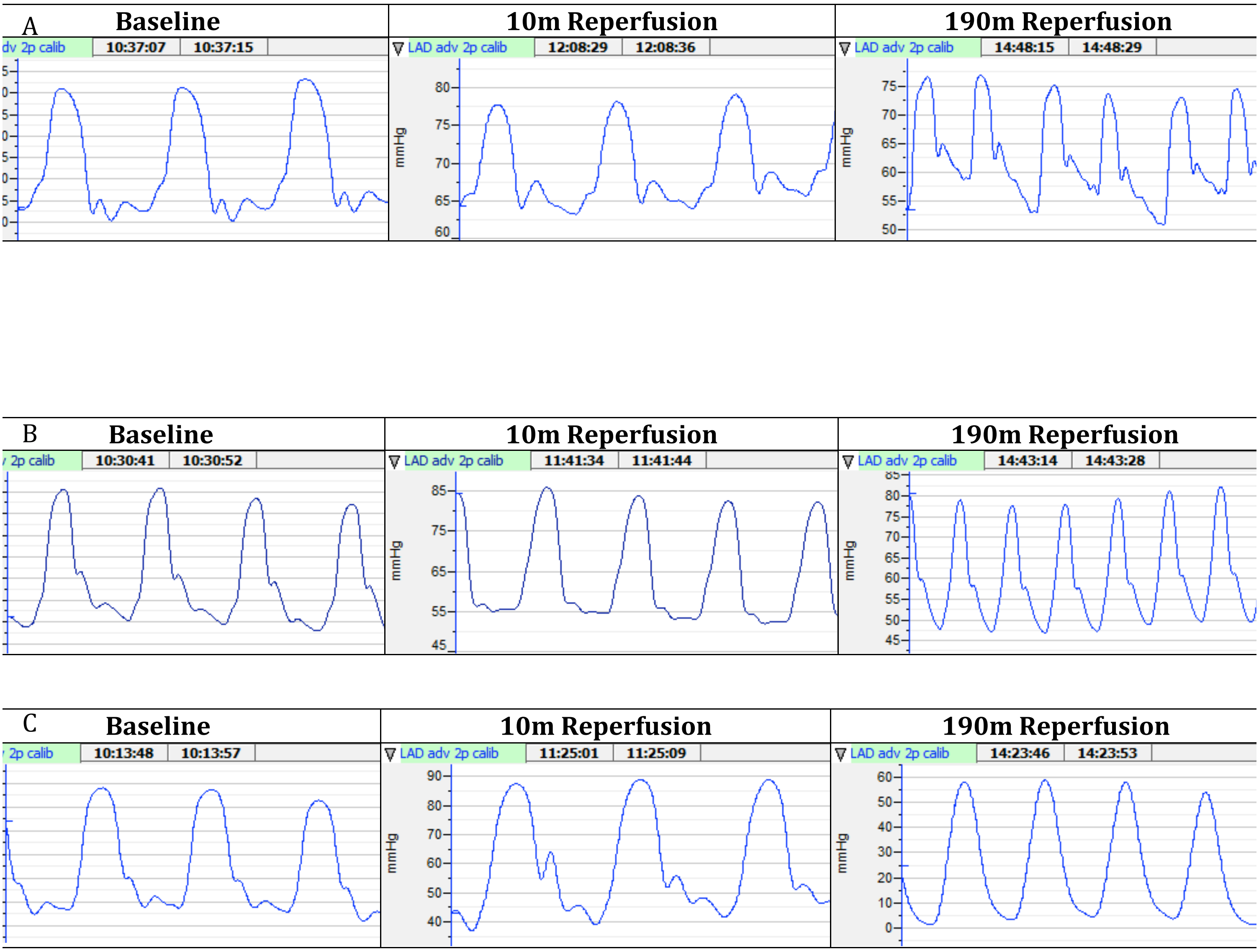

Figure 5: Exemplary real-time tracings of distal left anterior descending coronary artery (LAD) pressure from the 3 groups at different time points, (A) from group A with preserved diastolic pressure throughout the experiment, (B) from group B with preserved diastolic pressure throughout the experiment, and (C) from group C with lost diastolic pressure (ventricularization) at 180 minutes reperfusion.

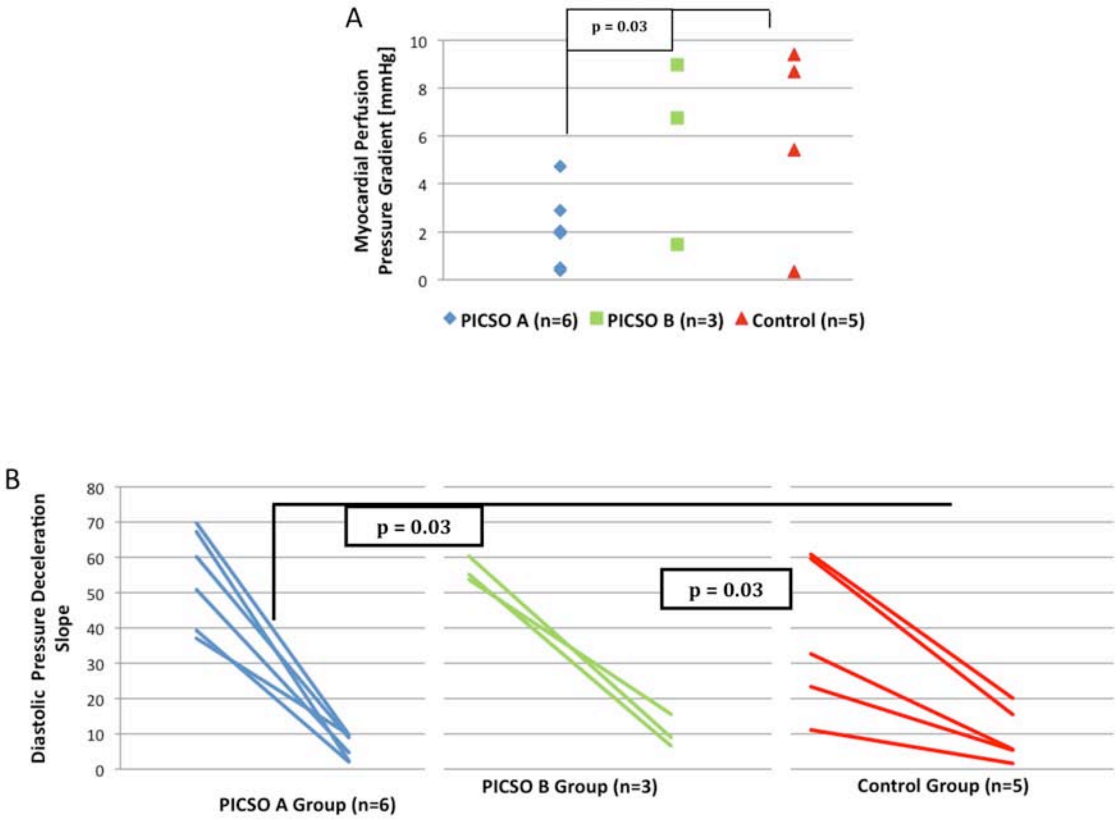

Figure 6: Coronary flow measurements indicative of microvascular obstruction. (A) Myocardial perfusion pressure gradient, (B) Diastolic pressure deceleration slope.

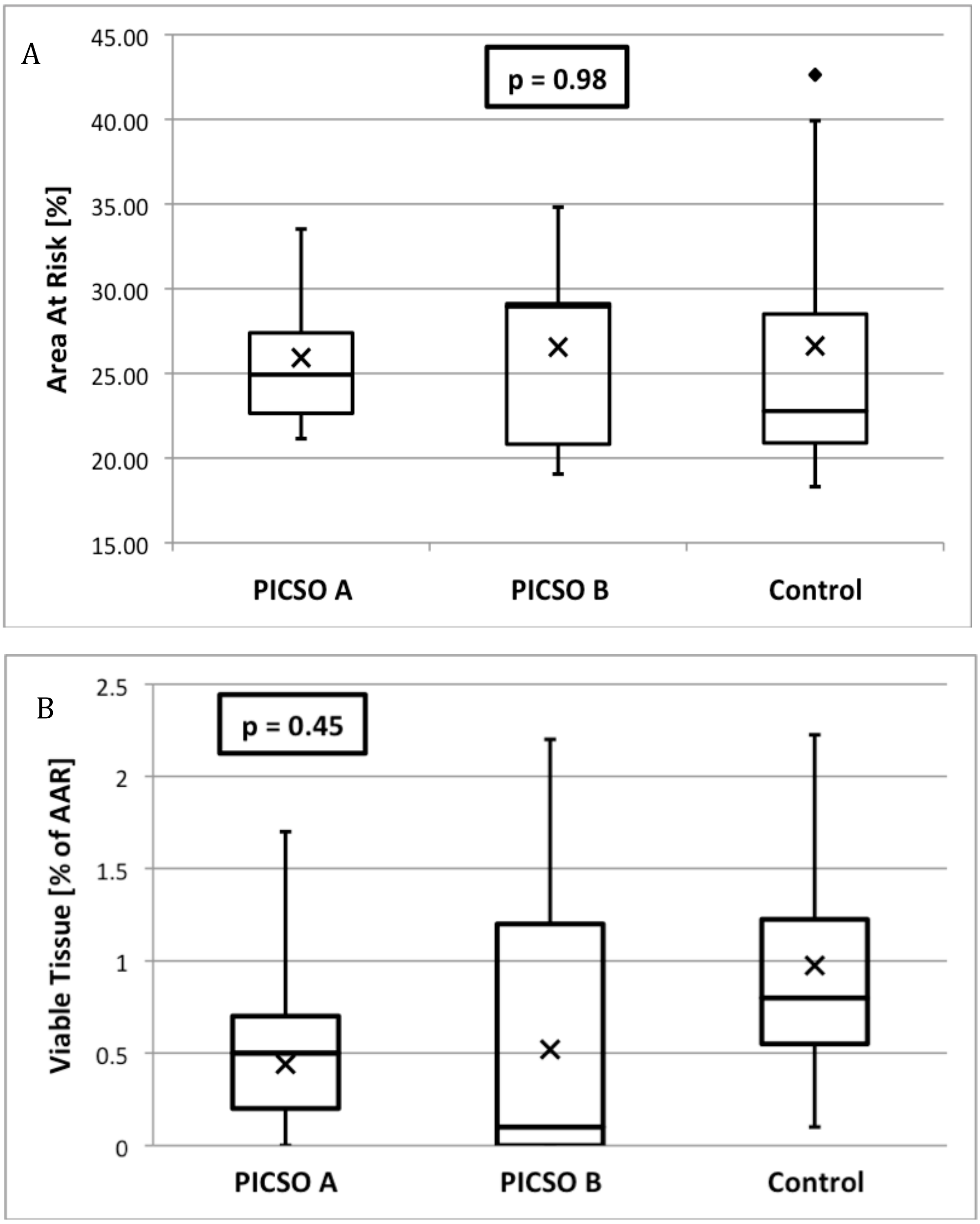

Figure 7: Area of the left ventricle subjected to ischemic risk (AAR) expressed as a percentage of the left ventricle (A). The viable ischemic tissue (VIT) was expressed as percentage of the AAR (B).

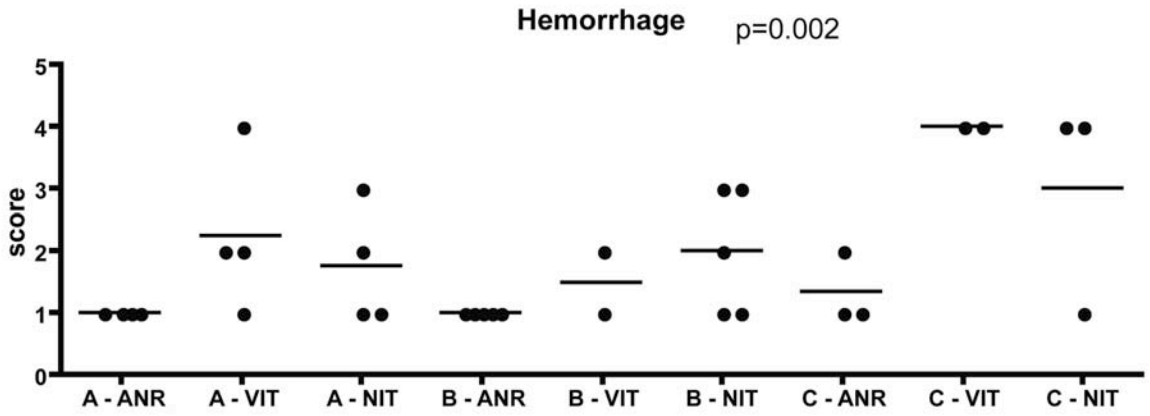

Figure 8: H&E staining of myocardial tissue showing significantly more hemorrhagic lesions in the ischemic tissue (necrotic and viable) of group C.

References:

1. Antman EM, Anbe DT, Armstrong PW, Bates ER, Green LA, Hand M, Hochman JS, Krumholz HM, Kushner FG, Lamas GA, Mullany CJ, Ornato JP, Pearle DL, Sloan MA, Smith SC Jr, Alpert JS, Anderson JL, Faxon DP, Fuster V, Gibbons RJ, Gregoratos G, Halperin JL, Hiratzka LF, Hunt SA, Jacobs AK. ACC/AHA guidelines for the management of patients with ST-elevation myocardial infarction–executive summary: a report of the American College of Cardiology/American Heart Association Task Force on Practice Guidelines (Writing Committee to Revise the 1999 Guidelines for the Management of Patients With Acute Myocardial Infarction). *Circulation* 2004;110:588–636.
2. Goel M, Dodge JT Jr, Rizzo M, McLean C, Ryan KA, Daley WL, Cannon CP, Gibson CM. The open artery hypothesis: past, present, and future. *J Thromb Thrombolysis* 1998;5:101–112.
3. Berger PB, Ellis SG, Holmes DR Jr, Granger CB, Criger DA, Betriu A, Topol EJ, Califf RM. Relationship between delay in performing direct coronary angioplasty and early clinical outcome in patients with acute myocardial infarction: results from the global use of strategies to open occluded arteries in Acute Coronary Syndromes (GUSTO-IIb) trial. *Circulation* 1999;100:14–20.
4. Roe MT, Ohman EM, Maas AC, Christenson RH, Mahaffey KW, Granger CB, Harrington RA, Califf RM, Krucoff MW. Shifting the open-artery hypothesis downstream: the quest for optimal reperfusion. *J Am Coll Cardiol* 2001;37:9–18.
5. Sorajja P, Gersh BJ, Costantini C, McLaughlin MG, Zimetbaum P, Cox DA, Garcia E, Tcheng JE, Mehran R, Lansky AJ, Kandzari DE, Grines CL, Stone GW. Combined prognostic utility of ST-segment recovery and myocardial blush after primary percutaneous coronary intervention in acute myocardial infarction. *Eur Heart J* 2005;26:667–674.
6. Wu KC, Zerhouni EA, Judd RM, Lugo-Olivieri CH, Barouch LA, Schulman SP, Blumenthal RS, Lima JA. Prognostic significance of microvascular obstruction by magnetic resonance imaging in patients with acute myocardial infarction. *Circulation* 1998;97:765–772.
7. Morishima I, Sone T, Okumura K, Tsuboi H, Kondo J, Mukawa H, Matsui H, Toki Y, Ito T, Hayakawa T. Angiographic no-reflow phenomenon as a predictor of adverse long-term outcome in patients treated with percutaneous transluminal coronary angioplasty for first acute myocardial infarction. *J Am Coll Cardiol* 2000;36:1202–1209.
8. Bolognese L, Carrabba N, Parodi G, Santoro GM, Buonamici P, Cerisano G, Antoniucci D. Impact of microvascular dysfunction on left ventricular remodeling and long-term clinical outcome after primary coronary angioplasty for acute myocardial infarction. *Circulation* 2004;109:1121–1126.
9. Mohl W, Glogar DH, Mayr H, Losert U, Sochor H, Pachinger O, Kaindl F, Wolner E. Reduction of infarct size induced by pressure-controlled intermittent coronary sinus occlusion. *Am J Cardiol* 1984;53:923-928.
10. Lazar HL, Rajaii A, Roberts AJ. Reversal of reperfusion injury after ischemic arrest with pressure controlled intermittent coronary sinus occlusion. *J Thorac Cardiovasc Surg* 1988;95:637-642.
11. Mohl W, Punzengruber C, Moser M, Kenner T, Heimisch W, Haendchen R, Meerbaum S, Maurer G, Corday E. Effects of pressure-controlled intermittent coronary sinus occlusion on regional ischemic myocardial function. *J Am Coll Cardiol* 1985;5:939-947.

12. Mohl W, Simon P, Neumann F, Schreiner W, Punzengruber C. Clinical evaluation of pressure controlled intermittent coronary sinus occlusion: randomized trial during coronary artery surgery. *AnnThorac Surg* 1988;46:192-201.
13. Schreiner W, Neumann F, Schuster J, Simon P, Froehlich KC, Mohl W. Intermittent coronary sinus occlusion in humans: pressure dynamics and calculation of diagnostic quantities. *Cardiovasc Res* 1988;22:277-286.
14. Mohl W, Glogar D, Kenner Th, Klepetko W, Moritz A, Moser M, Müller M, Schuster J and Wolner E. Enhancement of Washout Induced by Pressure Controlled Intermittent Coronary Sinus Occlusion (PICSO) In the Canine and Human Heart. In: Mohl W, editor. ICSO and PICSO. *Coronary Sinus Library*.
15. Faxon DP, Jacobs AK, Kellett MA, McSweeney SM, Coats WD, Ryan TJ. Coronary sinus occlusion pressure and its relation to intracardiac pressure. *Am J Cardiol* 1985;56:457-460.
16. Yamamoto K, Ito H, Iwakura K, Shintani Y, Masuyama T, Hori M, Kawano S, Higashino Y, Fujii K. Pressure-derived collateral flow index as a parameter of microvascular dysfunction in acute myocardial infarction. *J Am Coll Cardiol* 2001; 38:1383-1389.
17. Braunwald E. Myocardial reperfusion, limitation of infarct size, reduction of left ventricular dysfunction and improved survival. *Circulation* 1989;79:441–444.
18. Hii JTY, Traboulsi M, Mitchell LB, et al. Infarct artery patency predicts outcome of serial electropharmacological studies in patients with malignant ventricular tachyarrhythmias. *Circulation* 1993;87:764–772.
19. Brändle M, Wang W, Zucker IH. Hemodynamic correlates of baroreflex impairment of heart rate in experimental heart failure. *Basic Res Cardiol* 1996;91:147–154.
20. Bonnemeier H, Wiegand UKH, Friedlbinder J, et al. Heart Rate Turbulence in Patients Undergoing Direct Percutaneous Coronary Intervention for Acute Myocardial Infarction. *Circulation* 2003;108:958-964.
21. Bonnemeier H, Wiegand UKH, Bode F, et al. Impact of Infarct-Related Artery Flow on QT Dynamicity in Patients Undergoing Direct Percutaneous Coronary Intervention for Acute Myocardial Infarction. *Circulation* 2003;108:2979-2986.
22. Kassab GS, Navia JA, March K, Choy JS. Coronary venous retroperfusion: an old concept, a new approach. *J Appl Physiol* 2008;104:1266-1272.
23. Aldea GS, Zhang X, Rivers S, Shemin RJ. Salvage of ischemic myocardium with simplified and even delayed coronary sinus retroperfusion. *Ann Thorac Surg* 1996;62:9-15.
24. Gregg DE, Dewald D. The immediate effects of the occlusion of the coronary veins on collateral blood flow in the coronary arteries. *Am J Physiol* 1938;124:435-443.
25. Ido A, Hasebe N, Matsuhashi H, Kikuchi K. Coronary sinus occlusion enhances coronary collateral flow and reduces subendocardial ischemia. *Am J Physiol Heart Circ Physiol* 2001;280:H1361-1367.
26. Sato M, Saito T, Mitsugi M, Saitoh S, Niitsuma T, Maehara K, Maruyama Y. Effects of cardiac contraction and coronary sinus pressure elevation on collateral circulation. *Am J Physiol* 1996;271:H1433-1440.

27. Scheel KW, Williams SE, Parker JB. Coronary sinus pressure has a direct effect on gradient for coronary perfusion. *Am J Physiol* 1990;258:H1739-1744.
28. Toggart EJ, Nellis SH, Liedtke AJ. The efficacy of intermittent coronary sinus occlusion in the absence of coronary artery collaterals. *Circulation* 1987;76:667-677.
29. Scheel KW, Mass H, Williams SE. Collateral influence on pressure-flow characteristics of coronar circulation. *Am J Physiol* 1989;257:H717-725.
30. Mohl W, Glogar DH, Mayr H, Losert U, Sochor H, Pachinger O, et al. Reduction of infarct size induced by pressure-controlled intermittent coronary sinus occlusion. *Am J Cardiol* 1984;53:923-928.
31. Zalewski A, Goldberg S, Slysh S, Maroko PR. Myocardial protection via coronary sinus interventions: superior effects of arterializations compared with intermittent occlusion. *Circulation* 1985;71:1215-1223.
32. Guerci AD, Ciuffo AA, DiPaula AF, Weisfeldt ML. Intermittent coronary sinus occlusion in dogs: reduction of infarct size 10 days after reperfusion. *J Am Coll Cardiol* 1987;9:1075-1081.
33. Ikeoka K, Nakagawa Y, Kawashima S, Fujitani K, Iwasaki T. Effects of intermittent coronary sinus occlusion on experimental myocardial infarction and reperfusion hemorrhage. *Jpn Circ J* 1990;54:1258-1273.
34. Feindel CM, Cruz J, Sandhu R, Wilson GJ. The effectiveness of various modes of nonsynchronized retrovenous perfusion in salvage of ischemic myocardium in the pig. *Can J Cardiol* 1991;7:357-365.
35. Lazar HL, Haan CK, Yang X, Rivers S, Bernard S, Shemin RJ. Reduction of infarct size with coronary venous retroperfusion. *Circulation* 1992;86:II352-327.
36. Koke JR, Bittar N. Functional role of collateral flow in the ischaemic dog heart. *Cardiovasc Res* 1978;12:309-315.
37. Weisse AB, Kearney K, Narang RM, Regan TJ. Comparison of the coronary collateral circulation in dogs and baboons after coronary occlusion. *Am Heart J* 1976;92:193-200.
38. Schaper W, Flameng W, De Brabander M. Comparative aspects of coronary collateral circulation. *Adv Exp Med Biol* 1972;22:267-276.
39. Syeda B, Schukro C, Heinze G, Modaressi K, Glogar D, Maurer G, Mohl W. The salvage potential of coronary sinus interventions: meta-analysis and pathophysiologic consequences. *J Thorac Cardiovasc Surg* 2004;127:1703-1712.
40. De Wood MA, Spores J, Notske RN et al (1980) Prevalence of total coronary artery occlusion during the early hours of transmural myocardial infarction. *N Engl J Med* 303:897–902.
41. Habib GB, Heibig J, Forman SA, Brown BG, Roberts R, Terrin ML, Bolli R. Influence of coronary collateral vessels on myocardial infarct size in humans. Results of phase I thrombolysis in myocardial infarction (TIMI) trial. The TIMI Investigators. *Circulation* 1991;83:739-746.
42. Martin GV, Kennedy JW (1994) Choice of thrombolytic agent. In: Julian D, Braunwald E (eds) Management of Acute Myocardial Infarction. WB Saunders, London, pp 71–105.
43. Seiler C. Collateral Circulation of the Heart. 1st ed. London: Springer-Verlag; 2009.
44. Seiler C, Fleisch M, Garachemani A, Meier B. Coronary collateral quantitation in patients with coronary artery disease using intravascular flow velocity or pressure measurements. *J Am Coll Cardiol* 1998;32:1272-1279.

45. Traupe T, Gloekler S, de Marchi SF, Werner GS, Seiler C. Assessment of the human coronary collateral circulation. *Circulation* 2010;122:1210-1220.
46. Matsumura K, Jeremy RW, Schaper J, Becker LC. Progression of Myocardial Necrosis During Reperfusion of Ischemic Myocardium. *Circulation* 1998;97:795-804.
47. Amabile N, Jacquier A, Shuhab A, Gaudart J, Bartoli JM, Paganelli F, Moulin G. Incidence, predictors and prognostic value of intramyocardial hemorrhage lesions in St elevation myocardial infarction. *Catheter Cardiovasc Interv* 2011: in press.
48. Pratt FH. The nutrition of the heart through the vessels of Thebesian and the coronary veins. *Am J Physiol* 1898;1:86-103.
49. Bekkers SC, Yazdani SK, Virmani R, Waltenberger J. Microvascular obstruction: underlying pathophysiology and clinical diagnosis. *J Am Coll Cardiol* 2010;55:1649-1660.

Paper VI

Characterization of shed heparan sulfates in pig model of myocardial ischemia / reperfusion injury.

Pranitha J Kamat[1], Andrew Hamilton[2], Sally. E. Stringer[2], Robert Rieben[1]

[1]Department of Clinical Research, University of Bern, Switzerland, [2]Cardiovascular group, University of Manchester, UK

A layer of sugar and protein molecules called the endothelial glycocalyx covers the endothelium. Heparan sulfate is a major constituent of this layer and plays important role during ischemia/reperfusion injury by interacting specifically with many molecules involved in the pathology.

Aim: To characterize the different disaccharide components of shed heparan sulfates.

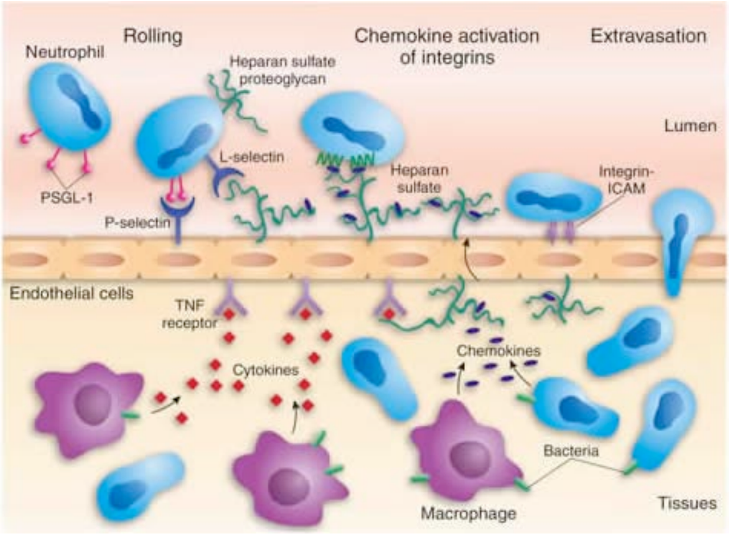
Neutrophil
Rolling
Heparan sulfate proteoglycan
Chemokine activation of integrins
Extravasation
Lumen
L-selectin
Heparan sulfate
Integrin-ICAM
PSGL-1
P-selectin
Endothelial cells
TNF receptor
Cytokines
Chemokines
Bacteria
Macrophage
Tissues

Interaction of heparan sulfate with molecules involved during inflammation which makes a major contribution to the patholgoy during ischemia reperfusion. Parish, 2005, Nat. Immunol (6) 861-862.

Model: Myocardial infarction in pigs with 60 minutes and 20 minutes ischemia followed by 6 hours reperfusion.

Conclusion: Heparan sulfates shed during ischemia/reperfusion have different disaccharide composition depending on the duration of ischemia.

Characterization of shed heparan sulfates in pig model of myocardial ischemia / reperfusion injury.

Pranitha J Kamat[1], Andrew Hamilton[2], Sally. E. Stringer[2], Robert Rieben[1]*

[1]Department of Clinical Research, University of Bern, Switzerland, [2]Cardiovascular group, University of Manchester UK

Running title: Characterization of heparan sulfate shed during myocardial infarction

(Manuscript in process of submission to: Journal of vascular surgery)

*Corresponding author

Prof. Robert Rieben

University Bern

Department of clinical research

Murtenstrasse 50, P.O. Box 44

3010 Bern, Switzerland

Tel: +41 31 632 9669

Fax: +41 31 6328837

Email: Robert.rieben@dkf.unibe.ch

Abstract

Heparan sulfate (HS), a major constituent of the endothelial glycocalyx participates in pathology during ischemia/reperfusion (IR). We therefore sought to characterize shed HS in a model of myocardial IR.

Method: Left anterior descending artery of pigs was occluded for 60 min (Group 1) or 20 min (Group 2). Myocardial viability was assessed after 6 hours reperfusion. Blood samples were collected at baseline, 50 min after ischemia and 2 min after reperfusion from which HS composition was analyzed by HPLC. Tissue expression of HS was analyzed by immunostaining.

Results: The myocardial necrosis was 20% to 66% (Group 1) and 0% (Group 2). Increased shedding of non- sulfated disaccharides and decreased shedding of 6S NS disaccharides at 2 min reperfusion from baseline was significant for group 2. Sulfated HS expression was higher in the ischemic myocardium when compared to non- ischemic myocardium for group 2

Conclusion: Group 2 with 0% necrosis may indicate the shedding of non- sulfated disaccharides to be protective. Decreased shedding and increased expression of sulfated disaccharides for group 2 may indicate the protective role of sulfated HS during IR. This is the first study showing differential shedding of HS disaccharides during IR, which is regulated by ischemic duration.

Keywords: Myocardial infarction, heparan sulfate, disaccharide sulfation, pig, ischemia reperfusion.

Introduction

In the last two decades a number of studies have shown the endothelium to be much more than simply an inert lining of blood vessels. It is now identified as the largest organ in human body maintaining vascular homeostasis [1, 2]. As an interface between blood and surrounding tissue and due to its large surface area, the vascular endothelium offers a platform for progression of pathology during ischemia reperfusion (IR).

The vascular endothelium is covered by a layer of glycocalyx that participates in the (patho) physiological functions of the endothelium. Heparan sulfate (HS) proteoglycans are a major constituent forming 50-90% of the endothelial glycocalyx [3-5]. HS consists of repeating disaccharide units attached to the endothelial membrane via a core protein, such as syndecan. The disaccharides are sulfated at different positions. Sulfation of disaccharides is highly regulated and determines functional interaction of HS with its ligands. During IR the glycocalyx is shed converting the native endothelium to an active pro-inflammatory/pro-coagulative state [6]. Alongside the glycocalyx has a role in three other pathways involved in IR injury. These are the generation of reactive oxygen species (ROS), innate immune reactions and the coagulation pathway.

During ischemia, the degradation of ATP leads to formation of xanthine, which is converted to superoxide ions by xanthine oxidase during reperfusion [7]. Reperfusion of previously ischemic tissue therefore comes with a burst of ROS, which later oxidizes surrounding biomolecules leading to tissue destruction. The role of glycocalyx in this pathway is suggested by its affinity for xanthine oxidase [8]. It is also shown that ROS generated by xanthine oxidase stimulate the synthesis of glycosaminoglycan chains that compose the glycocalyx [9].

Another source of injury during IR is the innate immune response. The immune response during IR is marked by the production of cytokines, which are unable to carry out their function unless bound to HS [10]. Many cytokines [13,14,15,16] and all chemokines have ability to bind to HS [11]. The pro inflammatory cytokines IL-8, MCP-1 and MIP-1α are upregulated during IR and bind specifically to N- and O- sulfated regions on HS [12]. IL-8 binding to HS is shown to correlate with the occurrence of -IdceA(2-OSO3)-GlcNSO3(6-OSO3)- disaccharide unit [13]. Another cytokine RANTES, the inhibition of which reduces myocardial IR injury also prefers O- sulfation on the HS [13]. The anti-inflammatory cytokine IL-10 induced during reperfusion binds explicitly to N-sulfation but not O-sulfation on the HS [14]. Supporting the specificity of chemokine binding to HS is the fact that chemokines show opposite effector functions based on the type of complexes they form with the HS and/or its core protein [15, 16]. HS also interacts with adhesion molecules E-, L- and P- selectin [17]. Infact in conditions of acute inflammation HS forms the primary ligand for L-selectin [17]. Growth factors mainly FGF, VEGF and PDGF have significant effects during IR and are widely studied in this context. Interestingly enough, these growth factors have highly specific binding sites on HS and participate in their signaling [19,20,21,13,14]. For instance, PDGF BB binding and signaling via HS is attenuated with reduction in N- sulfation on the HS chain. However, no significant effect is seen when the HS chain has extensive N- and 6- sulfation but reduced 2- sulfation on the iduronic acid residues [18].

As mentioned earlier, shedding of the glycocalyx triggers the coagulation pathway terminating in the production of thrombin. Thrombin has multiple functional roles in pathogenesis during IR [19]. This is emphasized with experiments that have shown attenuation of IR injury by inhibition of thrombin [20]. Antithrombin III is a natural thrombin inhibitor and elucidates its functions via binding through HS [21-25]. Interaction between HS and antithrombin III is specific wherein the 6-O-sulfate and the 3-O-sulfate group together bind antithrombin and accelerate its function (78, 79).

It is therefore clear the prominent role of the glycocalyx during IR for its interaction with the various molecules causing the injury. In vivo models and clinical studies in humans have detected shed HS and syndecan during IR [26-28]. Also, studies have demonstrated the attenuation of IR injury by using structural analogues to replace the shed HS [29]. However the HS shed during IR injury has not yet been subject to compositional analysis. Characterization of HS is important as many of these interactions depend highly upon the sulfation patterns within HS [30]. We therefore sought to characterize the shed HS during IR with a pig model of myocardial infarction, which would help us deduce the underlying pathological mechanism.

The tissue necrosis due to IR is dependant upon the duration of ischemia and is completely absent when ischemia is reduced to 20 min. In this study pigs were subjected to 20 min ischemia and were compared to pigs subjected to 60 min ischemia where considerable necrosis was expected. From this study we illustrate that the composition of shed HS varies during IR and is regulated by the duration of ischemia.

Material and methods

Experimental model

Piglets were pre-medicated with Narketan /Xylapan, Penthotal, Dormicum and Atropin, intubated, and mechanically ventilated with a Draeger respirator (O2/N2O 1:3, Isoflurane 1–1.5 vol.%). Central venous and arterial lines were introduced and a single bolus of unfractionated heparin (5000 IU) administered intravenously. 2500 IE of heparin was given 2hours after the first dose and at every hour from the second dose.

The left anterior descending (LAD) artery was occluded just distally of the first diagonal branch with a semi-compliant over-the-wire PCI catheter (Concerto, Occam, the Netherlands; balloon length 20 mm, diameter 3 mm). The balloon was inflated to completely occlude the vessel (EncoreTM 26 inflation device, Boston Scientific, Ireland; used pressure 4–6 atm) to render a part of the left ventricle ischemic. Localization of the balloon and state of inflation was controlled angiographically on a regular basis. At end of the ischemic period, deflating the balloon reperfused the ventricle. At end of reperfusion, the balloon was reoccluded at the same place and 60ml Evans blue injected intravenously to demarcate the ischemic area at risk (AAR). With an intravenous bolus of KCl the animal was sacrificed and the heart excised for further analysis. In the case of ventricular fibrillation, a biphasic defibrillator (150 J) was used for cardioconversion.

Pigs were divided into two groups. Group 1 underwent 60 min ischemia and group 2 underwent 20 min ischemia. Both groups were followed with 6 hours of reperfusion before the pig was sacrificed.

Infarct size and myocardial necrosis

The excised heart was cut into slices perpendicular to the septum until the mitral valve. From each slice the right ventricle was removed. The Evans Blue unstained non-blue parts were weighed and expressed as a percentage of the left ventricle to determine the AAR.

The AAR was then treated with triphenyl tetrazolium chloride (TTC) solution at 37°C for 20 min. The TTC unstained areas were the necrotic ischemic tissue (NIT) and TTC stained red areas were the viable ischemic tissue (VIT). Myocardial necrosis was expressed as the percentage of NIT within the AAR. Tissue samples were taken from the Evans Blue stained area not at risk (ANR), VIT and NIT for immunostaining.

Blood sampling

Systemic venous blood was collected directly into vacutainers containing serum clot activator. Tubes were centrifuged at 3000rpm for 10 min and the serum collected as supernatant stored at -20°C until used. Samples were taken at baseline after injection of heparin, 50 min after ischemia and 2 min after reperfusion.

Protein measurement

Before extraction of HS for HPLC, 5µl of 1:10 diluted serum in ddH2O was assayed to determine its protein concentration. This was performed using a BCA kit (Thermo Scientific, UK) according to the manufacturer's instructions. Measurements were performed at 570nm on an ELx800 absorbance microplate reader running Gen5 Software (BioTek Instruments, USA).

Characterization by HPLC

Sample preparation was carried out as described previously with minor changes [31]. 400µl of serum was and digested overnight with protease to liberate the HS chains from the core protein. The samples were then loaded onto a DEAE spin filter (Sartorius, UK), and following a wash with 400µl of 50mM sodium phosphate; 0.3M NaCl, GAGs were eluted using 400µl 50mM sodium phosphate; 1M NaCl. Samples were then desalted on a Biomax-5 spin filter (Millipore, Ireland), and further desalted using a PD10 column (GE Healthcare, UK) from which the elution volume of 2.5-4ml was collected. The samples were then lyophilized, re-suspended in 0.1M sodium acetate; 10mM calcium acetate with heparinase mix (heparinase I, II, III at final concentration 0.33mIU/ml each) and incubated at 37°C overnight. Samples were dried, re-dissolved in 12µl ddH$_2$O, then analyzed with a ProPac PA1 analytical column (Dionex, USA) running on an Agilent 1100 series high performance liquid chromatogram, as described by [31]. Quantification of each HS disaccharide was by calibration against HS standards of known concentration obtained from Seikagaku (Japan). Every sample was run in replicates and the ones with a complete histogram were considered for further analysis.

Accounting for heparin in circulation

In our in vivo model, heparin was injected in the pig as an anticoagulant to keep the catheters unclogged. Thus, the contribution of heparin to the disaccharide peaks obtained from the samples had to be considered for quantification of actual shed heparan sulfate. For this purpose, heparin alone was digested and run on HPLC column. 85% of disaccharides were eluted as tri- sulfated disaccharides. We therefore excluded this peak in all our analysis and expressed each disaccharide as a percentage of the sum of the rest of the peaks.

Immunostaining for heparan sulfate on tissue

Tissue sample were fixed with 2% formaldehyde at 4°C overnight and then transferred to 18% sucrose solution for 15 hours at room temperature. Samples were then embedded in Shandon M1 embedding matrix and stored at -20°C until use.

Samples were cut to 30μm thick sections and permeablized with TBS-Triton X100 solution. Sections were incubated with primary antibody (mouse anti HS; 10E4 clone; Siekagaku 370255) that is specific for sulfated epitopes on HS. After overnight incubation at 4°C, secondary antibody (anti mouse Cy3; Jackson Immunoresearch 115-167-020) incubation was done at room temperature for 90 min. Sections were washed with TBS-Triton X100 solution between incubations and mounted on gelatin coated glass slides.

Statistical analysis

One way ANOVA was conducted to compare the groups. Bonferroni’s post test was used to detect significant differences within a group.

Results

Myocardial area at ischemic risk and necrosis

The heart was excised at the end of the experiment as assessed for myocardial area at ischemic risk (AAR) and myocardial necrosis. The AAR was identified by Evans blue unstained areas of the left ventricle and were expressed as percentage of the total left ventricle. This ranged from 30-50% for all pigs (Table 1). The myocardial necrosis within the AAR was determined by TTC staining. This ranged from 20% to 60% for Group 1 and 0% for Group 2 (Table 1).

Total shed heparan sulfate

HS are known to shed during IR. We compared the total shed HS at baseline, 50 min after ischemia and 2 min after reperfusion. No significant differences were observed in shed HS in either of the groups (Figure 1).

Comparison of heparan sulfate disaccharides

The individual disaccharides quantified by HPLC were compared between the groups at different time points of baseline (Bl), 50 min after ischemia (Isch) and 2 min after reperfusion (Rep). Values are represented as percentage of baseline. Table 2 shows the values for groups 1 and 2. When compared by One way ANOVA, the groups were significantly different for non- sulfated (p=0.0006), NS- (p=0.0010), 6S NS- (p<0.0001) and 2S NS (p<0.0001) sulfated disaccharides. By Bonferroni's post test the time points within a group were compared for each type of disaccharide. The non-sulfated disaccharides increased from Bl to Isch for group 1 (p<0.05) and from Bl to Rep for group 1 (p<0.05) and group 2 (p<0.05). NS sulfated disaccharides significantly increased only for group 1 (p<0.001) from Bl to Rep. Opposite trend was seen with double sulfated disaccharides that decreased from Bl. For group 1 the 6S NS disaccharides decreased from Bl to Isch (p<0.01) and from Bl to rep (p<0.01). For group 2 significant reductions were seen for 2S NS disaccharides that decreased from BL to Isch (p<0.01) and Rep (p<0.001).

HS disaccharides were also compared based on %necrosis. Pigs were grouped into >50% necrosis, <50% necrosis and 100% necrosis groups (Table 3). Significant differences were observed between groups for non- (p=0.0002), NS- (p=0.0014), 6S NS- (p=0.0010) and 2S NS (p<0.0001) sulfated disaccharides. Significant rise in non-sulfated disaccharides from Bl to Isch was observed in <50% necrosis group (p<0.05). Their decrease from Bl to Rep was noticed for <50% necrosis (p<0.01) and 0% necrosis (p<0.05) groups. The NS sulfated disaccharides were significantly increased from Bl to Rep for >50% necrosis group (p<0.05) and not for <50% and 0% necrosis groups. The 6S NS disaccharides decreased from Bl to Rep for <50% necrosis group (p<0.05). The 2S NS sulfated disaccharides decreased significantly only in the 0% necrosis from Bl to Isch (p<0.05) and from Bl to Rep (p<0.01).

Total heparan sulfate on tissue

Tissue samples from group 1, ANR, VIT and NIT and from group 2, ANR and VIT were stained for heparan sulfate. No significant differences were found between the groups (Figure 2).

Discussion

Recent investigations on heparan sulfate and other glycosaminoglycans (GAGs) are increasingly adding to knowledge of their extensively dynamic nature. Along with the core protein and spatial conformation in which the HS are formed, the sulfation pattern on their disaccharides contributes significantly to the HS function. Under physiologic conditions the heparan sulfates are continuously shed and replaced [32]. In IR injury, the degree of shedding of the HS is directly proportional to the ischemic insult [27].

GAGs, mainly HS shed during IR have been quantified in several studies until now. These studies were conducted in isolated guinea pig hearts perfused with a nutrient rich oxygenated solution and the HS quantified by ELISA. The total shed HS was quantified to be 20 times more than baseline after 20 min ischemia followed by 10 min reperfusion [33-35]. In our study, in vivo in pig hearts after 20 min ischemia and 10min reperfusion, the total shed HS was similar to baseline. This was also the case for group 1 with 60 min ischemia (Figure 1). A major difference of the previous studies from this study is that the perfusion solution used in the in vitro model lack the presence of leukocytes and in general the systemic response that is also important in modulating the circulating HS. Other studies have measured HS in vivo during myocardial infarction by using polyclonal antibodies that recognize the core protein carrying HS chains [29]. Thus, it cannot be compared with the current study. A study of relevance with the current study was that from Rehm, et. al. where they measured HS in circulation of patients subjected to cardiopulmonary bypass. With help of a monoclonal antibody to HS they measured the amount of shed HS in the arterial blood by ELISA. The study showed almost 5 fold rise in shed HS at end of 90 min ischemia and 20 fold rise during early reperfusion [34]. However, the study did not account for heparin given to the patients that could contribute significantly to the circulating HS. In the context of IR injury, the current study is the first to characterize the different sulfated disaccharides of shed HS.

In this study, a pig model of myocardial infarction was used. The percentage of left ventricle subjected to ischemia was comparable among the pigs and ranged between 30-50%. Group 1 showed necrosis ranging from 20% to 66% and for group 2 the ischemic myocardium was 0% necrotic (Table 1). This was expected as it is known that an ischemic duration of 20 min or lesser causes no necrosis to the tissue.

Differential shedding of the disaccharides were observed based on the degree and pattern of sulfation. Non-sulfated disaccharides were increasingly shed already during ischemia for group 1 and during reperfusion for both group1 and group 2 (Table 2). The non-sulfated disaccharides could play the role of 'protective shedding' as indicated by no necrosis for group 2. This is further confirmed by increased shedding of non-sulfated disaccharides in the <50% necrosis and not >50% necrosis group. The double sulfated disaccharides showed opposite trends from the non sulfated by decreased shedding during ischemia and reperfusion. This was significant for the 6S NS disaccharide for group 1 and 2S NS disaccharide for group 2 (Table 2). Such subtle changes in position of sulfation in the shed HS based on ischemic duration highlight its dynamic nature in vivo. Furthermore, the group with <50% necrosis was different from group with >50% necrosis but showed similar trends to group with 0% necrosis. It has been shown that 20 min short ischemia leads to no necrosis of the myocardial tissue inspite of shedding of the glycocalyx [34]. This study confirms the previous finding and shows the composition of the shed glycocalyx.

Finally expression of sulfated HS locally in the ischemic myocardium (VIT, NIT) was compared with the non- ischemic myocardium (ANR) at the end of 6 hours reperfusion. Decreased HS expression for group 1 and increased expression for group 2 may indicate the importance of sulfated HS expression on the tissue. The decreased shedding of sulfated disaccharides in group 2 and <50% necrosis group could also be interpreted in this direction. Importance of sulfated HS was clearly demonstrated by use of low molecular weight DXS (an analogue of sulfated HS), which attenuated myocardial infarction in pigs when administered locally [29].

Modulation of HS composition and structure has been studied in many pathological conditions but not in IR injury [36-39]. This study is the first of its kind with a very small group size and results should be confirmed with a larger group size. However, two main observations/interpretations can be made from this study. The non-sulfated disaccharides are increasingly shed during IR and could be referred to as 'protective shedding', as shed HS is bioactive and chemotactically attracts leukocytes [40, 41]. The double sulfated disaccharides 6S NS and 2S NS are lesser in the circulation during IR. This may denote the importance of these high sulfated disaccharides to be retained by the glycocalyx to simply protect the endothelial cells from further injury. This is supported by studies that have shown specific binding of inflammatory molecules, leukocytes and growth factors to high sulfated domains on HS chains [18, 42, 43]. Also, the burst of reactive oxygen species may contribute to depolymerization of GAGs during IR. It is known that sulfated GAGs are more resistant to depolymerization by ROS when compared to non sulfated GAGs [44]. Increased shedding of NS sulfated disaccharides may directly indicate tissue injury as this was seen for group 1 and more specifically within the >50% necrosis group.

Several mechanisms could be proposed for the modulation of sulfation in the HS chains. It could be due to the activity of heparanase that is upregulated during hypoxia [45], and selectively sheds HS from endothelial glycocalyx [46] modulating HS chains by increasing their sulfation [47]. ROS generated during IR could contribute to this effect by influencing synthesis of new GAG chains whose sulfation extensively depends on the environment [9]. Once the HS chains are synthesized and presented on the endothelial surface, they are modulated by a set of enzymes, the endosulfatases. These enzymes remove the 6O sulfation on HS and regulate the activity of many growth factors by modulating the protein binding sites [48-50]. The activity of endosulfatases during IR has been shown previously in kidney where HS is modulated by an endosulfatase to form ligands for L-selectin and MCP-1 [51]. Also it is shown that in presence of proinflammatory cytokines, which is generated also during IR, the sulfation of HS increases on cultured endothelial cells [52]. Finally ROS is shown previously to mediate the modifications on the glycocalyx [53]. The possible existence of these many mechanisms and our lack in knowledge for their role IR marks the importance of such studies in future.

Shedding of the glycocalyx during IR can be due to the shear stress at the start of reperfusion along with the action of a cocktail of enzymes contained within the resident mast cells [35]. These enzymes could be produced by different sources including endothelial cells and surrounding mast cells [35]. A clear picture of the reason for shedding is yet to be elucidated. In our study, it is also unclear the exact location from where the HS is shed. It could be from the vessels within the area at ischemic risk as shown by Banz *et.al.* [54]. TNFα production is induced by ischemia and continued to be produced during reperfusion [55] and has the ability to denudate the glycocalyx [56]. The TNFα formed can easily join the circulation and cause systemic shedding of the glycocalyx. This is complex to be elucidated and would require either samples from specific locations or isolated model systems. To conclude, shedding of the glycocalyx during ischemia and during reperfusion is a functional shedding that is dynamically regulated by the sulfation pattern on the HS. The exact mechanism and function of its shedding is important and requires further investigation.

Acknowledgements

Swiss National Foundation grant number 3200B0-116618 and 32003B-135272 supported this study

Table 1: Myocardial area at ischemic risk and necrosis

	AAR as percentage LV	**Myocardial necrosis**
Group 1	32%	54%
(60min Ischemia)	32%	20%
	38%	66%
	44%	40%
	36%	45%
	50%	60%
Group 2	31%	0%
(20min Ischemia)	30%	0%
	39%	0%

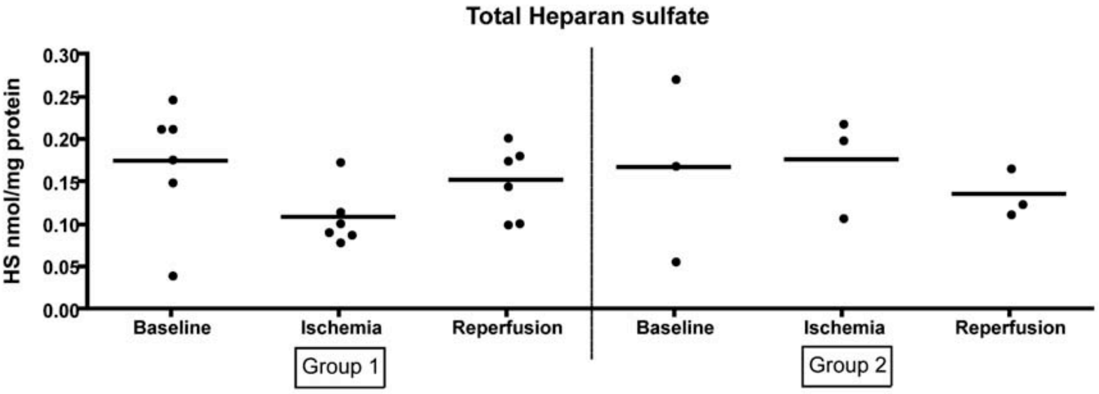

Figure 1: Total shed heparan sulfate in circulation

Total shed heparan sulfate in the circulation at baseline, 50 min after ischemia and 2 min after reperfusion were compared based on the ischemic duration. No significant differences were found between the groups.

Table 2: Comparison of different sulfated disaccharides based on ischemic duration.

	Time point	Group 1 (60 min Ischemia) (n=6)	Group 2 (20 min Ischemia) (n=3)
Non Sulfated P = 0.0006	Bl	100.00	100.00
	Isch	150.17*	160.30
	Rep	146.39*	188.76*
NS Sulfated P = 0.0010	Bl	100.00	100.00
	Isch	140.33	152.63
	Rep	152.03**	129.53
6S Sulfated	Bl	100.00	100.00
	Isch	91.46	84.74
	Rep	79.19	66.26
6S NS Sulfated P < 0.0001	Bl	100.00	100.00
	Isch	35.21**	36.31
	Rep	35.06**	28.81
2S NS Sulfated P < 0.0001	Bl	100.00	100.00
	Isch	53.87	37.78**
	Rep	62.64	26.35***

Values expressed as percentage of baseline. P=One way ANOVA, $*p < 0.05$, $**p<0.01$ and $***p < 0.001$

Table 3: Comparison of individual disaccharides based on necrosis.

	Time point	>50% Necrosis (n=3)	<50% Necrosis (n=3)	0% Necrosis (n=3)
Non Sulfated P = 0.0002	Bl	100.00	100.00	100.00
	Isch	126.10	182.10*	160.30
	Rep	114.25	193.43**	188.76*
NS Sulfated P = 0.0014	Bl	100.00	100.00	100.00
	Isch	137.35	143.94	152.63
	Rep	169.21*	124.65	129.53
6S Sulfated	Bl	100.00	100.00	100.00
	Isch	96.30	68.92	105.75
	Rep	75.76	61.37	91.56
6S NS Sulfated P = 0.0010	Bl	100.00	100.00	100.00
	Isch	75.73	32.76	37.78
	Rep	92.55	32.84*	26.35
2S NS Sulfated P<0.0001	Bl	100.00	100.00	100.00
	Isch	41.92	29.30	36.31*
	Rep	43.84	26.57	28.81**

Values expressed as percentage of baseline. P=One way ANOVA,*$p < 0.05$ and ** $p < 0.01$

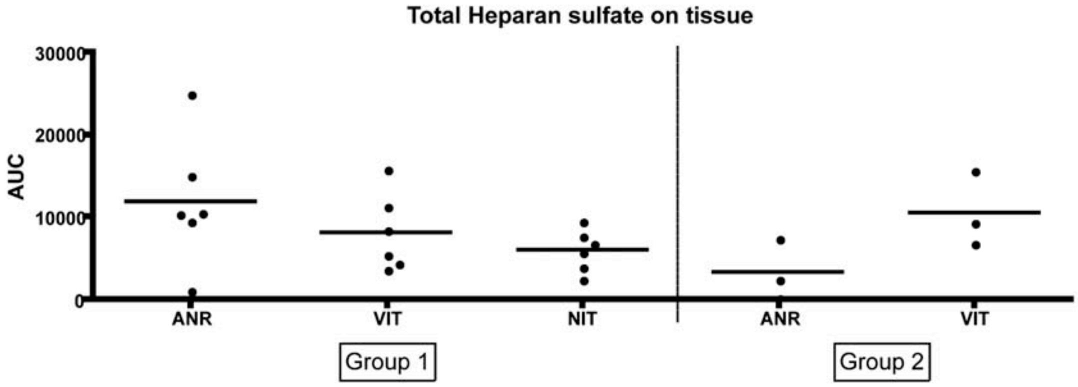

Figure 2 Total heparan sulfate on tissue

Tissue sections from group 1 area not at risk (ANR), viable ischemic tissue (VIT) and necrotic ischemic tissue (NIT) were stained for HS. Group 2 contains only ANR and VIT. No significant differences were found between the groups.

References

1 Nieuwdorp M, Meuwese MC, Vink H, Hoekstra JB, Kastelein JJ, Stroes ES: The endothelial glycocalyx: A potential barrier between health and vascular disease. Curr Opin Lipidol 2005;16:507-511.

2 Van Teeffelen JW, Brands J, Stroes ES, Vink H: Endothelial glycocalyx: Sweet shield of blood vessels. Trends Cardiovasc Med 2007;17:101-105.

3 Shibata S, Sasaki T, Harpel P, Fillit H: Autoantibodies to vascular heparan sulfate proteoglycan in systemic lupus erythematosus react with endothelial cells and inhibit the formation of thrombin-antithrombin iii complexes. Clin Immunol Immunopathol 1994;70:114-123.

4 Ihrcke NS, Wrenshall LE, Lindman BJ, Platt JL: Role of heparan sulfate in immune system-blood vessel interactions. Immunol Today 1993;14:500-505.

5 Kainulainen V, Wang H, Schick C, Bernfield M: Syndecans, heparan sulfate proteoglycans, maintain the proteolytic balance of acute wound fluids. J Biol Chem 1998;273:11563-11569.

6 Pries AR, Secomb TW, Gaehtgens P: The endothelial surface layer. Pflugers Arch 2000;440:653-666.

7 Granger DN, Rutili G, McCord JM: Superoxide radicals in feline intestinal ischemia. Gastroenterology 1981;81:22-29.

8 Adachi T, Fukushima T, Usami Y, Hirano K: Binding of human xanthine oxidase to sulphated glycosaminoglycans on the endothelial-cell surface. Biochem J 1993;289 (Pt 2):523-527.

9 Tanaka H, Okada T, Konishi H, Tsuji T: The effect of reactive oxygen species on the biosynthesis of collagen and glycosaminoglycans in cultured human dermal fibroblasts. Arch Dermatol Res 1993;285:352-355.

10 Parish CR: Heparan sulfate and inflammation. Nat Immunol 2005;6:861-862.

11 Handel TM, Johnson Z, Crown SE, Lau EK, Proudfoot AE: Regulation of protein function by glycosaminoglycans--as exemplified by chemokines. Annu Rev Biochem 2005;74:385-410.

12 Kuschert GS, Coulin F, Power CA, Proudfoot AE, Hubbard RE, Hoogewerf AJ, Wells TN: Glycosaminoglycans interact selectively with chemokines and modulate receptor binding and cellular responses. Biochemistry 1999;38:12959-12968.

13 Spillmann D, Witt D, Lindahl U: Defining the interleukin-8-binding domain of heparan sulfate. J Biol Chem 1998;273:15487-15493.

14 Salek-Ardakani S, Arrand JR, Shaw D, Mackett M: Heparin and heparan sulfate bind interleukin-10 and modulate its activity. Blood 2000;96:1879-1888.

15 Marshall LJ, Ramdin LS, Brooks T, PC DP, Shute JK: Plasminogen activator inhibitor-1 supports il-8-mediated neutrophil transendothelial migration by inhibition of the constitutive shedding of endothelial il-8/heparan sulfate/syndecan-1 complexes. J Immunol 2003;171:2057-2065.

16 Li Q, Park PW, Wilson CL, Parks WC: Matrilysin shedding of syndecan-1 regulates chemokine mobilization and transepithelial efflux of neutrophils in acute lung injury. Cell 2002;111:635-646.

17 Wang L, Fuster M, Sriramarao P, Esko JD: Endothelial heparan sulfate deficiency impairs l-selectin- and chemokine-mediated neutrophil trafficking during inflammatory responses. Nat Immunol 2005;6:902-910.

18 Abramsson A, Kurup S, Busse M, Yamada S, Lindblom P, Schallmeiner E, Stenzel D, Sauvaget D, Ledin J, Ringvall M, Landegren U, Kjellen L, Bondjers G, Li JP, Lindahl U, Spillmann D, Betsholtz C,

Gerhardt H: Defective n-sulfation of heparan sulfate proteoglycans limits pdgf-bb binding and pericyte recruitment in vascular development. Genes Dev 2007;21:316-331.

19 Raivio P, Lassila R, Petaja J: Thrombin in myocardial ischemia-reperfusion during cardiac surgery. Ann Thorac Surg 2009;88:318-325.

20 Jormalainen M, Vento AE, Lukkarinen H, Kaapa P, Kyto V, Lauronen J, Paavonen T, Suojaranta-Ylinen R, Petaja J: Inhibition of thrombin during reperfusion improves immediate postischemic myocardial function and modulates apoptosis in a porcine model of cardiopulmonary bypass. J Cardiothorac Vasc Anesth 2007;21:224-231.

21 Opal SM, Kessler CM, Roemisch J, Knaub S: Antithrombin, heparin, and heparan sulfate. Crit Care Med 2002;30:S325-331.

22 Mizutani A, Okajima K, Uchiba M, Isobe H, Harada N, Mizutani S, Noguchi T: Antithrombin reduces ischemia/reperfusion-induced renal injury in rats by inhibiting leukocyte activation through promotion of prostacyclin production. Blood 2003;101:3029-3036.

23 Okajima K, Uchiba M: The anti-inflammatory properties of antithrombin iii: New therapeutic implications. Semin Thromb Hemost 1998;24:27-32.

24 Roemisch J, Gray E, Hoffmann JN, Wiedermann CJ: Antithrombin: A new look at the actions of a serine protease inhibitor. Blood Coagul Fibrinolysis 2002;13:657-670.

25 Opal SM: Therapeutic rationale for antithrombin iii in sepsis. Crit Care Med 2000;28:S34-37.

26 Mulivor AW, Lipowsky HH: Inflammation- and ischemia-induced shedding of venular glycocalyx. Am J Physiol Heart Circ Physiol 2004;286:H1672-1680.

27 Rehm M, Bruegger D, Christ F, Conzen P, Thiel M, Jacob M, Chappell D, Stoeckelhuber M, Welsch U, Reichart B, Peter K, Becker BF: Shedding of the endothelial glycocalyx in patients undergoing major vascular surgery with global and regional ischemia. Circulation 2007;116:1896-1906.

28 Ward BJ, Donnelly JL: Hypoxia induced disruption of the cardiac endothelial glycocalyx: Implications for capillary permeability. Cardiovasc Res 1993;27:384-389.

29 Banz Y, Hess OM, Robson SC, Mettler D, Meier P, Haeberli A, Csizmadia E, Korchagina EY, Bovin NV, Rieben R: Locally targeted cytoprotection with dextran sulfate attenuates experimental porcine myocardial ischaemia/reperfusion injury. Eur Heart J 2005;26:2334-2343.

30 Kreuger J, Spillmann D, Li JP, Lindahl U: Interactions between heparan sulfate and proteins: The concept of specificity. J Cell Biol 2006;174:323-327.

31 Toyoda H, Kinoshita-Toyoda A, Selleck SB: Structural analysis of glycosaminoglycans in drosophila and caenorhabditis elegans and demonstration that tout-velu, a drosophila gene related to ext tumor suppressors, affects heparan sulfate in vivo. J Biol Chem 2000;275:2269-2275.

32 Lipowsky HH: Microvascular rheology and hemodynamics. Microcirculation 2005;12:5-15.

33 Chappell D, Dorfler N, Jacob M, Rehm M, Welsch U, Conzen P, Becker BF: Glycocalyx protection reduces leukocyte adhesion after ischemia/reperfusion. Shock 2010;34:133-139.

34 Chappell D, Jacob M, Hofmann-Kiefer K, Bruegger D, Rehm M, Conzen P, Welsch U, Becker BF: Hydrocortisone preserves the vascular barrier by protecting the endothelial glycocalyx. Anesthesiology 2007;107:776-784.

35 Chappell D, Hofmann-Kiefer K, Jacob M, Rehm M, Briegel J, Welsch U, Conzen P, Becker BF: Tnf-alpha induced shedding of the endothelial glycocalyx is prevented by hydrocortisone and antithrombin. Basic Res Cardiol 2009;104:78-89.

36 Lauer ME, Hascall VC, Wang A: Heparan sulfate analysis from diabetic rat glomeruli. J Biol Chem 2007;282:843-852.

37 Rops AL, van den Hoven MJ, Bakker MA, Lensen JF, Wijnhoven TJ, van den Heuvel LP, van Kuppevelt TH, van der Vlag J, Berden JH: Expression of glomerular heparan sulphate domains in murine and human lupus nephritis. Nephrol Dial Transplant 2007;22:1891-1902.

38 Korc M: Pancreatic cancer-associated stroma production. Am J Surg 2007;194:S84-86.

39 Properzi F, Lin R, Kwok J, Naidu M, van Kuppevelt TH, Ten Dam GB, Camargo LM, Raha-Chowdhury R, Furukawa Y, Mikami T, Sugahara K, Fawcett JW: Heparan sulphate proteoglycans in glia and in the normal and injured cns: Expression of sulphotransferases and changes in sulphation. Eur J Neurosci 2008;27:593-604.

40 Bernfield M, Gotte M, Park PW, Reizes O, Fitzgerald ML, Lincecum J, Zako M: Functions of cell surface heparan sulfate proteoglycans. Annu Rev Biochem 1999;68:729-777.

41 Kharabi Masouleh B, Ten Dam GB, Wild MK, Seelige R, van der Vlag J, Rops AL, Echtermeyer FG, Vestweber D, van Kuppevelt TH, Kiesel L, Gotte M: Role of the heparan sulfate proteoglycan syndecan-1 (cd138) in delayed-type hypersensitivity. J Immunol 2009;182:4985-4993.

42 Soker S, Goldstaub D, Svahn CM, Vlodavsky I, Levi BZ, Neufeld G: Variations in the size and sulfation of heparin modulate the effect of heparin on the binding of vegf165 to its receptors. Biochem Biophys Res Commun 1994;203:1339-1347.

43 Sugaya N, Habuchi H, Nagai N, Ashikari-Hada S, Kimata K: 6-o-sulfation of heparan sulfate differentially regulates various fibroblast growth factor-dependent signalings in culture. J Biol Chem 2008;283:10366-10376.

44 Moseley R, Waddington R, Evans P, Halliwell B, Embery G: The chemical modification of glycosaminoglycan structure by oxygen-derived species in vitro. Biochim Biophys Acta 1995;1244:245-252.

45 Sandwall E, Bodevin S, Nasser NJ, Nevo E, Avivi A, Vlodavsky I, Li JP: Molecular structure of heparan sulfate from spalax. Implications of heparanase and hypoxia. J Biol Chem 2009;284:3814-3822.

46 Chappell D, Jacob M, Rehm M, Stoeckelhuber M, Welsch U, Conzen P, Becker BF: Heparinase selectively sheds heparan sulphate from the endothelial glycocalyx. Biol Chem 2008;389:79-82.

47 Escobar Galvis ML, Jia J, Zhang X, Jastrebova N, Spillmann D, Gottfridsson E, van Kuppevelt TH, Zcharia E, Vlodavsky I, Lindahl U, Li JP: Transgenic or tumor-induced expression of heparanase upregulates sulfation of heparan sulfate. Nat Chem Biol 2007;3:773-778.

48 Uchimura K, Morimoto-Tomita M, Rosen SD: Measuring the activities of the sulfs: Two novel heparin/heparan sulfate endosulfatases. Methods Enzymol 2006;416:243-253.

49 Narita K, Staub J, Chien J, Meyer K, Bauer M, Friedl A, Ramakrishnan S, Shridhar V: Hsulf-1 inhibits angiogenesis and tumorigenesis in vivo. Cancer Res 2006;66:6025-6032.

50 Ai X, Kitazawa T, Do AT, Kusche-Gullberg M, Labosky PA, Emerson CP, Jr.: Sulf1 and sulf2 regulate heparan sulfate-mediated gdnf signaling for esophageal innervation. Development 2007;134:3327-3338.

51 Celie JW, Rutjes NW, Keuning ED, Soininen R, Heljasvaara R, Pihlajaniemi T, Drager AM, Zweegman S, Kessler FL, Beelen RH, Florquin S, Aten J, van den Born J: Subendothelial heparan sulfate proteoglycans become major l-selectin and monocyte chemoattractant protein-1 ligands upon renal ischemia/reperfusion. Am J Pathol 2007;170:1865-1878.

52 Carter NM, Ali S, Kirby JA: Endothelial inflammation: The role of differential expression of n-deacetylase/n-sulphotransferase enzymes in alteration of the immunological properties of heparan sulphate. J Cell Sci 2003;116:3591-3600.

53 Rubio-Gayosso I, Platts SH, Duling BR: Reactive oxygen species mediate modification of glycocalyx during ischemia-reperfusion injury. Am J Physiol Heart Circ Physiol 2006;290:H2247-2256.

54 Banz Y, Gajanayake T, Matozan K, Yang Z, Rieben R: Dextran sulfate modulates map kinase signaling and reduces endothelial injury in a rat aortic clamping model. J Vasc Surg 2009;50:161-170.

55 Shames BD, Barton HH, Reznikov LL, Cairns CB, Banerjee A, Harken AH, Meng X: Ischemia alone is sufficient to induce tnf-alpha mrna and peptide in the myocardium. Shock 2002;17:114-119.

56 Henry CB, Duling BR: Tnf-alpha increases entry of macromolecules into luminal endothelial cell glycocalyx. Am J Physiol Heart Circ Physiol 2000;279:H2815-2823.

Paper VII

Development of an in vitro system to grow and investigate vascular endothelial cells under physiological flow conditions

Pranitha J Kamat[1], Linda Moli-Hua Kam[1], Jakob Heier[2], Roland Hany[2], Robert Rieben[1]

[1]Department of Clinical Research, University of Bern, Switzerland, [2]EMPA, Dübendorf, Switzerland

Activation and damage of vascular endothelial cells is an important mechanism in the pathophysiology of several diseases and clinical entities. Therefore, extensive research is conducted in studying the mechanism and protection of endothelial cells. This involves large numbers of animal studies and currently available in vitro systems offer only limited possibilities to replace animal experiments

Aim: To develop an in vitro system for growing a native monolayer of endothelial cells that can allow the investigation of these cells like in an in vivo scenario.

Model: The model consists of thin glass tubes that are coated with nano features to help adhesion and growth of endothelial cells. The glass tube is connected to a pump system that allows controlled pulsatile flow within the fiber.

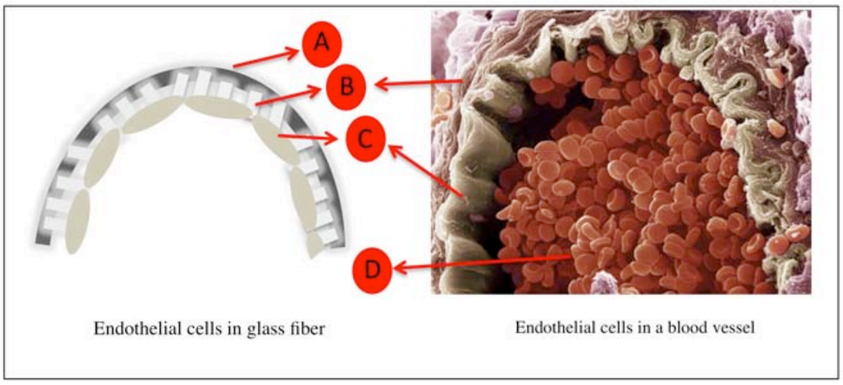
A
B
C
D
Endothelial cells in glass fiber
Endothelial cells in a blood vessel

On the left is the in vitro system showing the glass tube in which endothelial cells are grown. This is compared to a physiological blood vessel on the right. Inner layer of the glass fiber (A). Nano structures (left) and fibroblasts (right) that support endothelial cells in the in vitro system and blood vessel respectively (B). Endothelial cells (C), blood (D).

Conclusion: The system in still under development. Optimal conditions for seeding of cells inside the glass tube have been developed. Several nano features on flat substrates have been screened for supporting endothelial cell growth.

Development of an in vitro system to grow and investigate vascular endothelial cells under physiological flow conditions

Pranitha Kamat[1], Linda Kam[1], Jakob Heier[2], Roland Hany[2], Robert Rieben[1]*

[1]Department of Clinical Research, University of Bern, [2]EMPA Dübendorf

*Corresponding author

Robert Rieben

University Bern

Department of Clinical Research

Murtenstrasse 50

3008 Bern, Switzerland

Tel: +41 31 632 9669

Fax: +41 31 632 7594

E-mail: robert.rieben@dkf.unibe.ch

Abstract

Background: Vascular endothelial cells (EC) make an important area of research for its role in pathology of many clinical conditions. EC function during physiological and pathological conditions is regulated by its morphology, the glycocalyx layer on its surface and shear stress exerted on it. The aim of this study was to develop an in vitro system that would allow study of EC in normal and pathological (activated) state in order to replace animal experiments.

Method and Results: A pulsatile roller pump with maximum flow rate of 48 ml/min was adapted to render physiologically relevant shear stress of 16 Dynes. Porcine EC were grown in a glass tube for it to experience the volume to surface area ratio as in a vessel. Various cell seeding techniques inside the glass tube were tested to determine the optimal method to be 4 times manual rotation at 90° with reseeding at intervals of 30 min. Cells inside the tubes were confirmed by immunostaining for cell nucleus. Alamar Blue assay was developed to identify cell confluence within the glass tube, by testing the assay in normal cell culture flasks. To support EC morphology, coating of the inner lumen of glass tubes with nano- structures was considered. To start with, flat glass cover- slips coated with nano- surfaces were tested for porcine EC growth over two days. Among the nano- surfaces tested, the ones with a height ranging from 20 nm to 40 nm and period ranging from 500 nm to 1000 nm was found to be optimal for porcine EC growth.

Discussion: An in vitro system to study EC in normal and activated state has been set up. Cell seeding and incubation technique inside the glass tube has been determined, although with a scope for further optimization. Glass tubes allow for immunostaining of cells inside the tube and Alamar Blue assay was established for indentifying a confluent glass tube. Testing of more nano- surfaces should be conducted to determine the optimal surface for endothelial cell growth.

Conclusion: A preliminary prototype of the required in vitro system has been set up. Individual components of the system should be further optimized to attain the desired functionality.

Introduction

A large number of diseases that contribute to mortality in this modern world can be categorized under vascular diseases. The outcome of surgical interventions and transplantation is influenced by many factors, which mainly boils down to the vasculature of the tissue being handled. It is therefore not surprising that the vasculature, mainly the endothelial cells lining its inner most layer, are intensively studied in clinical research.

Endothelial cells (EC) form a highly specialized, metabolically active and dynamic layer of interface between blood and underlying tissue. Its main function is to maintain vascular homeostasis under normal physiologic and pathologic conditions. Several features of the EC help them to carry out their function. Among other things this includes their phenotypic morphology, the shear stress exerted on them by flowing blood and the protein/sugar molecules expressed on their surface referred to as the glycocalyx [1]. The behavior and response of EC is directed by these factors that are bound to change under different conditions. Thus, studying EC activation and damage is preferably conducted in vivo in animal models.

Considering the vast research directed on EC, an in vitro model to culture and investigate them would be highly advantageous especially in the interest of reducing animal experiments. Several in vitro models for studying endothelial cells have been designed but only few mimic the native endothelium by presenting the right phenotype under shear stress with a relevant glycocalyx.

Estrada et al. recently developed the endothelial cell culture model (ECCM) where cells are grown on a stretchable concave shaped polymetric film, which is placed in a rectangular cell culture channel [2]. Furthermore, with a scope to regulate pressure, stretch and shear stress the ECCM could be used to test drugs as pathophysiological flow patterns could be imitated. The model however falls short from imitating a native endothelium due to its two dimensionality affecting the cell surface area to volume ratio.

Other models have overcome this problem by growing EC on the inside of silastic or glass tubes [3-6]. These models also had the possibility to regulate flow conditions inside the tube and therefore could mimic closely the vascular endothelium in vivo. For studying EC under different flow and stress conditions the models served its purpose.

The aim of the current study was to develop an in vitro model that can initially aid a native EC culture and further facilitate a follow up on its activation and damage. In this model, pig EC's were cultured inside glass tubes that could then be hooked up to a pump system for pulsatile flow within the tube. Activation and damage of the pig EC's would be attained by replacing the cell culture media with human whole blood. In order to facilitate the study of activated and damaged EC inside the glass tubes, their attachment to the glass surface must be ensured and will be attained by using nano- coated glass tubes [7].

Materials and methods

In vitro system

The cells used in this project were porcine cells isolated from the aorta. To simulate in vivo conditions for these cells it was necessary to provide them with shear stress as in the aorta, which on an average is 16 dynes [8]. Based on this and the known internal diameter of the glass tube 1.6mm, we calculated the maximum flow rate required as below

$$Q = \frac{\tau \cdot \pi \cdot r^3}{4 \cdot \eta} = \frac{16 \cdot \pi \cdot 0.08^3}{4 \cdot 0.008} = 0.804 ml/\sec = \underline{\underline{48.24 ml/\min}}$$

$$\begin{aligned} &Q = f\,lowrate\left[ml/\sec\right] \\ &\tau = shear\ stress\left[dyne\right] \\ &r = glass\ tube\ radius\left[cm\right] \\ &\eta = media\ vis\cos ity\left[dyne\ \sec/cm^2\right] \end{aligned}$$

The required maximum flow rate helped us to choose an appropriate pump for the study which was ECOLINE VC-MS / CA4-12 pump (Ismatec ISM 1090). This pulsatile pump with a 12 roller pump head renders a flow rate ranging from 0.47 to 47 ml/min. An additional feature of the pump is its multichannel casket, which allows four different circuits to run simultaneously.

One circuit of our in vitro system consisted of the glass tube in which cells are grown, silicone tubings that connect all parts of the system (comes with the pump from Ismatec), media bottle, pump and the multichannel casket (Figure 1). The glass tubes have an internal diameter of 1.6 mm and can be coated with nano-structures inside its lumen (Figure 2).

Cell culture

Porcine aortic endothelial cells (PAEC) and porcine epithelial cell line (PK15) were cultured with DMEM+GlutaMAX^{TM}-I media (GIBCO 21885-025) to which we added 1% L-Glutamine 200mM (GIBCO 25030-024), 1% penicillin/streptomycin (GIBCO 15140-122) and 10% foetal bovine serum (GIBCO 10270-106). Cells were washed with PBS pH 7.4 and passaged by using 0.05% Trypsin EDTA (GIBCO 25300-054) at a centrifugation speed of 1200 rpm.

Isolation of porcine aortic endothelial cells

Porcine aortas were obtained in a transport media consisting of RPMI+GlutaMAX media (GIBCO 61870-010) with 20% heat inactivated foetal calf serum, 2% penicillin/streptomycin (GIBCO 15140-122) and 2% L-Glutamine (GIBCO 25030-024). The aorta was washed with sterile PBS and slit into half to expose the lumen. Cotton bud wetted in cell culture media was gently swiped over the lumen to have only the endothelial cells attached to the bud. The bud was then scratched into one well of a 6 well plate that was previously coated with fibronectin (Chemikon; FC 010) at final concentration of 12.5 μg/ml 1 mg/ml for at least 15 min in the incubator. The procedure was repeated over different areas on the lumen of the aorta and scratched onto different wells in the plate. The plate was let in the incubator for cells to grow to almost confluence, transferred to 25cm^2 and subsequently to 75cm^2 cell culture flask. Once cells reached confluence in this flask they were trypsinized and frozen at -150°C in DMEM media containing 20% FCS and 10% DMSO (Sigma Aldrich D5879). Before using for an experiment, the cells were washed three times in cell culture media and grown to confluence in a 75 cm^2 cell culture flask.

Optimization of cell seeding inside glass tubes

PAEC were seeded at a concentration of 0.8x10^5 live cells/ml in the glass tubes by using a 200μl pipette. To ensure even seeding throughout the glass tube, three techniques of incubation were tested.

1. Two squared silicon rubbers were fixed to the glass tubes kept in a petri dish. Tubes were rotated manually either 90° or 180° and different intervals between rotations were tested.
2. The second technique was similar to the first, but additionally, fresh cell suspension (0.8x10^5 cells/ml) was reseeded before each rotation. The reseeding procedure was thought to augment the amount of cells attaching to the glass surface.
3. Cell seeded glass tubes were attached to a mechanical rotator set to different rotation times inside the incubator.

After following either of the seeding procedures, cells were let to grow in the incubator and checked regularly under the microscope. Cell growth was followed for until about 5 days until there was no further growth (Table 1-3).

Glass tubes where cell growth was relatively successful (highlighted in the Table 1&2), were considered for immunostaining procedure.

Immunostaining inside glass tubes

Picric acid solution: 10g Paraformaldehyde was added to 75ml saturated parapicric acid, warmed and mixed with magnetic stirrer. 75μl of 1M NaOH was then added to the solution that was continuously warmed up until everything dissolved. 1.65g of $NaH_2PO_4.H_2O_4$ (Merck 6346) and 2.94g of NaH_2PO_4 (Fluka 71640) were separately dissolved in 250ml demineralized water. Finally all three solutions were mixed to make picric acid solution for cell fixation prior to immunostaining.

Glass tubes containing cells were filled with self made picric acid fixation solution for 10 minutes and then washed three times, 10 minutes each with PBS^{++} (PBS + $Cacl.2H_2O$ 0.185mg/ml + $MaCl_2.6H_2O$ 0.188mg/ml). Glass tubes were then filled with DAPI (Boehringer 236276) diluted in TBS-PBS-BSA 1% and incubated for 10 minutes at room temperature. Tubes were then filled with glycerol as the mounting media, sealed and stored at 4°C until observed under confocal microscope.

Coating glass tubes with gelatin

The glass tube was filled with a 0.1% gelatin solution (mixed with ultra pure water) and incubated at 37°C over night. After washing with PBS pH 7.3, the tube was filled with coomassie blue and rotated manually for 5 minutes. The glass tube was finally washed with PBS pH 7.3 for another 5 minutes.

Alamar blue assay

Alamar blue assay was established in confluent cell culture flasks to help in detection of confluent cells within glass tubes. PK15 was used for comparison with PAEC. Cells were seeded in cell culture flasks with 10% Alamar blue in the culture medium. Metabolically active cells reduce blue Resazurin dye in Alamar blue to fluorescent red Resofurin. 10μl of the culture media was taken from a confluent flask into a 96 well flat bottom plate containing 190μl of fresh media. Fluorescence was measured with an excitation wavelength of 525 nm and an emission wavelength of 590 nm.

Testing flat nano-coated surfaces.

By the technique of polymer demixing, nano-surfaces were created on flat glass cover slips. Two polymers polystyrene (PS) and poly venyl methyl ether (PVME) were mixed and added to the substrate cover slip. The mixture was annealed at 100°C under vacuum followed by dissolving the PVME with ultrapure water (Milipore). Surfaces with different nano-structures were created by controlling the ratio of PS/PVME and by regulating the process of dissolving PVME.

Surfaces were plasma sterilized before seeding them with $4x10^4$ cells/ml. Cells were allowed to grow for 2 days after which they were stained with Calcein AM (Molecular Probes, C-3100) and Ethidium homodimer (Molecular Probes, E-1169) for 15 min at room temperature. Cells were counted under a fluorescence microscope as live for green cells (stained by Calcein) and dead for red cells (stained by ethidium). An average of 20 frames was used to quantify the cells.

Results

Optimization of cell seeding inside glass tubes

Various cell seeding and incubation methods were tested in a total of 58 glass tubes (Table 1-3). Glass tubes were scored based on the amount of cells and surface area covered by the cells as seen under the light microscope. The scale for cell density used was: 1 = low density, 2 = intermediate density, 3 = high density, 4 = confluence. For distribution of cells the scale used was: 1 = ¼, 2 = 2/4, 3 = ¾, 4 = 4/4 of the tubes surface area. Glass tubes that only contained dead cells were excluded.

Among all tested methods, the incubation method of rotating manually and without reseeding of cells, 4 times rotation at 90° for 5 min each was found to be the most optimal (Table 1). For incubation with 4 times rotation at 90° with 30 min intervals and reseeding the outcome was slightly better than the one mentioned before (Table 2). The outcome was poorest when glass tubes were attached to the rotator (Table 3).

Immunostaining inside glass tubes

Cells inside glass tubes could be visualized by immunosatining them with a dye specific for cell nucleus (Figure 3)

Coating glass tubes with gelatin

Since maximum cell adhesion was still not attained in a plain glass tube the use of gelatin-coated glass tubes were considered. Gelatin coating has been previously used to grow endothelial cells [9]. The first step was to test if gelatin could be coated inside our glass tubes. Figure 4 shows staining for gelatin coated glass tube with coomassie and a control tube for the same staining without a gelatin coat.

Alamar blue assay

For regular monitoring of cell growth inside the glass tubes hooked up to the pump system inside an incubator, it would be necessary to detach the circuit to be taken under the microscope. To make this process easier, the Alamar Blue assay was adapted and tested in normal cell culture flasks. Two cell types PAEC and PK15 were compared for Alamar blue reduction at confluence (Figure 5). The average fluorescence intensity for PAEC was found to be 26816 and for PK15 it was 19202.

Testing flat nano-coated surfaces.

Nine different nano-coated surfaces were tested for PAEC adhesion and growth over two days. Figure 6 shows representative images of two surfaces with their corresponding staining for live/dead cells. The average number of dead cells for each surface was plotted on the z-axis of a 3D graph. On the x-axis of this graph was the average height of nano-structure and y-axis was the period of the nano-structure on which the cells grew (Figure 7). The 3D graph helped to identify the surface with fewer dead cells to have an average height of 20-40 nm and period of 500-1000 nm. Surfaces with highest number of dead cells had a height of 10-25 nm and period of 175-500 nm. One surface showed intermediate number of dead cells and the height of this surface was approximately 100 nm with a period of approximately 2500 nm.

Discussion

Vascular endothelial cells are in continuous interaction with their surrounding responding to and modulating the immediate micro- environment. For this purpose, EC needs to sense a stimulus and respond to it, which is known as endothelial cell activation. Be it under physiological or pathological conditions, the functions of EC's are determined by their morphology, the glycocalyx layer covering them and the shear stress exerted on them. It is therefore utmost important to consider these factors in the in vitro system that aims to replace animal experiments.

Vascular shear stress is the force exerted by the flowing blood on the vascular EC's. This can be determined by the flow rate for a known vessel diameter. The glass tube that replaces the vessel had an inner diameter of 1.6 mm and the maximum flow rate required for this was 48 ml/min. This would simulate the shear stress within an aortic vessel from where the cells to be experimented were isolated. The glycocalyx is a highly dynamic layer of the EC and are very sensitive to shear stress [10]. It is therefore upmost important to impart the right shear stress in order to study the important responses demonstrated by EC via its glycocalyx. EC morphology is an indicator for the health status of the cell and in our system the use of nano-structures is intended to support EC adhesion and growth in a normal and activated state.

To start with, different seeding and incubation methods were tested for PAEC inside the glass tubes. The most optimal of these was that with 4 times rotation at 90° with 30 min interval and additionally reseeding the tubes with fresh cell suspension between the intervals (Table 1). Such a low rate of manual rotation when compared to the other methods adapted was expected to be optimal, as EC need their time to adhere and grow on a foreign surface. Some of the successful glass tubes with cells were stained for DAPI and cells found to be attached but widely spread on the lumen of the tubes (Figure 3). Although the staining confirms the possibility to grow cells inside the tubes, the results need to be confirmed by checking for the viability of these cells. Furthermore, the results confirms the possibility of immunostaining the cells inside the glass tubes, which is in accordance with a previous study wherein glass tubes were exceptionally used for immunostaining [6].

As shown in Table 1- 3 various methods of EC seeding were tested but none gave complete confluence of cells. We considered to coat glass tuber with gelatin for it is known to support adherence and growth of EC. Overnight incubation of glass tubes filled with gelatin gave a good coating as stained by coomassie. However the coating was rather uneven with dense staining on the corners of the tube.

The entire in vitro system will be placed inside the incubator. In order to make regular monitoring if cells inside the glass tube easier and to determine cell confluence without bringing the tube out of the incubator, we sought to use the Alamar blue assay. The assay was established by comparing confluence of PAEC and PK15 cells in cell culture flasks. The fluorescence intensity varied within a cell type but was generally higher for PAEC than for PK15 (Figure 5), showing that reduction of the dye depends on the cell type. Although the standard deviation is low within a group, results from the assay for the glass tubes should be confirmed by viewing under the microscope.

The use of nano- or micro- fabricated surfaces have greatly come to use in the past decade for cellular engineering [11]. Recently it has been shown that EC's grow better on curved surfaces when coated with nano-structures [12]. Furthermore other studies have proven nano-structures to enhance EC adhesion and retention under flow [7, 13]. From our own experience we know this would be a major concern in our system especially when the media in the circuit would be replaced by human blood, in order to stimulate endolthelial cell activation [14]. Several studies in the past have been dedicated to determine the nano-dimensions required for optimal growth of EC's. These studies demonstrate nano- structures to be better than micro- structures for EC growth [15]. Cells were also shown to react to differences in the period (distance between two structures on the surface) of nano-surfaces. While Ranjan et al showed a height in nano meter range and period in micro- meter range to be optimal [16], others have gone far lower in the structural dimensions [17].

The nano- structures tested in this study also had mainly a low structure height ranging between 15 nm and 40 nm and a period ranging between 175 nm and 1000 nm. The best surface based on number of dead cells after 2 days of culture was the one with an average height ranging between 20 nm and 40 nm and a period ranging between 500 nm and 1000 nm. To this end, more samples must be tested in order to identify the best nano- coating for culture of porcine endothelial cells.

In conclusion, the current study is novel in its aim to culture endothelial cells and more importantly allow their investigation in settings that are very close to in vivo situations. This manuscript indicates the preliminary work done in setting up the system. Individual components of the system should be further optimized to attain the desired functionality.

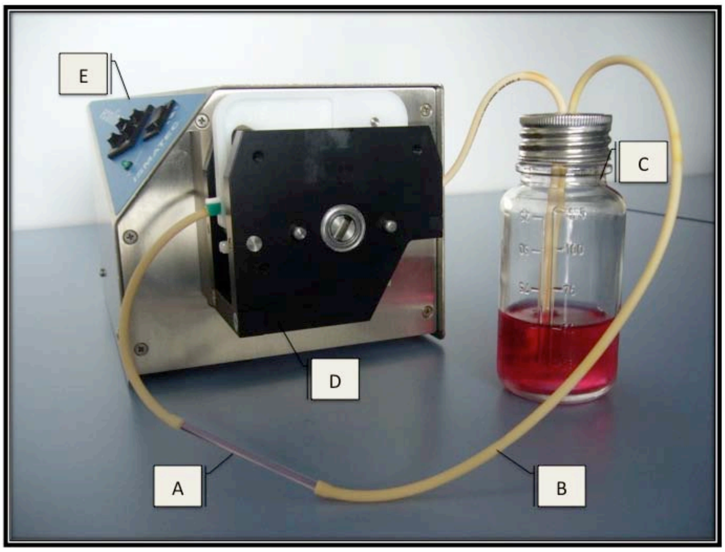

Figure 1: In vitro system to culture endothelial cells. Glass tubes in which endothelial cells are grown (A), silicone tubing connecting parts of the system (B), media bottle (C), 4-multichannel pump head (D), pulsatile pump (E).

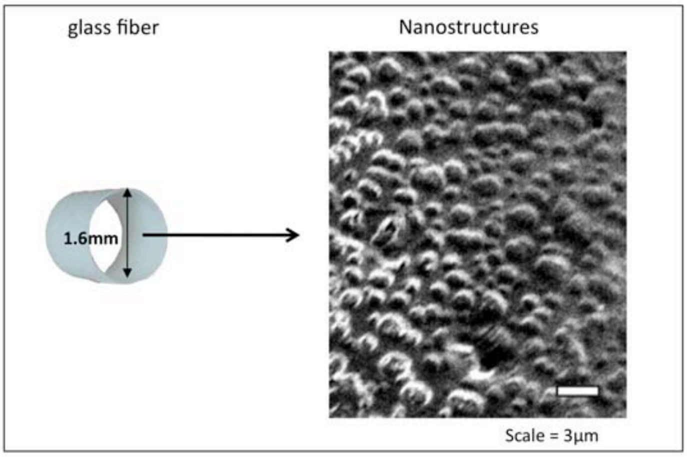

Figure 2: Nano structures within the glass tube. The glass tubes have an internal diameter of 1.6mm (left). Lumen of the tubes will be coated with nano-structures. A scanning electron microscope picture of nano-coating inside the tube (right)

Table 1. Incubation parameters for glass tubes rotated manually, without reseeding cells.

Rotation angle	Number of rotations	Interval of rotations	Number of glass tubes	Cell density	Covered surface
90°	4	30 min.	13	1.9	1.6
90°	4	15 min.	3	1.7	3
90°	**4**	**5 min.**	**8**	**2**	**4**
90°	8	2 min.	4	0	0
90°	4	2 min.	3	0	0
90°	4	20 min.	1	1	1
180°	2	60 min.	2	3	2
180°	1	24 hours	1	3	1

Table 2. Incubation parameters for glass tubes rotated manually and with reseeding cells.

Rotation angle	Number of rotations	Interval of rotations	Number of glass tubes	Cell density	Covered surface
90°	4	20 min.	2	2	2
90°	**4**	**30 min.**	**13**	**2.3**	**4**
180°	2	60 min.	1	2	2

Table 3. Incubation parameters for glass tubes attached to a rotator.

Rotations per minute	Time of rotation	Number of glass tubes	Cell density	Covered surface
1	60 min.	5	1	1
1	120 min.	2	3	2
10	24 hours	1	3	1

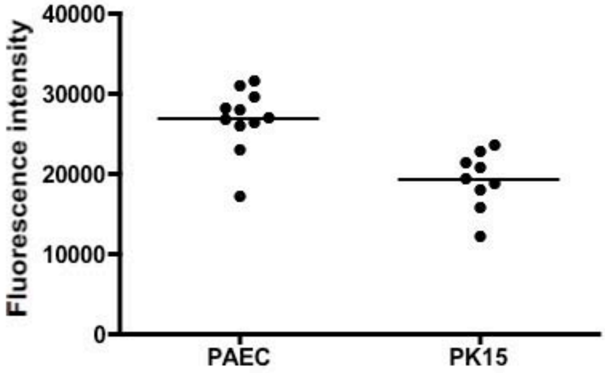

Figure 3: Alamar blue assay for detection of confluence. Reduction of alamar blue dye was measured as fluorescence intensity with confluent flasks of porcine aortic endothelial cells (PAEC) and porcine epithelial cell line (PK15). The average fluorescence intensity for a confluent flask of PAEC was 26816 and for PK15 it was 19202

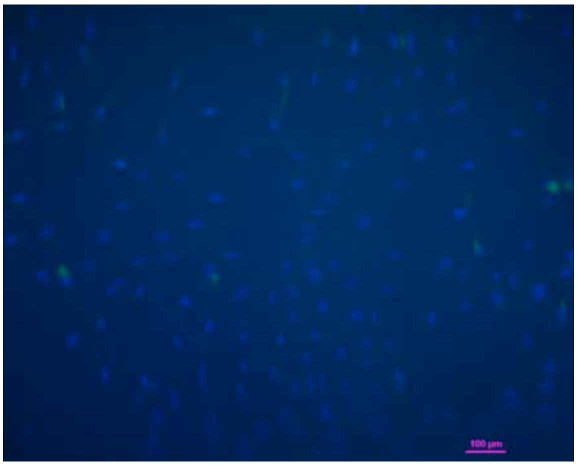

Figure 4: DAPI staining for PAEC in glass tube. Image taken under fluorescence microscope for PAEC cells inside the glass tube. Bright blue staining is the cell nucleus. Scale = 100μm.

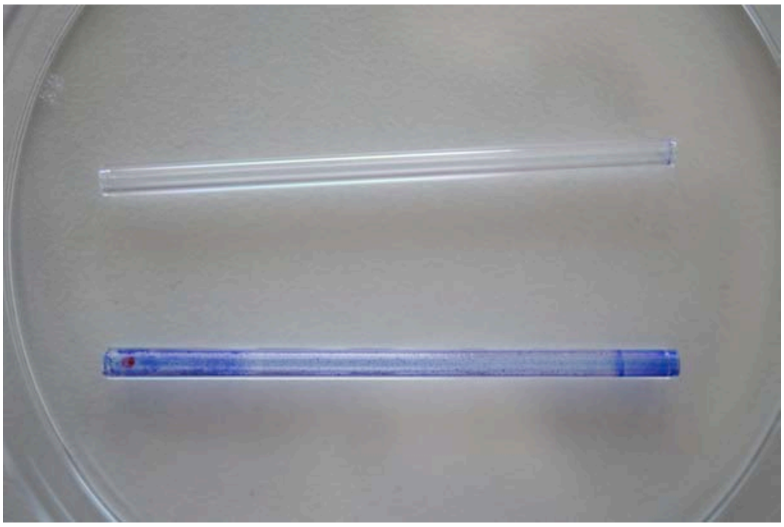

Figure 5: Gelatin coated glass fiber. Control glass tube without gelatin coating but with staining for gelatin (Above). Glass tube coated with gelatin and stained for the same (Below).

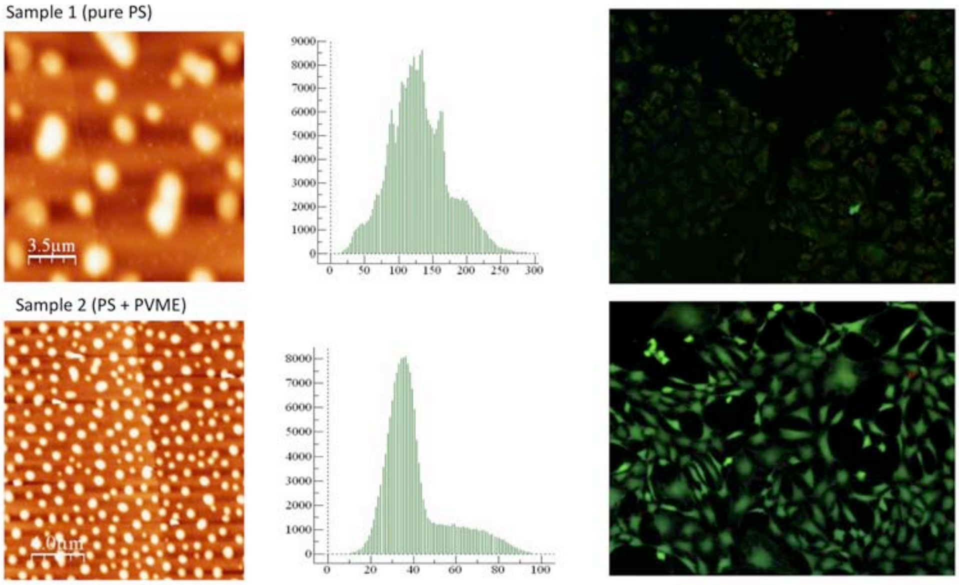

Figure 6: Testing nano-coated flat surfaces. Two types of nano-coated flat surfaces as seen under the scanning electron microscope are shown in the extreme left column. Variability of the nano-structures on these surfaces is shown in the middle column. On the x-axis is the height of the structures in nm and on the y-axis is the density. Live dead staining of cells grown for two days on these surfaces is shown in the extreme right column. Green staining is for live cells and red dots indicate dead cells.

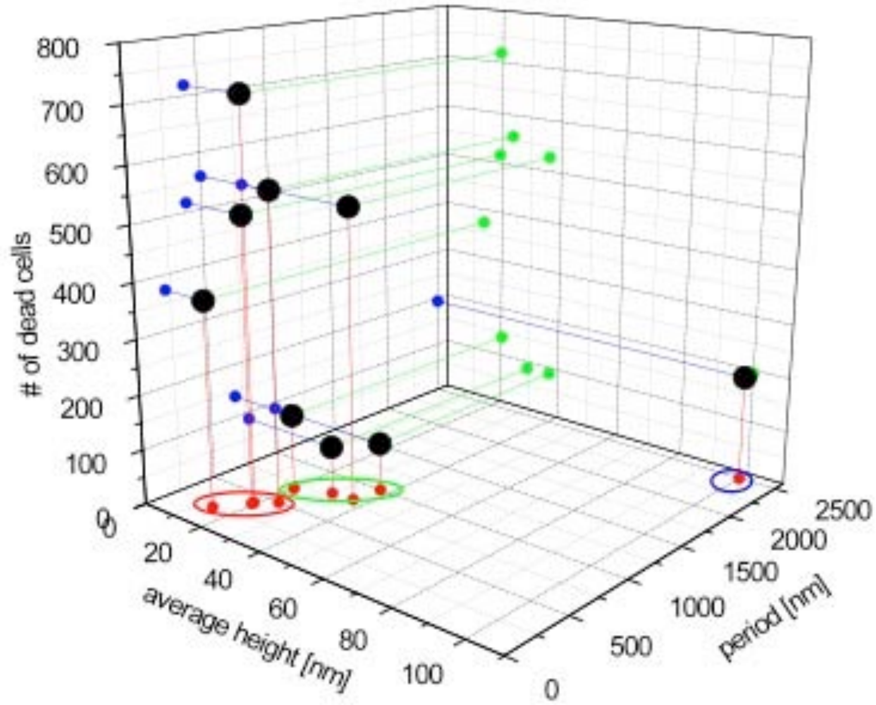

Figure 7: Comparing nano-coated flat surfaces. Nine flat surfaces coated with different nano-structures were compared. Every black dot indicates a surface. When black dots are extrapolated to the XZ-axis, surfaces with least number of dead cells have a height of 20-40nm and period of 500-1000nm (green circle). Surfaces with highest number of dead cells have a height of 10-25nm and period of 175-500nm (red circle). One surface with an intermediate number of dead cells had a height of approximately 100nm and period of approximately 2500nm (blue circle).

References

1 Reitsma S, Slaaf DW, Vink H, van Zandvoort MA, oude Egbrink MG: The endothelial glycocalyx: Composition, functions, and visualization. Pflugers Arch 2007;454:345-359.

2 Estrada R, Giridharan GA, Nguyen MD, Roussel TJ, Shakeri M, Parichehreh V, Prabhu SD, Sethu P: Endothelial cell culture model for replication of physiological profiles of pressure, flow, stretch, and shear stress in vitro. Anal Chem 2011;83:3170-3177.

3 Dai G, Tsukurov O, Orkin RW, Abbott WM, Kamm RD, Gertler JP: An in vitro cell culture system to study the influence of external pneumatic compression on endothelial function. J Vasc Surg 2000;32:977-987.

4 Benbrahim A, L'Italien GJ, Milinazzo BB, Warnock DF, Dhara S, Gertler JP, Orkin RW, Abbott WM: A compliant tubular device to study the influences of wall strain and fluid shear stress on cells of the vascular wall. J Vasc Surg 1994;20:184-194.

5 Benbrahim A, L'Italien GJ, Kwolek CJ, Petersen MJ, Milinazzo B, Gertler JP, Abbott WM, Orkin RW: Characteristics of vascular wall cells subjected to dynamic cyclic strain and fluid shear conditions in vitro. J Surg Res 1996;65:119-127.

6 Peng X, Recchia FA, Byrne BJ, Wittstein IS, Ziegelstein RC, Kass DA: In vitro system to study realistic pulsatile flow and stretch signaling in cultured vascular cells. Am J Physiol Cell Physiol 2000;279:C797-805.

7 Hwang SY, Kwon KW, Jang KJ, Park MC, Lee JS, Suh KY: Adhesion assays of endothelial cells on nanopatterned surfaces within a microfluidic channel. Anal Chem 2010;82:3016-3022.

8 Chien S: Significance of macrorheology and microrheology in atherogenesis. Ann N Y Acad Sci 1976;275:10-27.

9 Ma Z, He W, Yong T, Ramakrishna S: Grafting of gelatin on electrospun poly(caprolactone) nanofibers to improve endothelial cell spreading and proliferation and to control cell orientation. Tissue Eng 2005;11:1149-1158.

10 Pahakis MY, Kosky JR, Dull RO, Tarbell JM: The role of endothelial glycocalyx components in mechanotransduction of fluid shear stress. Biochem Biophys Res Commun 2007;355:228-233.

11 C.D.W. Wilkinson MR, M. Wood, J. Gallagher, A.S.G. Curtis The use of materials patterned on a nano- and micro-metric scale in cellular engineering. Materials Science and Engineering 2002;C:263–269.

12 Wang GJ, Lin YC, Hsu SH: The fabrication of plga microvessel scaffolds with nano-patterned inner walls. Biomed Microdevices;12:841-848.

13 Zorlutuna P, Rong Z, Vadgama P, Hasirci V: Influence of nanopatterns on endothelial cell adhesion: Enhanced cell retention under shear stress. Acta Biomater 2009;5:2451-2459.

14 Banz Y, Cung T, Korchagina EY, Bovin NV, Haeberli A, Rieben R: Endothelial cell protection and complement inhibition in xenotransplantation: A novel in vitro model using whole blood. Xenotransplantation 2005;12:434-443.

15 Lu J, Rao MP, MacDonald NC, Khang D, Webster TJ: Improved endothelial cell adhesion and proliferation on patterned titanium surfaces with rationally designed, micrometer to nanometer features. Acta Biomater 2008;4:192-201.

16 Ranjan A, Webster TJ: Increased endothelial cell adhesion and elongation on micron-patterned nano-rough poly(dimethylsiloxane) films. Nanotechnology 2009;20:305102.

17 Dalby MJ, Riehle MO, Johnstone H, Affrossman S, Curtis AS: In vitro reaction of endothelial cells to polymer demixed nanotopography. Biomaterials 2002;23:2945-2954.

General Conclusions

The current thesis is focused on acute mechanisms of ischemia reperfusion injury with mainly pig model of acute myocardial infarction as the working model. The state of research in this field is profound but still not complete. It highlights the major pathways involved and their degree of interaction in eliciting IR injury. The research I was involved in as mentioned in this thesis aids in understanding better the mechanisms of IR injury.

To begin with, our work has shown the involvement of heparan sulfates already during ischemia and at the onset of reperfusion via subtle changes in its composition (Paper VI). This directly reflects the importance of maintaining a native endothelium during IR, which is the driving hypothesis of the lab. Another key regulator of IR that appears early during reperfusion are the cytokines (Paper I). Role of complement was elucidated in Paper IV and its function other than contributing to tissue necrosis was confirmed. Strategies for the attenuation of injury during AMI were also tested. In Paper II a metal chelator was used to reduce the deleterious effects of reactive radicals and in Paper V we tried to restore the microvascular perfusion by regulating the coronary sinus pressure. The effect of these treatment strategies were restricted and showed no gross effect of reducing tissue necrosis, which would be favorable. All put together, the thesis confirms the importance of a native endothelium and immune response as essential players of IR injury. At least when compared to reactive radicals or regulation of sinus pressure. To conclude, the thesis has elucidated the minute changes that can regulate IR injury. Future research should therefore aim to develop strategies that would allow manipulation of the pathways of IR at a higher resolution.

Acknowledgements

I would like to acknowledge all the people who helped me start and finish this thesis. Firstly, my supervisor Prof. Dr. Robert Rieben, for realizing the potential in me and giving me the opportunity to carry out this PhD. He has undoubtedly given me support and encouragement through out my tenure, especially during my periods of frustration with science. I would like to thank my co-supervisor Prof Dr. Sylvia Miescher and my mentor Prof. Dr. Britta Engelhardt for their constant support during my thesis.

Big thanks to my colleagues at the cardiovascular research group starting with the Goddess Katja Matozan and Coochie Carmen Fleurkens for their technical support. My seniors Thusitha Gajanayake and Rolf Spirig (alias Jolfi) for their ever available help. Super big thanks to all my colleagues who also share the office with me: Claudia Dührkop for her 'Motherly-ness' when I was hyper- or hypo- active. Julie Denoyelle for her unbeatable support in helping me with my experiments. Anjan Bongoni, the 'Bioplex man' for his company in the lab during weekends and late evenings. Last but not the least, the new comers Yvonne Roschi and Philippe Montavon for adding to the spirit of the lab.

I would also like to thank all the people, whom I have met during my tenure including the short-term students Sabine Müller, Brigitte Jossen, Linda Kam and many more. My collaborators: Prof. Hans Imboden, Prof. Stijn Vandenberghe, Dr. Ahmed Khattab, Otto Aby and Prof. Stephan Christen and Dr. Lars Ebert for their scientific input and patience in answering my questions.

Once again I would like to thank everybody mentioned above and especially the ones not mentioned above.

Finally my family, to whom a 'thanks' is just not enough. Their trust in me has always kept me going. I am largely indebted to them for their understanding, patience, support and encouragement throughout my studies.

Curriculum Vitae

Personal details

Name:	Pranitha Jayadev Kamat
Date of Birth	17th April 1984
Nationality	Indian
Languages	Konkani, Hindi, English

Educational Background

2007- 2011	PhD in Immunology, University of Bern
2006-2007	MSc Drug Design and Biomedical Science Napier University, Edinburgh, UK
2003-2005	BSc Biotechnology Bangalore University, Bangalore, India

Awards

Napier University medal for graduating with distinction

Travel Award, 13th European meeting on complement in Human Disease, Leiden, Netehrlands

Manuscripts in preparation/submitted

P.J.Kamat, B.Juon, B.Jossen, T.Gajanayake, R.Rieben, E.Vögelin. Endothelial cell activation, Complement and Cytokines at the onset of Reperfusion after Tourniquet Application in Hand Surgery. Submitted to Journal of Inflammation.

P.J.Kamat, S.Vandenberghe, C.Stephan, O.Beslac, D.Mettler, B.Meier, O.M.Hess, R.Rieben, A.Khattab. Testing Dexrazoxane as an Attenuator of Ischemia/Reperfusion Injury in a Closed-Chest Porcine Model. Manuscript in preparation.

P.J.Kamat, A.Hamilton, S.Stringer, R.Rieben. Characterization of shed heparan sulfates in pig model of myocardial ischemia reperfusion injury. Manuscript in preparation.

T.Ruder, P.J.Kamat, A.Khattab, R.Rieben, M.Thali, L.Ebert. Detection of acute myocardial infarction by postmortem magnetic resonance imaging. Manuscript under preparation.

A.A.Khattab, S.Stieger, P.J.Kamat, O.Nitz, S.Vandenbherge, O.Beslac, J.H.Hoem, R.Rieben, W.Mohl. Effect of Pressure-Controlled Intermittent Coronary Sinus Occlusion (PICSO) on Myocardial Ischemia and Reperfusion in a Closed-Chest Porcine Model. Manuscript in preparation

P.Kamat, A.Broillet, A.Helbert, T.Bettinger, O.M.Hess, M.Schneider, R.Rieben. Antibodies and complement are deposited in viable myocardium in a porcine model of acute coronary syndrome

P.J.Kamat, L.Kam, J.Heier, R.Hany, R.Rieben. Development of an in vitro system to grow and investigate vascular endothelial cells under physiological flow conditions

Patent Pending

Title: Method of Coating Tubes with Controllable Internal Nanotopography

Published Abstracts

P. Kamat, A. Broillet, A. Helbert, T. Bettinger, O.M. Hess, M. Schneider, R. Rieben. Ultrasound molecular imaging of coronary endothelial P-selectin expression in a porcine model of acute myocardial ischemia and reperfusion. Journal of Vascular Research 2009 46(Suppl 3):36.

P. Kamat, A. Broillet, A. Helbert, T. Bettinger, F. Tranquart, M. Schneider, R. Rieben. The onset of reperfusion injury: Deposition of antibodies and complement in viable myocardium in a porcine model of acute coronary syndrome. Molecular Immunology 2010, 47:2275-2275.

P.Kamat, A.Broillet, A.Helbert, T.Bettinger, O.M.Hess, M.Schneider, R.Rieben. Antibodies and complement are deposited in viable myocardium in a porcine model of acute coronary syndrome. Molecular Immunology 2011, 48: 61-61

Oral presentations at international conferences

P.Kamat, B.Juon, B.Jossen, K.Matozan, R.Rieben, E.Vögelin. Studying endothelial damage in tourniquet induced ischemia/reperfusion injury in hand patients. European conference of scientists and plastic surgeons (ECSAPS) – Helsinki, 2010

P.Kamat, A.Broillet, A.Helbert, T.Bettinger, O.M.Hess, M.Schneider, R.Rieben. Antibodies and complement are deposited in viable myocardium in a porcine model of acute coronary syndrome. 13th European meeting on complement in Human Disease, Leiden, Netehrlands.

Poster presentations at international conferences

P.Kamat, A.Broillet, A.Helbert, T.Bettinger, F.Tranquart**,** M.Schneider, R.Rieben. The onset of reperfusion injury: Deposition of antibodies and complement in viable myocardium in a porcine model of acute coronary syndrome. 23rd International complement workshop – New York, 2010

P.Kamat, A.Broillet, A.Helbert, T.Bettinger, F.Tranquart**,** M.Schneider, R.Rieben. The onset of reperfusion injury: Deposition of antibodies and complement in viable myocardium in a porcine model of acute coronary syndrome. 2nd International symposium of defects in innate immunity – Zurich, 2011

P.J.Kamat, B.Juon, B.Jossen, T.Gajanayake, R.Rieben, E.Vögelin. Inflammatory Markers of Tourniquet-Induced Ischemia/Reperfusion Injury in Upper Limb Surgery. 13th European meeting on complement in Human Disease, Leiden, Netehrlands.

P.J.Kamat, A.Hamilton, S.Stringer, R.Rieben. Characterization of shed heparan sulfates in pig model of myocardial ischemia reperfusion injury. Gordon research conference-Glycobiology – Italy

Oral presentations at national conferences

P.J.Kamat, A.Hamilton, S.Stringer, R.Rieben. Characterization of shed heparan sulfates in pig model of myocardial ischemia reperfusion injury. Meeting of Swiss Immunology PhD students – Wolfsberg, 2011

Poster presentations at national conferences

P. Kamat, A. Broillet, A. Helbert, T. Bettinger, O.M. Hess, M. Schneider, R. Rieben. Ultrasound molecular imaging of coronary endothelial P-selectin expression in a porcine model of acute myocardial ischemia and reperfusion. Joint Meeting of the European Society of Microcirculation (ESM) and the Society of Microcirculation and Vascular Biology (GfMVB) – Bern, 2009

Contribution to writing of grant applications

Acute anti-inflammatory effects of reconstituted high-density lipoproteins (rHDL) and intravenous immunoglobulins (IVIG). Bern University research foundation

In vitro model to grow endothelial cells and study their activation, 3R research foundation.